

Cover Page



Universiteit Leiden



The handle <http://hdl.handle.net/1887/24264> holds various files of this Leiden University dissertation.

Author: Karper, Jacobus Cornelis (Jacco)

Title: Damage associated molecular patterns and toll like receptors in inflammation mediated vascular remodeling : mechanistic insights and therapeutic potentials

Issue Date: 2014-02-27

Damage Associated Molecular Patterns and Toll Like Receptors in Inflammation mediated Vascular Remodeling

Mechanistic insights and therapeutic potentials

Jacco C. Karper

Damage Associated Molecular Patterns and Toll Like Receptors in Inflammation mediated Vascular Remodeling

Mechanistic insights and therapeutic potentials

PROEFSCHRIFT

ter verkrijging van de graad van Doctor aan de Universiteit Leiden,
op gezag van Rector Magnificus prof. mr. C.J.J.M. Stolker,
volgens besluit van het College voor Promoties
te verdedigen op donderdag 27 februari 2014
klokke 16:15 uur

door

Jacobus Cornelis Karper

Geboren te Zwolle in 1984

Promotiecommissie

Promotores:

Prof. dr. P.H.A. Quax
Prof. dr. J.W. Jukema

Overige leden:

Prof. dr. M.J. Goumans
Prof. dr. J.F. Hamming
Prof. dr. J. Kuiper (LACDR, Leiden University)
Prof. dr. R.E. Toes
Dr. R. Arens
Dr. I.E. Hofer (University Medical Center Utrecht)

Financial support by the Dutch Heart Foundation for the publication of this thesis is gratefully acknowledged.

The research described in this thesis was performed at The Netherlands Organization for Applied Scientific Research (TNO), in the Eindhoven Laboratory for Experimental Vascular Medicine, at the department of Vascular Surgery of the Leiden University Medical Center, Leiden, The Netherlands and at Paris-Centre de Recherche Cardiovasculaire (PARCC), Paris, France

“In all things of nature there is something of the marvelous.”

Aristotle

Greek critic, philosopher, physicist, & zoologist (384 BC - 322 BC)

Voor mijn broer

Cover design: Geertjan Tromp and Jacco Karper
Collectie Rijksdienst voor het Cultureel Erfgoed, Amersfoort, objectnummer 10783-8697

Arterial typeface by Josh Sorosky (www.joshsorosky.com)

Printed by: Proefschriftmaken.nl | Uitgeverij BOXPress
Published by: Uitgeverij BOXPress, 's-Hertogenbosch

ISBN: 978-90-8891-797-4



Jacco C Karper

Damage Associated Molecular Patterns and Toll Like Receptors in Inflammation mediated Vascular Remodeling.

Proefschrift Leiden

Met literatuur opgave en Nederlandse Samenvatting

Copyright 2014 J.C. Karper

No parts of this thesis may be reproduced or transmitted in any form or by any means without prior permission of the author.

Financial support for the printing of this thesis was provided by Amgen B.V, Bayer Healthcare and Servier Nederland Farma B.V.

Table of Contents		<i>page</i>
Chapter 1	General introduction	11
Chapter 2	Small animal models to study restenosis and effects of (local) drug therapy. <i>Karper JC*</i> , <i>Ewing MM*</i> , <i>de Vries MR</i> , <i>Jukema JW</i> , <i>Quax PHA</i> . Coronary stent restenosis. Editor: IC Tintoiu. The Publishing House of the Romanian Academy, 2011.	21
Chapter 3	Future potential biomarkers for postinterventional restenosis and accelerated atherosclerosis. <i>Karper JC*</i> , <i>Ewing MM*</i> , <i>Jukema JW</i> , <i>Quax PH</i> . <i>Biomark Med</i> . 2012;6:53-66.	41
Chapter 4	Toll-like receptor 4 is involved in human and mouse vein graft remodeling, and local gene silencing reduces vein graft disease in hypercholesterolemic APOE*3Leiden mice. <i>Karper JC</i> , <i>de Vries MR</i> , <i>van den Brand BT</i> , <i>Hofer IE</i> , <i>Fischer JW</i> , <i>Jukema JW</i> , <i>Niessen HW</i> , <i>Quax PH</i> . <i>Arterioscler Thromb Vasc Biol</i> . 2011;31(5):1033-40.	61
Chapter 5	Blocking Toll-Like Receptors 7 and 9 Reduces Postinterventional Remodeling via Reduced Macrophage Activation, Foam Cell Formation, and Migration. <i>Karper JC</i> , <i>Ewing MM</i> , <i>Habets KL</i> , <i>de Vries MR</i> , <i>Peters EA</i> , <i>van Oeveren-Rietdijk AM</i> , <i>de Boer HC</i> , <i>Hamming JF</i> , <i>Kuiper J</i> , <i>Kandimalla ER</i> , <i>La Monica N</i> , <i>Jukema JW</i> , <i>Quax PH</i> . <i>Arterioscler Thromb Vasc Biol</i> . 2012;32(8):e72-80.	81
Chapter 6	Toll like receptors in vein graft remodeling: protective effects of TLR3 and downstream Interferon regulating factors. <i>de Vries M.R*</i> , <i>Karper J.C*</i> , <i>van der Pouw Kraan T.C</i> , <i>Peters H.A.B</i> , <i>de Jong R.C.M</i> , <i>Hamming J.F</i> , <i>Jukema J.W</i> , <i>Horrevoets A</i> , <i>Quax P.H</i> . Manuscript in preparation	105
Chapter 7	TLR accessory molecule RP105 (CD180) is involved in post-interventional vascular remodeling and soluble RP105 modulates neointima formation. <i>Karper JC</i> , <i>Ewing MM</i> , <i>de Vries MR</i> , <i>de Jager SC</i> , <i>Peters EA</i> , <i>de Boer HC</i> , <i>van Zonneveld AJ</i> , <i>Kuiper J</i> , <i>Huizinga EG</i> , <i>Brondijk TH</i> , <i>Jukema JW</i> , <i>Quax PH</i> <i>PLoS One</i> . 2013;8(7):e67923.	125
Chapter 8	RP105 deficiency aggravates cardiac dysfunction after myocardial infarction in mice. <i>Karper J.C*</i> , <i>Louwe M.C*</i> , <i>de Vries M.R</i> , <i>Bastiaansen A.J.N.M</i> , <i>van der Hoorn J.W.A</i> , <i>Willems van Dijk K</i> , <i>Rensen P.C.N</i> , <i>Steendijk P</i> , <i>Smit J.W.A</i> , <i>Quax P.H.A</i> Manuscript under revision	143
Chapter 9	An unexpected intriguing effect of TLR regulator RP105 (CD180) on atherosclerosis formation with alterations on B cell activation. <i>Karper J.C*</i> , <i>de Jager S.C.A*</i> , <i>Ewing M.M</i> , <i>de Vries M.R</i> , <i>Bot I</i> , <i>van Santbrink P.J</i> , <i>Redeker A</i> , <i>Mallat Z</i> , <i>Binder C.J</i> , <i>Arens R</i> , <i>Jukema J.W</i> , <i>Kuiper J</i> , <i>Quax P.H.A</i> <i>Arterioscler Thromb Vasc Biol</i> . 2013 Dec;33(12):2810-7	159
Chapter 10	Summary and general discussion	181
Chapter 11	Nederlandse samenvatting	187

		<i>page</i>
Chapter 12	List of publications	195
	Curriculum Vitae	

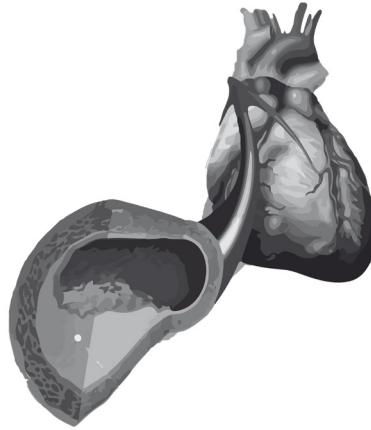
Supplemental material to chapter 2

T-cell co-stimulation by CD28-CD80/86 and its negative regulator CTLA-4 strongly influence accelerated atherosclerosis development *Ewing MM, Karper JC, Abdul S, de Jong RC, Peters HA, de Vries MR, Redeker A, Kuiper J, Toes RE, Arens R, Jukema JW, Quax PH* Int J Cardiol. 2013 Jan 22. 201

Annexin A5 prevents post-interventional accelerated atherosclerosis development in a dose-dependent fashion. *Ewing MM, Karper JC, Sampietro ML, de Vries MR, Pettersson K, Jukema JW, Quax PH.* Atherosclerosis 2012;221:333-340. 231



CHAPTER 1



General Introduction

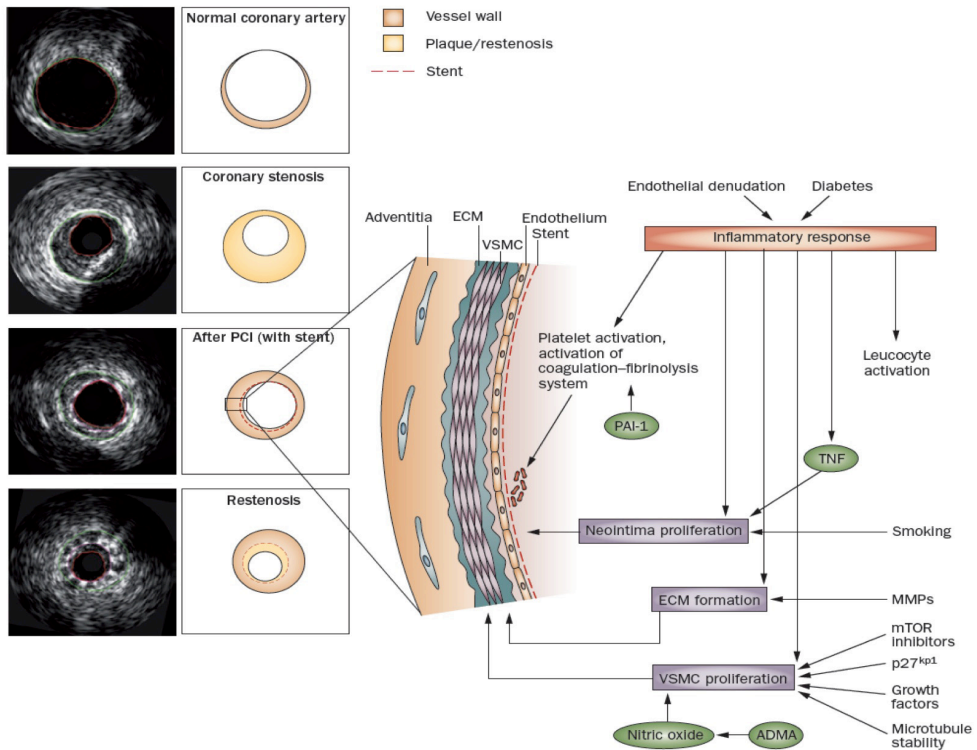
Introduction

Atherosclerosis

Atherosclerosis remains one of the main causes of mortality and contributes significantly to the increase of morbidity in the western world. The origin of this problem is initiated by changes in the endothelial layer caused by dyslipidemia, hypertension, and pro-inflammatory mediators that lead to the exposure of adhesion molecules and infiltration of circulating leukocytes into the arterial wall. The recognition of modified lipids, parts from damaged cells or modified matrix components by immune cells cause an ongoing inflammatory process that contributes to lesion and plaque formation.[1-3] Early atherosclerotic plaques consist of lipid depositions, foam cells and T cells and resides most in the large and middle arteries such as aorta, coronary arteries, carotid arteries and femoral arteries.[1] During progression of the plaque a fibrous cap is formed overlying the necrotic core of the plaque. This fibrous cap is formed by migration and proliferation of smooth muscle cell (SMC) and extracellular matrix depositions. Progression in growth of the atherosclerotic plaques narrows the vessel, limiting blood flow and thereby essential oxygen provision to the organs and tissues[4, 5]. A major problem occurs when the fibrous cap ruptures and the core of the plaque is exposed to the blood. This will cause platelets to aggregate and to form blood clots that will close up the total vessel causing immediate ischemia, an infarction[6]. This requires intervention strategies to re-open the vessel to restore bloodflow. Due to increased possibilities for the treatment and the prevention of a myocardial infarction (MI) survival chances of these patients have increased significantly.

Percutaneous Coronary Intervention

The invention of Percutaneous Coronary Intervention, also known as balloon angioplasty, has ensured that closed vessels could be re-opened without the requirement of heart surgery. Unfortunately, the results are not always satisfactory because in a significant number of patients the re-opened vessel narrows again at the place of initial treatment. This process is called restenosis a problem strongly mediated by inflammation, proliferation and matrix turnover as can be appreciated in figure 1. [7, 8].



Intravascular ultrasound images of the various stages of coronary artery disease. Indicated are the outer border of the vessel (green), the lumen (red), and the coronary stent (pink). Schematic representations are shown to the right of these images. The processes occurring in the vessel immediately after PCI with stent placement are highlighted in detail. Abbreviations: ADMA, asymmetric dimethylarginine; ECM, extra cellular matrix; MMPs, matrix metalloproteinases; mTOR, mammalian target of rapamycin; PAI-1, plasminogen activator inhibitor I; PCI, percutaneous coronary interventions; TNF, tumor necrosis factor; VSMC, vascular smooth muscle cell. (Jukema et al. *Nature Reviews Cardiology* 9, 53-62 2012)[7]

Risk factors of restenosis development are diabetes, smoking, stent type, lesion complexity and off-label use of stents. Although strong evidence for influence of inflammation has been provided, the exact pathophysiology of restenosis has not been fully elucidated yet. Gaining more insight in this process may be fundamental for the development of novel therapeutic strategies

In the late 70s rates of restenosis and procedural failures were still around 40%. As interventional cardiologist gained more experience with the procedure the number of failed procedures was significantly reduced. Restenosis rates however began to decline only after introduction of the stent. A stent is a small tube inserted into a natural passage/conduit to prevent or counteract a disease-induced, localized flow constriction. This stent prohibits the early phase of restenosis in which elastic recoil of the vessel after balloon angioplasty narrows the lumen. The intermediate phase of intimal hyperplasia and late phase of atherosclerosis formation however are not sufficiently prohibited by the stent. The vascular injury and presence of a foreign body even may cause a stronger inflammatory reaction leading to platelet aggregation, proliferation of smooth muscle cells in the vessel wall and influx of lipids and

immune cells derived from the circulation that all contribute to the formation of intimal hyperplasia, accelerated atherosclerosis and thereby the incidence of restenosis[7, 9, 10]. A novel invention to overcome this problem is the use of stents that secrete specific drugs, which inhibit the proliferation of cells, the so-called drug eluting stents (DES)[11, 12]. As a result restenosis numbers further decreased. Unfortunately, the reverse side is an increased risk for in-stent-thrombosis caused by a reduction in re-endothelialisation, activation of coagulation mediators such as tissue factor and is associated with high morbidity and mortality rates[7, 11, 13]. Therefore patients with DES have to take medication that inhibits platelet aggregation such as Aspirin and Clopidogrel for longer periods, thereby increasing bleeding risk but also experience a greater risk of in-stent thrombosis, and thus infarction, when they undergo non-cardiac surgery within one year after stent placement[14, 15]. Nowadays PCI is a safe and effective treatment of atherosclerotic coronary artery disease however restenosis remains an important complication after PCI with rates in daily practise of 5-15%.

Vein graft remodeling

The trade-off for the choice of intervention type is associated with the severity of the stenosis, strictures, and the number of occluded vessels[16]. In some cases it is not possible or unbeneficial to perform PCI and an alternative intervention strategy is provided by the use of a bypass. Nowadays thoracic surgeons make mainly use of arterial grafts, such as the left and right mammary artery. In some cases, however, when these vessels are unavailable or unusable, venous conduits offer an alternative. So vein grafts are still important conduits for revascularization during both coronary but also peripheral bypass surgery. Unfortunately vein graft failure is not an uncommon event.[17] Early graft failure is usually due to thrombosis, but long-term graft failure is caused by vein graft disease (VGD) induced by the wall thickening due to intimal hyperplasia, which is part of an inflammatory reaction. Vein graft wall thickening is in part characterized by smooth muscle cell (SMC) proliferation, matrix turnover, and an influx of lipids and inflammatory cells. When this process continues and additional atherosclerosis formation takes place the lumen slowly closes the vessel leading to a poor long-term graft patency[18-20]. The disadvantage of the vein is that it is rather weak with a thin vessel wall with limited musculature and is not adapted to the high pressures that are present in the arterial circuit. Via hyperplasia of smooth muscle cells in the vessel wall partial arterialization takes place, which ensures that the vein does not collapse under the increased pressure[21]. Due to the pressure differences however the endothelium is severely damaged offering a substrate for lipid and inflammatory cell influx and thereby atherosclerotic plaque formation[22]. This process together with the proliferation of the smooth muscle cells, that also may become foam cells, will severely narrow the lumen.

Inflammation

For many years the assumption was that atherosclerosis is merely a passive accumulation of cholesterol in the vessel wall[1] Nowadays, atherosclerosis and other vascular remodeling processes such as restenosis and vein graft remodeling, are considered to be chronic inflammatory diseases mediated by the immune system[3, 23]. The innate immune system is considered to be the first line of defence and to be non-specific. This means that the cells of the innate system recognize and respond to pathogens in a generic way without a long-lasting memory. Cells of the innate immunity such as dendritic cells, monocytes and macrophages recognize pathogens via their pattern recognition receptors (PRR) that bind pathogen associated molecular patterns (PAMPs) that are molecules broadly shared by pathogens but

not by host cells or tissues[24, 25]. Activation of innate immunity by PAMPs will result in cytokine/chemokine releases that further mediate the initiated inflammatory cascade[26]. On the other hand cell stress or tissue damage cause a release of host molecules that are known as Damage Associated Molecular Patterns (DAMPs) and are thought to mediate non-infectious “sterile” inflammatory responses in reaction to cell stress, apoptosis or necrosis[27]. Acquired or adaptive immunity consists of B and T lymphocytes and is considered to be the specific immune system. T-cell responses to immunogenic antigens are regulated by antigen recognition signals provided by peptide-MHC antigen complexes on antigen-presenting cells (APCs) that bind to the T-cell antigen receptor (TCR), which operates in concert with co-stimulatory signals[28]. In multiple vascular remodeling processes infiltration of multiple leukocyte subsets from both innate and adaptive immunity such as monocytes, macrophages, T cells, B cells and Mast cells can be appreciated in the vessel wall[1].

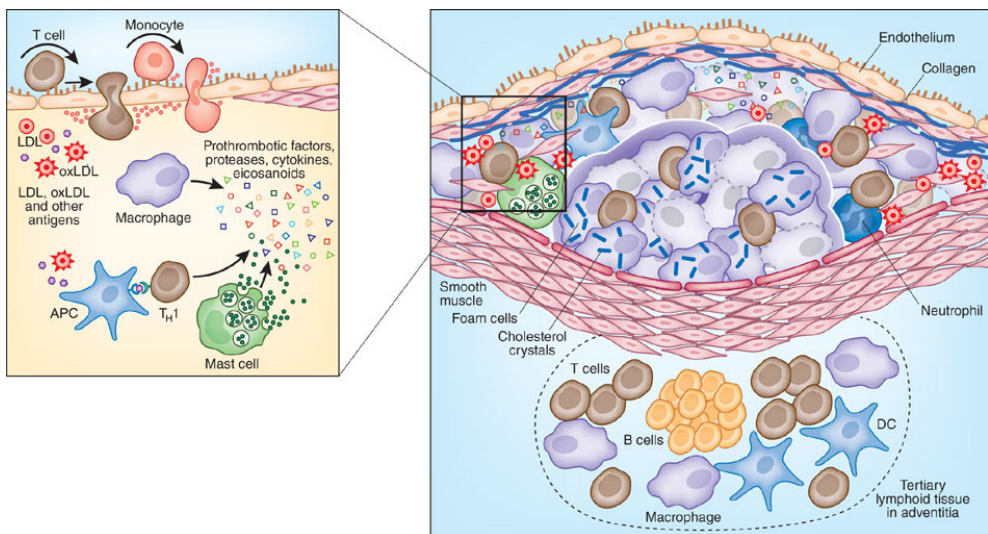


Figure 2: Activation of innate immune responses in the atheroma

From Göran K Hansson & Andreas Hermansson *Nature Immunology* 12, 204–212 (2011) [1]

Over time processes of cellular stress, apoptosis, necrosis and calcification take place within the plaque with the release of several DAMPs and multiple inflammatory cells can be appreciated that may further enhance the ongoing inflammation and luminal narrowing.

Toll Like Receptors

Toll Like Receptors are pattern recognition receptors (PRR) of the immune system known to recognize exogenous ligands that originate from bacteria or viruses (PAMPs) as well as endogenous ligands derived from host-cells (DAMPs). TLR4 is the most investigated TLR as a membrane bound receptor located on a variety of immune and non-immune cells including macrophages, endothelial cells and SMCs. It is the only TLR that makes use of all four adaptor proteins. The discovery by Dr. Beutler that TLR4 recognizes lipopolysaccharide (LPS), part of the cell membrane of gram negative bacteria, has had important implications and for which he was awarded the Nobel Prize in 2011 shared with Jules A. Hoffmann and

Ralph M. Steinman for their discoveries concerning the activation of innate immunity[29, 30]. Later TLR4 was found to be capable of initiating inflammatory responses upon DAMP activation[31-34]. The role of TLR4 in vascular remodeling, especially arterial remodeling has previously been demonstrated in various studies either directed at atherogenesis and plaque (de)stabilization or directed at the role of TLR4 in post-interventional arterial remodeling after angioplasty[35-38]. The TLR family consists of 13 members that all recognize multiple ligands from different source[24]. TLRs can reside in the cell membrane or endosomal. Endosomal TLRs comprising TLR3, TLR7, TLR8 and TLR9 recognize nucleic acid derived from viruses as well as endogenous nucleic acids (self DNA and RNA) while the other TLRs recognize mostly bacterial components and endogenous matrix components as hyaluronic acid, fibronectin EDA but also oxLDL[35, 39, 40]. These DAMPs may be released after tissue damage or cell stress initiated upon PCI, vein graft placement or myocardial infarction. TLRs make use of four different adaptor proteins of which Myd88 is considered to be the most important. Myd88 depended TLR signaling leads to NF κ B activation and up regulation of several pro-inflammatory cytokines also those that are considered to be important in vascular disease such as TNF and MCP1. The Myd88-independent or TRIF-pathway is only used by TLR3 and 4 and leads to phosphorylation of Interferon Regulating Factors (IRF) that after translocating to the nucleus cause the release of type 1 interferons[39]. Meanwhile a late response of TRIF activation may, via RIP1 and TAK1, initiate NF κ B activation and up regulation of several pro-inflammatory cytokines via a mechanism comparable to that of the Myd88-dependent pathway. Altogether TLRs regulate over more than thousand genes and subsequent processes[41, 42].

Specific accessory proteins or cofactors can regulate the complex mechanism of signaling that reflects and emphasizes the complexity and diversity of TLR ligand interaction and activation. Such molecules have different roles, for example as cofactors, signalling adaptors and molecules, and regulators of TLR function[43]. Activation of TLR4 is dependent on the presence of accessory molecule MD2 that is capable of binding LPS and a variety of other known endogenous ligands [44-46]. Next to MD2, RP105 (CD180) is an important accessory molecules acting as a regulator of TLR4[46-49]. Interestingly the role of RP105 in modulating inflammatory responses depends on the cell type making it unique in its role of either enhancing or suppressing TLR regulated inflammation in different cell types[43] This underlines the complex mechanism of TLR signalling which should be taken into account during the design of therapeutic strategies focused on TLR or DAMP interference.

Outline of the thesis

Studying pathophysiological processes in a pre-clinical setting requires resembling animal models. Chapter 2 reviews animal models that can be used for the study of post-interventional remodeling highlighting the murine arterial cuff model either or not in combination with a hypercholesterolemic pro-atherosclerotic background. This model not only allows studying this process but also the application of local therapy mimicking drug eluting balloons or drug eluting stents. Furthermore effects of local and systemic drug therapy are reviewed. The continuing problems of vascular remodeling and restenosis emphasize the need for specific biomarkers so that these processes can be detected early and / or can be treated in time. The underlying immune regulated inflammatory reactions may offer such biomarkers, which are discussed in chapter 3 with special interest in Damage Associated Molecular Patterns (DAMPs). A distinction in potential biomarkers is made between circulating, local and circulating cell-bound markers Chapter 4 describes the role of TLR4, one of the most



important recognizers of multiple DAMPs, in vein graft remodeling. TLR4 was up-regulated in reperfused human venous segments and was shown to serve as a potential local therapeutic target to reduce accelerated atherosclerosis in vein grafts in mice.

TLR7 and TLR9 are recognizers of PAMPs (CpG and DNA fragments) of viruses and DAMPs derived from the cell nucleus of dying cells and known to be involved in several autoimmune disorders. Chapter 5 shows the efficacy of a novel synthesized dual TLR7/9 antagonist on the prevention of accelerated atherosclerosis. The antagonist reduced restenosis via reduced leukocyte infiltration, hampered foam cell formation and an increase in anti-inflammatory cytokine IL10. TLR7 and TLR9 use signaling routes via Myd88 to release type I interferons that are known to be capable of successfully target viruses. Actually all TLRs make use of the Myd88 dependent pathway except for TLR3. TLR3 signals via the TIR-domain-containing adapter-inducing interferon- β (TRIF) and interferon regulatory factor (IRF)3 and IRF7 resulting in induction of type I interferons (IFNs). Chapter 6 describes the protective effects of TLR3 and downstream IRF factors on vein graft remodeling while other TLRs traditionally linked to vascular disease were shown to increase vein graft remodeling. Via pathway analysis we showed that the TLR and type 1 Interferon pathway belonged to the top 15 of regulated pathways in vein graft remodelling. Presence of intact TLR3, IRF3 or IRF7 resulted in reduced influx of inflammatory cell types compared to mice in which these genes were deleted.

TLR signalling is strongly mediated by TLR accessory molecules. RP105 is a TLR4 homolog and important regulator of TLR4 signalling. It is unique in its role of either enhancing or suppressing TLR4 signalling in different cell types. The function of RP105 in restenosis was studied in Chapter 7 where RP105 deficiency revealed enhanced restenosis rates. Analysis on the protein structure of purified MD1/RP105 showed a unique protein structure that is consistent with a hetero-tetrameric RP105₂MD1₂ complex, as was observed in the recently published crystal structures of the RP105-MD1 complex. This orientation is opposite to that of known ligand-induced TLR-homodimers. The soluble form of this protein was capable of reducing TLR induced inflammation ex-vivo and restenosis in vivo. The effects of RP105 deficiency on myocardial remodeling were described in Chapter 8. RP105 deficient mice showed a more prominent cardiac dilation after MI, but remained relatively good hemodynamic parameters by adequate compensation. No effects however were found on inflammatory cell infiltration. Chapter 9 describes the role of RP105 deficiency on haematopoietic cells in atherosclerotic plaque formation with an unexpected reduction of lesion size. Differences were found on B cell activation status, antibody production against oxLDL and cytokine expression profiles. Only moderate effects were detected on cells that are traditionally linked to TLR involvement in atherosclerosis.

In the supplemental material to chapter 2 it is shown how potential therapeutic therapies can be tested and mechanistic insights can be obtained by using the murine arterial cuff model. First the importance of T cell and co-stimulatory and co-inhibitory pathways in restenosis making use of knockout mice, antibodies and Abatacept is described. Abatacept, a recombinant CTLA4-Ig fusion protein, is registered for treatment of clinical-RA and prevents CD28 mediated T cell activation.

Furthermore the use of Annexin A5 to block the DAMP phosphatidylserine (PS) is described and reduced restenosis can be appreciated. Additionally associations were found between polymorphisms in the Annexin A5 gene and restenosis rates in humans making it highly relevant for the medical clinic.

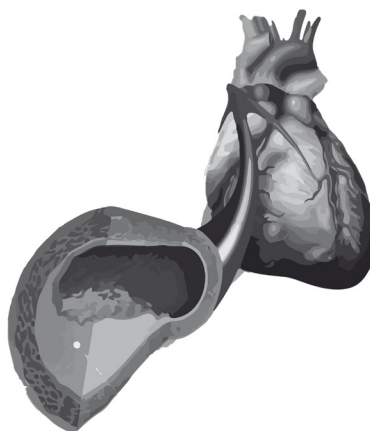
1. Hansson, G.K. and A. Hermansson, The immune system in atherosclerosis. *Nat Immunol*, 2011. 12(3): p. 204-12.
2. Libby, P., P.M. Ridker, and G.K. Hansson, Progress and challenges in translating the biology of atherosclerosis. *Nature*, 2011. 473(7347): p. 317-25.
3. Medzhitov, R., et al., Highlights of 10 years of immunology in *Nature Reviews Immunology*. *Nat Rev Immunol*, 2011. 11(10): p. 693-702.
4. Hansson, G.K., Inflammation, atherosclerosis, and coronary artery disease. *N Engl J Med*, 2005. 352(16): p. 1685-95.
5. Newby, A.C., Matrix metalloproteinases regulate migration, proliferation, and death of vascular smooth muscle cells by degrading matrix and non-matrix substrates. *Cardiovasc Res*, 2006. 69(3): p. 614-24.
6. Shah, P.K., Mechanisms of plaque vulnerability and rupture. *J Am Coll Cardiol*, 2003. 41(4 Suppl S): p. 15S-22S.
7. Jukema, J.W., et al., Restenosis after PCI. Part 1: pathophysiology and risk factors. *Nat Rev Cardiol*, 2012. 9(1): p. 53-62.
8. Weintraub, W.S., The pathophysiology and burden of restenosis. *Am J Cardiol*, 2007. 100(5A): p. 3K-9K.
9. Newby, A.C. and A.B. Zaltsman, Molecular mechanisms in intimal hyperplasia. *J Pathol*, 2000. 190(3): p. 300-9.
10. Koskinas, K.C., et al., Role of endothelial shear stress in stent restenosis and thrombosis: pathophysiologic mechanisms and implications for clinical translation. *J Am Coll Cardiol*, 2012. 59(15): p. 1337-49.
11. Jukema, J.W., et al., Restenosis after PCI. Part 2: prevention and therapy. *Nat Rev Cardiol*, 2012. 9(2): p. 79-90.
12. Walter, D.H., et al., Statin therapy, inflammation and recurrent coronary events in patients following coronary stent implantation. *J Am Coll Cardiol*, 2001. 38(7): p. 2006-12.
13. Dangas, G.D., et al., In-stent restenosis in the drug-eluting stent era. *J Am Coll Cardiol*, 2010. 56(23): p. 1897-907.
14. Holmes, D.R., Jr., et al., Stent thrombosis. *J Am Coll Cardiol*, 2010. 56(17): p. 1357-65.
15. Korte, W., et al., Peri-operative management of antiplatelet therapy in patients with coronary artery disease: joint position paper by members of the working group on Perioperative Haemostasis of the Society on Thrombosis and Haemostasis Research (GTH), the working group on Perioperative Coagulation of the Austrian Society for Anesthesiology, Resuscitation and Intensive Care (OGARI) and the Working Group Thrombosis of the European Society for Cardiology (ESC). *Thromb Haemost*, 2011. 105(5): p. 743-9.
16. Task Force on Myocardial Revascularization of the European Society of C., et al., Guidelines on myocardial revascularization. *Eur Heart J*, 2010. 31(20): p. 2501-55.
17. Lopes, R.D., et al., Relationship between vein graft failure and subsequent clinical outcomes after coronary artery bypass surgery. *Circulation*, 2012. 125(6): p. 749-56.
18. Owens, C.D., et al., Early remodeling of lower extremity vein grafts: inflammation influences biomechanical adaptation. *J Vasc Surg*, 2008. 47(6): p. 1235-42.
19. Ozaki, C.K., Cytokines and the early vein graft: strategies to enhance durability. *J Vasc Surg*, 2007. 45 Suppl A: p. A92-8.
20. Davies, M.G. and P.O. Hagen, Pathophysiology of vein graft failure: a review. *Eur J Vasc Endovasc Surg*, 1995. 9(1): p. 7-18.
21. Kwei, S., et al., Early adaptive responses of the vascular wall during venous arterialization in mice. *Am J Pathol*, 2004. 164(1): p. 81-9.
22. Stooker, W., et al., Perivenous support reduces early changes in human vein grafts: studies in whole blood perfused human vein segments. *J Thorac Cardiovasc Surg*, 2001. 121(2): p. 290-7.
23. Libby, P., Inflammation in atherosclerosis. *Arterioscler Thromb Vasc Biol*, 2012. 32(9): p. 2045-51.
24. Kawai, T. and S. Akira, The role of pattern-recognition receptors in innate immunity: update on Toll-like



- receptors. *Nat Immunol*, 2010. 11(5): p. 373-84.
25. Miyake, K., Innate immune sensing of pathogens and danger signals by cell surface Toll-like receptors. *Semin Immunol*, 2007. 19(1): p. 3-10.
 26. Takeuchi, O. and S. Akira, Pattern recognition receptors and inflammation. *Cell*, 2010. 140(6): p. 805-20.
 27. Bianchi, M.E., DAMPs, PAMPs and alarmins: all we need to know about danger. *J Leukoc Biol*, 2007. 81(1): p. 1-5.
 28. Lichtman, A.H., et al., Adaptive immunity in atherogenesis: new insights and therapeutic approaches. *J Clin Invest*, 2013. 123(1): p. 27-36.
 29. Poltorak, A., et al., Genetic and physical mapping of the Lps locus: identification of the toll-4 receptor as a candidate gene in the critical region. *Blood Cells Mol Dis*, 1998. 24(3): p. 340-55.
 30. Poltorak, A., et al., Defective LPS signaling in C3H/HeJ and C57BL/10ScCr mice: mutations in Tlr4 gene. *Science*, 1998. 282(5396): p. 2085-8.
 31. Ionita, M.G., et al., Endogenous inflammatory molecules engage Toll-like receptors in cardiovascular disease. *J Innate Immun*, 2010. 2(4): p. 307-15.
 32. Park, J.S., et al., Involvement of toll-like receptors 2 and 4 in cellular activation by high mobility group box 1 protein. *J Biol Chem*, 2004. 279(9): p. 7370-7.
 33. Gondokaryono, S.P., et al., The extra domain A of fibronectin stimulates murine mast cells via toll-like receptor 4. *J Leukoc Biol*, 2007. 82(3): p. 657-65.
 34. Taylor, K.R., et al., Hyaluronan fragments stimulate endothelial recognition of injury through TLR4. *J Biol Chem*, 2004. 279(17): p. 17079-84.
 35. Stewart, C.R., et al., CD36 ligands promote sterile inflammation through assembly of a Toll-like receptor 4 and 6 heterodimer. *Nat Immunol*, 2010. 11(2): p. 155-61.
 36. Hollestelle, S.C., et al., Toll-like receptor 4 is involved in outward arterial remodeling. *Circulation*, 2004. 109(3): p. 393-8.
 37. Kiechl, S., et al., Toll-like receptor 4 polymorphisms and atherogenesis. *N Engl J Med*, 2002. 347(3): p. 185-92.
 38. Hansson, G.K. and K. Edfeldt, Toll to be paid at the gateway to the vessel wall. *Arterioscler Thromb Vasc Biol*, 2005. 25(6): p. 1085-7.
 39. Kawai, T. and S. Akira, TLR signaling. *Semin Immunol*, 2007. 19(1): p. 24-32.
 40. Yu, L., L. Wang, and S. Chen, Endogenous toll-like receptor ligands and their biological significance. *J Cell Mol Med*, 2010. 14(11): p. 2592-603.
 41. Watters, T.M., E.F. Kenny, and L.A. O'Neill, Structure, function and regulation of the Toll/IL-1 receptor adaptor proteins. *Immunol Cell Biol*, 2007. 85(6): p. 411-9.
 42. Brikos, C. and L.A. O'Neill, Signalling of toll-like receptors. *Handb Exp Pharmacol*, 2008(183): p. 21-50.
 43. Lee, C.C., A.M. Avalos, and H.L. Ploegh, Accessory molecules for Toll-like receptors and their function. *Nat Rev Immunol*, 2012. 12(3): p. 168-79.
 44. Shimamoto, A., et al., Inhibition of Toll-like receptor 4 with eritoran attenuates myocardial ischemia-reperfusion injury. *Circulation*, 2006. 114(1 Suppl): p. I270-4.
 45. Kim, H.M., et al., Crystal structure of the TLR4-MD-2 complex with bound endotoxin antagonist Eritoran. *Cell*, 2007. 130(5): p. 906-17.
 46. Miyake, K., et al., RP105, a novel B cell surface molecule implicated in B cell activation, is a member of the leucine-rich repeat protein family. *J Immunol*, 1995. 154(7): p. 3333-40.
 47. Divanovic, S., et al., Regulation of TLR4 signaling and the host interface with pathogens and danger: the role of RP105. *J Leukoc Biol*, 2007. 82(2): p. 265-71.
 48. Divanovic, S., et al., Negative regulation of Toll-like receptor 4 signaling by the Toll-like receptor homolog RP105. *Nat Immunol*, 2005. 6(6): p. 571-8.
 49. Ogata, H., et al., The toll-like receptor protein RP105 regulates lipopolysaccharide signaling in B cells. *J*

Exp Med, 2000. 192(1): p. 23-9.

CHAPTER 2



Small animal models to study restenosis and effects of (local) drug therapy.

Karper JC, Ewing MM*, de Vries MR, Jukema JW, Quax PHA*

** both authors contributed equally*

Coronary stent restenosis. Editor: IC Tintoiu. Bucharest:
The Publishing House of the Romanian Academy, 2011.

Summary

In-stent restenosis remains the major drawback of coronary interventions and is a highly complex process, initiated by the induction of vascular injury and stent deployment, ultimately leading to negative vascular remodeling and reoccurrence of symptoms. Development, testing and validation of new therapies strongly depends on the availability of animal models that closely mimic human restenotic pathophysiology. Moreover, for a better understanding of the pathophysiology of the restenosis process adequate animal models mimicking the human restenosis process are essential.

Here, we review various animal models, predominately humanized mouse models, currently used to study the pathophysiology of restenosis. Larger animal models such as pigs and rabbits that are used for testing new therapeutic strategies such as new drug-eluting stents, will not be discussed in this chapter.

We will discuss the involvement of inflammatory and immune modulatory factors in the development and progression of restenosis. Furthermore, we will discuss in detail several new therapeutic options based on modulation of their anti-proliferative, anti-inflammatory or proteinase-interference abilities.

We can conclude highly-reproducible animal models for post-interventional vascular remodeling remain essential for the development of future anti-restenotic therapies.



Introduction

Pathophysiology of restenosis in humans and animals

Restenosis is defined angiographically in patients when neointimal tissue comprises over 50% of the luminal surface at the site of intervention of the affected artery. Restenosis is characterized by acute elastic recoil, negative remodeling and intimal hyperplasia due to inflammation, deposition of granulation tissue and extracellular matrix remodeling.

Intracoronary stenting has virtually eliminated elastic recoil and negative remodeling. However, after balloon angioplasty and stent placement neointimal formation still occurs due to de-endothelization and injury of the vessel wall including the atherosclerotic plaque.

Together, these effects lead to activation of the remaining endothelium, platelet adhesion and subsequent activation, fibrin formation and the expression of adhesion molecules, leukocyte adherence and infiltration. Adhered leukocytes release an array of inflammatory cytokines, chemokines, proteases such as matrix metalloproteinases and growth factors which not only promote inflammation, but also cause medial smooth muscle cell migration and proliferation, matrix degradation, local proteoglycan deposition and subsequent extracellular matrix remodeling. Under hypercholesterolemic conditions this is accompanied by influx and accumulation of low-density lipoprotein (LDL) cholesterol in the vessel wall. This will be taken up by macrophages, that become foam cells and initiate a process of accelerated atherosclerosis in these vessel segments¹. Patients receive platelet-inhibitors throughout interventional procedures to prevent arterial thrombosis and end-organ ischemia due to thrombotic occlusion of the affected vessel. Furthermore, this therapy partly prevents the initial pathophysiological events that eventually lead to restenosis development. Nonetheless, in patients limited local inflammatory processes are related to the healing of the vascular injury triggered by mechanical dilation, stent deployment and the continuous presence of stent struts against the arterial wall and their exposure to flowing blood^{2,3}. However, uncontrolled inflammatory processes may induce intimal hyperplasia.

Intravascular injury to diseased vessels with a hypercholesterolemic background is common in patients, but severely difficult to reproduce in healthy vessels of mainly young animals with a normocholesterolemic phenotype. Therefore, transgenic mouse models with a pro-atherosclerotic or hypercholesterolemic phenotype have attracted attention as humanized mouse models for mechanistic and pathophysiological restenosis research.

Animal models for restenosis and vascular remodeling

Various animal models, mainly in mice, are currently available to mimic human restenosis, extensively based on perivascular injury, aimed to induce local coagulation and subsequent inflammation, leading to accelerated atherosclerosis formation.

Balloon angioplasty of rat carotid arteries

A model of balloon-induced injury to the carotid artery in rats was described in 1983 by Clowes et al.⁴ and used many studies there after, amongst others by Ohlstein et al.⁵, in which an arterial embolectomy catheter is inserted into the common carotid artery and a balloon is inflated and drawn along the vessel wall to induce mechanical injury. Afterwards, the external carotid artery is ligated. This leads to severe SMC migration and proliferation and intimal thickening.

Common carotid artery ligation in mice

Neointimal formation can be elicited by completely ligating the common carotid artery just proximal to the carotid bifurcation to disrupt blood flow as has been described by Kumar et al.⁶ and since then has frequently been used by several groups. After 4 weeks, intimal thickening occurs and consists of both SMCs and leukocytes, indicating the pivotal role of inflammation in the formation of neointimal tissue. The model is hampered by its reproducibility, since morphometric analysis is very critical. The degree of the intimal hyperplasia depends on the position the analyzed section in regard to the point of ligation.

Mouse model of femoral artery denudation injury

Femoral artery transluminal injury can be induced by passage of a 0.25-mm diameter angioplasty guide wire in mice⁷. Four weeks after injury, neointima formation can be analyzed and consist predominately of migrated and proliferated SMCs, although inflammatory cells can already be observed early after injury.

Perivascular electrocoagulation injury

Electrocoagulation-induced injury to the femoral artery of mice was introduced in 1997 by Carmeliet et al.⁸, leading to loss of all endothelial and medial smooth muscle cells (SMCs) and formation of a mural non-occlusive platelet-rich thrombus. This leads to inflammatory cell recruitment and SMC migration and proliferation, eventually leading to intimal thickening.

Photochemical intravascular injury

Photochemical endothelial injury to the femoral artery of mice injected with rose Bengal solution using transluminal green light has been used by Kikuchi et al.⁹ in 1998 to induce a local thrombus formation, followed by endothelial denudation and medial SMC apoptosis and eventually intimal thickening. Unfortunately, the reproducibility of this model remains rather low.

Perivascular chemical injury

Chemical perivascular injury to the carotid artery of dyslipidemic mice using a filter paper saturated with a 10% ferric chloride solution was used by Zhu et al.¹⁰ to induce formation of an occlusive platelet-rich thrombus due to endothelial cell loss and medial SMC necrosis, triggering inflammatory cell recruitment and SMC migration and proliferation. Eventually, this promotes intimal thickening.

Inter-arterial venous engraftment

Accelerated atherosclerosis and vascular remodeling also appear in engrafted vascular segments, which are performed frequently to bypass occluded arterial segments in patients. Although bypass models do not mimic the pathophysiology of restenosis completely, they can be used excellently to study various aspects of restenotic disease. Models have been developed for several animal species. Only relatively recently have mouse models for vein graft disease become available, developed by Xu et al., (7), most often based on the model described by Lardenoye et al.¹¹, in which a venous interposition is made within the carotid artery of a mouse. For this, an inferior caval vein is harvested from littermate donor mice and preserved in a 0.9% NaCl solution containing 100U of heparin at 4°C, to prevent thrombosis. Afterwards, the carotid artery is dissected free from its surroundings, ligated twice and cut between the two 8.0 silk ligatures. Clamps are placed proximally and distally from the



ligatures to allow haemostatic control to the surgeon throughout the procedure, leaving free arterial ends over which a cuff can be placed. Next, the free arterial ends are everted over the cuffs and ligated with an 8.0 silk ligature, after which the harvested inferior caval vein is interpositioned between the ends of the artery. The connections are ligated together with an 8.0 silk suture and visible pulsations confirm successful engraftment.

When performed in hypercholesterolemic mice, concentric lesions are formed within 4 weeks and are friable, with extracellular lipid deposition and foam cell accumulation, underneath a poorly developed or absent fibrous cap. This morphology highly resembles the morphology observed in arterially-engrafted veins in patients. All aspects of rapid post-interventional vascular remodeling and accelerated atherosclerosis development are present in this very reproducible animal model.

Intravascular balloon dilatation injury

Intravascular injury models resembling invasive coronary procedures have been developed recently, but remain technically very demanding.

Kwak et al.¹² described a mouse model in which intravascular carotid balloon distension injury is performed, which a balloon catheter was introduced through an arteriotomy on the proximal external carotid artery and advanced into the common carotid artery and subsequently distended to induce controlled vessel wall distension. In this elegant model, distention could be matched to the animal's weight and the balloon was expanded using a water-filled inflation device. Vessel wall damage led to endothelial denudation, followed by leukocyte recruitment and medial SMC activation, leading to intimal thickening and luminal stenosis. Although this model is technically difficult to perform, vascular injury highly resembles the human situation and leads to a similar pathophysiological vessel wall response.

Inter-arterial stented-arterial engraftment

Ali et al.¹³ have taken intravascular stenting in mouse models a step further, which they reported in 2007. Donor mice receiving aspirin underwent stenting using a stainless-steel stent crimped onto an angioplasty balloon catheter, which was guided into place retrograde through the thoracic aorta, leaving the balloon and stent in the descending thoracic aorta. The balloon was inflated for 30 seconds until 8 times atmospheric pressure to induce stent deployment. Next, the stented-aorta was removed and kept in heparinised PBS solution, before being engrafted within the ligated carotid artery of a hypercholesterolemic recipient mouse, similarly to the vein graft procedure. After 28 days, intimal thickening was significantly increased in the stented arterial graft, when compared to the aorta and balloon-inflated aortic grafts. Lesions consisted predominately of SMCs, macrophages and foam cells, similarly to human coronary lesions after interventions.

Perivascular femoral arterial cuff placement

Already in 1989, it was shown by Booth et al.¹⁴ that placement of a perivascular non-constrictive plastic cuff around the common carotid artery of hypercholesterolemic rabbits results in intimal thickening based on SMC migration and proliferation, cholesterol deposition and foam cell formation as seen in human restenotic lesions. This is due to mechanical vascular damage and an inflammatory response evoked by the cuff. There was no need for endothelial cell damage and the formation of a transient occlusive thrombus in this model.

When this attractive model was downscaled to mice¹⁵, this offered the unique opportunity to employ a mechanically-induced inflammatory-based restenosis model in an animal species of

which an enormous range of strains with genetic variations existed, including atherosclerosis prone transgenic strains.

Since like the human genome, the murine genome has currently been completely mapped and multiple humanized-mouse models have been developed, this has allowed researchers to investigate the role of specific genotypic and general phenotypic traits in restenosis development. The aim was to identify pathophysiological changes leading to restenosis and accelerated atherosclerosis development, and subsequently identify key targets for prevention and treatment of restenosis in patients in a clinical setting.

The technical procedure of perivascular cuff placement¹⁵ is described in detail in the next section.

Before surgery, mice are anaesthetized with an intraperitoneal injection with a combination of 5 mg/kg Midazolam (Roche, Basel, Switzerland), 0.5 mg/kg Medetomidine (Orion, Helsinki, Finland) and 0.05 mg/kg Fentanyl (Janssen, Geel, Belgium). This combination of anesthetics gives complete narcosis, lasting minimally one hour and can be antagonized using Antisedan 2.5 mg/kg (Orion), Anexate 0.5 mg/kg (Roche) and Buprenorphine 0.08 mg/kg (Schering-Plough, Kenilworth, NJ, USA).

A microscope with 10-15x total magnification is used during the microsurgery procedures (Olympus SZX9 microscope). Basic instruments required are a blunt micro forceps (length: 10.5cm, height: 0.3mm, Medicon Instruments, Tuttlingen, Germany), a sharp micro forceps (length: 10.5cm, height: 0.3mm, Medicon Instruments), a micro scissor (length: 12.5cm, height: 10mm, Medicon Instruments) and a micro needle holder (length: 18.5cm, Medicon Instruments).

A longitudinal incision is made at the internal side of the thigh and the femoral artery is dissected from the femoral nerve and vein. The femoral artery is looped twice with a ligature (USP: 6/0, Metric: 0.7., Silkam natural silk, B. Braun, Melsungen, Germany) and a non-constrictive fine bore polyethylene tubing (0.40mm inner diameter, 0.80mm outer diameter, Portex, Kent, UK) is cut 2.0mm length and longitudinally opened and sleeved loosely around the femoral artery. The cuff is closed with two 6/0 ligature knots in the extremities of the cuff. Finally, the skin incision is closed with a running suture (USP: 6/0, Metric: 0.7., Silkam silk, B. Braun). After surgery, animals are placed in a clean cage on top of a heating pad for four hours. A schematic representation and photomicrograph of the femoral arterial cuff placement are shown in figure 1.

For histological analysis, animals are typically sacrificed 2-3 weeks after cuff placement. After anesthesia, the thorax is opened and a mild pressure-perfusion (100 mmHg) with 4% formaldehyde in 0.9% NaCl is performed for 5 minutes by cardiac puncture. After perfusion, a longitudinal incision is made in the internal side of the thigh and the cuffed femoral artery is harvested as a whole and fixed overnight in 4% formaldehyde.

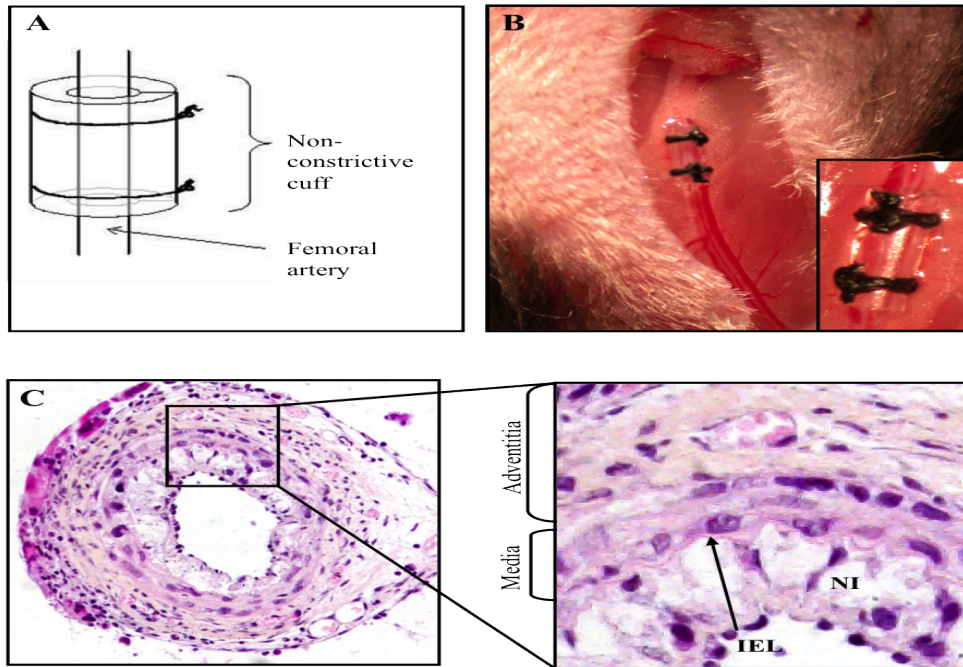


Figure 1. Schematic representation of non-constrictive cuff placed loosely around a murine femoral artery, held in place by two ligatures (A) and a photomicrograph (B) of a positioned cuff in vivo. (C) Photomicrograph of the restenosis lesion in the cuffed femoral artery in the mouse. Indicated are the internal elastic lamina (IEL) and the neointima (NI) formed within the vessel wall.

Preclinical application of drug-eluting stents and balloons

Intracoronary stenting decreased restenosis rates by preventing elastic recoil and negative remodeling, although in-stent restenosis due to neointimal proliferation remains the major limiting factor of the success rate for coronary interventions as treatment for coronary artery disease. Drug-eluting stents with a polymer coating have been developed which are loaded with various types of drugs designed to prevent in-stent restenosis. These drugs, some originally used as chemotherapeutic agents, against transplant rejection or as immunosuppressive drugs, tend to prevent the local inflammatory reaction, SMC proliferation and migration or promote local healing due to a slow local release.

Drug-eluting balloons are coated with similar drugs, but are designed to deliver the drug only for a very short period of time whilst the balloon is left inflated, to prevent solely the initial local responses to balloon inflation and vessel wall distention.

Limited (post-mortem) pathological data is available from stented human coronary arteries, since histology is usually not readily available. All in vitro and in vivo effects of new drug-eluting stents should be evaluated for safety and efficiency before being applied in human studies. Preclinical animal studies can also provide insight in the method-of-action, dose-response and side-effects of these new stents. Additionally, they can be used for investigation into specific genes involved in restenosis development. Genes of interest can be found in large prospective follow up studies, such as the GENDER study¹⁶, in which the association between gene polymorphisms and clinical outcome can be studied. Additionally, these

highly-reproducible models can be used to screen candidate compounds, without the need for expensive, large, long-lasting and time-consuming clinical trials.

Drug-eluting stents can be mimicked in mice by placement of a perivascular non-constrictive drug-eluting cuff¹⁷, comprised of a poly(ϵ -caprolactone) (PCL) polymer and non-toxic polyethylene glycol, loaded with the candidate drug, shown in figure 2. This polymer cuff allows encapsulation and local sustained release of compounds over a longer period of time. Depending on the ratio between PCL and polyethylene glycol, the duration of drug-release can be extended up until 21 days after cuff placement, to allow local vessel wall drug-exposure throughout the entire study period, even in non-hypercholesterolemic mice which develop restenotic lesions relatively slowly.

An alternative for local delivery of active compounds to the mouse vessel wall is the use of local administration of the compound dissolved in pluronic gel or gelatin in and around the cuff. This allows short period of delivery of compounds locally in the murine cuff model as the gelatin or the pluronic gel will degrade in a short period of time. The set-up of this local application of pluronic gel in the cuff is shown in figure 3.

In patients, drug-eluting stents release the drug intraluminally, whilst in this model drugs are released from the adventitial side of the vessel wall. However, the vessel wall in the mouse is smaller, therefore penetration of the compound will be efficient, although applied via the adventitia. Nonetheless, this drug-eluting PCL cuff is certainly an extremely useful and practical tool to evaluate the effects of new candidate anti-restenotic drugs on local vessel wall pathology and intimal thickening as part of post-interventional vascular remodeling.

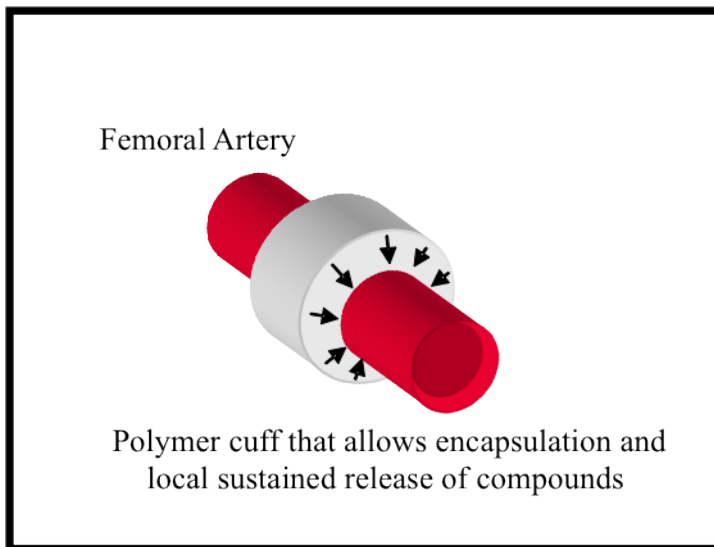


Figure 2. Schematic representation of a drug-eluting femoral arterial cuff and method-of-action

Suitable mouse strains

Contrary to patients, wild-type mouse strains have low levels of pro-atherosclerotic low-density-lipoprotein and high plasma levels of anti-atherosclerotic high-density lipoprotein and therefore do not readily develop native atherosclerosis. Inbred mice used for studies into



accelerated atherosclerosis and restenosis tend to respond to restenotic stimuli by displaying either a type 1 or type 2 helper T cell (Th1 or Th2) response. The Th1 response, typical of the C57BL/6 mouse strain, leads to macrophage differentiation into proatherogenic M1 macrophages and production of inflammatory cytokines and chemokines, which promote lesion formation¹⁸. The Th2 response, typical of the BALB/C mouse strain, promotes the differentiation of macrophages into anti-inflammatory M2 macrophages, which produce anti-inflammatory and anti-atherogenic cytokines, eventually leading to a healing response within the damaged vessel wall. For this reason, mouse strains with a C57BL/6 background are favored for studying pathophysiological changes leading to restenosis. When the perivascular non-constrictive cuff procedure is performed in this mouse strain¹⁹, concentric lesions develop within 21 days after surgery and typically consist of collagen and α -actin positive SMCs.

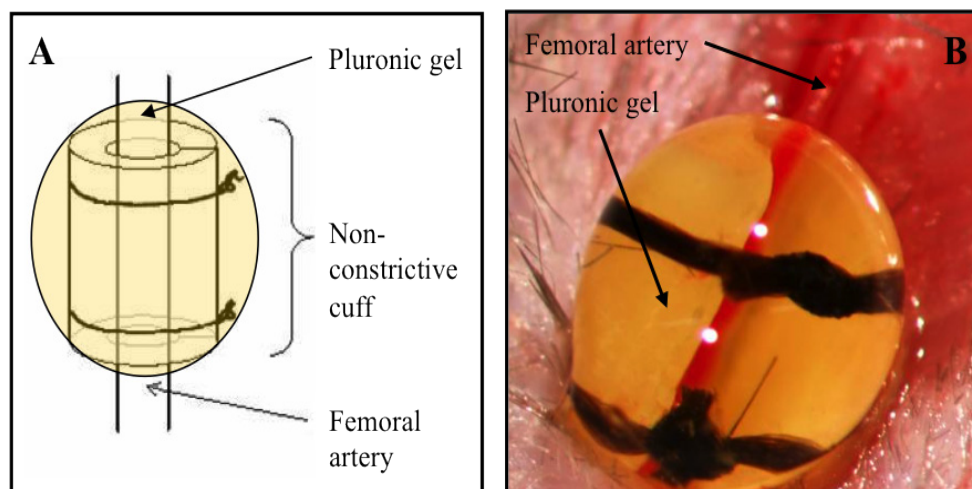


Figure 3. Schematic representation of non-constrictive cuff around a murine femoral artery, covered by hardened pluronic gel (A). Photomicrograph cuff in vivo, with hardened (40%) pluronic gel applied to the cuffed vessel segment, loaded with an anti-restenotic drug (yellow) (B).

Dyslipidemic mouse strains

Intravascular injury by balloon inflation and stent placement in diseased human vessels in hypercholesterolemic patients can be mimicked by cuff placement in hypercholesterolemic knock-out or transgenic mouse strains.

Apolipoprotein (Apo) E is an important part of circulating very (V) LDL and LDL cholesterol and acts as a ligand for the LRL-R, thus leading to uptake of proatherosclerotic cholesterol from the circulation. Genetic ApoE deficiency therefore leads to hypercholesterolemia due to insufficient LDL-receptor(R)-mediated VLDL and LDL clearance, especially when fed a high-cholesterol diet, and spontaneous atherosclerotic and interventional-induced lesion formation. Drawbacks of this mouse strain are plasma cholesterol levels that are mainly determined by the VLDL fraction, that exceed by far any physiological level and that all other atheroprotective (anti-inflammatory, anti-platelet and anti-proliferative) properties of ApoE are lost²⁰.

Patients with familial hypercholesterolemia display mutations in the LDL-R gene, leading to insufficient LDL clearance and dyslipidemia. Similarly, LDL-R knockout mice develop

mild hypercholesterolemia, which increases strongly when fed a high-cholesterol diet. Since cholesterol elevation is mainly determined by the LDL fraction and spontaneous atherosclerotic lesions develop more slowly than in ApoE knockout mice, this is classified as a more moderate model. Nonetheless, both mouse strains can be used to study post-interventional restenosis development²⁰.

Mutations in the ApoE3 gene are associated with dysbetaipoproteinemia in patients. One of these mutations is the ApoE3Leiden mutation²¹. By introducing an ApoE3 and ApoC1 gene construct in the C57BL/6 mice, the transgenic ApoE3*Leiden mouse strain was generated²². Since the animals still express endogenous ApoE proteins, contrary to the ApoE knockout animals, the uptake of ApoE-containing lipoproteins is merely reduced and not completely inhibited. Animals have diet-induced increased plasma cholesterol concentrations, mainly in VLDL and LDL fractions. They are very responsive to high-cholesterol feeding.

Desired plasma cholesterol concentrations can be obtained by varying dietary cholesterol content. Additionally, since both ApoE and LDL-R are still present, plasma cholesterol levels are subject to modulation by lipid-lowering drugs that influence endogenous chylomicron and VLDL production and indirectly affect LDL-R expression, such as statins. Restenotic lesions after cuff placement develop moderately and consist predominately of SMCs, foam cells and extracellular matrix formation, very similar to human lesions¹⁵.

New mechanistic and therapeutic insights

Agents currently used or under investigation to prevent and treat restenosis can be divided between either drugs with cytotoxic/anti-proliferative and anti-inflammatory effects or drugs that target proteolytic systems. Here we give an overview how animal models may contribute to gain further insight into the mechanism of restenosis and to test new therapeutic strategies.

Proliferation

Rapamycin (sirolimus)

Immunosuppressive drugs like rapamycin are currently widely used in drug-eluting stents to prevent the development of in-stent restenosis. Rapamycin is a macrolide antibiotic drug with anti-proliferative and immunosuppressive effects that targets protein translation, resulting in a G1 arrest of the cell cycle which is known to inhibit vascular SMC proliferation and migration in vitro by inhibiting DNA synthesis and cell growth²³⁻²⁵. Rapamycin has been shown to effectively inhibit the arterial proliferative response after PCTA in a porcine restenosis model, without toxicity in low doses. Local rapamycin application in the murine cuff model was performed using a rapamycin-eluting cuff and it was observed that locally released rapamycin led to an inhibition of neointima formation by 75±6% for all tested concentrations. Experiments demonstrated that perivascular sustained release was restricted to the cuffed vessel segment, with no systemic adverse effects. Moreover, when applying the rapamycin eluting cuff to a diseased atherosclerotic vessel segment in ApoE3Leiden mice, no progression of the atherosclerotic lesion development could be observed, nor any systemic side effects

Paclitaxel

Paclitaxel belongs to the taxanes, which are potent anti-proliferatives widely used to treat patients suffering from cancer. It leads to polymerization of the α - and β -units of tubulin and thus stabilizes microtubules, which are necessary for the G₂ transition of a dividing cell into the M phase. Paclitaxel causes almost complete inhibition of cell growth and SMC



proliferation and migration by targeting cytoskeleton structure. SMC proliferation and migration are both induced by balloon inflation and stent placement during interventional procedures. In a murine femoral arterial cuff model, drug-eluting cuffs containing high paclitaxel concentrations (1–5%) have been shown to reduce intimal thickening by $76 \pm 2\%$. When placing the paclitaxel eluting cuff in hypercholesterolemic mice or even over an existing atherosclerotic lesion in mice, dose dependent negative side effects were observed. High dosage of paclitaxel significantly increased apoptosis (also in the media), disruption of the elastic laminae and decrease medial and intimal smooth muscle cell as well as collagen content. These findings show elegantly the added value of testing drug eluting devices in atherosclerotic animal model. Many clinical trials^{26–28} have investigated the effectiveness of (non) polymer-based paclitaxel-eluting stents and have shown to be very effective in the prevention of restenosis development, however, negative effects on the vascular pathology were not detected, emphasizing that the femoral arterial cuff model is of high predictive value in the screening for new candidate drugs for efficacy and local adverse side effects.

Inflammation

Although neointima formation is characterized by proliferation and migration of smooth muscle cells (SMC) and extracellular matrix turnover it is now broadly accepted that these processes are triggered by inflammatory activation of the vessel wall¹⁶. Evidence that inflammation is the initial trigger for vascular remodeling has accumulated over the past years and the role of various cytokines and chemokines as pro-inflammatory factors as well as immune modulation in general has been the focus of many studies on vascular remodeling and restenoses. In the next section we would like to illustrate this with a couple of representative examples. Starting with the description of the effects of the general anti-inflammatory factor dexamethason, we will further zoom in on the effects of specific cytokines (TNF α , IL10), chemokines (MCP-1) and the role of the innate immune system (complement, Toll-like receptors) on restenosis in the mouse models.

Dexamethason

Dexamethason is a corticosteroid with strong glucocorticoid properties and is widely used as a broad anti-inflammatory and immunosuppressant drug. Prolonged systemic delivery is associated with multiple side effects in humans and animals. These effects could be abolished by local delivery using a drug-eluting cuff (DEC), mimicking the potential effect of drug eluting stents. Local delivery of dexamethason via DEC delivery inhibited neointima formation drastically without systemic side effects, indicating a beneficial effect of local suppression of inflammation over systemic delivery as was tested by applying dexamethason via the drinking water in the same model. However pathobiological examination of the murine arteries revealed a dose-dependent medial atrophy, a reduction in vascular smooth muscle cells and collagen content, an increase in apoptotic cell count and disruption of the internal elastic lamina²⁹. Short term systemic delivery in a model for vein graft remodeling showed a reduction in intimal hyperplasia formation without serious side effects probably due to the short period of delivery³⁰. These results not only emphasize the importance of the immune system and the role of inflammation in restenosis more specifically and systematically, but also show that the use of small (hypercholesterolemic) animal models does have predictive value in regard to negative side effects on vascular pathology after local drug application.

Innate immunity

Innate immunity is very important in triggering inflammation and can be divided into a humoral and a cellular component. It comprises multiple cell types, receptors and mechanisms such as the Complement system and Toll like receptors (TLRs) that are very important in host defense. The innate immune system is considered to be highly involved in regulation of intimal hyperplasia and atherogenesis. This could very elegantly be demonstrated using specific mouse models in combination with cuff placement or vein grafting as described in the section below.

Complement

The complement system comprises the humoral mechanism of the innate immune system. C3 cleavage plays a central role in the complex regulation of complement activation and can be initiated via the classical, alternative or the lectin pathway. The role of complement was studied in the model of vein graft restenosis combined with accelerated atherosclerosis in the ApoE3*Leiden mouse. The expression of complement components C1q, C3, and the regulatory proteins CD59 and complement receptor-related gene γ (Crry) could be detected on the protein and mRNA level in the grafts. A reduction in vein graft thickening and intimal hyperplasia was accomplished after interference with C3 activation by systemic administration of either Cobra Venom Factor or Crry-Ig protein. The latter was associated with a reduced number of inflammatory cells in the vessel wall³¹, indicating that blocking the central factor in the complement activation cascade, C3, results in a profound reduction of vascular remodeling. This underscores a role of the innate immune system in restenosis related vascular remodeling.

Toll-like Receptors

TLRs are membrane bound receptors located on a variety of immune and non-immune cells including macrophages, endothelium and SMCs. Cell stress and tissue damage may cause a release of Damage Associated Molecular Patterns (DAMPs) that function as endogenous TLR ligands. Balloon inflation and stent placement or bypass grafting lead to injury to the vessel wall and may cause up regulation of DAMPs such as Heat Shock Protein 60 (HSP60), Fibronectin-EDA, Tenascin C and Biglycan. HSP60 binds directly to TLR2 or TLR4 thereby initiating proliferation of VSMC³². In response to peri-adventitial cuff induced injury TLR4 expression is up regulated in the vessel wall during at least 7 days (unpublished data). A causal role for TLR4 in restenosis was demonstrated by a reduced cuff induced neointima formation in TLR4 deficient mice³³. Moreover, local adventitial TLR4 activation by LPS application strongly augmented neointima formation in both mouse models, so with and without involvement of accelerated atherosclerosis³⁴. The same method was used to stimulate TLR2 with Pam3Cys and resulted in an increase in neointima formation in C57/B6 mice and in APOE^{-/-} mice that develop atherosclerotic lesions³⁵.

We believe that the release upon vascular injury of specific DAMPs as endogenous TLR ligands is one of the earliest triggers in vascular remodeling in restenosis and are convinced that the TLR signaling pathway has a crucial function in the restenosis process. This is supported by the SNPs found in the TLR4 gene that correlate with an increased risk for cardiovascular event and/or restenosis after an initial PCI³⁶⁻³⁸

Cytokines

Activation of the immune system results in secretion of multiple pro and anti-inflammatory



cytokines. These cytokines can be seen as hormones of the immune system that communicate, can attract and activate different cell types importantly involved in restenosis and atherosclerosis like SMC and macrophages. A disturbance in the cytokine balance, locally or systemically, alters the inflammatory status thereby mediating inflammatory processes. Since many cytokines have their role in multiple inflammatory reactions it is important to know whether they are involved, can be a therapeutic target or may function as biomarker for the process of restenosis.

TNF α

Tumor Necrosis Factor alpha (TNF α) is a cytokine that regulates immune cells and promotes the inflammatory response. It is produced by many cells including endothelial cells, VSMCs and macrophages. The GENDER project systematically genotyped for six polymorphisms in the TNF α gene and found associations with an increased clinical and angiographic risk for restenosis in humans³⁹. In a rat balloon-injury model blockade of the TNF α caused a reduction in neointima formation via acceleration of endothelium repair⁴⁰. In mice, after common carotid artery (CCA) ligation, TNF α mRNA expression was found in intimal lesions itself. Application of the same model in knockout mice showed a decrease in lesion size⁴¹. After peri-adventitial cuff placement TNF α mRNA is rapidly up regulated to levels 4000 times to original mRNA levels and deficiency of TNF α in a murine study of restenosis with accelerated atherosclerosis, performed in ApoE*3-Leiden-TNFalpha knockout mice, caused a marked reduction in neointima formation. Interestingly, the use of a DEC for local delivery of thalidomide as a potent TNFalpha biosynthesis inhibitor demonstrated a powerful reduction of the neointima formation after cuff placement to levels similar to those observed in the ApoE*3-Leiden-TNFalpha knockout model³⁹. TNFalpha is clearly an important cytokine in the inflammatory process that take place in the vessel wall during restenosis and its role can be studied in detail using the specific mouse models for restenosis, cuff and drug eluting cuff placement.

CCR2/MCP1

The chemokine Monocyte Chemoattractant Protein1 (MCP1) or CCL2 is a cytokine that is capable of attracting immune cell types like monocytes that are known to infiltrate the vessel wall as a one of the first in neointima formation. Furthermore MCP1 influences SMC proliferation and is expressed in various stages of vascular remodeling. MCP1 binds to its receptor CC chemokine receptor 2 (CCR2) that belongs to the family of G-coupled receptors. Femoral artery transluminal injury by passage of a 0.25-mm diameter angioplasty guide wire was done in a CCR2^{-/-} mice⁷. Four weeks after injury, CCR2^{-/-} mice showed a 61.4% reduction in neointima formation and a 62% reduction in intima/media ratio. The effects of MCP1 in vivo were studied in the murine vein graft model as well as in the femoral cuff model. Systemic overexpression of a dominant negative form of MCP-1, 7ND-MCP, by electroporation of a plasmid into the calf muscle resulted in circulating levels of this MCP-1 inhibitor that were sufficient to decrease intimal hyperplasia significantly, both in the cuff model⁴² as well as in the vein graft model⁴³.

In addition, in the mouse vein graft restenosis model perivascular local vector application for lentiviral shRNA targeting CCR2 reduced intimal hyperplasia in the vein grafts by approximately 50%⁴⁴. These studies demonstrate the role of these models in evaluation of experimental therapeutic strategies.

Interleukin 10

Interleukin 10 (IL-10) is one of the most prominent anti-inflammatory cytokines and functions pleiotropic. It may suppress antigen presentation and is capable of inhibiting pro-inflammatory cytokine production. These capacities make IL-10 a very attractive candidate for anti restenotic and anti atherosclerotic therapy. Three polymorphisms significantly increased the risk of restenosis in patients and demonstrate that IL-10 is associated with restenosis. This set interest for anti-inflammatory genes to be involved in the development of restenosis⁴⁵. The functional role of IL-10 in restenosis was assessed by Feldman et al.⁴⁶ and showed beneficial effects of recombinant human IL-10 after balloon angioplasty or stenting in hypercholesterolemic rabbits. Per-adventitial cuff placement in hypercholesterolemic APOE*3-Leiden-IL-10^{-/-} mice (hypercholesterolemic mice deficient for IL-10) resulted in an increased neointima formation indicating a protective role for IL-10 in a murine model for restenosis and accelerated atherosclerosis⁴⁷. Electroporation of an IL-10 plasmid into the calf muscle resulted in IL-10 overexpression in ApoE3*Leiden mice and caused a reduction in cholesterol and neointima formation two weeks after cuff placement, underscoring the therapeutic potential of IL10 in restenosis.

Protease inhibition in restenosis

Proteases of the Matrix metalloproteinase (MMP) system and of the plasminogen activator system are thought to play an important role in the matrix degradation and smooth muscle cell migration during vascular remodeling and are upregulated after coronary angioplasty⁴⁸. Studies in mice showed a decreased neointima formation in MMP2^{-/-}, MMP9^{-/-} mice and augmented neointima formation in TIMP1^{-/-} mice⁴⁹⁻⁵¹. By use of the electrocoagulation vascular injury model Lijnen et al.⁵² studied whether the plasminogen activation system, a system that also may activate the MMP system, and the MMP system itself play a role in neointima formation using knockout mice. Neointima formation was reduced in urokinase-type plasminogen activator knockout (uPA^{-/-}) and Plasminogen (Plg) knockouts (Plg^{-/-}) but no effect was seen in the tissue-type Plg activator knockout (tPA^{-/-}) mice.

To study the therapeutic potential of these findings a hybrid protein consisting of the receptor-binding amino-terminal fragment of uPA (ATF), linked to the potent protease inhibitor bovine pancreas trypsin inhibitor (BPTI) was constructed and cloned into an adenoviral vector⁵³. Mice were infected with the combined ATF.BPTI vector or single vectors for ATF or BPTI and cuffs were placed around the femoral arteries to induce neointima formation. Only the ATF.BPTI showed a strong inhibition of neointima formation by selective binding to the uPA receptor and inhibiting plasmin activity⁵⁴. Infection with the same vector in a balloon injury model also showed significant inhibition of neointima formation in rats⁵⁵ as well as in mice after cuff placement⁵³. In 2002 a novel hybrid protein consisting of the tissue inhibitor of metalloproteinase-1 (TIMP-1) domain, as MMP inhibitor, linked to ATF (TIMP-1.ATF) was constructed. By binding to the u-PA receptor this protein blocks binding of u-PA and attaches TIMP-1 directly to the cell surface. This construct was able to inhibit SMC migration and neointima formation *in vitro*⁵⁶. *In vivo* intimal hyperplasia combined with accelerated atherosclerosis was studied in murine vein grafts. Plasmids encoding ATF, TIMP-1, TIMP-1.ATF, were injected and electroporated (non-viral gene transfer) in both calf muscles of hypercholesterolemic ApoE*3Leiden mice. Although all constructs reduced vein graft thickening compared with the controls, the luminal area was best preserved in the TIMP-1.ATF-treated mice⁵⁷.

Finally a non-viral expression vector encoding the hybrid protein TIMP-1.ATF.BPTI (TAB)



was constructed and validated. After four weeks, vein graft thickening was significantly inhibited in mice treated with the single domains TIMP-1, ATF or BPTI. In the TAB treated mice vein graft thickening was reduced and was also significantly stronger as compared to the individual domains⁵⁸.

Conclusions

For restenosis research animal models are definitely essential for testing new anti-restenosis devices, such as new drug eluting stent, as well as for unraveling the underlying pathophysiological mechanism and identifying new therapeutic targets.

It is important to work with models that mimic the human situation as good as possible, either in vascular anatomical aspects (size, diameter, wall thickness) or disease stage related aspects (hypercholesterolemia, vessel with atherosclerotic lesions).

In the current chapter we have focused on the later group of animal models, those humanized models that have the best predictive value for the pathophysiological process in the development of restenosis, intimal hyperplasia and accelerated atherosclerosis in the lesions. Various vascular interventions in transgenic mouse models have been described, with a strong focus on the mouse femoral artery cuff model and these mouse models have proven to be technically suitable for the study into restenosis development.

Next, to study effects of (local) drug therapy, animals should be susceptible to the treatment of interest, have similar metabolic levels, coagulatory phenotype and react in a human-like fashion. The use of humanized (transgenic) animal models has extensively increased the similarity between human and animal lesions and the translation of new therapies into in the clinical setting.

Mechanistic and pathophysiological studies have shown that local vessel wall inflammation, proliferation and proteolysis play important roles in the post-interventional vascular remodeling, both in humans and in the animal models used.

In addition, these animal models are extremely suitable to identify new potential therapeutic targets to prevent restenosis and test new experimental strategies for therapy, e.g. based on systemic or local gene delivery of inhibitory factors (anti-proliferative, anti-inflammatory or anti-proteolytic). These studies clearly demonstrate the importance and value of animal models for clinical medicine.

We can conclude that highly-reproducible animal models for post-interventional vascular remodeling remain essential for studying the process of restenosis and the development of future anti-restenotic therapies.

1. Pires NM, Jukema JW, Daemen MJ, Quax PH. *Drug-eluting stents studies in mice: do we need atherosclerosis to study restenosis?* *Vascul Pharmacol* 2006 May;44(5):257-64.
2. Landau C, Lange RA, Hillis LD. *Percutaneous transluminal coronary angioplasty.* *N Engl J Med* 1994 April 7;330(14):981-93.
3. Mehilli J, Kastrati A, Bollwein H, Dibra A, Schuhlen H, Dirschinger J, Schomig A. *Gender and restenosis after coronary artery stenting.* *Eur Heart J* 2003 August;24(16):1523-30.
4. Clowes AW, Reidy MA, Clowes MM. *Mechanisms of stenosis after arterial injury.* *Lab Invest* 1983 August;49(2):208-15.
5. Ohlstein EH, Douglas SA, Sung CP, Yue TL, Loudon C, Arleth A, Poste G, Ruffolo RR, Jr., Feuerstein GZ. *Carvedilol, a cardiovascular drug, prevents vascular smooth muscle cell proliferation, migration, and neointimal formation following vascular injury.* *Proc Natl Acad Sci U S A* 1993 July 1;90(13):6189-93.
6. Kumar A, Lindner V. *Remodeling with neointima formation in the mouse carotid artery after cessation of*

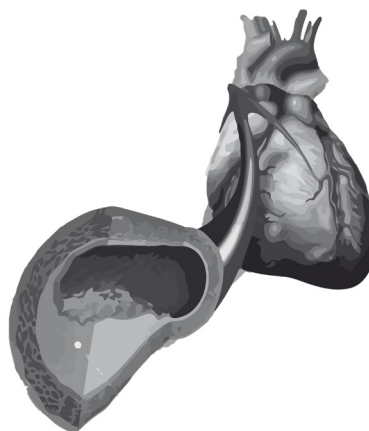
- blood flow*. *Arterioscler Thromb Vasc Biol* 1997 October;17(10):2238-44.
7. Roque M, Kim WJ, Gazdoin M, Malik A, Reis ED, Fallon JT, Badimon JJ, Charo IF, Taubman MB. *CCR2 deficiency decreases intimal hyperplasia after arterial injury*. *Arterioscler Thromb Vasc Biol* 2002 April 1;22(4):554-9.
 8. Carmeliet P, Moons L, Stassen JM, De MM, Bouche A, van den Oord JJ, Kockx M, Collen D. *Vascular wound healing and neointima formation induced by perivascular electric injury in mice*. *Am J Pathol* 1997 February;150(2):761-76.
 9. Kikuchi S, Umemura K, Kondo K, Saniabadi AR, Nakashima M. *Photochemically induced endothelial injury in the mouse as a screening model for inhibitors of vascular intimal thickening*. *Arterioscler Thromb Vasc Biol* 1998 July;18(7):1069-78.
 10. Zhu Y, Farrehi PM, Fay WP. *Plasminogen activator inhibitor type 1 enhances neointima formation after oxidative vascular injury in atherosclerosis-prone mice*. *Circulation* 2001 June 26;103(25):3105-10.
 11. Lardenoye JH, de Vries MR, Lowik CW, Xu Q, Dhore CR, Cleutjens JP, van Hinsbergh VW, van Bockel JH, Quax PH. *Accelerated atherosclerosis and calcification in vein grafts: a study in APOE*3 Leiden transgenic mice*. *Circ Res* 2002 October 4;91(7):577-84.
 12. Kwak BR, Veillard N, Pelli G, Mulhaupt F, James RW, Chanson M, Mach F. *Reduced connexin43 expression inhibits atherosclerotic lesion formation in low-density lipoprotein receptor-deficient mice*. *Circulation* 2003 February 25;107(7):1033-9.
 13. Ali ZA, Alp NJ, Lupton H, Arnold N, Bannister T, Hu Y, Mussa S, Wheatcroft M, Greaves DR, Gunn J, Channon KM. *Increased in-stent stenosis in ApoE knockout mice: insights from a novel mouse model of balloon angioplasty and stenting*. *Arterioscler Thromb Vasc Biol* 2007 April;27(4):833-40.
 14. Booth RF, Martin JF, Honey AC, Hassall DG, Beesley JE, Moncada S. *Rapid development of atherosclerotic lesions in the rabbit carotid artery induced by perivascular manipulation*. *Atherosclerosis* 1989 April;76(2-3):257-68.
 15. Lardenoye JH, Delsing DJ, de Vries MR, Deckers MM, Princen HM, Havekes LM, van Hinsbergh VW, van Bockel JH, Quax PH. *Accelerated atherosclerosis by placement of a perivascular cuff and a cholesterol-rich diet in ApoE*3Leiden transgenic mice*. *Circ Res* 2000 August 4;87(3):248-53.
 16. Monraats PS, Pires NM, Agema WR, Zwinderman AH, Schepers A, de Maat MP, Doevendans PA, de Winter RJ, Tio RA, Waltenberger J, Frants RR, Quax PH, van Vlijmen BJ, Atsma DE, van der Laarse A, van der Wall EE, Jukema JW. *Genetic inflammatory factors predict restenosis after percutaneous coronary interventions*. *Circulation* 2005 October 18;112(16):2417-25.
 17. Pires NM, van der Hoeven BL, de Vries MR, Havekes LM, van Vlijmen BJ, Hennink WE, Quax PH, Jukema JW. *Local perivascular delivery of anti-restenotic agents from a drug-eluting poly(epsilon-caprolactone) stent cuff*. *Biomaterials* 2005 September;26(26):5386-94.
 18. Hansson GK. *Inflammation, atherosclerosis, and coronary artery disease*. *N Engl J Med* 2005 April 21;352(16):1685-95.
 19. Krom YD, Pires NM, Jukema JW, de Vries MR, Frants RR, Havekes LM, van Dijk KW, Quax PH. *Inhibition of neointima formation by local delivery of estrogen receptor alpha and beta specific agonists*. *Cardiovasc Res* 2007 January 1;73(1):217-26.
 20. Zadelaar S, Kleemann R, Verschuren L, de Vries-Van der Weij, van der Hoorn J, Princen HM, Kooistra T. *Mouse models for atherosclerosis and pharmaceutical modifiers*. *Arterioscler Thromb Vasc Biol* 2007 August;27(8):1706-21.
 21. Havekes L, de WE, Leuven JG, Klasen E, Utermann G, Weber W, Beisiegel U. *Apolipoprotein E3-Leiden. A new variant of human apolipoprotein E associated with familial type III hyperlipoproteinemia*. *Hum Genet* 1986 June;73(2):157-63.
 22. van den Maagdenberg AM, de KP, Stalenhoef AF, Gevers Leuven JA, Havekes LM, Frants RR. *Apolipoprotein E*3-Leiden allele results from a partial gene duplication in exon 4*. *Biochem Biophys Res*

- Commun 1989 December 15;165(2):851-7.
23. Gallo R, Padurean A, Jayaraman T, Marx S, Roque M, Adelman S, Chesebro J, Fallon J, Fuster V, Marks A, Badimon JJ. *Inhibition of intimal thickening after balloon angioplasty in porcine coronary arteries by targeting regulators of the cell cycle.* Circulation 1999 April 27;99(16):2164-70.
 24. Marx SO, Jayaraman T, Go LO, Marks AR. *Rapamycin-FKBP inhibits cell cycle regulators of proliferation in vascular smooth muscle cells.* Circ Res 1995 March;76(3):412-7.
 25. Poon M, Marx SO, Gallo R, Badimon JJ, Taubman MB, Marks AR. *Rapamycin inhibits vascular smooth muscle cell migration.* J Clin Invest 1996 November 15;98(10):2277-83.
 26. Gershlick A, De S, I, Chevalier B, Stephens-Lloyd A, Camenzind E, Vrints C, Reifart N, Missault L, Goy JJ, Brinker JA, Raizner AE, Urban P, Heldman AW. *Inhibition of restenosis with a paclitaxel-eluting, polymer-free coronary stent: the European evaluation of paclitaxel eluting stent (ELUTES) trial.* Circulation 2004 February 3;109(4):487-93.
 27. Grube E, Silber S, Hauptmann KE, Mueller R, Buellesfeld L, Gerckens U, Russell ME. *TAXUS I: six- and twelve-month results from a randomized, double-blind trial on a slow-release paclitaxel-eluting stent for de novo coronary lesions.* Circulation 2003 January 7;107(1):38-42.
 28. Park SJ, Shim WH, Ho DS, Raizner AE, Park SW, Hong MK, Lee CW, Choi D, Jang Y, Lam R, Weissman NJ, Mintz GS. *A paclitaxel-eluting stent for the prevention of coronary restenosis.* N Engl J Med 2003 April 17;348(16):1537-45.
 29. Pires NM, Schepers A, van der Hoeven BL, de Vries MR, Boesten LS, Jukema JW, Quax PH. *Histopathologic alterations following local delivery of dexamethasone to inhibit restenosis in murine arteries.* Cardiovasc Res 2005 December 1;68(3):415-24.
 30. Schepers A, Pires NM, Eefting D, de Vries MR, van Bockel JH, Quax PH. *Short-term dexamethasone treatment inhibits vein graft thickening in hypercholesterolemic ApoE3Leiden transgenic mice.* J Vasc Surg 2006 April;43(4):809-15.
 31. Schepers A, de Vries MR, van Leuven CJ, Grimbergen JM, Holers VM, Daha MR, van Bockel JH, Quax PH. *Inhibition of complement component C3 reduces vein graft atherosclerosis in apolipoprotein E3-Leiden transgenic mice.* Circulation 2006 December 19;114(25):2831-8.
 32. de Graaf R, Kloppenburg G, Kitslaar PJ, Bruggeman CA, Stassen F. *Human heat shock protein 60 stimulates vascular smooth muscle cell proliferation through Toll-like receptors 2 and 4.* Microbes Infect 2006 June;8(7):1859-65.
 33. Vink A, Schoneveld AH, van der Meer JJ, Van Middelaar BJ, Sluijter JP, Smeets MB, Quax PH, Lim SK, Borst C, Pasterkamp G, de Kleijn DP. *In vivo evidence for a role of toll-like receptor 4 in the development of intimal lesions.* Circulation 2002 October 8;106(15):1985-90.
 34. Hollestelle SC, de Vries MR, van Keulen JK, Schoneveld AH, Vink A, Strijder CF, Van Middelaar BJ, Pasterkamp G, Quax PH, de Kleijn DP. *Toll-like receptor 4 is involved in outward arterial remodeling.* Circulation 2004 January 27;109(3):393-8.
 35. Schoneveld AH, Oude Nijhuis MM, van MB, Laman JD, de Kleijn DP, Pasterkamp G. *Toll-like receptor 2 stimulation induces intimal hyperplasia and atherosclerotic lesion development.* Cardiovasc Res 2005 April 1;66(1):162-9.
 36. Boekholdt SM, Agema WR, Peters RJ, Zwinderman AH, van der Wall EE, Reitsma PH, Kastelein JJ, Jukema JW. *Variants of toll-like receptor 4 modify the efficacy of statin therapy and the risk of cardiovascular events.* Circulation 2003 May 20;107(19):2416-21.
 37. Hamann L, Gomma A, Schroder NW, Stamme C, Glaeser C, Schulz S, Gross M, Anker SD, Fox K, Schumann RR. *A frequent toll-like receptor (TLR)-2 polymorphism is a risk factor for coronary restenosis.* J Mol Med 2005 June;83(6):478-85.
 38. Kiechl S, Lorenz E, Reindl M, Wiedermann CJ, Oberhollenzer F, Bonora E, Willeit J, Schwartz DA. *Toll-like receptor 4 polymorphisms and atherogenesis.* N Engl J Med 2002 July 18;347(3):185-92.

39. Monraats PS, Pires NM, Schepers A, Agema WR, Boesten LS, de Vries MR, Zwiderman AH, de Maat MP, Doevendans PA, de Winter RJ, Tio RA, Waltenberger J, 't Hart LM, Frants RR, Quax PH, van Vlijmen BJ, Havekes LM, van der Laarse A, van der Wall EE, Jukema JW. *Tumor necrosis factor-alpha plays an important role in restenosis development*. FASEB J 2005 December;19(14):1998-2004.
40. Krasinski K, Spyridopoulos I, Kearney M, Losordo DW. *In vivo blockade of tumor necrosis factor-alpha accelerates functional endothelial recovery after balloon angioplasty*. Circulation 2001 October 9;104(15):1754-6.
41. Rectenwald JE, Moldawer LL, Huber TS, Seeger JM, Ozaki CK. *Direct evidence for cytokine involvement in neointimal hyperplasia*. Circulation 2000 October 3;102(14):1697-702.
42. Egashira K, Zhao Q, Kataoka C, Ohtani K, Usui M, Charo IF, Nishida K, Inoue S, Katoh M, Ichiki T, Takeshita A. *Importance of monocyte chemoattractant protein-1 pathway in neointimal hyperplasia after periarterial injury in mice and monkeys*. Circ Res 2002 June 14;90(11):1167-72.
43. Schepers A, Eefting D, Bonta PI, Grimbergen JM, de Vries MR, van W, V, de Vries CJ, Egashira K, van Bockel JH, Quax PH. *Anti-MCP-1 gene therapy inhibits vascular smooth muscle cells proliferation and attenuates vein graft thickening both in vitro and in vivo*. Arterioscler Thromb Vasc Biol 2006 September;26(9):2063-9.
44. Eefting D, Bot I, de Vries MR, Schepers A, van Bockel JH, van Berkel TJ, Biessen EA, Quax PH. *Local lentiviral short hairpin RNA silencing of CCR2 inhibits vein graft thickening in hypercholesterolemic apolipoprotein E3-Leiden mice*. J Vasc Surg 2009 July;50(1):152-60.
45. Monraats PS, Kurreeman FA, Pons D, Sewgobind VD, de Vries FR, Zwiderman AH, de Maat MP, Doevendans PA, de Winter RJ, Tio RA, Waltenberger J, Huizinga TW, Eefting D, Quax PH, Frants RR, van der Laarse A, van der Wall EE, Jukema JW. *Interleukin 10: a new risk marker for the development of restenosis after percutaneous coronary intervention*. Genes Immun 2007 January;8(1):44-50.
46. Feldman LJ, Aguirre L, Ziolkowski M, Bridou JP, Nevo N, Michel JB, Steg PG. *Interleukin-10 inhibits intimal hyperplasia after angioplasty or stent implantation in hypercholesterolemic rabbits*. Circulation 2000 February 29;101(8):908-16.
47. Eefting D, Schepers A, de Vries MR, Pires NM, Grimbergen JM, Lagerweij T, Nagelkerken LM, Monraats PS, Jukema JW, van Bockel JH, Quax PH. *The effect of interleukin-10 knock-out and overexpression on neointima formation in hypercholesterolemic APOE*3-Leiden mice*. Atherosclerosis 2007 August;193(2):335-42.
48. Hojo Y, Ikeda U, Katsuki T, Mizuno O, Fujikawa H, Shimada K. *Matrix metalloproteinase expression in the coronary circulation induced by coronary angioplasty*. Atherosclerosis 2002 March;161(1):185-92.
49. Galis ZS, Johnson C, Godin D, Magid R, Shipley JM, Senior RM, Ivan E. *Targeted disruption of the matrix metalloproteinase-9 gene impairs smooth muscle cell migration and geometrical arterial remodeling*. Circ Res 2002 November 1;91(9):852-9.
50. Johnson C, Galis ZS. *Matrix metalloproteinase-2 and -9 differentially regulate smooth muscle cell migration and cell-mediated collagen organization*. Arterioscler Thromb Vasc Biol 2004 January;24(1):54-60.
51. Lijnen HR, Soloway P, Collen D. *Tissue inhibitor of matrix metalloproteinases-1 impairs arterial neointima formation after vascular injury in mice*. Circ Res 1999 December 3;85(12):1186-91.
52. Lijnen HR, Van HB, Lupu F, Moons L, Carmeliet P, Collen D. *Function of the plasminogen/plasmin and matrix metalloproteinase systems after vascular injury in mice with targeted inactivation of fibrinolytic system genes*. Arterioscler Thromb Vasc Biol 1998 July;18(7):1035-45.
53. Quax PH, Lamfers ML, Lardenoye JH, Grimbergen JM, de Vries MR, Slomp J, de Ruiter MC, Kockx MM, Verheijen JH, van Hinsbergh VW. *Adenoviral expression of a urokinase receptor-targeted protease inhibitor inhibits neointima formation in murine and human blood vessels*. Circulation 2001 January 30;103(4):562-9.
54. Lamfers ML, Wijnberg MJ, Grimbergen JM, Huisman LG, Aalders MC, Cohen FN, Verheijen JH, van

- Hinsbergh VW, Quax PH. *Adenoviral gene transfer of a u-PA receptor-binding plasmin inhibitor and green fluorescent protein: inhibition of migration and visualization of expression*. *Thromb Haemost* 2000 September;84(3):460-7.
55. Lamfers ML, Lardenoye JH, de Vries MR, Aalders MC, Engelse MA, Grimbergen JM, van Hinsbergh VW, Quax PH. *In vivo suppression of restenosis in balloon-injured rat carotid artery by adenovirus-mediated gene transfer of the cell surface-directed plasmin inhibitor ATF.BPTI*. *Gene Ther* 2001 April;8(7):534-41.
56. Lamfers ML, Grimbergen JM, Aalders MC, Havenga MJ, de Vries MR, Huisman LG, van Hinsbergh VW, Quax PH. *Gene transfer of the urokinase-type plasminogen activator receptor-targeted matrix metalloproteinase inhibitor TIMP-1.ATF suppresses neointima formation more efficiently than tissue inhibitor of metalloproteinase-1*. *Circ Res* 2002 November 15;91(10):945-52.
57. Eefting D, de Vries MR, Grimbergen JM, Karper JC, van Bockel JH, Quax PH. *In vivo suppression of vein graft disease by nonviral, electroporation-mediated, gene transfer of tissue inhibitor of metalloproteinase-1 linked to the amino terminal fragment of urokinase (TIMP-1.ATF), a cell-surface directed matrix metalloproteinase inhibitor*. *J Vasc Surg* 2010 February;51(2):429-37.
58. Eefting D, Seghers L, Grimbergen JM, de Vries MR, de Boer HC, Lardenoye JW, Jukema JW, van Bockel JH, Quax PH. *A novel urokinase receptor-targeted inhibitor for plasmin and matrix metalloproteinases suppresses vein graft disease*. *Cardiovasc Res* 2010 July 23.

CHAPTER 3



Future potential biomarkers for postinterventional restenosis and accelerated atherosclerosis.

Karper JC, Ewing MM*, Jukema JW, Quax PH.*

** both authors contributed equally*

Biomark Med. 2012;6:53-66.

Abstract

New circulating and local arterial biomarkers may help the clinician with risk stratification or diagnostic assessment of patients and selecting the proper therapy for a patient. Additionally they may be used for follow-up and testing efficacy of therapy, which is not provided by current biomarkers. Processes leading to post-interventional restenosis and accelerated atherosclerosis are complex due to many biological variables mediating the specific inflammatory and immunogenic responses involved. Adequate assessment of these processes requires different and more specific biomarkers. Post-interventional remodeling is associated with cell stress and tissue damage causing apoptosis, release of damage-associated molecular patterns (DAMPs) and upregulation of specific cyto/chemokines that could serve as suitable clinical biomarkers. Furthermore, plasma titers of pathophysiological process-related (auto) antibodies could aid in the identification of restenosis risk or lesion severity. This review provides an overview of a number of potential biomarkers selected on the basis of their role in the remodeling process.

Key-words

Atherosclerosis; inflammation; damage associated molecular patterns; innate immunity



Introduction

The current concept that inflammation plays a key role in the development of (post-interventional) atherosclerotic vascular remodeling has led to the investigation of inflammatory factors to serve as biomarkers for cardiovascular risk prediction. Multiple local arterial and blood-based biomarkers have been identified and selected for their association with a more adverse cardiovascular risk profile independently of known traditional risk factors such as dyslipidemia, hypertension, diabetes and smoking. Many of these markers have been incorporated into risk prediction models to improve risk assessment accuracy in addition to current diagnostic strategies [1]. Of these, C-reactive protein (CRP) is currently the best-validated inflammatory biomarker. Despite the value of plasma lipoprotein profiling and CRP measurements the picture is not yet clear. Many patients but not all continue to develop vascular remodeling following revascularization procedures and ongoing investigations into newer and more accurate or combined biomarker risk profiles remain necessary[2]. This review retracts the underlying pathophysiology of atherosclerosis and post-interventional vascular remodeling and the value of recently discovered inflammatory biomarkers[3] in the prediction of cardiovascular events in the biological context that require target lesion revascularization, highlighting their potential clinical value. Other biomarkers including genetic differences such as polymorphisms are not taken into account in this review.

Background of atherosclerosis and restenosis

Native atherosclerosis

Atherosclerosis is a chronic inflammatory disease of the large and medium-sized arteries and is initiated by a qualitative change in the endothelial monolayer by irritative stimuli such as dyslipidemia, hypertension, and pro-inflammatory mediators that lead to the exposure of adhesion molecules and infiltration of circulating leukocytes into the arterial wall[4]. Such mediators could be of high value when measured as biomarkers of lesion progression and stage of severity. Changes in endothelial permeability provoke the retention of cholesterol-containing low-density lipoprotein (LDL) particles that are endocytosed by monocytes-derived macrophages leading to foam cell and atheromatous lesion formation in the arterial tree(5, 6). Tunica media-derived smooth muscle cell (SMC) migration and proliferation and extracellular matrix deposition lead to the formation of a fibrous cap overlying a necrotic core due to inefficient efferocytosis[5, 7]. Physical disruption of the plaque exposes the underlying thrombogenic material to the circulation triggering thrombosis formation, that may be monitored as biomarkers, and luminal occlusion with progressing ischemia in distal tissues[6], eventually leading to infarction requiring angioplasty or bypass-grafting[6, 8].

Post-interventional restenosis

Restenosis following angioplasty and stent implantation has been the major problem limiting the success rate of coronary interventions and tremendous efforts have been made to target this problem[9]. Acute and long-term vessel occlusion requiring target lesion revascularization following balloon angioplasty occurred in 30-60% of all patients due to elastic recoil and negative remodeling. The introduction of bare-metal stents (BMS) prevented elastic recoil and has reduced this incidence of restenosis to 16-44%, but also led to the development of neointimal hyperplasia[10]. Drug-eluting stents (DES) have been developed to counter this phenomenon, although incidence rates of 5-10% of in-stent restenosis (ISR) are still reported, encompassing over 200.000 revascularizations annually in the United States alone[11].

Inflammation has been shown to be the driving factor behind these remodeling processes, pointing to a role as biomarker for this factor in the analysis of disease progression. DES have been successful in the prevention of neointimal hyperplasia, but have not been able to completely prevent the process of ISR. These figures support the need for development of new biomarker assays that allow careful screening of patients at risk for restenosis. Restenosis is defined as more than 50% luminal loss at follow-up angiography with clinical restenosis defined as recurrence of symptoms such as angina pectoris or ischemia at rest, requiring repeat revascularization[12]. It has been proposed to be the result of an overshooting healing response that originally occurred in three distinctive phases: early loss due to elastic recoil, which occurs within minutes and has been successfully countered by the application of intracoronary stenting, followed by neointimal hyperplasia and eventually accelerated atherosclerosis development[13]. Neointimal hyperplasia is evoked by injury to the endothelium and underlying atherosclerotic plaque, with exposure of thrombogenic content to flowing blood, supporting the adhesion and activation of thrombocytes and thrombosis. Platelets release mitogens, which can be traced throughout the plasma to serve as biological markers of thrombosis extent, and promote SMC migration and proliferation to the tunica intima with local extracellular matrix deposition[14]. This process is prevented or delayed (e.g. by many years) by DES compared to BMS implantation through the release of drugs that affect SMC migration and proliferation. This process is ultimately followed by a phase of vascular remodeling, in which accelerated atherosclerosis and concentric adventitial compression together further comprise lumen patency[13].

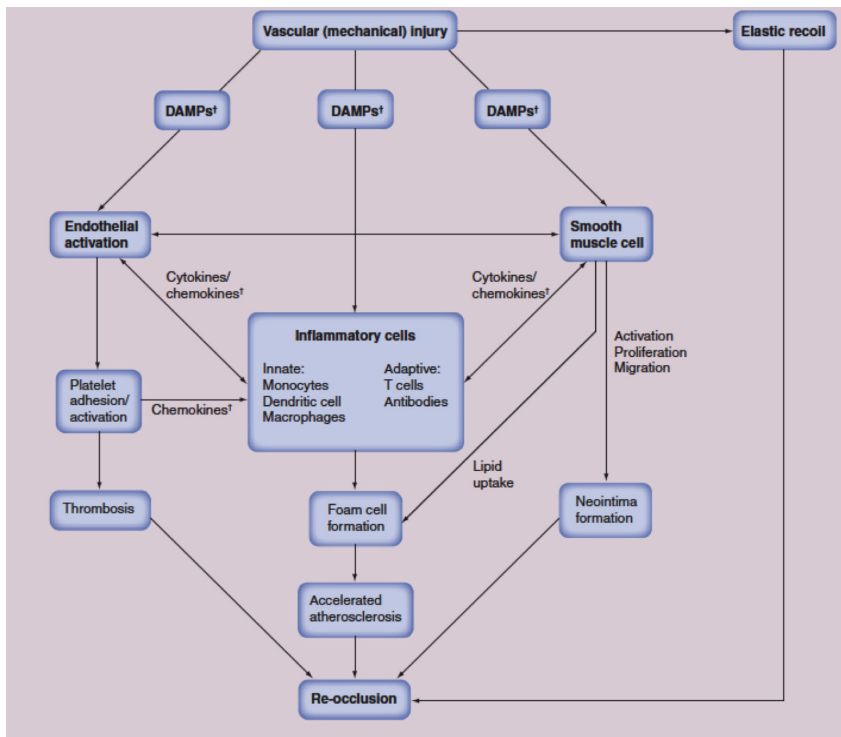


Figure 1. The complex interactions between various cell types that are involved in vascular remodeling, activating processes and factors modulating vascular remodeling. All these factors and processes may provide new biomarkers.

†Potential future biomarkers.

DAMP: Damage-associated molecular pattern.



Underlying causes of restenosis

The underlying causes of restenosis can be divided into four general causes, namely biological, arterial, stent and implantation factors[10, 12]. Biological factors encompass the natural (genetic) vascular wall resistance to anti-proliferative drugs and the development of a sustained hypersensitivity reaction directed towards the polymer or metallic stent platform. Additionally, the initial levels of proteinases that determine SMC proliferation and migration are of great importance to treatment success[10]. These effects of proteinase of SMC proliferation and migration may be direct or indirect effects. In vascular remodeling matrix metalloproteinases may regulate migration, proliferation, and death of vascular smooth muscle cells by degrading matrix and non-matrix substrates[15], but also may play a role in activating other factors such as growth factor or other pericellular proteases[16]. Arterial factors that influence the vascular response are comprised of factor regulated by local wall shear stress levels, the progression of original atherosclerosis lesions growth within a stented segment, but also previous positive vascular remodeling. Stent factors that contribute to the development of ISR are the specific type of coating used, drug concentration and sustained period of release and to a lesser extent the drug of choice[17, 18]. Differences between effectiveness rates of specific drugs are determined by their ability to meet the biological threshold that exists and determines the initiation of an inflammatory response and the eventual occurrence of neointimal hyperplasia, which could be tracked with biomarker levels in plasma[10]. The stent gap, strut thickness and possible polymer disruption or cracking and eventual fractures are all important for proper stent effectiveness in the prevention of ISR[10]. Finally, technical implantation factors can limit therapeutic effectiveness that stenting could offer, such as an incomplete stent expansion and geographical misses, where the stent is deployed short of or beyond the complete lesion area[12]. During every interventional procedure the eventually of barotrauma to unstented segments and the deployment of a DES in a clot-laden arterial segment remains, that raise the chance of ISR after discontinuation of anti-thrombotic drugs. These factors support the search for biomarkers that could offer diagnostic insight at the time of procedure. These markers should be an adequate reflection of acute vessel injury.

Inflammation status as biomarker

The overall requirement of a cardiovascular disease biomarker is to enhance the ability to optimally manage the patient, identification of patients, to differentiate patients, assess the likelihood of a therapeutic response, the risk of future recurrences and progression of disease[19]. The use of BMS or DES may have different effects on the pathophysiological process initiated and thereby on the inflammatory response and eventual potential biomarkers related to restenosis or in-stent thrombosis. For potential novel biomarkers it would be of major importance to be easily detectable and that levels correlate with disease progression. Since inflammation is importantly involved in vascular disease many studies focused on CRP as a biomarker. CRP is a strong marker of inflammation and upregulated in response to pro-inflammatory cytokines. No association was found for major cardiovascular events and high sensitivity-CRP, IL6 or TNF α by Sukhija and co-workers[20]. However, CRP seemed to be an excellent marker for post-stenting inflammation since it was produced mostly in response to pro-inflammatory cytokines released as a response upon the vascular damage initiated by the procedure(1). In addition pre-procedural serum CRP-level proved to be an independent predictor of adverse outcome after coronary stent implantation, suggesting that a systemically detectable inflammatory activity is associated with proliferative responses within successfully implanted stents[21]. Higher baseline CRP levels of patients undergoing BMS implantation

are a predictor of restenosis[22]. Interactions were also found between CRP levels, statin treatment and restenosis-incidence[23]. No clear association of CRP and restenosis was found during application of drug-eluting stents[1]. A study on first cardiovascular events and death based on the Framingham Offspring Study by Wang and co-workers showed that the most informative circulating biomarkers for predicting death proved to be B-type natriuretic peptide, C-reactive protein, homocysteine, renin, and the urinary albumin-to-creatinin ratio[2]. Other studies focused on CRP levels did not find a direct relation with restenosis[24]. Currently the limitation of existing biomarkers is that even in combination, they only add moderately to the prediction of risk in an individual person[2]. This statement is confirmed by Ware who explains that a risk factor must have a much stronger association with the disease outcome than we ordinarily see in etiologic research if it is to provide a basis for early diagnosis or prediction in individual patients. Most studies are of limited value for the risk stratification of individual patients as we have discovered new biologic variables that lie on the complex pathway leading to chronic disease and death[25]. Therefore the role of experimental research is very important in identifying novel biomarkers since it provides the tools to focus more specifically on the pathophysiological process.

Currently a lot of contradicting data is available of using CRP as a biomarker in cardiovascular disease, a notion merely worsened by the use of different stents types. The approaches thus far may not be specific enough to serve as good reflectors of the pathophysiological process that is initiated by the interventional procedure. CRP is possibly just an indirect reflection of inflammation which is easily become upregulated by other underlying inflammatory processes. The application of individual biomarkers only contributes moderately to risk assessment of individual patients. The prospect of combining multiple known markers could possibly contribute significantly more to the optimization of patient selection and individual tailor-made treatment[1]. The future success of biomarker strategies in this field could possibly depend on the discovery of new biomarkers to complement the current markers and diagnostic strategies. The identification of patients at elevated risk based upon biomarker assessment could be of additive value for the management of patients receiving stent implantation. In this review, we provide an overview of considered novel potential biomarkers in post-interventional atherosclerotic vascular remodeling with the emphasis on inflammation.

Future biomarkers

Circulating Factors

Several factors involved in the pathophysiological process of post-interventional remodeling may be detected in the circulation soon after the interventional damage, thereby forming potential biomarkers that are easily available such as damage-associated molecular patterns (DAMPs). DAMPs are endogenous structures that can be released upon tissue damage and can be recognised by receptors on inflammatory cells e.g. Toll Like Receptors. Balloon angioplasty with or without stent placement will cause damage to the vessel wall that will cause al release of DAMPs and activate toll-like receptors that cause a release of several inflammatory cytokines and chemokines[26, 27]. Also antibodies may be formed upon (auto-) antigens that become present after the intervention. Original papers on this subject are summarized in the citation overview below.



Annexin A5

Annexin A5 is a member of the annexin family, a group of highly-conserved Ca^{2+} dependent proteins that bind to negatively-charged phospholipid surfaces. Annexin A5 is primarily an intracellular protein that is released upon injury and binds specifically and with high affinity to phosphatidylserine (PS) [28]. PS becomes externalized and presented upon the outer cellular membrane during the process of apoptosis, but also during platelet activation and erythrocyte aging[29]. For this reason annexin A5, alone and bound to contrast agents, has been used world-wide for the detection of apoptosis in vitro and in pilot experiments in vivo in patients [28].

PS serves as an 'eat-me' signal on apoptotic cells for circulating phagocytes. Annexin A5 then binds PS leading to the formation two-dimensional crystals. Annexin A5 thereby may act as a lattice shielding PS from phagocytes and from interacting in phospholipid-dependent coagulation reactions[30, 31]. In addition to its anti-thrombogenic properties, annexin A5 binds with high affinity to oxLDL cholesterol which together with apoptotic cells is present in native atherosclerotic and restenotic lesions in high concentrations[32]. For this reason, annexin A5 is also detectable in high concentrations in (accelerated) atherosclerotic lesions[33].

Next to its presence in the vascular wall, annexin A5 has been suggested in the prevention of pro-inflammatory microparticle formation. Stimulated platelets and apoptotic cells expressing PS on their membrane have been shown to shed PS-containing membrane-derived microparticles. Annexin A5 is able to inhibit the formation of microparticles by binding to PS on these cells[30].

Annexin A5 is partially removed from the circulation by binding to specific components of atherosclerotic tissues, such as oxLDL and activated or damaged cells. Measurement of plasma annexin A5 concentration requires only limited amounts of venous blood and is therefore an easy-to-perform diagnostic test. Although this information does not allow discrimination between a restenotic and a de novo atherosclerotic lesion, it could certainly be of much additive value to current diagnostic strategies and screening purposes. In addition, it was found that the prognostic value of the oxLDL / annexin A5 ratio is even more sensitive than annexin A5 alone, stressing the importance of combined biomarkers for disease screening[34].

The presence of high concentrations of annexin A5 in atherosclerotic lesions leads to annexin A5 release in the circulation following myocardial infarction[35]. Increased annexin A5 levels are therefore indicative of the extent of myocardial tissue damage. Since annexin A5 levels provide both information on plaque severity in the stable period of atherosclerosis and on infarction severity during acute episodes of plaque rupture, annexin A5 is a highly potential future biomarker of cardiovascular disease progress.

Damage Associated Molecular Patterns (DAMPs)

Restenosis is a late process, although it is believed that events that take place within 72 hours after intervention are already triggering the restenosis process. The intervention will cause severe damage to the vessel wall leading to a release of DAMPs. DAMPs can be seen as endogenous fragments that are recognized by the immune system by toll-like receptors (TLR) [26]. During the whole process of restenosis a continuous process of cell stress, lipid influx, inflammation and matrix degradation, the release of DAMPs will continue. The last decade much focus has been towards the involvement of TLR in cardiovascular disease where the TLRs were predominantly found on circulating cells and in vascular lesions[36-38]. TLRs are

membrane-bound receptors located on a variety of immune and non-immune cells including macrophages, endothelium, SMCs and platelets. Release of the DAMPS as endogenous TLR ligands may have serious consequences due to the activation of the TLR signalling pathway on variety of cells carrying TLRs. These cells may then initiate a severe inflammatory response with direct activation of the vessel wall but also platelet activation and infiltration of inflammatory cells[26, 39, 40]. A causal role for TLR4 in post-interventional vascular remodeling was previously demonstrated. Neointima formation, arterial outward remodeling as well as vein graft remodelling were decreased by in TLR4 deficient mice, and TLR4 ligands and TLR4 silencing tools could modify these processes[41-43]. Furthermore TLR4 is importantly involved in the sterile inflammatory response upon CD36 activation by oxLDL particles[44]. Two very important DAMPs that can be linked to multiple TLRs are high mobility group box 1 (HMGB1) and fibronectin-EDA (FN-EDA) that also come available in the circulation upon their release. These DAMPS may potentially serve as ideal biomarkers since they are only upregulated in response to tissue damage, have direct inflammatory effects via multiple TLRs and can also be detected in the plasma[27, 49-51].

Nuclear HMGB1 may become present in the cytoplasm or even outside the cell where it is known to act as TLR2 and TLR4 ligand[45, 49]. Not only can this release be initiated upon cell stress but also activated macrophages are capable of releasing HMGB1[26, 49-51]. Previously our group was able to detect intra- and extra-nuclear HMGB1 in remodeled vein grafts[42]. Furthermore presence of HMGB1 was detected in atherosclerotic plaques. Although the number of macrophages increased markedly in fatty streaks and fibrofatty lesions, the proportion that expressed HMGB1 did not alter significantly. However, the proportion of macrophages containing HMGB1 in both cytoplasm and nuclei increased markedly[52]. Others showed that elevation of serum HMGB1 level is associated with severe cardiac remodeling complications such as pump failure, cardiac rupture, and eventually in-hospital cardiac death. This was in association with an increased serum C-reactive protein level in these patients. However, in an animal model for myocardial infarction blockade of HMGB1 caused impaired infarct healing and marked scar thinning thereby worsening left ventricular remodelling[53]. Furthermore, HMGB1 serum levels are markedly increased upon surgical thoracic aortic aneurysm repair[54]. HMGB1 is also of interest in other inflammatory disease processes like SLE and kidney ischemia reperfusion[55, 56]. HMGB1 also has pro-thrombogenic features by increasing tissue factor expression on monocytes and inhibiting anti-coagulant protein C pathway in vitro. In vivo the combined administration of thrombin and HMGB1 caused prolonged plasma clotting times[57]. The effect of HMGB1 on platelets via direct TLR4 activation is still unknown.

Fibronectin is a part of the extracellular matrix that undergoes severe stress during interventional procedures. Fibronectin-EDA (FN-EDA) is an adhesive glycoprotein spliced from fibronectin and is important in wound healing and can be produced by activated endothelium and fibroblasts. FN-EDA has been implicated in fibroblast differentiation, proliferation and migration and is capable of monocytes activation and induction of inflammation through upregulation of cytokines like interleukin-1 α and β and matrix metalloproteinases. Interestingly, FN-EDA is the only spliced variant of FN that binds and activates TLR4[58, 59]. FN-EDA targets antigen to TLR4-expressing cells and induces cytotoxic T cell responses[60]. FN-EDA is also considered to be a TLR2 ligand and therefore has the potential to activate the two most important TLRs in vascular disease. We showed that lack of FN-EDA prevents myocardial remodeling and preserves pump function after infarction[61]. FN-EDA was also found in restenotic lesions with features of accelerated



atherosclerosis and in the myocardium in the early phase of the remodeling process following infarction[61]. Additionally absence of FN-EDA reduced atherosclerosis formation. In normal aortas the spliced FN-EDA could not be found, although FN-EDA was found in atherosclerotic plaques and in plasma of atherosclerotic mice. FN-EDA was shown to have effects in both plasma lipoprotein metabolism and in macrophage foam cell formation[59, 62]. Studies with atherosclerotic mice that lack FN-EDA indeed showed that cholesterol levels were lowered[59, 62]. In addition, FN-EDA may influence post-interventional remodeling directly via inducing an inflammatory reaction but also via effects on lipid metabolism.

Cytokines and chemokines

Cytokines and chemokines are important mediators of inflammatory responses and can be easily measured in serum. Both lowered and elevated concentrations of cytokines and chemokines are associated with cardiovascular risk profiles and specifically post-interventional vascular remodeling due to accelerated atherosclerosis development. Nevertheless their levels can strongly differ due to different pathophysiological processes initiated by different treatment strategies. The treatment strategy (BMS vs. DES) therefore may have strong influence on the reliability of a selected cytokine or chemokine as biomarker[1, 22]. Interestingly conditions after acute myocardial infarction could exacerbate post-angioplasty restenosis by stimulating signaling via $TNF\alpha$ [63]. This may cause differences for patients that undergo scheduled PCI versus patients that had an acute myocardial infarction before PCI. It may therefore be important to look for combinations of specific cytokines besides a selected biomarker. Activation of innate immune response via TLRs will lead to nuclear factor kappa B (NF κ B) activation followed by upregulation of cytokines and chemokines[26, 39]. Many different cytokines have been studied in relation to post-interventional remodeling and may be used in combination with specific biomarkers to correlate DAMP presence with remodeling related cytokines. Additionally this may provide better insight in the underlying mechanism of the pathophysiological process and thereby indications for proper treatment strategies. Cytokines could also be interesting to measure the effect of these treatment strategies by checking ratios of pro- and anti-inflammatory cytokines. Here we discuss a few cytokines/chemokines that have been intensively researched in relation to cardiovascular disease and have showed biomarker potential

Tumor necrosis factor α

Tumor necrosis factor (TNF) α is a pro-inflammatory cytokine that is importantly involved in inflammatory responses. Multiple cells including endothelial cells, vascular smooth muscle cells and monocytes-derived macrophages can secrete it. Several studies have shown that blockade of TNF α caused a reduction in neointimal formation via acceleration of endothelium repair, found increased mRNA expression of TNF α in the neointima of damaged vessels which may be upregulated 4000 times compared to resting levels. These kinds of studies also showed a relation with accelerated atherosclerosis[64, 65].

Interestingly, the local delivery of thalidomide as a potent TNF α biosynthesis inhibitor demonstrated a powerful reduction of the neointima formation in mice. In humans single nucleotide polymorphisms in the TNF α gene were found and showed associations with an increased clinical and angiographic risk for restenosis[66]. Angioplasty in peripheral arterial segments gave increased levels of TNF α within 1 hour, although no statistically significant correlation was found between failed angioplasty and the following inflammatory response[67]. Kubica et al stated that the combined analysis of CRP and TNF α might be an

effective approach to the clinical restenosis prediction and long-term outcome is markedly influenced by the periprocedural activation of inflammation[68].

Monocyte chemoattractant protein 1

Monocyte chemoattractant protein (MCP)-1 binds to its receptor CC chemokine receptor 2 (CCR2) that belongs to the family of G-coupled receptors and is a chemokine that is capable of attracting immune cells like monocytes. Upon vascular injury MCP-1 recruits monocytes, memory T cells and dendritic cells to the injured site. Attracted monocytes infiltrate the vessel and contribute importantly to neointima formation[69]. MCP-1 is strongly expressed locally in different stages of the remodeling process. Furthermore, it has strong influence on SMC proliferation. Both mouse models for arterial restenosis as for vein graft remodeling showed a MCP-1 inhibitor showed sufficient reduction in neointima formation. Furthermore studies in which the receptor for MCP-1 was targeted gave similar results[70-72]. No differences in MCP-1 concentrations between patients with acute MI, patients with stable coronary artery disease and healthy individuals were found[73]. However, an inverse correlation was found between MCP-1 concentration at baseline and the time to reperfusion, and a significant decrease in MCP-1 concentration immediately after PCI and lower MCP-1 concentrations over time in patients who developed restenosis within 6 months were found[73]. Elevated baseline level of MCP-1 was associated both with traditional risk factors for atherosclerosis as well as an increased risk for death or myocardial infarction, independent of baseline variables. Interestingly MCP-1 levels are not associated with CRP levels indicating the importance of selecting specific inflammatory markers in stead of general markers like CRP[74]. MCP-1 levels are different amongst patients that received a BMS versus a DES[75]. Furthermore in the same study they found increased monocyte CCR-2 expression 24 hr and 48 hr after stenting in the BMS but not the DES group and changes in plasma MCP-1 after stenting correlated significantly with in-stent lumen loss. Previously another Japanese study already showed a correlation between MCP-1 and the risk for restenosis after stenting[76].

Interleukin 10

Interleukin 10 (IL-10) is one of the most prominent anti-inflammatory cytokines. It may suppress antigen presentation and is capable of inhibiting pro-inflammatory cytokine production. Different animal models for restenosis and atherosclerosis showed protective effects of IL-10 by the use of recombinant human IL-10 or using animals deficient in IL-10. In humans three polymorphisms significantly increased the risk of restenosis in patients and demonstrate that IL-10 is associated with restenosis[77-79]. IL-10 is however upregulated together with pro-inflammatory cytokines to maintain a balance between pro- and anti-inflammatory cytokines. Most of the time upregulation of pro-inflammatory cytokines exerts the upregulation of IL-10. Peripheral therapeutic angioplasty gave no difference in IL-10 levels compared to patients that underwent only angiography[67]. In a study using BMS after PCI a significant low IL-10 levels was associated with an increase in restenosis after 6 months[80]. The use of undergoing zotarolimus-eluting (Zotarolimus is a semi-synthetic derivative of rapamycin that works as immunosuppressant) stent implantation combined with pioglitazone significantly reduced neointimal hyperplasia within the stented lesion and attenuated total plaque burden in the in-segment regions of the stent at the 8-month follow-up. These changes were preceded by an elevated IL-10 concentration 10 days after implantation[81].

RANTES/CCL5

CCL5 (RANTES) deposition was involved in wire-induced intimal hyperplasia and blocking of RANTES receptors attenuates neointima formation and macrophage infiltration in animal studies[82]. Two clinical studies focused on the relation of RANTES levels and restenosis. While one of these studies found a decrease of RANTES in time in the non-restenosis group another found a significant time-dependent increase in the restenosis group[83, 84]. No association was found between RANTES promoter genotype and restenosis[85].

Plasma antibodies

Recent results from murine interventional studies indicate that inflammation and (auto) immune mechanisms are both strong contributors to the development of post-interventional restenosis development have led to the hypothesis that (auto)antibodies are both causally related to restenosis development, and titers could serve as biological biomarkers for the identification of restenosis risk or lesion severity. Longitudinal studies will be required to determine both the diagnostic and predictive values of antibody profiles, but promising candidates have emerged over the past decade, which will be discussed below.

The immune system can be divided into the innate and adaptive systems, which are closely linked and regulated. The innate immunity forms the first line of defense and offers a quick but unspecific response to invading microorganisms, whilst adaptive immunity takes longer to develop, but targets highly specific antigen-bearing foreign intruders. To this end, the former system is comprised of various toll-like receptors, the complement system and cytokines and chemokines, whilst the latter depends on the vast variety of B and T cell receptors and antigen-specific immunoglobulines.

Anti-oxidized LDL and phosphorylcholine antibodies

Immune responses against oxidized forms of cholesterol-containing LDL particles play a critical role in activation and regulation of the inflammatory process that characterizes all stages of atherosclerosis[86]. LDL cholesterol is the most important risk factor for cardiovascular disease and cholesterol-lowering therapy (statins) alone can reduce CVD-risk by 30-40%. LDL has been found to play a key role in lesion development and LDL oxidation by enzymes such as lipoxygenases primarily occurs in the extracellular matrix in the arterial wall. Oxidative modification of phospholipid fatty acids, degradation of apoB-100 into peptide fragments and modification of these structures by aldehydes derived from oxidized fatty acids leads to the development of immunogenic neo-antigens[87, 88]. These contain pathogen-associated molecular patterns (PAMPs) that are recognized by the pathogen recognition receptors (PRRs) from the immune system, of which TLRs and scavenger receptors are considered to be the most important. TLRs occur both intra- and extracellular and are activated by lipopolysaccharide (LPS) and various other (viral) micro-biological antigens, but also by endogenous ligands such as heat shock proteins and fibronectin extra-domain A[89]. Their activation stimulates MyD88-dependent and independent intracellular cascades that eventually all lead to increased NF κ B transcription and inflammation.

In both mouse and man, natural anti-oxLDL IgM and IgG antibodies occur, whilst in vitro, antibodies are directed towards malondialdehyde (MDA) and copper-oxidized LDL[87]. These antibodies proved to be exactly similar to those produced by natural occurring T15 B-1 cell clones and all recognize the phosphorylcholine (PC) antigen on oxLDL[90], but also on apoptotic cells and *Streptococcus pneumoniae*, which share molecular mimicry[91, 92]. These antibodies are suggested to block the oxLDL-uptake by scavenger receptor-

bearing macrophages and block foam cell and atherosclerotic lesion formation, but could also serve as risk markers for atherosclerotic and restenotic lesion development. Several studies have reported increased plasma titers of IgG anti-oxLDL antibodies in patients with angiographically verified coronary artery disease and with acute myocardial infarction[93-95]. Many studies found that low levels of IgM anti-oxLDL antibodies are associated with increased atherosclerosis in hypertensive patients and low levels of IgM anti-PC antibodies with acute myocardial infarction, ischemic stroke and cardiovascular disease in general in both the general population and patients with either hypertension or SLE[93-96]. Therefore, this could also hold true for restenosis due to accelerated atherosclerosis development and the severity of lesion development. In general, these studies have identified anti-oxLDL and specifically anti-PC antibodies as biomarkers for cardiovascular disease monitoring with potentially high additive value to current diagnostic strategies.

Microparticles

Thrombocytes, monocytes and those cellular types lining the arterial wall including endothelial cells and SMCs have been shown to vesiculate and release membrane-shed microparticles in response to cellular activation and apoptosis such as occur during the development of atherosclerotic and restenotic lesions[97, 98]. Membrane integrity is largely controlled by intracellular calcium and caspase homeostasis[99]. Disorganization of the cytoskeleton enables blebbing to occur and disruption of the membrane phospholipid symmetry supports PS externalization[99]. These PS-containing microparticles have been implicated in the development, progression and complications of atherosclerotic lesions and patients suffering from atherosclerotic or restenotic cardiovascular disease display high levels of circulating microparticles and since these microparticles are absent in healthy individuals, their circulating levels prove to allow excellent follow-up of lesion progression and serve as surrogate markers for vascular function[99].

Specifically endothelium-derived microparticles, but not those originating from other cellular types, have been shown to bear high prognostic value in the risk assessment of mortality and major adverse cardiovascular events in patients with coronary artery disease, but also pulmonary hypertension and end-stage renal failure[98].

What can we learn from the lesion itself for selecting novel biomarkers?

In an ideal situation we would like to extract our biomarkers directly out of the lesion since this area previously gave problems and here postinterventional remodeling will start again. Previously detectable CRP levels in the arterial intima were found preceding the appearance of monocytes. Furthermore, CRP had actually chemotactic capacities by direct influence on monocyte recruitment both in vitro as in vivo[100]. Another study showed that immunoreactivity to CRP was localized to macrophages, SMCs and necrotic areas. Moreover, the immunoreactivity to CRP in coronary atheromatous plaque increases in culprit lesions of unstable angina and it affects restenosis[101]. This may indicate that local CRP levels are much more specific to study while the role of circulating CRP and the relation with post-interventional remodeling may still be difficult to assess since it may be upregulated in multiple ways even independently of the interventional procedure. Another factor of which its plaque levels were more than 70 times higher in plaques than in plasma is oxLDL in patients undergoing carotid endarterectomy[102]. The same authors also found differences in the oxLDL amount in macrophages rich plaques versus macrophage poor plaques. Interestingly plasma oxLDL levels were only significantly different between control patients and patients



with macrophage-rich plaques which may indicate that when studying only oxLDL on the plasma level will not discriminate patients without or patients with a macrophage-poor plaque and may be more helpful in determination of plaque vulnerability than just plaque formation or progression[102]. Bamberg and co-workers showed that different biomarkers of inflammation, vascular remodeling, oxidation, and lipoprotein metabolism maybe associated with different patterns of coronary atherosclerosis as quantified by coronary CT angiography[103]. So lesion phenotype may be very important for the selection of proper novel biomarkers. Only recently a novel study was conducted that uses the knowledge of specific lesions to study the disease process and use it as a predictor of future restenosis and or atherosclerosis occurrence even at other sites than the initial lesion. This Athero-Express study was the first study to provide prospective evidence that plaque composition may predict the risk of restenosis after endarterectomy. Here they found associations for non-vulnerable plaque phenotype to be more prone to develop restenosis[104]. The Athero-Express biobank was also used for a proteomics search approach to identify local biomarkers (selected proteins that have been identified earlier in experimental set-ups with any cardiovascular phenotype but not necessarily with atherosclerosis, osteopontin (OPN) and Macrophage migration inhibitory factor (MIF)) in the atherosclerotic plaque to predict atherosclerotic plaque development in other vascular beds. The authors collected plaques from carotids as well as plaques from femoral arteries and in both cases they found plaque osteopontin (OPN) levels highly predictive for secondary atherosclerotic development. Furthermore, plaque MIF levels were strongly associated with secondary cardiovascular events and showed that the concept not only applies for OPN[105]. Although beyond the scope of this review, the field of proteomic research is evolving and could contribute substantially to the discovery of new biomarkers in post-interventional restenosis and accelerated atherosclerosis.

Most studies are of limited value for the risk stratification of individual patients with the current available biomarkers[25] and are therefore playing a very little role in the prediction of restenosis and decision-making for its exploration and treatment. Furthermore, in many clinical centers it is not possible yet to sample and extract tissue to select for biomarkers patient specifically however combining results of these kind of studies on plaque development and progression together with increased specific knowledge on the complex pathways extracted from experimental research may help us in understanding not only the pathophysiological process but also to select novel biomarkers. They probably will contribute largely to our knowledge and selection of novel biomarkers and may find new correlations between local and circulating levels of biomarkers and post-interventional remodeling and accelerated atherosclerosis. In addition these local studies may even come up with novel biomarkers inside the plaque that can not be detected in plasma due to their low plasma levels, incapacity of being released outside the plaque or just being plaque specific.

Conclusion

Recently published studies have demonstrated that both lowered and elevated concentrations of local arterial and circulating biomarkers are associated with cardiovascular risk profiles and specifically post-interventional vascular remodeling due to accelerated atherosclerosis development. These associations are independent of traditional risk factors and could serve as helpful tools for risk stratification or diagnostic assessment of patients eligible for intensified treatment for clinicians performing target lesion revascularization interventions. Improved assays have identified not only circulating biomarkers, but also cellular-expressed receptors, co-factors and microparticles that all directly causally involved in disease progress, but also indirectly as biomarkers of inflammatory status and vascular function. Provided these

findings are replicated in other studies, the combined power of current diagnostic strategies with the latest tools and multiple biological risk markers could contribute significantly to the optimization of patient selection and future individual tailor-made treatment.

Executive summary
Background <ul style="list-style-type: none">▪ Coronary heart disease remains the leading cause of death and is caused by atherosclerosis, a chronic inflammatory disease.
Underlying causes of restenosis <ul style="list-style-type: none">▪ Postpercutaneous coronary intervention restenosis is determined by biological, arterial, stent and technical factors.
Inflammation status as a biomarker <ul style="list-style-type: none">▪ Biomarkers can be divided into local, circulating and circulating cell-bound markers, and are most valuable when causally related to disease progression.
Circulating biomarkers <ul style="list-style-type: none">▪ Circulating markers and ligands of the innate immune system such as fibronectin, inflammatory cytokines, annexin A5 and natural antibodies towards oxidized low-density lipoprotein cholesterol and high mobility group box 1 can be highly predictive.▪ Inflammatory receptors on circulating leukocytes such as Toll-like receptors and scavenger receptors, and also microparticles, are directly implicated in and strongly indicative of atherosclerotic vascular remodeling.
What can we learn from the lesion itself for selecting novel biomarkers? <ul style="list-style-type: none">▪ Biobanks containing mRNA and protein profiles from numerous atherosclerotic plaques are highly valuable for local biomarker screening.
Conclusion <ul style="list-style-type: none">▪ Biomarkers of inflammation status possess the highest predictive value for accelerated atherosclerosis disease progression, especially when combined and in addition to current diagnostic strategies.

Future perspective

The insight into the development of atherosclerosis and post-PCI restenosis has developed very quickly over the past decade. Ever since, atherosclerosis is primarily viewed as a chronic inflammatory disease due to a dysfunctional immune response towards the arterial wall. To this end, the focus on atherosclerotic biomarkers has shifted from traditional markers that serve as risk factors, such as hypercholesterolemia, towards markers of systemic inflammation (e.g. C-reactive protein) and arterial dysfunction. The important notion remains that causal factors are additionally powerful predictors of disease progression and the same would apply for inflammatory markers. The field of diagnostic and treatment-evaluation markers will shift in the same direction, guided by new insights, and rely heavily on the additional value of new biomarkers to the current diagnostic strategies. Epidemiologic assessment of additional value from combining biomarkers is a powerful tool to discover new biomarkers entities for the development of highly specific assays, specifically for genetic biomarkers such as polymorphisms that are associated with disease risk.

The field of biomarkers for accelerated atherosclerosis and post-interventional vascular remodeling has changed due to the introduction of drug-eluting stents. These stents have rendered various markers of little use, since they closely followed the inflammatory reaction towards BMS placement and are currently prevented by adequate local drug release. Their usefulness could be further compromised in future due to the ever-increasing application of drug-eluting balloons. Nevertheless, new inflammatory factors such as intraplaque and circulating proteins, natural antibodies, microparticles and cellular receptor expression could prove to be of highly-specific and diagnostic value. Furthermore, application of such screening assays would allow for optimal treatment evaluation such as occurred in the past with the introduction of cholesterol-lowering statin therapy.

Development and application of future biomarkers requires clinical validation, which remains a time-consuming and expansive entity, and this uncertainty is inherently (most notably on safety issues) present at the final stages of drug validation, limiting future biomarker

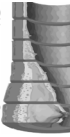


development. In spite of this, investigations continue to proceed and will improve diagnostic and treatment accuracy of post-interventional atherosclerotic vascular remodeling.

Reference List

1. Niccoli G, Montone RA, Ferrante G, Crea F: The evolving role of inflammatory biomarkers in risk assessment after stent implantation. *J. Am. Coll. Cardiol.* 56, 1783-1793 (2010).
2. Wang TJ, Gona P, Larson MG et al. : Preprocedural C-reactive protein levels and cardiovascular events after coronary stent implantation. *N. Engl. J. Med.* 355, 2631-2639 (2006).
3. Dahlöf B: Cardiovascular disease risk factors: epidemiology and risk assessment. *Am. J. Cardiol.* 105, 3A-9A (2010).
4. Andersson J, Libby P, Hansson GK: Adaptive immunity and atherosclerosis. *Clin. Immunol.* 134, 33-46 (2010).
5. Hansson GK: Inflammation, atherosclerosis, and coronary artery disease. *N. Engl. J. Med.* 352, 1685-1695 (2005).
6. Libby P, Ridker PM, Hansson GK: Progress and challenges in translating the biology of atherosclerosis. *Nature* 473, 317-325 (2011). **This review describes current immunological insights in the field of experimental and clinical atherosclerosis research**
7. Tabas I: Apoptosis and efferocytosis in mouse models of atherosclerosis. *Curr. Drug Targets.* 8, 1288-1296 (2007).
8. Libby P, Ridker PM, Hansson GK: Inflammation in atherosclerosis: from pathophysiology to practice. *J. Am. Coll. Cardiol.* 54, 2129-2138 (2009).
9. van der Hoeven BL, Pires NM, Warda HM, et al : Inflammation in atherosclerosis: from pathophysiology to practice. *Int. J. Cardiol.* 99, 9-17 (2005).
10. Farooq V, Gogas BD, Serruys PW: Restenosis: delineating the numerous causes of drug-eluting stent restenosis. *Circ. Cardiovasc. Interv.* 4, 195-205 (2011).
11. Garg S, Serruys PW: Coronary stents: current status. *J. Am. Coll. Cardiol.* 56, S1-42 (2010).
12. Dangas GD, Claessen BE, Caixeta A, Sanidas EA, Mintz GS, Mehran R: In-stent restenosis in the drug-eluting stent era. *J. Am. Coll. Cardiol.* 56, 1897-1907 (2010).
13. Weintraub WS: The pathophysiology and burden of restenosis. *Am. J. Cardiol.* 100, 3K-9K (2007).
14. Pires NM, Jukema JW, Daemen MJ, Quax PH: Drug-eluting stents studies in mice: do we need atherosclerosis to study restenosis? *Vascul. Pharmacol.* 44, 257-264 (2006).
15. Newby AC: Matrix metalloproteinases regulate migration, proliferation, and death of vascular smooth muscle cells by degrading matrix and non-matrix substrates. *Cardiovasc. Res.* 69, 614-624 (2006).
16. van Hinsbergh VWM, Engelse MA, Quax PHA: Pericellular proteases in angiogenesis and vasculogenesis. *Arterioscler. Thromb. Vasc. Biol.* 26, 716-728 (2006).
17. Jukema JW, Verschuren JJ, Ahmed TA, Quax PHA: Restenosis after PCI. Part 1: pathophysiology and risk factors. *Nat Rev Cardiol.* 9, 53-62 (2011)
18. Jukema JW, Ahmed TA, Verschuren JJ, Quax PHA: Restenosis after PCI. Part 2: prevention and therapy. *Nat Rev Cardiol.* (2011) Oct 11. epub ahead doi: 10.1038
19. Vasan RS: Biomarkers of cardiovascular disease: molecular basis and practical considerations. *Circulation* 113, 2335-2362 (2006). **This review provides an overview of the molecular basis of biomarker discovery and selection and the practical considerations that are a prerequisite to their clinical use.**
20. Sukhija R, Fahdi I, Garza L, et al : Inflammatory markers, angiographic severity of coronary artery disease, and patient outcome. *Am. J. Cardiol.* 99, 879-884 (2007).
21. Walter DH, Fichtlscherer S, Sellwig M, et al: Preprocedural C-reactive protein levels and cardiovascular events after coronary stent implantation. *J. Am. Coll. Cardiol.* 37, 839-846 (2001).

22. Ferrante G, Niccoli G, Biasucci LM, *et al*: Association between C-reactive protein and angiographic restenosis after bare metal stents: an updated and comprehensive meta-analysis of 2747 patients. *Cardiovasc. Revasc. Med.* 9, 156-165 (2008).
23. Walter DH, Fichtlscherer S, Britten MB, *et al*: Statin therapy, inflammation and recurrent coronary events in patients following coronary stent implantation. *J. Am. Coll. Cardiol.* 38, 2006-2012 (2001).
24. Aronson D: Inflammatory markers: linking unstable plaques to coronary event, an interventional perspective. *Int. J. Cardiovasc. Intervent.* 6, 110-118 (2004).
25. Ware JH: The limitations of risk factors as prognostic tools. *N. Engl. J. Med.* 355, 2615-2617 (2006).
26. Kawai T, Akira S: The role of pattern-recognition receptors in innate immunity: update on Toll-like receptors. *Nat. Immunol.* 11, 373-384 (2010). **This review describes the recent advances that have been made by research into the role of TLR biology in host defense and disease.**
27. Miyake K: Innate immune sensing of pathogens and danger signals by cell surface Toll-like receptors. *Semin. Immunol.* 19, 3-10 (2007). **This review describes how TLRs can recognize not only exogenous ligands but also endogenous danger signals.**
28. Boersma HH, Kietse-laer BL, Stolk LM, *et al*: Past, present, and future of annexin A5: from protein discovery to clinical applications. *J. Nucl. Med.* 46, 2035-2050 (2005).
29. Cederholm A, Frostegard J: Annexin A5 as a novel player in prevention of atherothrombosis in SLE and in the general population. *Ann. N. Y. Acad. Sci.* 1108, 96-103 (2007).
30. van Genderen HO, Kenis H, Hofstra L, Narula J, Reutelingsperger CP: Extracellular annexin A5: functions of phosphatidylserine-binding and two-dimensional crystallization. *Biochim. Biophys. Acta* 1783, 953-963 (2008). **A clear overview of the important functions of extracellular annexin A5 in the field of cellular and vascular biology.**
31. Cederholm A, Frostegard J: Annexin A5 multitasking: a potentially novel antiatherothrombotic agent? *Drug News Perspect.* 20, 321-326 (2007).
32. Cederholm A, Frostegard J: Annexin A5 in cardiovascular disease and systemic lupus erythematosus. *Immunobiology* 210, 761-768 (2005).
33. Ewing MM, de Vries MR, Nordzell M, *et al*: Annexin A5 therapy attenuates vascular inflammation and remodeling and improves endothelial function in mice. *Arterioscler. Thromb. Vasc. Biol.* 31, 95-101 (2011).
34. van Tits LJ, van Heerde WL, van der Vleuten GM, *et al*: Plasma annexin A5 level relates inversely to the severity of coronary stenosis. *Biochem. Biophys. Res. Commun.* 356, 674-680 (2007).
35. Hofstra L, Heymans S: Annexin A5 and the failing heart; lost or found in translation? *Eur. Heart J.* 28, 2695-2696 (2007).
36. Michelsen KS, Wong MH, Shah PK, *et al*: Lack of Toll-like receptor 4 or myeloid differentiation factor 88 reduces atherosclerosis and alters plaque phenotype in mice deficient in apolipoprotein E. *Proc. Natl. Acad. Sci. U. S. A* 101, 10679-10684 (2004).
37. Hansson GK, Hermansson A: The immune system in atherosclerosis. *Nat. Immunol.* 12, 204-212 (2011).
38. Hansson GK, Lundberg AM: Toll in the vessel wall--for better or worse? *Proc. Natl. Acad. Sci. U. S. A* 108, 2637-2638 (2011).
39. Ionita MG, Arslan F, de Kleijn DP, Pasterkamp G: Endogenous inflammatory molecules engage Toll-like receptors in cardiovascular disease *J. Innate. Immun.* 2, 307-315 (2010).
40. Andonegui G, Kerfoot SM, McNagny K, Ebbert KV, Patel KD, Kubes P: Platelets express functional Toll-like receptor-4. *Blood* 106, 2417-2423 (2005).
41. Hollestelle SC, de Vries MR, van Keulen JK *et al*: Toll-like receptor 4 is involved in outward arterial remodeling. *Circulation* 109, 393-398 (2004).
42. Karper JC, de Vries MR, van den Brand BT *et al*: Toll-like receptor 4 is involved in human and mouse vein graft remodeling, and local gene silencing reduces vein graft disease in hypercholesterolemic APOE*3Leiden mice. *Arterioscler. Thromb. Vasc. Biol.* 31, 1033-1040 (2011).



43. Vink A, Schoneveld AH, van der Meer JJ *et al*: In vivo evidence for a role of toll-like receptor 4 in the development of intimal lesions. *Circulation* 106, 1985-1990 (2002).
44. Stewart CR, Stuart LM, Wilkinson K *et al*: CD36 ligands promote sterile inflammation through assembly of a Toll-like receptor 4 and 6 heterodimer. *Nat. Immunol.* 11, 155-161 (2010).
45. Park JS, Svetkauskaite D, He Q *et al*: Involvement of toll-like receptors 2 and 4 in cellular activation by high mobility group box 1 protein. *J. Biol. Chem.* 279, 7370-7377 (2004).
46. Park JS, Gamboni-Robertson F, He Q *et al*: High mobility group box 1 protein interacts with multiple Toll-like receptors. *Am. J. Physiol Cell Physiol* 290, C917-C924 (2006).
47. Yu M, Wang H, Ding A *et al*: HMGB1 signals through toll-like receptor (TLR) 4 and TLR2. *Shock* 26, 174-179 (2006).
48. Gondokaryono SP, Ushio H, Niyonsaba F *et al*: The extra domain A of fibronectin stimulates murine mast cells via toll-like receptor 4. *J. Leukoc. Biol.* 82, 657-665 (2007).
49. Lotze MT, Tracey KJ: High-mobility group box 1 protein (HMGB1): nuclear weapon in the immune arsenal. *Nat. Rev. Immunol.* 5, 331-342 (2005).
50. Abraham E, Arcaroli J, Carmody A, Wang H, Tracey KJ: HMG-1 as a mediator of acute lung inflammation. *J. Immunol.* 165, 2950-2954 (2000).
51. Wang H, Bloom O, Zhang M *et al*: HMG-1 as a late mediator of endotoxin lethality in mice *Science* 285, 248-251 (1999).
52. Kalinina N: Increased expression of the DNA-binding cytokine HMGB1 in human atherosclerotic lesions: role of activated macrophages and cytokines. *Arteriosclerosis, thrombosis, and vascular biology* 24, 2320-2325 (2004).
53. Kohno T, Anzai T, Naito K *et al*: Role of high-mobility group box 1 protein in post-infarction healing process and left ventricular remodelling. *Cardiovasc. Res.* 81, 565-573 (2009).
54. Kohno T, Anzai T, Shimizu H *et al*: Impact of serum high-mobility group box 1 protein elevation on oxygenation impairment after thoracic aortic aneurysm repair. *Heart Vessels* 26, 306-312 (2011).
55. Leelahavanichkul A, Huang Y, Hu X *et al*: Chronic kidney disease worsens sepsis and sepsis-induced acute kidney injury by releasing High Mobility Group Box Protein-1. *Kidney Int* (2011).
56. Urbonaviciute V, Voll RE: HMGB1 represents a potential marker of disease activity and novel therapeutic target in SLE. *J. Intern. Med* (2011).
57. Ito T, Kawahara K, Nakamura T *et al*: High-mobility group box 1 protein promotes development of microvascular thrombosis in rats. *J. Thromb. Haemost.* 5, 109-116 (2007).
58. Okamura Y, Watari M, Jerud ES *et al*: The extra domain A of fibronectin activates Toll-like receptor 4. *J. Biol. Chem.* 276, 10229-10233 (2001).
59. Tan MH, Sun Z, Opitz SL *et al*: Deletion of the alternatively spliced fibronectin EIIIA domain in mice reduces atherosclerosis. *Blood* 104, 11-18 (2004).
60. Lasarte JJ, Casares N, Gorraiz M *et al*: The extra domain A from fibronectin targets antigens to TLR4-expressing cells and induces cytotoxic T cell responses in vivo. *J. Immunol.* 178, 748-756 (2007).
61. Arslan F, Smeets MB, Riem Vis PW *et al*: Lack of fibronectin-EDA promotes survival and prevents adverse remodeling and heart function deterioration after myocardial infarction. *Circ. Res.* 108, 582-592 (2011).
62. Babaev VR, Porro F, Linton MF, Fazio S, Baralle FE, Muro AF: Absence of regulated splicing of fibronectin EDA exon reduces atherosclerosis in mice. *Atherosclerosis* 197, 534-540 (2008).
63. Takaoka M, Uemura S, Kawata H *et al*: Inflammatory response to acute myocardial infarction augments neointimal hyperplasia after vascular injury in a remote artery. *Arterioscler. Thromb. Vasc. Biol.* 26, 2083-2089 (2006).
64. Krasinski K, Spyridopoulos I, Kearney M, Losordo DW: In vivo blockade of tumor necrosis factor-alpha accelerates functional endothelial recovery after balloon angioplasty. *Circulation* 104, 1754-1756 (2001).
65. Rectenwald JE, Moldawer LL, Huber TS, Seeger JM, Ozaki CK: Direct evidence for cytokine involvement

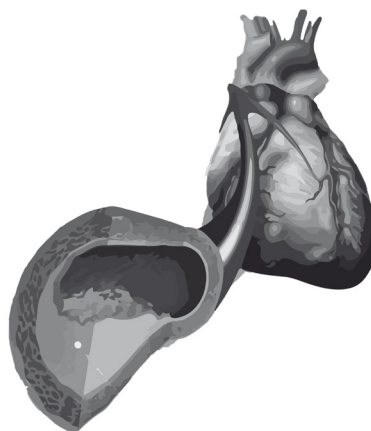
- in neointimal hyperplasia. *Circulation* 102, 1697-1702 (2000).
66. Monraats PS, Pires NM, Schepers A *et al*: Tumor necrosis factor- α plays an important role in restenosis development. *FASEB J.* 19, 1998-2004 (2005).
 67. Parmar JH, Aslam M, Standfield NJ: Percutaneous transluminal angioplasty of lower limb arteries causes a systemic inflammatory response. *Ann. Vasc. Surg.* 23, 569-576 (2009).
 68. Kubica J, Kozinski M, Krzewina-Kowalska A *et al*: Combined periprocedural evaluation of CRP and TNF- α enhances the prediction of clinical restenosis and major adverse cardiac events in patients undergoing percutaneous coronary interventions. *Int. J. Mol. Med.* 16, 173-180 (2005).
 69. Rogers C, Welt FG, Karnovsky MJ, Edelman ER: Monocyte recruitment and neointimal hyperplasia in rabbits. Coupled inhibitory effects of heparin. *Arterioscler. Thromb. Vasc. Biol.* 16, 1312-1318 (1996).
 70. Egashira K, Zhao Q, Kataoka C *et al*: Importance of monocyte chemoattractant protein-1 pathway in neointimal hyperplasia after periarterial injury in mice and monkeys. *Circ. Res.* 90, 1167-1172 (2002).
 71. Roque M, Kim WJ, Gazdoin M *et al*: CCR2 deficiency decreases intimal hyperplasia after arterial injury. *Arterioscler. Thromb. Vasc. Biol.* 22, 554-559 (2002).
 72. Schepers A, Eefting D, Bonta PI *et al*: Anti-MCP-1 gene therapy inhibits vascular smooth muscle cells proliferation and attenuates vein graft thickening both in vitro and in vivo. *Arterioscler. Thromb. Vasc. Biol.* 26, 2063-2069 (2006).
 73. Korybalska K, Pyda M, Grajek S, Lanocha M, Breborowicz A, Witowski J: Serum profiles of monocyte chemoattractant protein-1 as a biomarker for patients recovering from myocardial infarction. *Clin. Res. Cardiol.* 99, 315-322 (2010).
 74. de Lemos JA, Morrow DA, Sabatine MS *et al*: *Circulation* 107, 690-695 (2003).
 75. Sako H, Miura S, Iwata A *et al*: Changes in CCR2 chemokine receptor expression and plasma MCP-1 concentration after the implantation of bare metal stents versus sirolimus-eluting stents in patients with stable angina. *Intern. Med.* 47, 7-13 (2008).
 76. Oshima S, Ogawa H, Hokimoto S *et al*: Plasma monocyte chemoattractant protein-1 antigen levels and the risk of restenosis after coronary stent implantation. *Jpn. Circ. J.* 65, 261-264 (2001).
 77. Eefting D, Schepers A, de Vries MR *et al*: The effect of interleukin-10 knock-out and overexpression on neointima formation in hypercholesterolemic APOE*3-Leiden mice. *Atherosclerosis* 193, 335-342 (2007).
 78. Feldman LJ, Aguirre L, Zioli M *et al*: Interleukin-10 inhibits intimal hyperplasia after angioplasty or stent implantation in hypercholesterolemic rabbits. *Circulation* 101, 908-916 (2000).
 79. Monraats PS, Kurreeman FA, Pons D *et al*: Interleukin 10: a new risk marker for the development of restenosis after percutaneous coronary intervention. *Genes Immun.* 8, 44-50 (2007).
 80. Zurakowski A, Wojakowski W, Dzielski T *et al*: Plasma levels of C-reactive protein and interleukin-10 predict late coronary in-stent restenosis 6 months after elective stenting. *Kardiol. Pol.* 67, 623-630 (2009).
 81. Hong SJ, Kim ST, Kim TJ *et al*: Cellular and molecular changes associated with inhibitory effect of pioglitazone on neointimal growth in patients with type 2 diabetes after zotarolimus-eluting stent implantation. *Arterioscler. Thromb. Vasc. Biol.* 30, 2655-2665 (2010).
 82. Schober A, Manka D, von Hundelshausen P *et al*: Deposition of platelet RANTES triggering monocyte recruitment requires P-selectin and is involved in neointima formation after arterial injury. *Circulation* 106, 1523-1529 (2002).
 83. Inami N, Nomura S, Manabe K, Kimura Y, Iwasaka T: Platelet-derived chemokine RANTES may be a sign of restenosis after percutaneous coronary intervention in patients with stable angina pectoris. *Platelets* 17, 565-570 (2006).
 84. Satoh D, Inami N, Shimazu T *et al*: Soluble TRAIL prevents RANTES-dependent restenosis after percutaneous coronary intervention in patients with coronary artery disease. *Journal of thrombosis and thrombolysis* 29, 471-476 (2010).
 85. Vogiatzi K, Voudris V, Apostolakis S *et al*: Genetic diversity of RANTES gene promoter and susceptibility

- to coronary artery disease and restenosis after percutaneous coronary intervention. *Thrombosis research* 124, 84-89 (2009).
86. Hartvigsen K, Chou MY, Hansen LF *et al*: The role of innate immunity in atherogenesis. *J. Lipid Res.* 50 Suppl, S388-S393 (2009).
 87. Nilsson J, Nordin FG, Schiöpu A, Shah PK, Jansson B, Carlsson R: Oxidized LDL antibodies in treatment and risk assessment of atherosclerosis and associated cardiovascular disease. *Curr. Pharm. Des* 13, 1021-1030 (2007).
 88. de Faire U, Frostegard J: Natural antibodies against phosphorylcholine in cardiovascular disease. *Ann. N. Y. Acad. Sci.* 1173, 292-300 (2009).
 89. Frantz S, Ertl G, Bauersachs J: Mechanisms of disease: Toll-like receptors in cardiovascular disease. *Nat. Clin. Pract. Cardiovasc. Med.* 4, 444-454 (2007).
 90. Amabile N, Rautou PE, Tedgui A, Boulanger CM: Microparticles: key protagonists in cardiovascular disorders *Semin. Thromb. Hemost.* 36, 907-916 (2010).
 91. Chou MY, Fogelstrand L, Hartvigsen K *et al*: Oxidation-specific epitopes are dominant targets of innate natural antibodies in mice and humans. *J. Clin. Invest* 119, 1335-1349 (2009).
 92. Binder CJ, Horkko S, Dewan A *et al*: Pneumococcal vaccination decreases atherosclerotic lesion formation: molecular mimicry between *Streptococcus pneumoniae* and oxidized LDL. *Nat. Med.* 9, 736-743 (2003).
This study demonstrates the vital molecular mimicry between oxLDL and pathogens that are recognized by the innate immune system in atherosclerosis development.
 93. Fiskesund R, Stegmayr B, Hallmans G *et al*: Low levels of antibodies against phosphorylcholine predict development of stroke in a population-based study from northern Sweden. *Stroke* 41, 607-612 (2010).
 94. Frostegard J: Low level natural antibodies against phosphorylcholine: a novel risk marker and potential mechanism in atherosclerosis and cardiovascular disease *Clin. Immunol.* 134, 47-54 (2010).
 95. Su J, Georgiades A, Wu R, Thulin T, de Faire U, Frostegard J: Antibodies of IgM subclass to phosphorylcholine and oxidized LDL are protective factors for atherosclerosis in patients with hypertension. *Atherosclerosis* 188, 160-166 (2006).
 96. de Faire U, Su J, Hua X, Frostegard A *et al*: Low levels of IgM antibodies to phosphorylcholine predict cardiovascular disease in 60-year old men: effects on uptake of oxidized LDL in macrophages as a potential mechanism. *J. Autoimmun.* 34, 73-79 (2010).
 97. Leroyer AS, Tedgui A, Boulanger CM: Role of microparticles in atherothrombosis *J. Intern. Med.* 263, 528-537 (2008).
 98. Dignat-George F, Boulanger CM: The many faces of endothelial microparticles *Arterioscler. Thromb. Vasc. Biol.* 31, 27-33 (2011).
 99. Rautou PE, Vion AC, Amabile N *et al*: Microparticles, vascular function, and atherothrombosis. *Circ. Res.* 109, 593-606 (2011).
 100. Torzewski M, Rist C, Mortensen RF *et al*: C-reactive protein in the arterial intima: role of C-reactive protein receptor-dependent monocyte recruitment in atherogenesis. *Arterioscler. Thromb. Vasc. Biol.* 20, 2094-2099 (2000).
 101. Ishikawa T, Hatakeyama K, Imamura T *et al*: Involvement of C-reactive protein obtained by directional coronary atherectomy in plaque instability and developing restenosis in patients with stable or unstable angina pectoris. *Am. J. Cardiol.* 91, 287-292 (2003).
 102. Nishi K, Itabe H, Uno, M *et al*: Oxidized LDL in carotid plaques and plasma associates with plaque instability. *Arterioscler. Thromb. Vasc. Biol.* 22, 1649-1654 (2002).
 103. Bamberg F, Truong QA, Koenig W *et al*: Differential associations between blood biomarkers of inflammation, oxidation, and lipid metabolism with varying forms of coronary atherosclerotic plaque as quantified by coronary CT angiography. *Int. J. Cardiovasc. Imaging* (2011).
 104. Hellings WE, Moll FL, de Vries JP *et al*: Atherosclerotic plaque composition and occurrence of restenosis

after carotid endarterectomy. *JAMA* 299, 547-554 (2008).

105. de Kleijn DP, Moll FL, Hellings WE *et al*: Local atherosclerotic plaques are a source of prognostic biomarkers for adverse cardiovascular events. *Arterioscler. Thromb. Vasc. Biol.* 30, 612-619 (2010).

CHAPTER 4



Toll-like receptor 4 is involved in human and mouse vein graft remodeling, and local gene silencing reduces vein graft disease in hypercholesterolemic APOE*3Leiden mice.

Karper JC, de Vries MR, van den Brand BT, Hofer IE, Fischer JW, Jukema JW, Niessen HW, Quax PH

Arteriocler Thromb Vasc Biol. 2011;31(5):1033-40.

Abstract:

Objective Explore the role of TLR4 in vein graft remodeling and disease.

Methods and Results First, expression of TLR4 was analyzed in human Saphenous Veins (huSV), either freshly isolated, or freshly isolated huSV *ex vivo* perfused in an extracorporeal circulation or in huSV used as coronary vein grafts. Marked induction of focal TLR4 expression was observed in perfused fresh huSV. Moreover, TLR4 was abundantly present in lesions in fresh huSV or in intimal hyperplasia in coronary vein grafts. Secondly mouse venous bypass grafting was performed. In grafts of hypercholesterolemic APOE*3Leiden mice increased TLR4 mRNA and protein was detected over time by RT-PCR and immunohistochemistry. Furthermore local presence of the endogenous TLR4-ligands HSP60, HMGB1, Tenascin-C and biglycan in the grafts was demonstrated.

TLR4 deficiency in C3H-*Tlr4*^{LPS-d} mice resulted in 48±12% less vein graft wall thickening (p=0.04) than in Balb/c controls. Moreover, local TLR4 gene silencing in hypercholesterolemic APOE*3Leiden mice using lentiviral-shRNA against TLR4 administered perivascularly around vein grafts led to a 44±13% reduction of vessel wall thickening compared to controls (p=0.0059).

Conclusion: These results indicate that TLR4 is involved in vein graft remodeling and can be used as a local therapeutic target against vein graft disease.

**Introduction:**

Vein grafts are important conduits for revascularization during both coronary and peripheral bypass surgery although vein grafts sometimes have poor long term patency. Early graft failure is usually due to thrombosis but long term graft failure is caused by vein graft disease (VGD) induced by wall thickening due intimal hyperplasia that is triggered by inflammation. Vein graft wall thickening is in part characterized by smooth muscle cell (SMC) proliferation, matrix turnover and influx of lipids and inflammatory cells^{1, 2}.

The innate immune system contains multiple receptors that recognize a broad variety of molecular structures. Toll Like Receptors (TLRs) have a key role in driving inflammation regulating the innate response after binding pathogen associated molecular patterns (PAMPs) or damage associated molecular patterns (DAMPs), respectively³⁻⁷. TLR4 is a membrane bound receptor located on a variety of immune and non-immune cells including macrophages, endothelial and SMCs. Cell stress and tissue damage may cause a release of DAMPS that function as endogenous TLR4 ligands and lead to activation and up-regulation of the expression of TLR4 resulting in a pro-inflammatory response^{6, 8-10}. The role of TLR4 in vascular remodeling, especially arterial remodeling has previously been demonstrated in various studies either directed at atherogenesis and plaque (de)stabilization or directed at the role of TLR4 in postinterventional arterial remodeling after angioplasty¹¹⁻¹⁶. However the role of TLR4 and its endogenous ligands in remodeling of venous segments e.g. in vein graft remodeling is still unknown. Furthermore it is suggested that unactivated arterial VSMC do not express TLR4 and that TLRs may have a vessel specific profile which may also vary due to changes in cellular activation, differentiation and other local processes.¹⁷ Interestingly non-activated VSMC from huSV do express TLR4¹⁸.

To modulate atherosclerotic plaque formation by interfering in the TLR4 pathway, systemic therapeutic interventions would be required. However, due to its important role in the host defense mechanism, such a systemic approach would be undesirable. In contrast, venous bypass grafts do permit local therapeutic interventions. From the point of therapeutic interventions in the TLR4 pathway to reduce vascular remodeling VGD is of more interest and potential. Local therapy against VGD can be done easily e.g. by topical inhibitor application to the adventitial layer since adventitial cells contribute extensively to proliferation and migration of SMC and subsequent vein graft remodeling.¹⁹⁻²³ Therefore local gene transfer in order to silence TLR4 expression would be an interesting approach for therapy to improve graft survival, once the role of TLR4 in VGD is established.

In the current study we focus on the role for TLR4 in vein graft remodeling by illustrating the presence and upregulation of TLR4 and its endogenous ligands in both human and murine venous segments used for vein grafting. Moreover, a causal role of TLR4 was studied by performing vein grafting in TLR4 deficient mice (C3H-*Tlr4*^{LPS-d} mice) or by local TLR4 gene silencing in murine vein graft using a lentiviral shRNA construct against TLR4. The latter study was performed in hypercholesterolemic APOE*3Leiden mice in order to mimic the situation vein grafting in hypercholesterolemic patients as close as possible.

Material and methods:

For a detailed description of all materials and methods used see the online supplement (available online at <http://atvb.ahajournals.org>)

In brief, immunohistochemistry for TLR4 was performed on paraffin embedded sections of human saphenous vein (huSV) segments, either freshly isolated, or freshly isolated and ex vivo perfused in an extracorporeal circulation for 4h or huSV used for at least 5 years as coronary vein grafts. Also murine vein graft segments were analyzed for TLR4 expression, but also its endogenous ligands HPS60, HMGB1, Tenascin-C and biglycan.

Lentiviral shRNA vectors against murine TLR4 were established based on the “Mission” library (Sigma Aldrich, the Netherlands).

Vein grafting in mice was performed by placing a venous interposition (vena cava) in the carotid artery of either Balb/c mice, TLR4 deficient (C3H-Tlr4^{LPS-d}) mice or hypercholesterolemic APOE*3Leiden mice. In the APOE*3Leiden mice grafts were treated locally with the lentiviral shTLR4 construct.

Results

TLR4 presence in human saphenous veins and coronary vein grafts.

Human vein graft obtained in the operating room during coronary artery bypass grafting procedures one segment directly taken for histologic and immunohistochemical examination and the remaining segment was placed in a perfusion circuit that was connected to the heart lung machine. Samples were perfused with autologous whole blood, with a pressure of 60 mm Hg (nonpulsatile flow). After 4 hours of perfusion, segments were taken for histologic and immunohistochemical examination. Furthermore vein grafts that served as coronary arterial bypass grafts for more than 6 years were derived at autopsy. To study the presence of TLR4 during remodeling in huSV TLR4 expression was analyzed in the freshly isolated huSV, in pre-existing intimal lesions within these segments and the coronary vein grafts. In the fresh huSVs TLR4 expression could be detected especially in the circular smooth muscle cell layer (Figure 1A). Also the endothelial layer and adventitial vessels stained positive for TLR4 (not shown). Some of the venous segments contained spontaneous lesions, indicated by intimal hyperplasia formation. These lesions represent a focal area of spontaneous remodeling and demonstrated a marked presence of TLR4 (Figure 1B). Additionally a profound TLR4 expression was observed in severely remodeled coronary vein grafts with a saphenous vein origin (Figure 1C). These grafts were obtained at autopsy, had been in situ for more than 5yrs and are representative sections of remodeled vein grafts.

Focal TLR4 expression after graft perfusion.

In vein grafting, early damage to the vessel wall is initiated immediately by surgical manipulation and after transplantation due to increased shear stress and wall tension initiated by increased perfusion pressure. Non-perfused fresh huSV showed only little TLR4-positive cells in sub-endothelial longitudinal muscle layer (Figure 2A). Parallel sections of the same fresh huSV were subjected to 4hrs perfusion with autologous blood on arterial pressure. These sections showed an impressive focal increase of TLR4 expression within the longitudinal layer (Figure 2B).

TLR4 expression in murine vein grafts during remodeling

As the above presented findings indicate an increase of TLR4 presence during huSV remodeling, TLR4 presence on protein and mRNA level was analyzed during remodeling in mice. Therefore a murine vein graft model was used that represents human vein graft

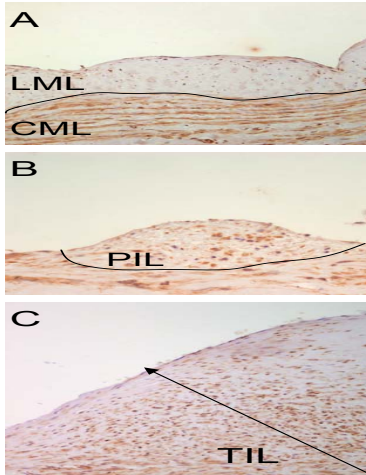


Figure 1: TLR4 expression on cross-sections of huSV. Freshly harvested huSV stained positive for TLR4 on the circular muscle layer (A). Pre-existing intimal lesions in freshly harvested huSV showed several TLR4 positive spots (B) and coronary huSV grafts derived at autopsy showed a profound expression of TLR4 in the thickened vein graft wall (C). CML= circular muscle layer, LML= longitudinal muscle layer, PIL= pre-existent intimal lesion, TIL= thickened intimal layer.

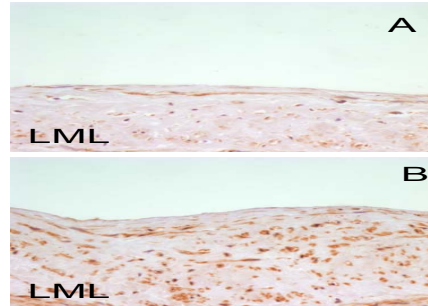


Figure 2: Freshly isolated huSV was divided into two parts. One part was directly fixated (and paraffin embedded) while the other part was placed into an extra-corporeal system for 4h with arterial pressure before fixation. Cross sections of both huSV parts were stained for TLR4. The longitudinal muscle layer of directly fixated huSV showed a few TLR4 positive spots (A). A rapid increase of TLR4 expression was seen in the longitudinal muscle layer of huSV after 4h perfusion with arterial pressure (B). LML= longitudinal muscle layer.

thickening and accelerated atherosclerosis. TLR4 protein presence was studied by IHC during progression of remodeling over time in hypercholesterolemic APOE*3Leiden mice. A marked expression of TLR4 was detectable in these vein grafts. In the early remodeling phase, when the graft is only a single to a couple of cell layers thick, TLR4 positive spots were observed (Figure 3AB). At $t=7$ and $t=14d$ vessel wall thickness has increased markedly. Within these segments focal areas of intense TLR4 protein expression could be detected (Figure 3CD). Rabbit IgG isotype control showed no staining (Figure 3E). Expression of TLR4 mRNA during remodeling was detected by RT-PCR in hypercholesterolemic APOE*3Leiden mice over time at $t=0$, 6hours, 1, 3, 7 and 28d after graft placement. A rapid increase in TLR4 mRNA could be detected in the early remodeling phase. During intermediate and late phase remodeling TLR4 mRNA remained up regulated (Figure 3F) ($t=0$ vs 6h $p=0.03$, $t=0$ vs 1d $p=0.0039$, $t=0$ vs 3d $p=0.02$, $t=0$ vs 7d $p=0.1$, $t=0$ vs 28d $p=0.09$). Increase of TLR4 expression may be partly related to an influx of $cd68+$ cells ($t=0$ vs 6h $p=0.6$, $t=0$ vs 1d $p=0.0037$, $t=0$ vs 3d $p=0.0026$, $t=0$ vs 7d $p=0.0032$, $t=0$ vs 28d $p=0.0003$ during remodeling and proliferation/migration of SMC ($t=0$ vs 6h $p=0.07$, $t=0$ vs 1d $p=0.0007$, $t=0$ vs 3d $p=0.17$, $t=0$ vs 7d $p=0.02$, $t=0$ vs 28d $p=0.006$, Figure 3GH).

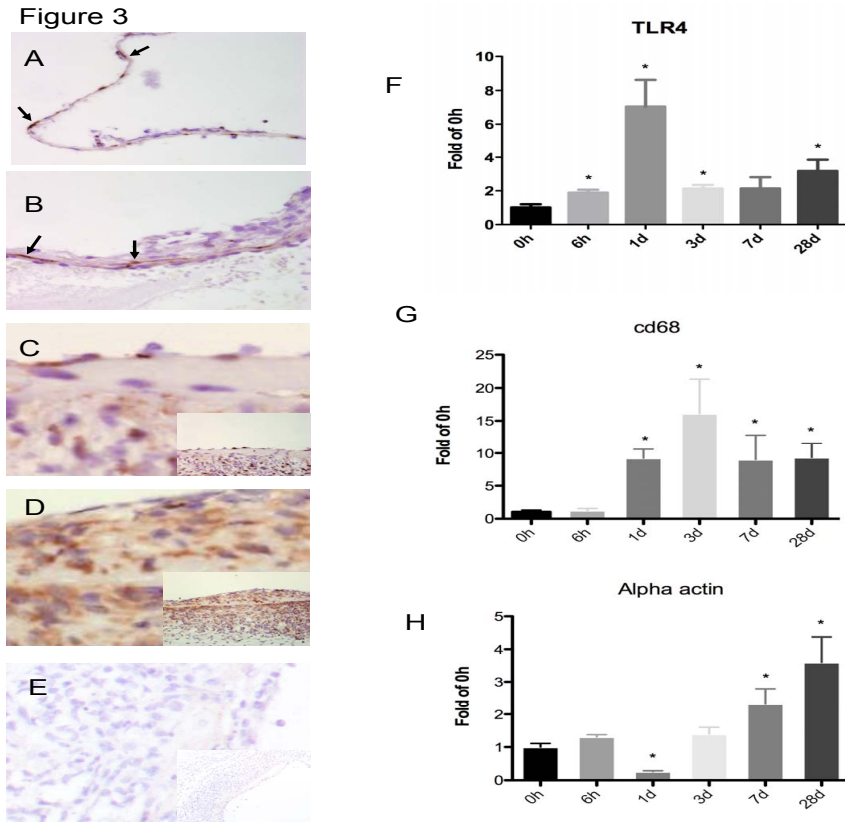


Figure 3: TLR4 expression on murine vein grafts of hypercholesterolemic APOE*3Leiden mice was detected by IHC and RT-PCR. Over time analysis was done at grafts harvested $t=1$ (A), 3 (B), 7 (C) and 14d (D) after surgery. Rabbit IgG isotype control (E). Arrows indicate positive TLR4 staining. RT-PCR of TLR4 (F) CD68 (G) and α SMA (H) mRNA at $t=0$ h, 6h, 1, 3, 7 and 28d after surgery. A student's t -test was used for statistical analysis, * = $P < 0.05$ compared to $t=0$.

Presence of endogenous TLR4 ligands in murine vein grafts

Remodeled grafts have been subjected to proliferation, migration and turnover of cells and matrix components. These processes may cause an upregulation of DAMPs that can be recognized by TLR4. We localized several of these DAMPs in vein grafts of hypercholesterolemic APOE3*Leiden mice harvested at $t=14$ d. Proteins in response to cellular stress like Heat Shock Protein 60 (HSP60) and High Mobility Group Box 1 (HMGB1) are known TLR4 ligands. Presence of HSP60 was detected especially in the sub-endothelial layer of the thickened vessel wall (Figure 4A). HMGB1, normally at rest located inside the nucleus, was now detected in the cytoplasm where it is known to act in a cytokine-like way (Figure 4B)²⁴. In addition, matrix components that are expressed during matrix turnover were studied. Glycoprotein Tenascin-C was demonstrated especially at the matrix rich adventitial site of the graft but also near the luminal site in matrix containing areas (Figure 4C). These endogenous ligands could potentially colocalize with TLR4 since they were present in the lesions site and in areas that also express TLR4 at the same time point (Figure 3D and 4ABC).



Furthermore mRNA expression of matrix component Biglycan (BGN), that may function as TLR4 ligand, was studied in time and a more than 10-fold increase of mRNA was detectable after 7d. This increase in Biglycan expression remained up regulated during the remodeling process ($t=0$ vs 6h $p=0.25$, $t=0$ vs 1d $p=0.017$, $t=0$ vs 3d $p=0.21$, $t=0$ vs 7d $p=0.004$, $t=0$ vs 28d $p=0.021$, Figure 4D).

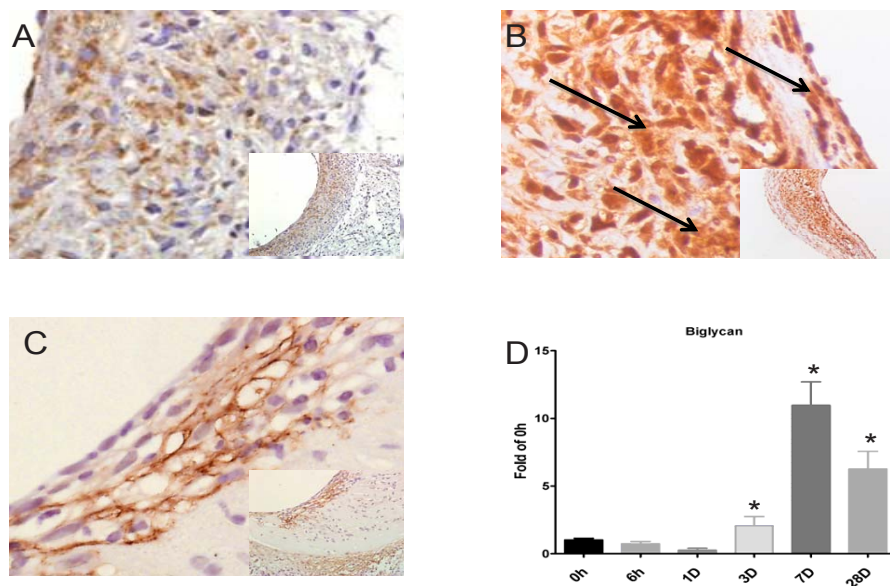


Figure 4: Endogenous TLR4 ligands were detected in vein grafts of hypercholesterolemic APOE*3Leiden mice. Presence of HSP60 (A), HMGB1 (B) and Tenascin-C (C) was detected by IHC in vein grafts 14 days after surgery. RT-PCR on matrix component Biglycan mRNA was performed at $t=0$ h, 6h, 1, 3, 7 and 28d after surgery ($n=3-4$ per timepoint) (D). A students *t*-test was used for statistical analysis, * = $P < 0.05$ compared to $t=0$.

Functional role of TLR4 in murine vein graft remodeling

To explore whether TLR4 has a functional role in vein graft thickening, an essential step in vein graft disease leading to vein graft failure, a venous interposition was placed in the carotid artery of Balb/c ($n=8$) and TLR4 deficient (C3H-*Tlr4*^{LP^S-d}) mice ($n=7$). C3H-*Tlr4*^{LP^S-d} mice showed $48 \pm 12\%$ ($0.264 \pm 0.06 \text{mm}^2$ vs. $0.136 \pm 0.02 \text{mm}^2$, $p=0.04$) less wall thickening than Balb/c controls (Figure 5A). Graft patency was kept by compensatory outward remodeling in the Balb/c mice indicated by a significantly larger total vessel wall area ($0.60 \pm 0.03 \text{mm}^2$ vs. $0.42 \pm 0.05 \text{mm}^2$, $P=0.01$) (figure 5B) and thereby only a small difference in ratio lumen/total vessel wall area (online supplement figure I). Furthermore the reduced vessel wall thickening correlated with a reduced alpha-SMC-actin positive area in the C3H-*Tlr4*^{LP^S-d} mice. ($0.022 \pm 0.003 \text{mm}^2$ vs $0.047 \pm 0.009 \text{mm}^2$, $p=0.035$) (Figure 5C).

TLR4 silencing in vitro

To create a tool for local TLR4 gene silencing five lentiviral based shRNAs were produced and validated by measurement of murine TLR4/MD2 expression on CHO cells by FACS analysis and the best vector was selected (not shown). The selected vector showed a dose

dependent down regulation of TLR4 protein expression (online supplement figure II). Murine 3T3 fibroblasts were then transduced by selected lenti-shTLR4 (TRCN0000065787), lenti-control or PBS and subsequently stimulated with different pro-inflammatory stimuli to obtain insight on its specificity in reducing TLR4 induced NF κ B activation. Lenti-shTLR4 gave a significant reduction in NF κ B activation after administration of TLR4 ligand LPS ($P < 0.01$). Application of Pam3Cys, TNFa or IL1beta gave no different effects on NF κ B activation when compared to the controls (online supplement figure III).

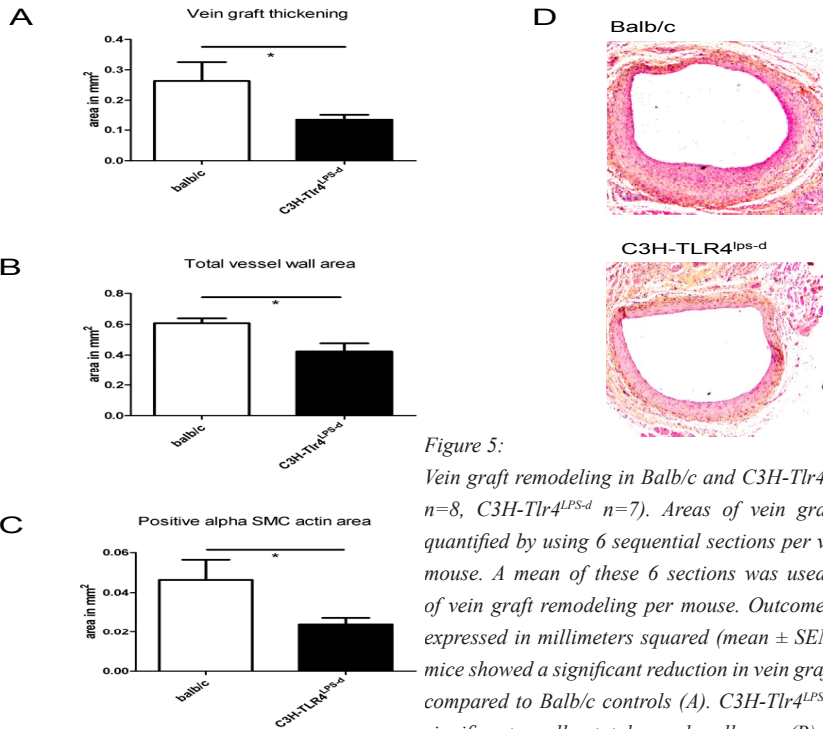


Figure 5:

Vein graft remodeling in Balb/c and C3H-Tlr4^{LPS-d} mice (balb/c n=8, C3H-Tlr4^{LPS-d} n=7). Areas of vein graft sections were quantified by using 6 sequential sections per vein graft of each mouse. A mean of these 6 sections was used as the outcome of vein graft remodeling per mouse. Outcomes of analysis are expressed in millimeters squared (mean \pm SEM). C3H-Tlr4^{LPS-d} mice showed a significant reduction in vein graft wall thickening compared to Balb/c controls (A). C3H-Tlr4^{LPS-d} mice showed a significant smaller total vessel wall area (B). Total of positive alpha SMC actin area was significantly smaller in C3H-Tlr4^{LPS-d} mice (C)

Representative HPS stained sections of Balb/c and C3H-Tlr4^{LPS-d} vein grafts (D), * = $P < 0.05$. Statistical analysis was performed by use of a Mann-Whitney test.

Local TLR4 silencing in hypercholesterolemic APOE*3Leiden mice

To validate the potential of TLR4 as a local therapeutic in vein graft disease, a study was pursued using local TLR4 gene silencing to diminish vein graft disease in APOE*3Leiden mice. These mice, when fed a high cholesterolemic diet, are well known to develop massive vein graft disease due to neointima formation and accelerated atherosclerosis. After graft placement in APOE*3Leiden mice pluronic gel (pg) with PBS (n=8), lenti-control (n=9) or lenti-shTLR4 (n=7) was lubricated around the graft. Mice were fed a western type diet for total duration of the experiment, starting 3 weeks before surgery. No significant differences between groups in cholesterol levels (PBS 9.6 \pm 0.9 mmol/L, lenti-control 9.7 \pm 1.0 mmol/L and lenti-shTLR4 10.2 \pm 0.6 mmol/L) and body weights were observed (not shown).

Local gene silencing of TLR4 led to a 44 \pm 13% reduction of vessel wall thickening in the graft segment (PBS 0.40 \pm 0.04mm², lenti-control 0.42 \pm 0.04mm², lenti-shTLR4 0.23 \pm 0.03mm²)

(PBS vs. lenti-shTLR4 $p=0.0059$, lenti-control vs. lenti-shTLR4 $p=0.0052$, PBS vs. lenti-control $p=0.96$). A difference in total vessel wall area was only found between lenti-control vs. lenti-shTLR4. Additionally a beneficial lumen/total cross sectional ratio showed a beneficial outcome for the lenti-shTLR4 treated group (PBS $0.45\pm 0.05\text{mm}^2$, lenti-control $0.54\pm 0.04\text{mm}^2$, lenti-shTLR4 $0.70\pm 0.03\text{mm}^2$) (PBS vs. lenti-shTLR4 $p=0.0012$, lenti-control vs. lenti-shTLR4 $p=0.0079$, PBS vs. lenti-control $p=0.14$) (Figure 6A-D). Furthermore although quantitative interpretation of immunohistochemistry has to be done with extreme caution, treatment with lenti-shTLR4 gave a reduction in focal TLR4 expression in the graft (Figure 6E). After TLR4 silencing in the vein grafts of APOE*3Leiden mice the area positive for macrophages (MAC3 positive area) and SMC (alpha-SMC-actin positive area) was reduced by 54% and 61% respectively when compared to the PBS group. (details: Table I online supplement)

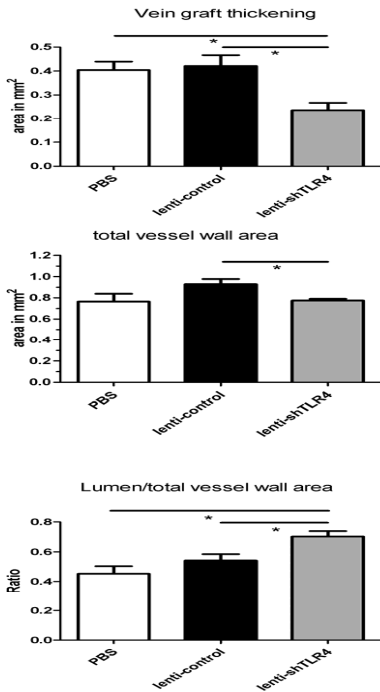
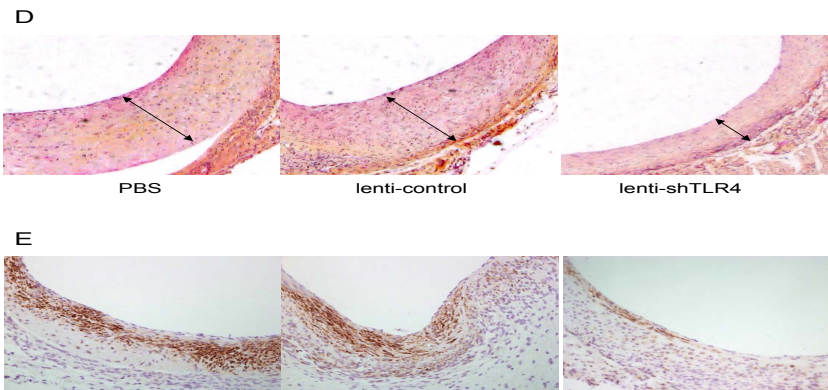


Figure 6: Vein graft remodeling after local TLR4 silencing in hypercholesterolemic APOE*3Leiden mice (PBS $n=8$, lenti-control $n=9$, lenti-shTLR4 $n=7$). Areas of vein graft sections were quantified by using 6 sequential sections per vein graft vein graft of each mouse. A mean of these 6 sections was used as the outcome of vein graft remodeling per mouse. Outcomes of analysis are expressed in millimeters squared (mean \pm SEM). Vein graft wall thickening was reduced in the lenti-shTLR4 treated group compared to the controls (A). Total vessel wall area was smaller in the lenti-shTLR4 group compared to the lenti-control (B). A beneficial lumen/total cross-sectional area ratio was observed in the lenti-shTLR4 treated group (C). Representative HPS stained sections of focal vein graft wall thickening (D). Focal TLR4 expression in vein grafts locally treated with PBS (1), lenti-control (2) and lenti-shTLR4 (3) (E), $*= P < 0.01$. Statistical analysis was performed with a one-way ANOVA.



Discussion

The present study describes the role of TLR4 in vein graft remodeling in human and mice with a profound presence TLR4, endogenous TLR4 ligands during remodeling and the therapeutic potential for local TLR4 silencing. Abundant TLR4 presence was noticed in freshly isolated huSV. Additionally in remodeled areas of fresh huSV, in fresh huSV after reperfusion and in coronary vein grafts derived at autopsy an up regulation of TLR4 protein was observed. In murine vein grafts of hypercholesterolemic APOE*3Leiden mice TLR4 expression is present over time at protein and mRNA level and a series of endogenous TLR4 ligands, HSP60, HMGB1, Tenascin C and Biglycan was expressed. Furthermore TLR4 deficient mice show a significant reduction in vein graft thickening and less outward remodeling after vein grafting. Moreover, local gene silencing of TLR4 gives a clear reduction in vein graft thickening and a beneficial lumen/total cross sectional area ratio.

Nowadays TLR4 is considered to be an important factor in inflammatory mediated diseases. VGD is strongly mediated by remodeling initiated by wall stress, cell damage and inflammation. The level of TLR4 expression may vary amongst different vessel specimens and is dependent on activation and local environmental changes like wall stress, cell damage and inflammation.¹⁷ Furthermore these differences may also be relevant for the presence and levels of endogenous TLR4 ligands. Therefore it is of major importance to evaluate TLR4 expression, function and therapeutic potential in a VGD related setting. Here we report presence of TLR4 on the circular muscle layer of fresh huSV and a rapid increase of focal TLR4 expression within 4 hours of reperfusion in an extracorporeal circulation set up with arterial pressure on sections of fresh huSV. Increased TLR4 expression may be initiated by damage inducing processes like ischemia/reperfusion and increased wall tension/shear stress due to pressure and flow disturbances^{25, 26}. Additionally, the initiated damage to the vessel contributes, most likely by inducing the release of endogenous ligands, to proliferation and migration of VSMC and influx of inflammatory cells like macrophages resulting in thickening of the vessel wall. These cells playing an important role in vascular remodeling have been shown to express TLR4^{13, 18, 27, 28}. In support we notice abundant TLR4 presence within the thickened vessel wall of severely remodeled areas in vein grafts of human and mouse origin. Previously, localization of TLR4 has been shown in remodeled arteries during atherogenesis and after angioplasty and that presence of TLR4 ligands may alter its expression^{13, 14, 16}.

The discovery that these TLR4 ligands can be of endogenous origin further emphasize the importance of TLR4 in inflammatory mediated diseases³. The endogenous ligands, most often referred as DAMPs, are most often danger signals or degradation products of matrix component that become available in response to injury. Bypass surgery itself and the subsection of the transplanted vessel to hypoxia and increased blood pressure can cause a release of powerful inducers of cellular stress and tissue damage. The observed presence of Heat Shock Protein 60 (HSP60), extracellular High Mobility Group Box 1 (HMGB1), Tenascin-C and up regulation of Biglycan mRNA during remodeling are nice examples of this. Previously Hochleitner et al. described the release of HSP60 after shear stress²⁹ and others showed the capability of HSP60 to bind directly to TLR4 thereby initiating proliferation of VSMC³⁰. Cellular stress may also cause passive release of HMGB1 by a variety of cell types including endothelium and monocytes/macrophages and acts like a cytokine capable of binding to TLR4 thereby initiating a pro-inflammatory response^{8, 31, 32}. Matrix turnover importantly mediates vein graft remodeling. Extracellular matrix glycoprotein Tenascin-C is related to tissue repair and injury. Normally Tenascin-C is not present in huSV but after graft placement its expression is significantly increased in huSV grafts^{33, 34}. If present it is



capable of promoting SMC migration³⁵, growth³⁶ and effecting important genes in vascular remodeling. Recently Tenascin-C was found to be an endogenous TLR4 ligand without the need for CD14 or MD-2 as accessory molecules for signal transduction and therefore Tenascin-C may act in vein grafts also via TLR4 signaling³⁷. The matrix component Biglycan is co-immunoprecipitated with TLR4 and by signaling via TLR4 on macrophages it has a pro-inflammatory effect. Moreover it enhances SMC proliferation^{36, 38}. The observed increase in Biglycan expression over time in the vein graft point towards an increased TLR4 signaling in murine vein grafts with Biglycan as ligand.

The reduced vein graft wall thickening in the C3H-*Tlr4*^{LPS-d} mice by reducing total SMC amount demonstrates that TLR4 and its endogenous ligands are not just only expressed in the remodeling vein graft segments, but TLR4 is also causally involved in vein graft remodeling. As the current results indicate presence and even causal involvement of TLR4 and up regulation of multiple endogenous ligands in VGD, several new targets can be proposed for therapeutic interference. Long-term systemic anti-inflammatory treatment against TLR4 would be difficult and undesirable due to expected adverse side effects. Furthermore targeting of a single DAMP would be not a good option since multiple DAMPS are up regulated and are able to trigger TLR4 signalling involved in vascular remodeling making it difficult to select them as therapeutic targets individually. Local RNA interference (RNAi) for TLR4 may overcome this problem. Short hairpin RNA constructs are able to inhibit gene translation into protein thereby initiating effective gene silencing^{39, 40}. Previously our group showed that local graft transduction using a lentivirus can be performed efficiently *in vivo*⁴¹. In support, others have shown encouraging results for the applicability of local gene therapy^{42, 43}.

Therefore local lentiviral infection with the selected TLR4 shRNA was performed in on vein grafts positioned in the carotid artery of hypercholesterolemic APOE*3Leiden mice. The specificity of the shRNA construct used was demonstrated by its capacity to decrease murine TLR4 expression on transformed CHO cells and to reduce NFκB activation in murine fibroblasts after LPS activation. NFκB activation after challenging the cells with other stimuli than the TLR4-ligand LPS, such as Pam3Cys, TNFα or IL1b, was not affected demonstrating the specificity of the construct.

Morphometric analysis after silencing TLR4 demonstrates a reduction in vessel wall thickening which is supported by a focal decrease in TLR4 expression and a reduction in total amount of macrophages in the lesions. Like in the TLR4 deficient mice reduction of total SMC in the lenti-shTLR4 treated group correlated with the decrease in vessel wall thickening. Furthermore local TLR4 silencing increases the ratio of lumen versus total cross sectional area. This indicates a beneficial effect of local TLR4 silencing on vein graft remodeling with effects on graft patency on long term.

This also might have impact for the treatment of patients since vein grafts can readily be treated locally *ex vivo* during surgery thus presenting a unique opportunity for gene transfer or gene inhibition to alter the remodeling response.

In summary, upregulation of TLR4 expression (both in human and mouse) as well as its endogenous ligands in vein grafts during graft remodeling and the reduced vein graft thickening in TLR4 deficient C3H-*Tlr4*^{LPS-d} mice point out important involvement of TLR4 and its endogenous ligands in vein graft disease. Furthermore the reduction of vein graft vessel wall thickening in hypercholesterolemic APOE*3Leiden mice after local lentiviral shRNA mediated interference in the TLR4 pathway indicate the potential of TLR4 as a local therapeutic target to improve vein graft survival.

Reference List

1. Davies MG, Hagen PO. Pathophysiology of vein graft failure: a review. *Eur J Vasc Endovasc Surg* 1995;9:7-18.
2. Newby AC, Zaltsman AB. Molecular mechanisms in intimal hyperplasia. *J Pathol* 2000;190:300-9.
3. Foell D, Wittkowski H, Roth J. Mechanisms of disease: a 'DAMP' view of inflammatory arthritis. *Nat Clin Pract Rheumatol* 2007;3:382-90.
4. Kawai T, Akira S. TLR signaling. *Semin Immunol* 2007;19:24-32.
5. Mullick AE, Tobias PS, Curtiss LK. Toll-like receptors and atherosclerosis: key contributors in disease and health? *Immunol Res* 2006;34:193-209.
6. Sabroe I, Parker LC, Dower SK, Whyte MK. The role of TLR activation in inflammation. *J Pathol* 2008;214:126-35.
7. Akira S, Takeda K, Kaisho T. Toll-like receptors: critical proteins linking innate and acquired immunity. *Nat Immunol* 2001;2:675-80.
8. Park JS, Svetkauskaite D, He Q, Kim JY, Strassheim D, Ishizaka A, Abraham E. Involvement of toll-like receptors 2 and 4 in cellular activation by high mobility group box 1 protein. *J Biol Chem* 2004;279:7370-7.
9. Taylor KR, Trowbridge JM, Rudisill JA, Termeer CC, Simon JC, Gallo RL. Hyaluronan fragments stimulate endothelial recognition of injury through TLR4. *J Biol Chem* 2004;279:17079-84.
10. Xu D, Komai-Koma M, Liew FY. Expression and function of Toll-like receptor on T cells. *Cell Immunol* 2005;233:85-9.
11. Hansson GK, Edfeldt K. Toll to be paid at the gateway to the vessel wall. *Arterioscler Thromb Vasc Biol* 2005 June;25:1085-7.
12. Hansson GK. Inflammation, atherosclerosis, and coronary artery disease. *N Engl J Med* 2005;352:1685-95.
13. Xu XH, Shah PK, Faure E, Equils O, Thomas L, Fishbein MC, Luthringer D, Xu XP, Rajavashisth TB, Yano J, Kaul S, Arditani M. Toll-like receptor-4 is expressed by macrophages in murine and human lipid-rich atherosclerotic plaques and upregulated by oxidized LDL. *Circulation* 2001;104:3103-8.
14. Hollestelle SC, De Vries MR, van Keulen JK, Schoneveld AH, Vink A, Strijder CF, Van Middelaar BJ, Pasterkamp G, Quax PH, de Kleijn DP. Toll-like receptor 4 is involved in outward arterial remodeling. *Circulation* 2004;109:393-8.
15. Kiechl S, Lorenz E, Reindl M, Wiedermann CJ, Oberhollenzer F, Bonora E, Willeit J, Schwartz DA. Toll-like receptor 4 polymorphisms and atherogenesis. *N Engl J Med* 2002;347:185-92.
16. Vink A, Schoneveld AH, van der Meer JJ, Van Middelaar BJ, Sluijter JP, Smeets MB, Quax PH, Lim SK, Borst C, Pasterkamp G, de Kleijn DP. In vivo evidence for a role of toll-like receptor 4 in the development of intimal lesions. *Circulation* 2002;106:1985-90.
17. Pryshchep O, Ma-Krupa W, Younge BR, Goronzy JJ, Weyand CM. Vessel-specific Toll-like receptor profiles in human medium and large arteries. *Circulation* 2008;118:1276-84.
18. Sasu S, LaVerda D, Qureshi N, Golenbock DT, Beasley D. Chlamydia pneumoniae and chlamydial heat shock protein 60 stimulate proliferation of human vascular smooth muscle cells via toll-like receptor 4 and p44/p42 mitogen-activated protein kinase activation. *Circ Res* 2001;89:244-50.
19. Conte MS, Mann MJ, Simosa HF, Rhynhart KK, Mulligan RC. Genetic interventions for vein bypass graft disease: a review. *J Vasc Surg* 2002;36:1040-52.
20. Conte MS. Molecular engineering of vein bypass grafts. *J Vasc Surg* 2007;45 Suppl A:A74-A81.
21. Hu Y, Zhang Z, Torsney E, Afzal AR, Davison F, Metzler B, Xu Q. Abundant progenitor cells in the adventitia contribute to atherosclerosis of vein grafts in ApoE-deficient mice. *J Clin Invest* 2004;113:1258-65.
22. Maiellaro K, Taylor WR. The role of the adventitia in vascular inflammation. *Cardiovasc Res* 2007;75:640-8.
23. Siow RC, Churchman AT. Adventitial growth factor signalling and vascular remodelling: potential of



- perivascular gene transfer from the outside-in. *Cardiovasc Res* 2007;75:659-68.
24. Lotze MT, Tracey KJ. High-mobility group box 1 protein (HMGB1): nuclear weapon in the immune arsenal. *Nat Rev Immunol* 2005;5:331-42.
 25. Wu H, Chen G, Wyburn KR, Yin J, Bertolino P, Eris JM, Alexander SI, Sharland AF, Chadban SJ. TLR4 activation mediates kidney ischemia/reperfusion injury. *J Clin Invest* 2007;117:2847-59.
 26. Yang J, Yang J, Ding JW, Chen LH, Wang YL, Li S, Wu H. Sequential expression of TLR4 and its effects on the myocardium of rats with myocardial ischemia-reperfusion injury. *Inflammation* 2008;31:304-12.
 27. Akashi S, Shimazu R, Ogata H, Nagai Y, Takeda K, Kimoto M, Miyake K. Cutting edge: cell surface expression and lipopolysaccharide signaling via the toll-like receptor 4-MD-2 complex on mouse peritoneal macrophages. *J Immunol* 2000;164:3471-5.
 28. Stewart CR, Stuart LM, Wilkinson K, van Gils JM, Deng J, Halle A, Rayner KJ, Boyer L, Zhong R, Frazier WA, Lacy-Hulbert A, Khoury JE, Golenbock DT, Moore KJ. CD36 ligands promote sterile inflammation through assembly of a Toll-like receptor 4 and 6 heterodimer. *Nat Immunol* 2010;11:155-61.
 29. Hochleitner BW, Hochleitner EO, Obrist P, Eberl T, Amberger A, Xu Q, Margreiter R, Wick G. Fluid shear stress induces heat shock protein 60 expression in endothelial cells in vitro and in vivo. *Arterioscler Thromb Vasc Biol* 2000;20:617-23.
 30. de Graaf R, Kloppenburg G, Kitslaar PJ, Bruggeman CA, Stassen F. Human heat shock protein 60 stimulates vascular smooth muscle cell proliferation through Toll-like receptors 2 and 4. *Microbes Infect* 2006;8:1859-65.
 31. Degryse B, Bonaldi T, Scaffidi P, Muller S, Resnati M, Sanvito F, Arrighi G, Bianchi ME. The high mobility group (HMG) boxes of the nuclear protein HMG1 induce chemotaxis and cytoskeleton reorganization in rat smooth muscle cells. *J Cell Biol* 2001;152:1197-206.
 32. Li W, Sama AE, Wang H. Role of HMGB1 in cardiovascular diseases. *Curr Opin Pharmacol* 2006;:130-5.
 33. Wallner K, Li C, Fishbein MC, Shah PK, Sharifi BG. Arterialization of human vein grafts is associated with tenascin-C expression. *J Am Coll Cardiol* 1999;34:871-5.
 34. Wallner K, Li C, Shah PK, Fishbein MC, Forrester JS, Kaul S, Sharifi BG. Tenascin-C is expressed in macrophage-rich human coronary atherosclerotic plaque. *Circulation* 1999;99:1284-9.
 35. LaFleur DW, Chiang J, Fagin JA, Schwartz SM, Shah PK, Wallner K, Forrester JS, Sharifi BG. Aortic smooth muscle cells interact with tenascin-C through its fibrinogen-like domain. *J Biol Chem* 1997;272:32798-803.
 36. Jones PL, Rabinovitch M. Tenascin-C is induced with progressive pulmonary vascular disease in rats and is functionally related to increased smooth muscle cell proliferation. *Circ Res* 1996;79:1131-42.
 37. Midwood K, Sacre S, Piccinini AM, Inglis J, Trebaul A, Chan E, Drexler S, Sofat N, Kashiwagi M, Orend G, Brennan F, Foxwell B. Tenascin-C is an endogenous activator of Toll-like receptor 4 that is essential for maintaining inflammation in arthritic joint disease. *Nat Med* 2009;15:774-80.
 38. Schaefer L, Babelova A, Kiss E, Hausser HJ, Baliova M, Krzyzankova M, Marsche G, Young MF, Mihalik D, Gotte M, Malle E, Schaefer RM, Grone HJ. The matrix component biglycan is proinflammatory and signals through Toll-like receptors 4 and 2 in macrophages. *J Clin Invest* 2005;115:2223-33.
 39. Hannon GJ. RNA interference. *Nature* 2002;418:244-51.
 40. Stewart SA, Dykxhoorn DM, Palliser D, Mizuno H, Yu EY, An DS, Sabatini DM, Chen IS, Hahn WC, Sharp PA, Weinberg RA, Novina CD. Lentivirus-delivered stable gene silencing by RNAi in primary cells. *RNA* 2003;9:493-501.
 41. Eefting D, Bot I, De Vries MR, Schepers A, van Bockel JH, Van Berkel TJ, Biessen EA, Quax PH. Local lentiviral short hairpin RNA silencing of CCR2 inhibits vein graft thickening in hypercholesterolemic apolipoprotein E3-Leiden mice. *J Vasc Surg* 2009;50:152-60.
 42. Eichstaedt HC, Liu Q, Chen Z, Bobustuc GC, Terry T, Willerson JT, Zoldhelyi P. Gene transfer of COX-1 improves lumen size and blood flow in carotid bypass grafts. *J Surg Res* 2010;161:162-7.
 43. Tatewaki H, Egashira K, Kimura S, Nishida T, Morita S, Tominaga R. Blockade of monocyte chemoattractant

protein-1 by adenoviral gene transfer inhibits experimental vein graft neointimal formation. *J Vasc Surg* 2007;45:1236-43.



Supplement Material

Materials and Methods

Mice

All animal experiments were approved by the animal welfare committee of our institute.

10 week old male Balb/c, C3H-Tlr4LPS-d and APOE*3Leiden mice, bred in our laboratory, were used. C3H-Tlr4LPS-d mice have a Balb/c background but carry a mutation that causes a deficiency in TLR4 signaling.

APOE*3Leiden were fed a western-type diet (Arie Blok, The Netherlands), starting 3 weeks before surgery and continued during the experiment to develop a diet dependent hypercholesterolemia.

All mice received water and food ad libitum. One week before surgery cholesterol levels in serum were determined (Roche Diagnostics, The Netherlands).

Production of lentiviral shRNA against TLR4

Out of the “Mission Library” (Sigma Aldrich, The Netherlands) 5 sequence-verified short hairpin RNA (shRNA) lentiviral-plasmids against TLR4 were isolated and produced. Lentiviral packaging vectors (pCMV-VSVG, pMDLg-RREgag/pol, pRSV-REV) and transfer vector (pLKO.1-puro Vector) were co-transfected in HEK293T cells using calcium-phosphate precipitation method. Lentiviral particles were concentrated using sucrose cushion centrifugation (30.000rpm, 2h). Quantification of lentiviral titer was done by p24 ELISA (ZeptoMetrix, USA).

The vectors encoded the shRNAs sequences against TLR4 (lenti-shTLR4) as indicated:

	TRCN0000065783	NM_021297.1-3054s1c1
	TRCN0000065784	NM_021297.1-1246s1c1
	TRCN0000065785	NM_021297.1-1568s1c1
	TRCN0000065786	NM_021297.1-509s1c1
*	TRCN0000065787	NM_021297.1-2247s1c1

* Selected and in vivo applied lenti-shTLR4

In vitro targeting of murine TLR4 expression

CHO cells expressing murine TLR4/MD2 and control cells (kindly provided by Dr. A. Garritsen, Merck Sharp Dome, The Netherlands) were transduced with the 5 different lentiviral based shRNAs in a 0.1:1, 0.5:1, 1:1 and 2:1 ratio (lentiviral particles/cells) in DMEM (Invitrogen, The Netherlands) containing 0.8ug/ml polybrene (Sigma Aldrich, The Netherlands) with 5% Fetal Calf Serum. After overnight transduction medium was replaced by fresh medium. Subsequent TLR4 expression was measured by FACS analysis with a TLR4-MD2 FITC antibody (HyCult biotechnology, The Netherlands) after 5d.

Transduction of murine 3T3 fibroblasts:

NIH 3T3 mouse fibroblasts stably transfected with a 5xNFκB-Luciferase vector as described 1. After overnight adherence, cells were transduced with, lenti-control (lentivirus-GFP) or lenti-shTLR4 (TRCN0000065787) per well (MOI of 7.5) or PBS. Medium was discarded after 4h transduction and replaced by fresh medium. Cells were cultured for 5d followed by stimulation with LPS, TNFα, Pam3Cys, or IL1β. After 6h stimulation, cells were washed with 0.9% NaCl and lysed for 15min on ice. Bright-Glo was added and luminescence was measured on the Lumistar Optima.

Murine vein graft model

In the mouse carotid artery a venous interposition was placed as described previously². Caval veins of donor mice were placed as vein grafts in the right carotid artery of recipient mice.

Lentiviral transduction of the vein graft in situ

Before wound closure, in the APOE*3Leiden mice, 150μl 20% pluronic gel (Sigma Aldrich, The Netherlands) containing 1.5×10^6 lentiviral particles (P24 Elisa, ZeptoMetrix, USA) and 0.8μg/ml DEAE (Sigma Aldrich, The Netherlands) was lubricated around the graft.

Vein graft thickening quantification

Mice were sacrificed 28d (or as stated otherwise) after surgery for histological analysis. Vein graft segments were harvested after perfusion fixation with 4% formaldehyde, fixated overnight and paraffin-embedded using an automated tissue processor (Leica, Germany). Cross-sections were made throughout the embedded vein grafts. Six representative sections per vessel segment were stained with Haematoxylin-Phloxine- Saffron (HPS) for histological and morphometric analysis (Leica, Germany). Vein graft thickening was defined as the area between lumen and adventitia and determined by subtracting the luminal area from the total vessel wall area.

Human vein graft tissue

Veins were surplus segments of huSVs that were collected in the operating room from patients undergoing coronary artery bypass grafting (CABG). Vessel specimens were freshly collected under sterile conditions. One part of the segment was directly fixated for histopathological examination and another part was perfused on an extracorporeal perfusion circuit connected to the heart-lung machine during the CABG procedure with autologous blood and under arterial pressure (60mmHg) as described by Stoker³. The study was approved by the local ethics committee. Patients were included in the study after providing informed consent. Non-perfused fresh huSV segments (n=6 patients) and parallel fresh huSV segments that were perfused for 4h respectively (n=6 patients) were analyzed huSV segments that have served as coronary bypass for more than 5yrs (n=5 patients) were derived at autopsy. Use of patient material after completion of the diagnostic process is part of the patient contract in the VU University Medical Centre.



Immunohistochemistry

Paraffin embedded sections (5 μ m) were deparaffinized in xylene. Peroxidase activity was blocked by incubation in 0.3% (v/v) H₂O₂ in methanol for 20min. Antigen retrieval was performed and tissue sections were pre-incubated with 5% bovine serum albumin (BSA), followed by incubation with detecting antibody.

TLR4 presence was stained with TLR4 antibody (sc-10741 rabbit anti-human, Santa Cruz, United States), HSP60 (rabbit anti-mouse, Abcam, UK), HMGB1 (rabbit anti-mouse Abcam, UK), Tenascin C (rabbit anti-mouse, Millipore, USA), SMCs with α -smooth muscle cell actin staining (Roche Applied Biosciences, Germany) and macrophages with MAC3ab (BD Pharmingen, USA). After washing in PBS, sections were incubated for 1h with a secondary antibody (Donkey anti-Rabbit, GE Healthcare, USA), washed in PBS, incubated for 1h with AB complex (Vector laboratories, The Netherlands) and visualized with Novared (Vector laboratories) or DAB (Dako, Denmark). Slides were counterstained with haematoxylin.

Immunopositive areas of SMC and macrophages were calculated as percentage of total vein graft area in cross-sections by morphometry (Leica, Germany). To increase the TLR4 detection after AB complex slides were incubated for 10 minutes with biotinylated thymids and again 1h with AB complex prior to visualization with Novared. As control parallel sections were incubated with 1% PBS/BSA alone or with Rabbit IgG isotype without adding detecting antibodies. Controls were all negative (not shown).

RT-PCR

Total RNA was isolated using Tri-Reagent (Sigma-Aldrich) according to the manufacturer's protocol. The expression levels of TLR4 and Biglycan were analyzed by RT-PCR (real time polymerase chain reaction). The relative mRNA expression levels were determined by using GAPDH as house keeping gene and the $2^{-\Delta\Delta C(T)}$ method. Values were expressed as fold of respective controls.

Statistical analysis

Values are presented as mean \pm standard error of the mean (SEM). Statistical significance was calculated in SPSS for Windows-17.0. Differences between groups were determined using a non parametric Mann-Whitney and One-way ANOVA (Kruskal-Wallis, non-parametric Dunn's Multiple Comparison Test) tests. A Student's t-test was used for statistical analysis of in vitro assays. Probability values of less than 0.05 were considered statistically significant.

Acknowledgements

This work was performed within the framework of Dutch Top Institute Pharma, project D1-101.

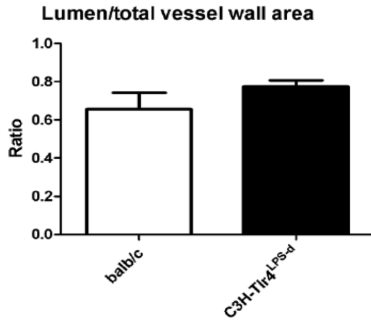


Figure I: Ratio lumen/total vessel wall area of vein grafts of balb/c (n=8) and TLR4 deficient C3H-Tlr4LPS-d mice (n=7)

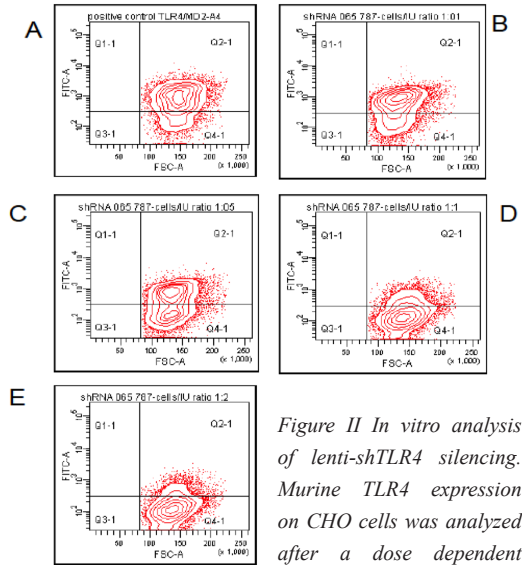


Figure II In vitro analysis of lenti-shTLR4 silencing. Murine TLR4 expression on CHO cells was analyzed after a dose dependent transduction with lenti-shTLR4. Positive control (A). Dose dependent transduction of lenti-shTLR4 in a 1:0.1 (B) 1:0.5 (C) 1:1 (D) 1:2 lentiviral particles/cells ratio showed a profound dose dependent reduction of TLR4 expression (E).

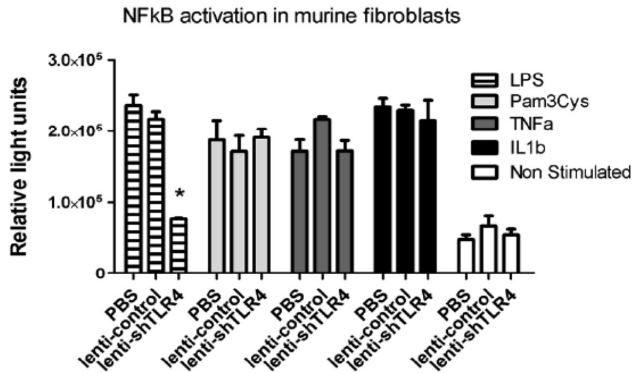


Figure III: Murine 3T3 fibroblast were transduced with PBS, lenti-control or lenti-shTLR4 and subsequently stimulated with LPS, 100ng/ml; Pam3Cys, 10µg/ml; TNF-α, 10ng/ml; IL-1β, 10ng/ml; Non Stimulated. NFkB activation due to LPS stimulation was significantly reduced in the lenti-shTLR4 transduced fibroblasts (F), A students t-test was used for statistical analysis * = P<0.01.

Tabel I:

	PBS	Lenti-control	Lenti-shTLR4
Macrophages	406±53µm ² *	446±87µm ²	187±64µm ²
SMC	1289±120µm ² *	515±169µm ²	511±63µm ²

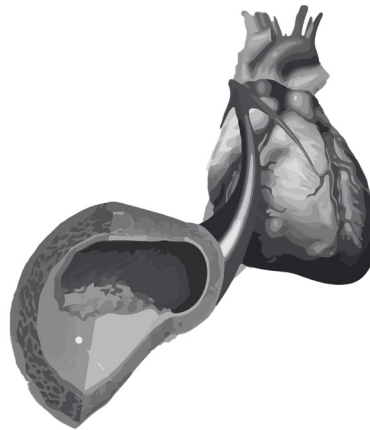
Macrophages: PBS vs. lenti-shTLR4 p=0.037, lenti-control vs. lenti-shTLR4 p=0.054, PBS vs. lenti-control p=1.00. SMC: PBS vs. lenti-shTLR4 p=0.00006, lenti-control vs. lenti-shTLR4 p=0.53, PBS vs. lenti-control p=0.0059.

References

1. Smeets RL, van de Loo FA, Joosten LA, Arntz OJ, Bennink MB, Loesberg WA, Dmitriev IP, Curiel DT, Martin MU, van den Berg WB. Effectiveness of the soluble form of the interleukin-1 receptor accessory protein as an inhibitor of interleukin-1 in collagen-induced arthritis. *Arthritis Rheum* 2003;48:2949-2958.
2. Lardenoye JH, de Vries MR, Lowik CW, Xu Q, Dhore CR, Cleutjens JP, van Hinsbergh VW, van Bockel JH, Quax PH. Accelerated atherosclerosis and calcification in vein grafts: a study in APOE*3 Leiden transgenic mice. *Circ Res* 2002 ;91:577-584.
3. Stooker W, Niessen HW, Baidoshvili A, Wildevuur WR, Van Hinsbergh VW, Fritz J, Wildevuur CR, Eijssman L. Perivenous support reduces early changes in human vein grafts: studies in whole blood perfused human vein segments. *J Thorac Cardiovasc Surg* 2001;121:290-297.
4. Edfeldt K, Swedenborg J, Hansson GK, Yan ZQ. Expression of toll-like receptors in human atherosclerotic lesions: a possible pathway for plaque activation. *Circulation* 2002 ;105:1158-1161.



CHAPTER 5



Blocking Toll-Like Receptors 7 and 9 Reduces Postinterventional Remodeling via Reduced Macrophage Activation, Foam Cell Formation, and Migration.

Karper JC, Ewing MM, Habets KL, de Vries MR, Peters EA, van Oeveren-Rietdijk AM, de Boer HC, Hamming JF, Kuiper J, Kandimalla ER, La Monica N, Jukema JW, Quax PH.

Arterioscler Thromb Vasc Biol. 2012;32(8):e72-80.

Abstract

Objective The role of Toll-like Receptors in vascular remodeling is well established. However, the involvement of the endosomal TLRs is unknown. Here we study the effect of combined blocking of TLR7 and TLR9 on post-interventional remodeling and accelerated atherosclerosis.

Methods and Results In hypercholesterolemic APOE*3Leiden mice femoral artery cuff placement led to strong increase of TLR7 and 9 presence, demonstrated by immunohistochemistry (IHC). Blocking TLR7/9 with a dual antagonist in vivo reduced neointimal thickening and foam cell accumulation 14d after surgery by 65.6% (p=0.0079). Intima/media ratio was reduced by 64.5%, and luminal stenosis by 62.8%. The TLR7/9 antagonist reduced the arterial wall inflammation, with reduced macrophage infiltration, decreased cytoplasmic High Mobility Group Box1 expression and altered serum IL10 levels. Stimulation of cultured macrophages with TLR7 and TLR9 ligands enhanced TNF α expression, which is decreased by TLR7/9 antagonist co-administration. Additionally, the antagonist abolished the TLR7/9 enhanced LDL uptake. The antagonist also reduced oxLDL induced foam cell formation, most likely not via decreased influx but via increased efflux, since CD36 expression was unchanged whereas IL-10 levels were higher (36.1 \pm 22.3pg/ml vs. 128.9 \pm 6.6pg/ml; p=0.008).

Conclusion, blocking TLR7 and TLR9 reduced post-interventional vascular remodeling and foam cell accumulation indicating TLR7 and TLR9 as novel therapeutic targets.

Introduction

Post-interventional remodeling is a critical determinant of long-term efficacy of Percutaneous Coronary Interventions (PCI). Restenosis is characterized by acute elastic recoil and intimal hyperplasia due to inflammation, smooth muscle cell proliferation and extracellular matrix turnover.¹ Under hypercholesterolemic conditions this is accompanied by influx and accumulation of low-density lipoprotein (LDL) cholesterol in the vessel wall that becomes oxidized and taken up by macrophages. Thereby these macrophages become foam cells and initiate a process of accelerated atherosclerosis.² Previously, we and others described an important causal role for extracellular Toll-like Receptors (TLRs) in post-interventional remodeling. It has been shown that TLR4 and the Myd88-dependent pathway play an important role in restenosis and postinterventional accelerated atherosclerosis³⁻⁶. Similarly a crucial role for TLR 2 has been described⁷

TLRs as part of the innate immune system are pattern recognition receptors (PRR) known to recognize exogenous ligands that originate from bacteria or viruses as well as endogenous ligands. These endogenous ligands may be released after tissue damage or cell stress, processes that may be initiated by PCI. Myd88-dependent signaling is the dominant activation pathway of TLR signaling leading to NF κ B activation and upregulation of several pro-inflammatory cytokines. Since TLR2 and TLR4 are known to be expressed on the cell surface of vascular cells and activated in vascular disease processes via Damage-Associated Molecular Patterns (DAMPs) as endogenous ligands, such as Heat Shock Proteins, Fibronectin-EDA, Tenascin C and High Mobility Group Box1 (HMGB1)⁸⁻¹¹, research in the cardiovascular field mainly focused on TLR2 and TLR4.

Little is known about the role of endosomal TLRs that are mostly studied for their recognition of viral/bacterial DNA and RNA fragments and were originally considered absent in the healthy arterial vessel wall.¹² Activation of endosomal TLRs like TLR7 and TLR9 may lead to up regulation of IFN α , IL-6, IL-12 or TNF α by innate immune cells, e.g. macrophages. Recently, increased TLR7 mRNA was found in atheroma of human carotids.¹³ Moreover TLR9 was also found in human atherosclerotic plaques¹⁴ and arterial cells were responsive to TLR9 ligand.¹⁵ Interestingly, it has been suggested that these receptors may also recognize self DNA/RNA that is exposed after cell stress and damage causing a sterile inflammatory reaction.¹⁶⁻¹⁹ TLR7 and TLR9 have also been shown to recognize immune complexes containing self nucleic acids in autoimmune diseases.^{16, 20} PCI is considered to cause severe damage to the endothelium allowing influx of lipids and inflammatory cells into the vessel wall. Concurrently, deeper layers in the vessel wall experience severe stress and cellular death at the place of intervention may cause a release of self RNA/DNA or proteins that enhance the direct recognition of nucleic acids by intracellular TLRs or binding of these nucleic acids to intracellular TLR signaling regulators such as HMGB1.²¹ Most interestingly, activation of TLR9 is also reported to increase the secretion of HMGB1, the endogenous ligand for TLR4²²

Recently, we have identified a novel class of oligonucleotide-based compounds that act as dual antagonists of TLR7 and TLR9 and inhibit immune responses mediated through these receptors.^{23, 24} In the current study we focus on the therapeutic potential of targeting TLR7 and TLR9 to reduce post-interventional remodeling by preventing neointimal formation and accelerated atherosclerosis. We illustrate the presence and upregulation of TLR7 and TLR9 and their co-localization with macrophages/foam cells in a murine model for neointimal formation and accelerated atherosclerosis. A causal role of the TLR7/9 was studied in a murine model for postinterventional vascular remodeling in hypercholesterolemic APOE*3Leiden

mice by the use of the TLR7/9 antagonist. Furthermore, we studied activation and antagonism of TLR7 and TLR9 on cultured macrophages and on foam cell formation using a novel TLR7/9 dual antagonist.

Material and methods:

For a detailed description of all materials and methods used see the online supplement (available online at <http://atvb.ahajournals.org>).

In brief, non-constricted polyethelene cuffs were placed around the femoral arteries as a well-established model for neointima formation and accelerated atherosclerosis in hypercholesterolemic ApoE3Leiden mice. Immunohistochemistry for TLR7 and TLR9 was performed on paraffin embedded sections of cuffed arteries of hypercholesterolemic ApoE3Leiden mice at t=0 and t=14. A TLR7/TLR9 dual antagonist was synthesized and specificity was determined. We studied its effect on neointima formation and accelerated atherosclerosis in hypercholesterolemic APOE*3Leiden mice after femoral arterial cuff placement by injecting the antagonist biweekly to get sufficient TLR7/9 blockade. Intimal lesions were analysed for CD45, MAC3 and HMGB1 by immunohistochemistry. The antagonist was used to study the effect of blocking of TLR7/9 on macrophage activation and lipid accumulation in macrophages. Cytokine levels of TNF α , IP-10, IL6, IL12 and IL10 were quantified by ELISA.

Results

Arterial injury leads to TLR7 and TLR9 presence in the vessel wall

Little is known about the presence of TLR7 and TLR9 in the vessel wall after surgical intervention. Using immunohistochemical analysis, we explored whether TLR7 and TLR9 are expressed in cuffed remodeled arteries with neointimal lesions after 14d and in non-cuffed arteries of hypercholesterolemic APOE*3Leiden mice, since TLR expression may differ amongst different arterial segments and also in response to vessel damage^{12, 13}. Cuff placement for 14d provoked severe neointimal thickening and showed presence of TLR7/9 profoundly in the tunica media of these arterial segments. Presence of either TLR7 or TLR9 could not be observed in non-cuffed femoral arteries (Figure 1A-D). Lesions in cuffed arteries of wild type mice on a chow diet that consist dominantly of vascular smooth muscle cells were also negative for TLR7 and TLR9 (Supplemental figure I AB). Negative controls showed no staining (Supplemental Figure I C). The area with positive staining for both TLRs contained many macrophages while in mice with a normal cholesterol these lesions do hardly show any of these cells. (Supplemental figure I DE)

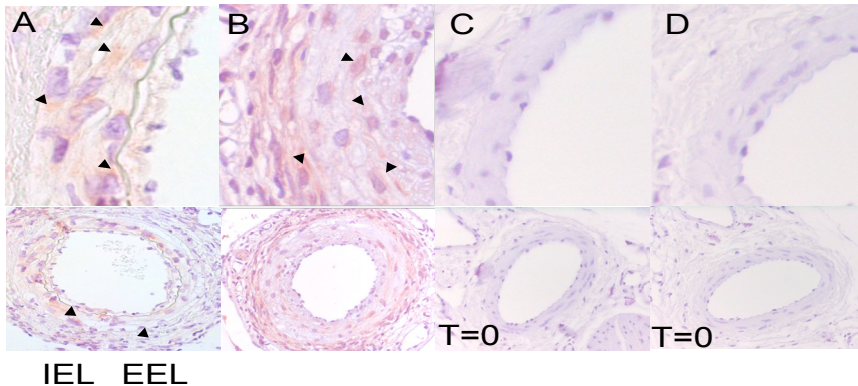


Figure 1: TLR expression in injured femoral artery lesions of hypercholesterolemic APOE3*Leiden mice. TLR7 expression (A) and TLR9 expression on femoral arteries with neointima 14 days after cuff placement (B). Non-cuffed femoral arteries stained for TLR7 (C) and TLR9 (D). IEL= Internal Elastic Lamina. EEL= External Elastic Lamina.

Inhibition of TLR7- and TLR9-mediated immune responses by antagonist

Splenocytes cultured with 0.01 to 10 μ g/ml of the dual TLR7/9 antagonist in combination with TLR3, TLR4, TLR7 or TLR9 agonist. The antagonist showed a dose dependent reduced production of TNF, IL6 and IP-10 upon either TLR7 or TLR9 activation. Activation of TLR4, the most robust signaling TLR, was not affected. Also cytokine production via activation of intracellular TLR3, that recognizes double-stranded RNA, was not affected by the antagonist. (Supplemental figure II A-D) Culturing of splenocytes with the antagonist alone did not induce cytokine production (not shown). Administration of either TLR7 or TLR9 agonists alone to mice resulted in elevated inflammation indicated by increased levels of serum IL-12. Mice administered with antagonist prior to TLR7 or TLR9 agonist administration displayed lower levels of serum IL-12. TLR7/9 antagonist alone did not induce IL-12 expression, suggesting it does not induce immune responses. At the dose used, antagonist showed about 64% and 85% inhibition of TLR9 and TLR7 agonist induced IL-12 in mice, respectively.

(Supplemental figure III). Control oligo showed no inhibition of either TLR7- or TLR9-mediated immune response in mice (Figure 2).

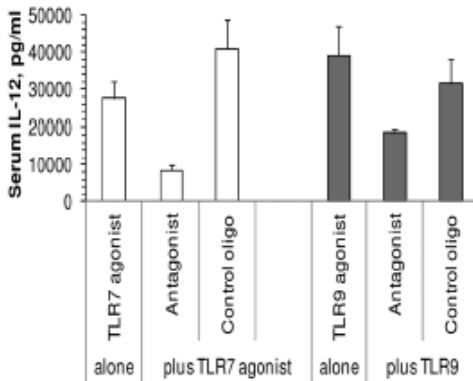


Figure 2: Antagonist or control oligo was injected at 5 mg/kg, s.c. in the left flank of 6-8 week old female C57BL/6 mice (n=2/group). RNA-based TLR7 agonist at 10 mg/kg, s.c. or TLR9 agonist at 0.25 mg/kg, s.c. was injected 48 hr later in the right flank. Two hours post TLR agonist administration, blood was collected and serum IL-12 level was determined by ELISA. TLR7 or TLR9 agonist alone was used as a positive control. Data shown are representative of at least two independent experiments.

TLR7/9 antagonist reduced neointima formation and accelerated atherosclerosis

After detecting TLR7 and TLR9 presence in remodeled arteries we focused on vascular remodeling. By in vivo administration of the antagonist the causal involvement of TLR7/9 activation in intimal hyperplasia and accelerated atherosclerosis was assessed in hypercholesterolemic APOE*3Leiden mice that underwent femoral arterial cuff placement, a widely applied model for restenosis. These mice were fed a Western-type diet, starting 3 weeks before surgery to induce hypercholesterolemia and are well known to develop intimal lesions due to neointima formation and accelerated atherosclerosis. No significant difference in plasma total cholesterol levels was detected before surgery (control 9.3 ± 0.60 mmol/L, TLR7/9 antagonist 9.0 ± 0.46 mmol/L), nor had antagonist-treated mice significant altered cholesterol levels compared to control mice after 14 days at sacrifice (control 8.4 ± 0.4 mmol/L, TLR7/9 antagonist 7.7 ± 0.8 mmol/L). HPS stained sections were used to study vessel wall composition and showed a profound neointima formation with foam cell formation, which was clearly reduced in the antagonist treated group. After quantification, we observed reduction in neointima formation of 66% (n=9 vs. n=7) ($5838 \pm 1158 \mu\text{m}^2$ vs. $2008 \pm 223 \mu\text{m}^2$, $p=0.0079$) a beneficial intima/media ratio ($0.473 \pm 0.09 \mu\text{m}^2$ vs. $0.168 \pm 0.018 \mu\text{m}^2$, $p=0.0021$) and a reduction in percentage of lumen stenosis of 64% ($33.9 \pm 6.6\%$ vs. $12.5 \pm 2.9\%$, $p=0.0021$) after administration of antagonist biweekly. No differences in total vessel wall area or media area were found (Figure 3A-G). In addition we found a difference in IL10 serum levels that were significantly higher in the antagonist treated mice 14 days after cuff placement (0.43 vs 15.46 pg/ml, $p=0.0003$) (supplemental figure IV). At sacrifice the antagonist treated mice had a higher number of circulating Ly6C^{low} monocytes compared to PBS treated controls (supplemental figure V). In the lesions of the antagonist treated mice, a reduced number of macrophages (MAC-3 positive cells) was observed (figure 3). This difference may be due to reduced infiltration of the vessel wall by the circulating monocytes since the expression of adhesion molecule CD11b was decreased on the cells of the antagonist treated mice (Figure 3H). Non-specific oligonucleotide administration not only had no effect on the number of circulating (Ly6C^{low}) monocytes or CD11b expression compared to PBS treatment, it also did not affect neointima formation (Figure 3I,J).

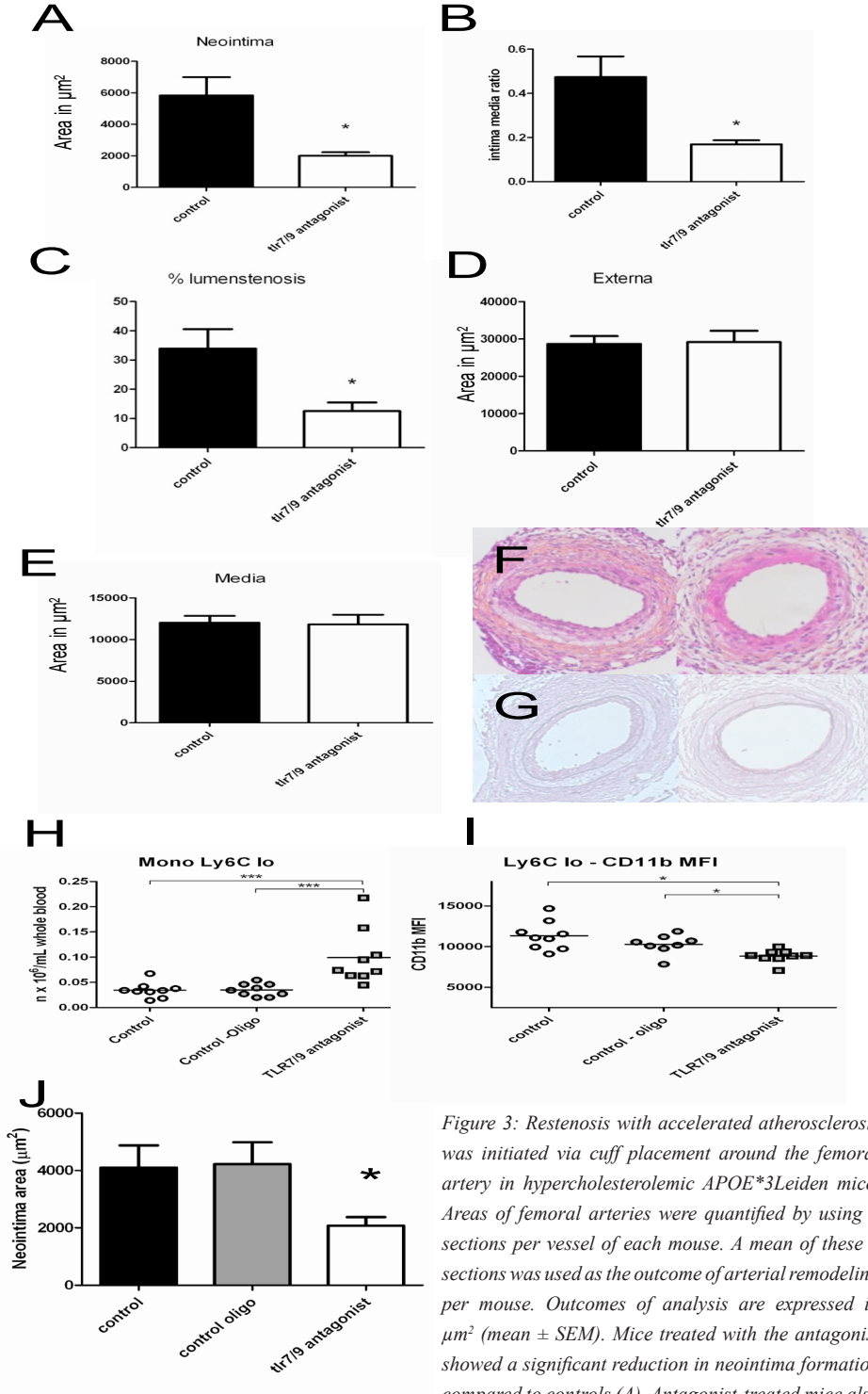


Figure 3: Restenosis with accelerated atherosclerosis was initiated via cuff placement around the femoral artery in hypercholesterolemic APOE*3Leiden mice. Areas of femoral arteries were quantified by using 6 sections per vessel of each mouse. A mean of these 6 sections was used as the outcome of arterial remodeling per mouse. Outcomes of analysis are expressed in μm^2 (mean \pm SEM). Mice treated with the antagonist showed a significant reduction in neointima formation compared to controls (A). Antagonist-treated mice also

showed a decrease in percentage of lumen stenosis (B) and a beneficial intima/media ratio (C). Neither total vessel wall area, nor media area was altered (D-E). Representative Hematoxylin-Phloxine-Saffron (HPS) (F) and Weigert's Elastin (G) stained cross-sections of control mice and antagonist-treated mice 14d after cuff placement. Number of circulating $Ly6c^{Low}$ monocytes (corrected for total white blood cell count) (H). Expression of adhesion molecule $CD11b$ on $Ly6c^{Low}$ monocytes (I) Neointima formation of cuffed mice treated with PBS, control-oligo and TLR7/9 antagonist (J). * = $P < 0.05$ Statistical analysis was performed by use of a non-parametric Mann-Whitney test, * =

TLR7/9 blockade reduced macrophage/foam cell positive area

As stated above we observed a significant reduced MAC-3 positive area. This was the case in both media ($2445 \pm 327 \mu m^2$ vs. $661 \pm 199 \mu m^2$, $p = 0.002$) as well as neointima ($268 \pm 59 \mu m^2$ vs. $26 \pm 9 \mu m^2$, $p = 0.003$) indicating less infiltration of macrophages that are importantly involved in the remodeling process.

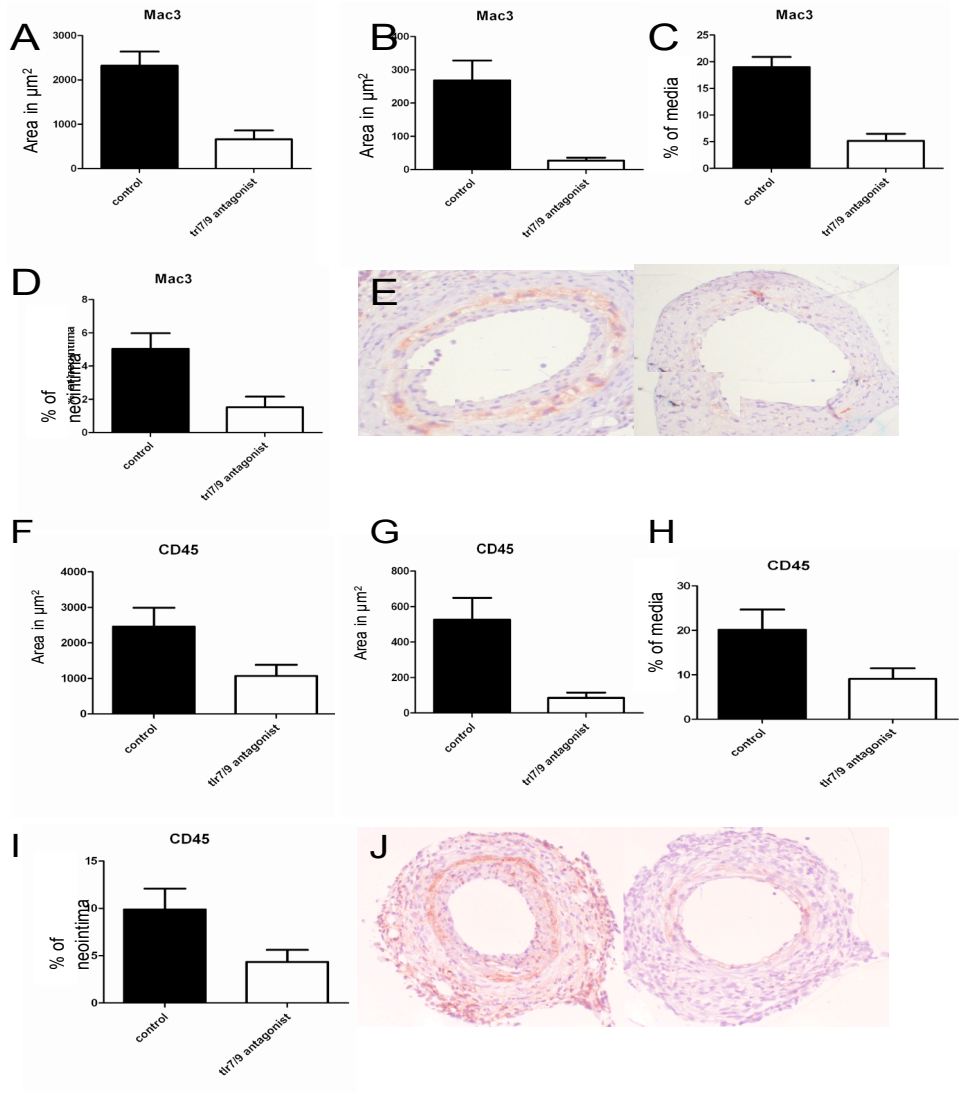


Figure 4 (previous page): Lesion composition after treatment with TLR7/9 antagonist in hypercholesterolemic APOE*3Leiden mice. Sections were stained for Mac3 and CD45. Positive staining in areas of femoral arteries was quantified by using 6 sequential sections per artery of each mouse. A mean of positive staining of these 6 sections was used as the outcome of positive immuno staining per mouse. Outcomes of analysis are expressed in μm^2 (mean \pm SEM) and percentage of area of either media or neointima. Macrophage infiltration was significantly reduced in the antagonist treated group compared to the controls in both neointima (A) as well as media (B). Percentage of positive staining for Mac3 was reduced in this group in both media (C) and neointima (D). Representative pictures of control mice and antagonist treated mice (E). Leukocyte infiltration in the antagonist treated group compared to the controls in media (F) as well as neointima (G). Percentage of positive staining for CD45 in the media (H) and neointima (I). Representative pictures of CD45 stained sections of control mice and antagonist treated mice (J). Statistical analysis was performed with a non-parametric Mann Whitney test * = $P < 0.05$

The percentage of positive area was also significantly reduced indicating a reduction of positive cells per μm^2 in both media as well as in the formed neointima. We also checked whether the effects observed in vivo could be related to the accumulation of total leukocytes in the lesions. Therefore, we quantified the area of the vessel segments that was positive for CD45, a pan-leukocyte marker. Vessels of the antagonist-treated mice showed a trend towards a reduced CD45 positive area which was significant in the neointima (Figure 4A-J).

TLR7/9 blockade reduced cytoplasmic High Mobility Group Box 1

Layers in the vessel wall undergo severe stress upon intervention. Together with our finding of a significant decrease in macrophages we searched for presence of cytoplasmic or extra-cellular HMGB1 that is a marker of cell stress and macrophage activation. HMGB1 can be directly up regulated by TLR9 activation and is an important TLR7/9 signaling regulator and an endogenous TLR2/4 ligand. Kalinina et al previously showed that HMGB1 could be detected in atherosclerotic plaques. Furthermore the showed that this was dominant in macrophages and that in these macrophages there was a markedly increase of HMGB1 in the cytoplasm²⁵. Therefore we performed analysis for the presence of cytoplasmic HMGB1 in the arterial wall. Since TLR7/9 was predominately expressed in the tunica media, were most macrophages/foam cells were present, the media area of the vessel segments that was positive for HMGB1 outside the nucleus was quantified. We found a significant decrease in percentage of positive cytoplasmic HMGB1 in the media area of mice treated with antagonist ($12.97 \pm 1.03\%$ vs. $7.80 \pm 1.28\%$, $p = 0.011$) (Figure 5A-C). This is of special interest, since HMGB1 release is increased upon TLR7/9 activation, regulates TLR7/9 signaling and is known to function as an endogenous ligand for TLR2 and TLR4 (Figure 5A-C)

TLR7/9 blockade reduced macrophage pro-inflammatory cytokine production upon TLR7/9 activation

Macrophage activation and foam cell accumulation play a crucial role in lesion formation and accelerated atherosclerosis development after cuff placement. As we found less macrophages and HMGB1 after blocking TLR7/9 we studied the effects of modulation of the TLR7/9 signaling in cultured Bone Marrow Derived (BMD) macrophages. BMD macrophages were cultured for 7d and then stimulated with either TLR7 ligand imiquimod, TLR9 ligand CpG-ODN or a combination of both for 24hours. Activation was monitored by analysis of TNF α expression, a key pro-inflammatory cytokine also known to be regulated in vivo after cuff placement.²⁶ Co-administration of TLR7/9 ligands with the antagonist caused a significant reduction in production of TNF α while LPS induced production of TNF α was not altered by the antagonist (Figure 6A)

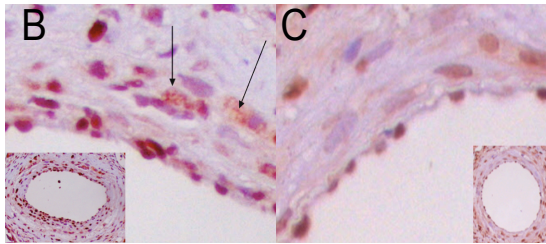
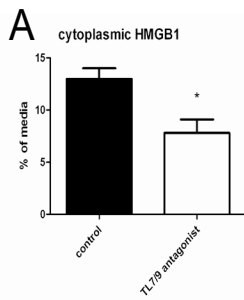


Figure 5: Presence of cytoplasmic HMGB1 in the injured vessel wall of hypercholesterolemic ApoE3*Leiden mice, 14d after surgery. Sections were stained for HMGB1. Positive staining in areas of femoral arteries was quantified by using 6 sequential sections per artery of each mouse. A mean of positive staining of these 6 sections was used as the outcome of positive immuno staining per mouse. Outcome of cytoplasmic HMGB1 analysis in percentage (mean±SEM) of area of media (A). Representative pictures of HMGB1 staining in control mice (B) and antagonist-treated mice (C). Statistical analysis was performed with a non-parametric Mann Whitney test * = $P < 0.05$.

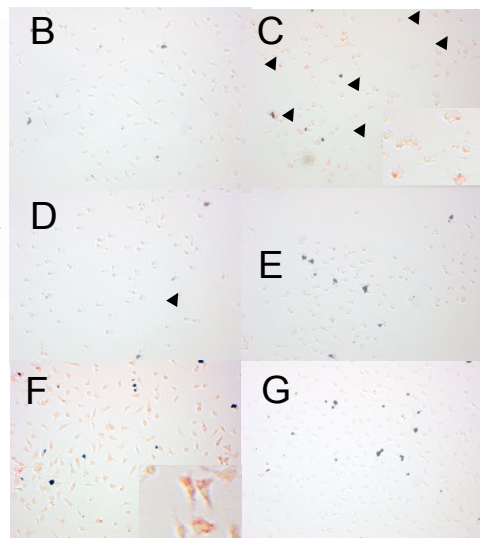
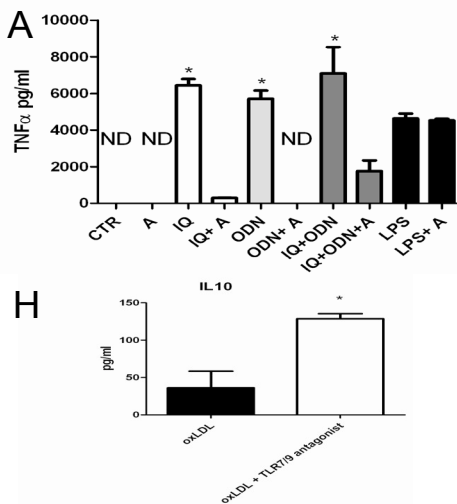
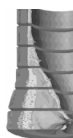


Figure 6: Bone marrow-derived macrophages cultured with imiquimod (IQ) as a ligand for TLR7, CpG-ODN as a ligand for TLR9 or TLR7/9 antagonist for 24hours. IQ and CpG induced macrophage activation. Use of the TLR7/9 antagonist caused a decrease in TNF α production. TLR4 (LPS) induced activation was not altered by the antagonist. (A) Foam cell formation was studied on cultured macrophages in the presence of either empty medium, native LDL, imiquimod (IQ), IQ + LDL, IQ + LDL + antagonist. All wells were screened for positive Oil-Red-O (ORO) staining and representative pictures are shown. Macrophages with native LDL showed no lipid uptake after staining with ORO (B). Positive staining in the presence IQ with native LDL (C). IQ + LDL + antagonist (D). IQ (E). Foam cell formation independent of direct TLR activation was studied on cultured macrophages in the presence of oxLDL or oxLDL + antagonist. All wells were screened for positive Oil-Red-O (ORO) staining and representative pictures are shown. Macrophages with oxLDL showed lipid uptake after staining with Oil Red O (ORO) (F) but only a few positive spots in the presence of TLR7/9 antagonist (G). Analysis by ELISA showed a significant difference in IL10 levels in the presence of TLR7/9 antagonist (H) A students *t*-test was used for statistical analysis, * = $P < 0.05$.



TLR7/9 blockade reduced foam cell formation by macrophages

Additionally to the direct effect of pro-inflammatory cytokine excretion by macrophages we looked to effect on lipid accumulation by macrophages since both processes are very important in post-interventional remodeling. Since macrophage-induced cytokine production and foam cell formation are major contributors to neointima formation and accelerated atherosclerosis, we studied whether TLR7 activation in combination with native LDL could induce lipid uptake by macrophages as was shown previously for TLR9. Reduced TLR9 activation was previously described to be important in foam cell formation via oxidation of native LDL cholesterol that normally is not capable of causing foam cell formation.²⁷ Furthermore we were interested in whether our antagonist could block this process efficiently like it did on inflammation with only the agonists. Presence of native LDL with TLR7 stimulation alone caused lipid accumulation shown by positive Oil-Red-O (ORO) staining in the macrophages while native LDL cholesterol alone showed no staining at all (figure 6A+B). The use of antagonist showed a clear reduction in lipid uptake and thus foam cell formation indicated by less intracellular ORO staining in the fixed macrophages (Figure 6B-E). TLR9 activation and blockade in the presence of LDL gave the same results and was described previously^{27, 28} (data not shown).

Foam cells, formed by oxLDL uptake of macrophages, die releasing lipids, intracellular molecules and necrotic debris which can further activate the remaining macrophages via endosomal receptors like TLR7/TLR9²⁹. Therefore we cultured macrophages in the presence of oxLDL cholesterol (Figure 6F) and to check whether the antagonist also could influence this lipid accumulation if we combined oxLDL administration with the antagonist. ORO staining was found in the oxLDL treated macrophages while combination with the antagonist showed only a few slightly positive cells (figure 6F+G). To see if this effect was dependent on influx or efflux of lipids we analyzed expression of scavenger receptor CD36 and IL10 production. CD36 scavenger receptor expression was not different (positive CD36 macrophages; control 41.48% vs antagonist 41.32%) (supplemental figure V) however we noticed significant change in IL10 levels (figure 6G) indicating effects on lipid efflux while IL-10 enhances lipid efflux via the PPARgamma-LXR-ABCA1/ABCG1 pathway³⁰.

Discussion

The present study describes the role of a novel TLR7/9 dual antagonist in restenosis and accelerated atherosclerosis in mice. Individual presence of both TLR7 and TLR9 was noticed in femoral arteries of hypercholesterolemic APOE*3Leiden mice with neointimal lesions and accelerated atherosclerosis after 14d. These have to be infiltrating cells e.g macrophages while normal arteries or arterial lesion from normal mice that consist dominantly of VSMC stained negative for both TLRs and macrophages. In vivo administration of antagonist showed a significant reduction in neointima formation with a beneficial intima/media ratio in hypercholesterolemic APOE*3Leiden mice. Moreover, blockade of TLR7/9 signaling led to a reduction in CD45 and Mac3 positive cells in both media as well as in the neointimal lesions and we notice a decrease in cytoplasmic HMGB1 indicating a decrease in cellular stress and a difference in serum IL10. In vitro, macrophages showed a significant increase in TNF α production upon TLR7 or TLR9 activation that was reduced after receiving TLR7/9 dual antagonist. Administration with TLR7 ligand imiquimod or TLR9 agonist CpG caused lipid accumulation in macrophages that could be sufficiently blocked by the antagonist. Moreover oxLDL induced foam cell formation was inhibited by antagonist possibly via upregulation of IL-10.

Previously, we and others described involvement of TLR2 and TLR4 in post interventional neointima formation.^{3, 6, 7} Recently, a protective role for intracellular receptor TLR3, important in recognition of double stranded RNA, was found in vascular remodeling.³¹ Neointima formation due to post interventional remodeling is strongly mediated by local activation and physiological changes, such as increased wall stress, cell damage and inflammation. In the present study, we were able to notice presence of TLR7 and TLR9 in post interventional remodeled arteries whereas non-cuffed vessels show no presence of these TLRs at all. This can probably be related to leukocytes that express these TLRs and infiltrate the vessel wall due to the damage of the intervention such as macrophages and start to clear apoptotic cells and infiltrated lipids. The level of TLR expression may vary among different vessel specimens and may be influenced by these changes.¹² Other studies in addition to the present showed TLR7 expression in atheroma of carotids¹³ and TLR9 presence in human atherosclerotic plaques¹⁴ that may be activated via unmethylated CpG motifs from bacteria.³² Furthermore, DNA from 17 different bacterial genera that can activate TLR9 were found in atherosclerotic carotids¹⁵, together indicating a possibly important contribution of these PRRs to vascular remodeling.

Blocking TLR7/9 signaling by antagonist strongly inhibited neointima formation thereby reducing the percentage of lumen stenosis. Neointima formation is strongly mediated by smooth muscle cell (SMC) proliferation/migration and macrophage activation and lipid uptake. Since TLR7/9 presence could not be detected in undamaged arteries it is unlikely that there is a direct activation of SMC. However, indirect activation of SMC is still possible via cytokines produced by leukocytes which express these TLRs. Our results may be explained, at least in part, by the difference in IL-10 production. On the other hand TLR7 and TLR9 stimulation by their ligands cause a strong increase in the upregulation of TNF α , which is important in post-interventional vascular remodeling, indicating a direct influence of TLR7/9 activation on inflammation. This response was nicely blocked by the antagonist in macrophages. Furthermore, we observed lower levels of HMGB1 in the cytoplasm after cuff placement in the antagonist treated mice, thereby reducing its effect via direct activation of TLR2/4 and activation of intracellular TLRs via its binding to their nucleic acid ligands.^{21, 33} Moreover, there were significantly less numbers of macrophages/foam cells present in media as well as neointima.

Activation of TLR7/9 leads to NF κ B-mediated upregulation of pro-inflammatory cytokines. Furthermore, it is known that TLR9 activation causes release of nuclear HMGB1 that may become available in the cytoplasm or even outside the cell where it is known to act as TLR2 and TLR4 ligand and was seen in macrophages in atherosclerotic plaques.^{22, 25, 33, 34} Not only can this release be initiated upon cell stress but also activated macrophages are capable of releasing HMGB1.^{34, 35} Previously we were able to detect HMGB1 in remodeled vein grafts in and outside the nucleus.⁴ Upon cuff placement we noticed presence of HMGB1 in the cytoplasm as well. Others previously showed that CpG-ODN stimulates macrophages to secrete HMGB1 and extracellular HMGB1 is known to accelerate the delivery of CpG-ODNs to its receptor, leading to a TLR9-dependent enhancement of IL-6, IL-12, and TNF α .²² Interestingly, HMGB1 is also known as a regulator of TLR7/9 signaling itself since the absence of HMGBs also severely impairs the activation of TLR3, TLR7 and TLR9 by their cognate nucleic acids.²¹ Therefore these intracellular TLRs are thought to play a very important role in autoimmune and other inflammatory diseases.^{20, 21} Our data confirm causal involvement of TLR7 and TLR9 in vascular-related diseases and development of a novel TLR7/9 dual antagonist may have important implications for understanding and treatment



of exacerbation periods of other inflammatory diseases such as rheumatoid arthritis and after vascular interventions that cause direct vessel damage.

Blocking TLR7/9 signaling leads to a reduction in inflammation and reduced lipid accumulation. The role for TLR7/9 may therefore indicate regulation of cell stress and thereby providing activation of e.g. macrophages to start scavenging lipids, dying cells and attracting more leukocytes to the inflammatory hazard. Our results confirm macrophage activation via TLR7/9 ligands and show a decrease of the presence of macrophages in the vessel wall after cuff placement in the TLR7/9 antagonist-treated mice.

Several studies have demonstrated the effect of intracellular TLR activation on lipid uptake^{27, 28, 36, 37}. Both TLR7 and TLR9 agonists cause up regulation of adipocyte differentiation-related protein that is involved in lipid droplet formation in macrophages.³⁸ TLR9 was previously described to be involved in foam cell formation via up regulation of NOX1, LOX1 and Perilipin 3.^{27, 28} This foam cell formation was NF κ B and IRF7 dependent and can be countered via LXR activation.³⁷ Both NF κ B and IRF7 are also very important mediators of TLR7 signaling and additionally we show that TLR7 stimulation in the presence of LDL leads to lipid uptake in macrophages. Our data show that blocking of TLR7 receptor results in no lipid uptake in macrophages that receive only LDL. Interestingly, the antagonist was capable of decreasing lipid accumulation of oxLDL in macrophages probably via IL-10. This might be due to altered efflux of lipids rather than decreased influx since CD36 expression is not altered whereas IL10, like in vivo, is upregulated. Macrophage IL-10 is known to enhance the efflux of cholesterol.³⁰ Different mechanisms, directly related to TLR signaling, can be involved in changes IL10 levels. Martin et al. showed that GSK3 can differentially regulate TLR mediated cytokine production³⁹. In the normal TLR activation situation there is little PI(3)K stimulation and GSK3 primarily remains constitutively active promoting the expression of IL12. Alternative situations, with different pathogenic stimuli or blocking antagonists (small molecule inhibitors, RNA inhibitors), can lead to TLR dependent activation of PI(3)K and thereby inhibition of GSK3 that causes a decrease in IL-12 production and an increase in IL10 production. Woodgett and Ohashi have provided a nice overview about this GSK3 in TLR signaling.⁴⁰ Alternatively it was previously described that TLR4 activation can cause an increase of HMGB1 in macrophages and that this HMGB1 is capable of reducing IL10 levels⁴¹. Oxidized LDL triggers inflammatory signaling through a heterodimer of TLR 4 and TLR6. Assembly of this newly identified heterodimer is regulated by signals from the scavenger receptor CD36⁴². Foam cells die releasing lipids, intracellular molecules and necrotic debris which can further activate the remaining macrophages via endosomal receptors like TLR7/TLR9²⁹. While HMGB1 can also be upregulated via TLR9 activation and it further enhances TLR7/9 activation this might be a mechanism that cause the differences seen in IL10 levels. Previously it was already shown on regulatory T cells that additional TLR9 activation could inhibit IL10 synthesis⁴³. Further studies are needed to fully elucidate the mechanisms causing differences in IL10 levels in the relation to TLR signaling and blockade. In summary, we observed upregulation of TLR7/9 expression during arterial restenosis and reduced macrophage activation and foam cell formation after TLR7/9 blockade which was accompanied with increase in IL-10 production. Additional blocking of TLR7/9 leads to a reduction in neointima formation, increased IL10 production, reduced macrophage presence in the lesions as well as less HMGB1 release, indicating the important role of TLR7 and TLR9 in post-interventional remodeling via reducing inflammation as well as lipid accumulation thereby making it an interesting therapeutic target to reduce restenosis and accelerated atherosclerosis after vascular intervention.

Acknowledgements

This work was supported by the Dutch Top Institute Pharma (project D1-101) (JCK) and the Research Program of the BioMedical Materials Institute (HABP).

Disclosures

JCK, MME, KLLH, MRdV, HABP, AMOR, HCdB, JFH, JK, JWJ, PHAQ; none
ERK; vice president Discovery, Idera Pharmaceuticals
NLM; vice president Biology, Idera Pharmaceuticals

Reference List

1. Pires NM, Jukema JW, Daemen MJ, Quax PH. Drug-eluting stents studies in mice: do we need atherosclerosis to study restenosis? *Vascul Pharmacol* 2006;44:257--264.
2. Lardenoye JH, Delsing DJ, De Vries MR, Deckers MM, Princen HM, Havekes LM, van Hinsbergh VW, van Bockel JH, Quax PH. Accelerated atherosclerosis by placement of a perivascular cuff and a cholesterol-rich diet in ApoE*3Leiden transgenic mice. *Circ Res* 2000;87:248--253.
3. Hollestelle SC, De Vries MR, Van Keulen JK, Schoneveld AH, Vink A, Strijder CF, Van Middelaar BJ, Pasterkamp G, Quax PH, de Kleijn DP. Toll-like receptor 4 is involved in outward arterial remodeling. *Circulation* 2004;109:393--398.
4. Karper JC, De Vries MR, van den Brand BT, Hoefler IE, Fischer JW, Jukema JW, Niessen HW, Quax PH. Toll-Like Receptor 4 Is Involved in Human and Mouse Vein Graft Remodeling, and Local Gene Silencing Reduces Vein Graft Disease in Hypercholesterolemic APOE*3Leiden Mice. *Arterioscler Thromb Vasc Biol* 2011;31:1033--1040.
5. Michelsen KS, Wong MH, Shah PK, Zhang W, Yano J, Doherty TM, Akira S, Rajavashisth TB, Ardit M. Lack of Toll-like receptor 4 or myeloid differentiation factor 88 reduces atherosclerosis and alters plaque phenotype in mice deficient in apolipoprotein E. *Proc Natl Acad Sci U S A* 2004;101:10679--10684.
6. Vink A, Schoneveld AH, van der Meer JJ, Van Middelaar BJ, Sluijter JP, Smeets MB, Quax PH, Lim SK, Borst C, Pasterkamp G, de Kleijn DP. In vivo evidence for a role of toll-like receptor 4 in the development of intimal lesions. *Circulation* 2002;106:1985--1990.
7. Schoneveld AH, Oude Nijhuis MM, van MB, Laman JD, de Kleijn DP, Pasterkamp G. Toll-like receptor 2 stimulation induces intimal hyperplasia and atherosclerotic lesion development. *Cardiovasc Res* 2005;66:162--169.
8. Arslan F, Smeets MB, Riem Vis PW, Karper JC, Quax PH, Bongartz LG, Peters JH, Hoefler IE, Doevendans PA, Pasterkamp G, de Kleijn DP. Lack of fibronectin-EDA promotes survival and prevents adverse remodeling and heart function deterioration after myocardial infarction. *Circ Res* 2011;108:582--592.
9. Hochleitner BW, Hochleitner EO, Obrist P, Eberl T, Amberger A, Xu Q, Margreiter R, Wick G. Fluid shear stress induces heat shock protein 60 expression in endothelial cells in vitro and in vivo. *Arterioscler Thromb Vasc Biol* 2000;20:617--623.
10. Li W, Sama AE, Wang H. Role of HMGB1 in cardiovascular diseases. *Curr Opin Pharmacol* 2006;6:130--135.
11. Midwood K, Sacre S, Piccinini AM, Inglis J, Trebaul A, Chan E, Drexler S, Sofat N, Kashiwagi M, Orend G, Brennan F, Foxwell B. Tenascin-C is an endogenous activator of Toll-like receptor 4 that is essential for maintaining inflammation in arthritic joint disease. *Nat Med* 2009;15:774--780.
12. Pryshchep O, Ma-Krupa W, Younge BR, Goronzy JJ, Weyand CM. Vessel-specific Toll-like receptor profiles in human medium and large arteries. *Circulation* 2008;118:1276--1284.
13. Edfeldt K, Swedenborg J, Hansson GK, Yan ZQ. Expression of toll-like receptors in human atherosclerotic lesions: a possible pathway for plaque activation. *Circulation* 2002;105:1158--1161.
14. Niessner A, Sato K, Chaikof EL, Colmegna I, Goronzy JJ, Weyand CM. Pathogen-sensing plasmacytoid dendritic cells stimulate cytotoxic T-cell function in the atherosclerotic plaque through interferon-alpha.

- Circulation* 2006;114:2482--2489.
15. Erridge C, Burdess A, Jackson AJ, Murray C, Riggio M, Lappin D, Milligan S, Spickett CM, Webb DJ. Vascular cell responsiveness to Toll-like receptor ligands in carotid atheroma. *Eur J Clin Invest* 2008;38:713--720.
 16. Boule MW, Broughton C, Mackay F, Akira S, Marshak-Rothstein A, Rifkin IR. Toll-like receptor 9-dependent and -independent dendritic cell activation by chromatin-immunoglobulin G complexes. *J Exp Med* 2004;199:1631--1640.
 17. Kawai T, Akira S. The role of pattern-recognition receptors in innate immunity: update on Toll-like receptors. *Nat Immunol* 2010;11:373--384.
 18. Means TK, Latz E, Hayashi F, Murali MR, Golenbock DT, Luster AD. Human lupus autoantibody-DNA complexes activate DCs through cooperation of CD32 and TLR9. *J Clin Invest* 2005;115:407--417.
 19. Uccellini MB, Busconi L, Green NM, Busto P, Christensen SR, Shlomchik MJ, Marshak-Rothstein A, Viglianti GA. Autoreactive B cells discriminate CpG-rich and CpG-poor DNA and this response is modulated by IFN- α . *J Immunol* 2008;181:5875--5884.
 20. Krieg AM, Vollmer J. Toll-like receptors 7, 8, and 9: linking innate immunity to autoimmunity. *Immunol Rev* 2007;220:251--269.
 21. Yanai H, Ban T, Wang Z, Choi MK, Kawamura T, Negishi H, Nakasato M, Lu Y, Hangai S, Koshiba R, Savitsky D, Ronfani L, Akira S, Bianchi ME, Honda K, Tamura T, Kodama T, Taniguchi T. HMGB proteins function as universal sentinels for nucleic-acid-mediated innate immune responses. *Nature* 2009;462:99--103.
 22. Ivanov S, Dragoi AM, Wang X, Dallacosta C, Louten J, Musco G, Sitia G, Yap GS, Wan Y, Biron CA, Bianchi ME, Wang H, Chu WM. A novel role for HMGB1 in TLR9-mediated inflammatory responses to CpG-DNA. *Blood* 2007;110:1970--1981.
 23. Wang D, Bhagat L, Yu D, Zhu FG, Tang JX, Kandimalla ER, Agrawal S. Oligodeoxyribonucleotide-based antagonists for Toll-like receptors 7 and 9. *J Med Chem* 2009;52:551--558.
 24. Yu D, Wang D, Zhu FG, Bhagat L, Dai M, Kandimalla ER, Agrawal S. Modifications incorporated in CpG motifs of oligodeoxynucleotides lead to antagonist activity of toll-like receptors 7 and 9. *J Med Chem* 2009;52:5108--5114.
 25. Kalinina N, Agrotis A, Antropova Y, DiVitto G, Kanellakis P, Kostolias G, Ilyinskaya O, Tararak E, Bobik A. Increased expression of the DNA-binding cytokine HMGB1 in human atherosclerotic lesions: role of activated macrophages and cytokines. *Arterioscler Thromb Vasc Biol* 2004;24:2320--2325.
 26. Monraats PS, Pires NM, Schepers A, Agema WR, Boesten LS, De Vries MR, Zwinderman AH, de Maat MP, Doevendans PA, de Winter RJ, Tio RA, Waltenberger J, 't Hart LM, Frants RR, Quax PH, van Vlijmen BJ, Havekes LM, van der Laarse A, van der Wall EE, Jukema JW. Tumor necrosis factor- α plays an important role in restenosis development. *FASEB J* 2005;19:1998--2004.
 27. Lee JG, Lim EJ, Park DW, Lee SH, Kim JR, Baek SH. A combination of Lox-1 and Nox1 regulates TLR9-mediated foam cell formation. *Cell Signal* 2008;20:2266--2275.
 28. Gu JQ, Wang DF, Yan XG, Zhong WL, Zhang J, Fan B, Ikuyama S. A Toll-like receptor 9-mediated pathway stimulates perilipin 3 (TIP47) expression and induces lipid accumulation in macrophages. *Am J Physiol Endocrinol Metab* 2010;299:E593--E600.
 29. Huang Q, Pope RM. Toll-like receptor signaling: a potential link among rheumatoid arthritis, systemic lupus, and atherosclerosis. *J Leukoc Biol* 2010;88:253--262.
 30. Han X, Kitamoto S, Wang H, Boisvert WA. Interleukin-10 overexpression in macrophages suppresses atherosclerosis in hyperlipidemic mice. *FASEB J* 2010;24:2869--2880.
 31. Cole JE, Navin TJ, Cross AJ, Goddard ME, Alexopoulou L, Mitra AT, Davies AH, Flavell RA, Feldmann M, Monaco C. Unexpected protective role for Toll-like receptor 3 in the arterial wall. *Proc Natl Acad Sci U S A* 2011;108:2372--2377.



32. Chen WH, Kang TJ, Bhattacharjee AK, Cross AS. Intranasal administration of a detoxified endotoxin vaccine protects mice against heterologous Gram-negative bacterial pneumonia. *Innate Immunol* 2008;14:269--278.
33. Park JS, Svetkauskaite D, He Q, Kim JY, Strassheim D, Ishizaka A, Abraham E. Involvement of toll-like receptors 2 and 4 in cellular activation by high mobility group box 1 protein. *J Biol Chem* 2004;279:7370--7377.
34. Lotze MT, Tracey KJ. High-mobility group box 1 protein (HMGB1): nuclear weapon in the immune arsenal. *Nat Rev Immunol* 2005;5:331-342.
35. Wang H, Bloom O, Zhang M, Vishnubhakat JM, Ombrellino M, Che J, Frazier A, Yang H, Ivanova S, Borovikova L, Manogue KR, Faist E, Abraham E, Andersson J, Andersson U, Molina PE, Abumrad NN, Sama A, Tracey KJ. HMG-1 as a late mediator of endotoxin lethality in mice. *Science* 1999;285:248--251.
36. Chen S, Sorrentino R, Shimada K, Bulut Y, Doherty TM, Crother TR, Ardit M. Chlamydia pneumoniae-induced foam cell formation requires MyD88-dependent and -independent signaling and is reciprocally modulated by liver X receptor activation. *J Immunol* 2008;181:7186--7193.
37. Sorrentino R, Morello S, Chen S, Bonavita E, Pinto A. The activation of liver X receptors inhibits toll-like receptor-9-induced foam cell formation. *J Cell Physiol* 2010;223:158--167.
38. Feingold KR, Kazemi MR, Magra AL, McDonald CM, Chui LG, Shigenaga JK, Patzek SM, Chan ZW, Lontos C, Grunfeld C. ADRP/ADFP and Mal1 expression are increased in macrophages treated with TLR agonists. *Atherosclerosis* 2010;209:81--88.
39. Martin M, Rehani K, Jope RS, Michalek SM. Toll-like receptor-mediated cytokine production is differentially regulated by glycogen synthase kinase 3. *Nat Immunol* 2005;6:777--784.
40. Woodgett JR, Ohashi PS. GSK3: an in-Toll-erant protein kinase? *Nat Immunol* 2005;6:751--752.
41. El GM. HMGB1 modulates inflammatory responses in LPS-activated macrophages. *Inflamm Res* 2007;56:162--167.
42. Stewart CR, Stuart LM, Wilkinson K, van Gils JM, Deng J, Halle A, Rayner KJ, Boyer L, Zhong R, Frazier WA, Lacy-Hulbert A, El KJ, Golenbock DT, Moore KJ. CD36 ligands promote sterile inflammation through assembly of a Toll-like receptor 4 and 6 heterodimer. *Nat Immunol* 2010;11:155--161.
43. Urry Z, Xystrakis E, Richards DF, McDonald J, Sattar Z, Cousins DJ, Corrigan CJ, Hickman E, Brown Z, Hawrylowicz CM. Ligation of TLR9 induced on human IL-10-secreting Tregs by 1alpha,25-dihydroxyvitamin D3 abrogates regulatory function. *J Clin Invest* 2009;119:387-398.



Supplemental Material and Methods

Animals

All animal experiments were approved by the animal welfare committee of our institute and are performed according to the regulatory guidelines. Ten week old male hypercholesterolemic APOE*3Leiden mice bred in our laboratory were used as previously described elsewhere.¹ Mice were fed a Western-type diet starting three weeks before surgery that was continued throughout the entire experiment. Mice were allocated randomly to different treatment groups. Cholesterol levels were measured one day before surgery and at sacrifice. All mice received water and food ad libitum.

Murine model for neointima formation

Non-constricted polyethylene cuffs were placed around the femoral arteries as a well-established model for neointima formation and accelerated atherosclerosis.¹ Mice were sacrificed 14 days after cuff placement. All mice received a subcutaneous (s.c) injection with either 200µl sterile water (n=9) or 200µl TLR7/9 antagonist (n=7) (15mg/kg dissolved in sterile water) for sufficient blocking of TLR7/9 continuously without infectious complications. The first injection was administered directly after cuff placement and injections were repeated 4 times (schedule of two injection per week) until sacrifice of the mice. Antagonist activity for TLR7 and TLR9 was assessed in six-to-eight-week-old female C57BL/6 mice obtained from Charles River Labs, (Wilmington, MA). Experimental procedures were performed according to the approved protocols and guidelines of the Institutional Animal Care and Use Committee of Idera Pharmaceuticals. Mice (N=2) were injected subcutaneously (s.c.) with 5 mg/kg antagonist. This was followed twenty- four hours later by 0.25 mg/kg TLR9 agonist 2 or 10 mg/kg of an RNA-based TLR7 agonist.³ Two hours post agonist administration, blood was collected by retro-orbital bleeding.

Morphological Quantification

At sacrifice blood was taken for cholesterol measurement and perfusion/fixation was done at 100mmHg with 4% formaldehyde via the left ventricle. Paraffin-embedded cross- sections were stained with either Weigert's Elastin stain or Hematoxylin-Phloxine- Saphrane (HPS) to visualize overall morphology. Six sections (5 µm thick) equally spaced throughout the cuffed segment were used to quantify intimal lesions, media and total vessel size using image analysis software for morphometric analysis (Qwin, Leica, Germany).

Cell cultures and reagents

Macrophages were derived from bone marrow from tibia and femur and seeded at a density of 250.000 cells/well in 6-wells plates and cultured for 7 days in RPMI GlutaMax (Gibco) supplemented with 100U/ml penicillin/streptavidin, 25% Fetal Calf Serum (FCS) and 20mcg/ml M-CSF (Myltec Biotechnologies) as described previously.⁴ Cells were cultured in the presence of the TLR7 agonist imiquimod (5µg/ml, Invivogen), the TLR9 agonist ODN-CpG (10µg/ml, Invivogen), oxLDL 50 mcg/ml or native LDL 50 mcg/ml (Myltec Biotechnologies) and TLR7/9 antagonist (10mcg/ml antagonist, Idera

Pharmaceuticals). All analysis was done on triplicate wells each in three independent experiments. C57BL/6 spleen cells (1x10⁶ cells/ml) were cultured with 0.01 to 10 µg/ml of a TLR7/9 antagonist in combination with 1 µg/ml of a TLR9 agonist (DNA), 200µg/ml of a TLR7 (sRNA) agonist or 50 µg/ml of a TLR4 agonist (LPS) or 1µg/ml TLR3 agonist (Poly I:C). As controls, spleen cells were cultured with medium alone, TLR9, 7, 4 or 3 agonist alone, or highest dose (10 µg/ml) of the TLR7/9 antagonist alone. After 24 hours, culture supernatants were collected and induction of selected cytokines and chemokines was assessed. All analysis was done on triplicate wells each in three independent experiments.

FACS analysis

Circulating monocytes were stained with anti-mouse CD11b (Biolegend 101224) and Ly6C (Bioconnect MCA2389A488). BMD Macrophages (non-stimulated, antagonist, oxLDL or oxLDL+antagonist, 24h) were stained anti-mouse CD36-PE, clone 72-1, isotype Rat IgG2a (Ebioscience) and analyzed by FACS (BDcalibur).

TLR7/9 antagonist

TLR7 and TLR9 antagonist (5'-TGUCG*TTCT-X-TCTTG*CUGT-5'; wherein, G/U are 2'-O-methyl-ribonucleotides, G* is 7-deaza-dG, and X is glycerol linker) was synthesized at Idera Pharmaceuticals on solid support on an automated DNA/RNA synthesizer with phosphorothioate backbone, purified by HPLC, and analyzed. The purity of full-length antagonist was over 93% with the material balance comprised of oligonucleotides shorter than the full-length product (n-1 and n-2) as determined by anion-exchange HPLC, capillary gel electrophoresis and/or denaturing polyacrylamide gel electrophoresis. Sequence integrity was confirmed by MALDI-TOF mass spectral analysis. Antagonist contained less than 0.2 EU/ml of endotoxin, as determined by the Limulus assay (Bio-Whittaker). A novel control oligo was created with similar chemical modulations in the backbone as in our antagonist since these modifications are crucial to the functional activities of the antagonist. The following sequence was used as a control oligo=: 5'-CACCCAAGACAGCAGAAAG-3'; It is a phosphorothioate oligodeoxynucleotide with 2'-O-methyl-ribonucleotides at each end (nucleotides shown in bold).

Assessment of foam cell formation

Foam cell formation was assessed in macrophages that were either stimulated with native LDL 50 mcg/ml or oxLDL 50mcg/ml (Myltec Biotechnologies). Incubation with native LDL was used to study the effect of TLR7 and TLR9 agonists (IQ, and ODN CpG) on lipid accumulation in macrophages, whereas oxLDL was used under conditions where effects the antagonist are studied. Oil-red-O staining of macrophages was used to identify foam cells. Cells were washed with PBS, fixed in 4%formaldehyde and pretreated with 60% isopropanol followed by staining with 1% Oil-Red-O solution (Sigma Aldrich). Cells were washed with 60% isopropanol followed by three times washing with PBS and examined by light microscopy. Foam cell designation required positive Oil-Red-O staining. Each condition was tested in triplicate.

ELISA assays

ELISA assays were performed with cell free supernatant using commercial available kits following the instructions of the manufacturer for TNF α , IL6, IL10 (BD Biosciences) and IP-10 (Ebioscience)

Immunohistochemistry

Paraffin-embedded sections (5 μ m thick) were stained with antibodies against TLR7 (AbD serotec), TLR9 (AbD serotec), CD45 (BD Biosciences), Mac3 (BD Biosciences), HMGB1 (Abcam, Cambridge, United Kingdom) followed by the appropriate secondary antibody (Donkey anti Rabbit, GE Healthcare) (Goat anti Rat, Jackson labs) and incubated with AB complex (Vector laboratories) and were visualized with Novared (Vector laboratories). Slides were counterstained with haematoxylin.

To confirm the specificity of the IHC staining, parallel sections were incubated with 1% PBS/BSA alone without adding the primary antibody or with Rabbit IgG or Rat IgG controls or staining without 1st antibody or staining without the 2nd antibody. Sections were incubated with the secondary antibody, AB complex and were visualized with Novared. Controls were all negative.

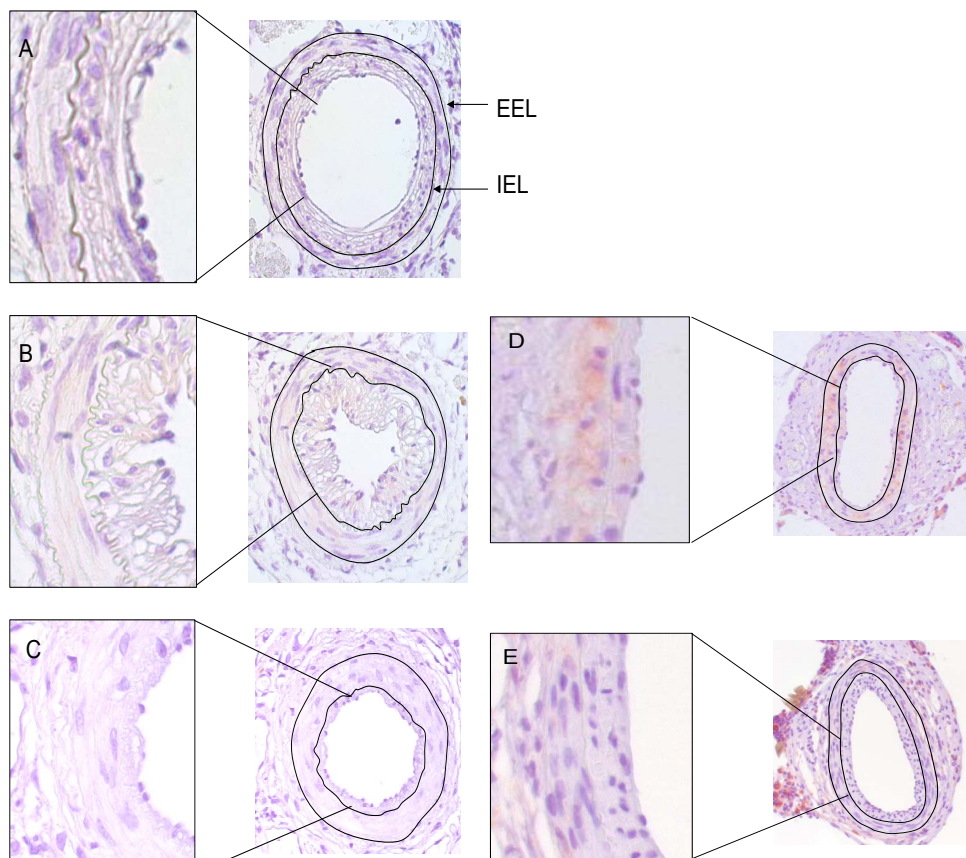
Statistics

For to the animal experiments, values are presented as mean \pm standard error of the mean (SEM). Statistical significance was calculated in SPSS for Windows 17.0. Differences between groups were determined using a non-parametric Mann-Whitney test. In vitro assays are presented as mean \pm standard error of the mean (SEM) and were statistically analyzed with a students T test.

References:

1. Lardenoye JH, Delsing DJ, De Vries MR, Deckers MM, Princen HM, Havekes LM, van Hinsbergh VW, van Bockel JH, Quax PH. Accelerated atherosclerosis by placement of a perivascular cuff and a cholesterol-rich diet in ApoE*3Leiden transgenic mice. *Circ Res* 2000;87:248--253.
2. Yu D, Wang D, Zhu FG, Bhagat L, Dai M, Kandimalla ER, Agrawal S. Modifications incorporated in CpG motifs of oligodeoxynucleotides lead to antagonist activity of toll-like receptors 7 and 9. *J Med Chem* 2009;52:5108--5114.
3. Kalinina N, Agrotis A, Antropova Y, DiVitto G, Kanellakis P, Kostolias G, Ilyinskaya O, Tararak E, Bobik A. Increased expression of the DNA-binding cytokine HMGB1 in human atherosclerotic lesions: role of activated macrophages and cytokines. *Arterioscler Thromb Vasc Biol* 2004;24:2320--2325.
4. Monraats PS, Pires NM, Schepers A, Agema WR, Boesten LS, De Vries MR, Zwinderman AH, de Maat MP, Doevendans PA, de Winter RJ, Tio RA, Waltenberger J, 't Hart LM, Frants RR, Quax PH, van Vlijmen BJ, Havekes LM, van der Laarse A, van der Wall EE, Jukema JW. Tumor necrosis factor-alpha plays an important role in restenosis development. *FASEB J* 2005;19:1998--2004.

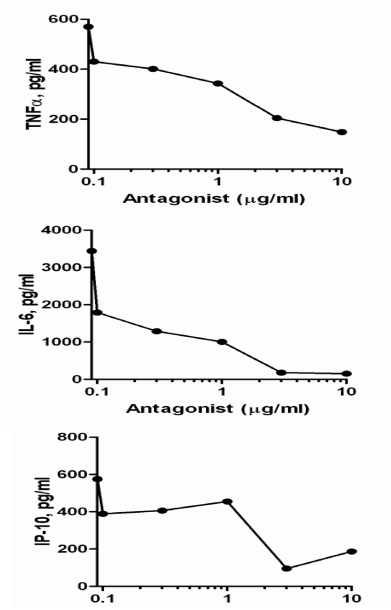




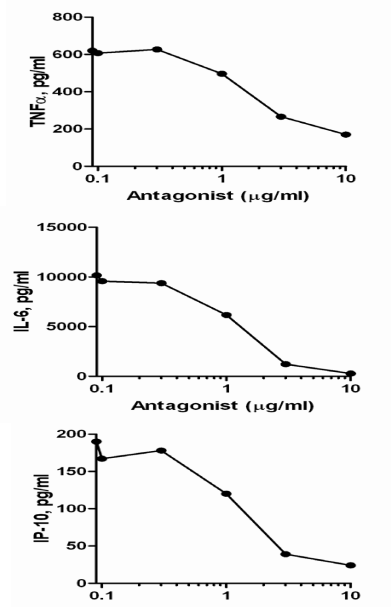
Supplemental figure I: TLR7 staining on arterial lesion of wild type mice (A). TLR9 staining on arterial lesion of wild type mice (B). Example of negative control (C), Macrophage staining in lesions of hypercholesterolemic mice (D) and in wild type mice (E). N= 4 mice per staining; at least 6 sections per mouse were stained for either TLR7 or TLR9.

IEL= Internal Elastic Lamina. EEL= External Elastic Lamina

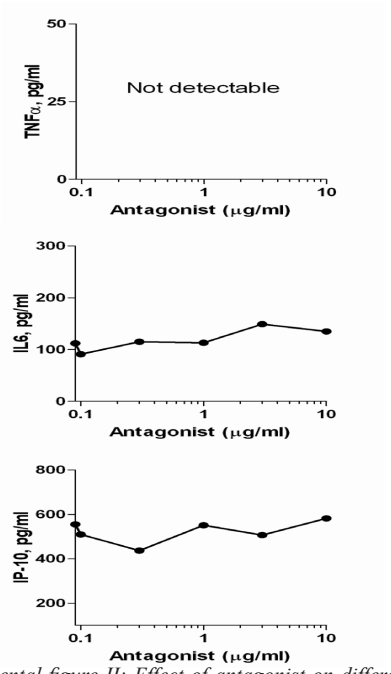
A



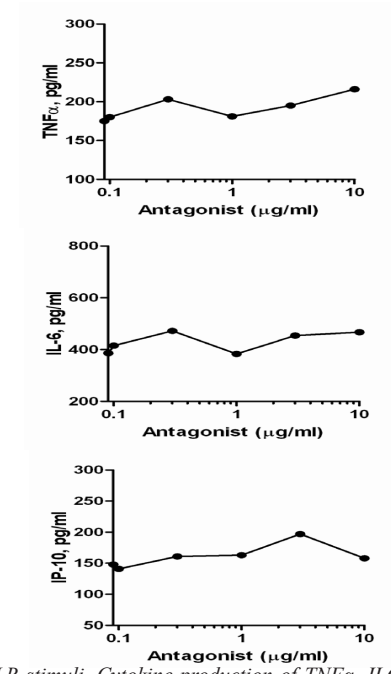
B



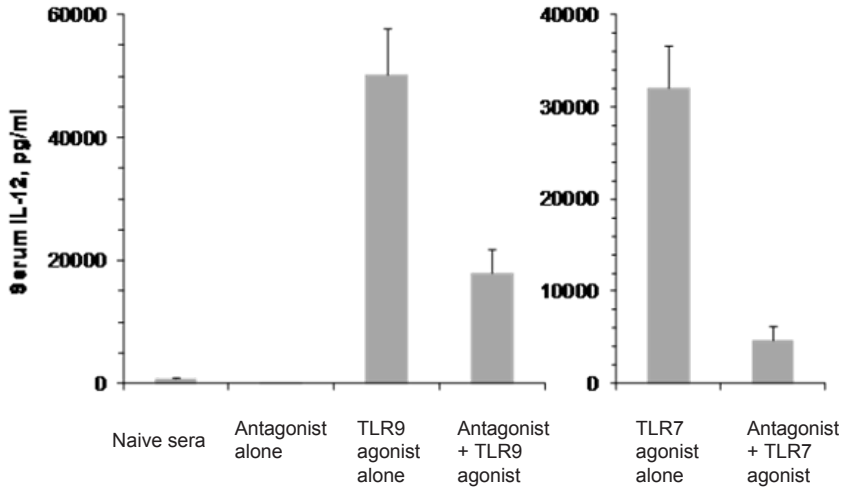
C



D

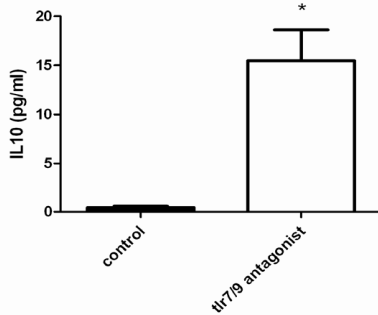


Supplemental figure II: Effect of antagonist on different TLR stimuli. Cytokine production of TNF α , IL6 and IP-10 upon TLR activation in the presence of 0.01 to 10 μ g/ml of the TLR7/9 antagonist. TLR7 agonist IQ+ TLR7/9 antagonist (A), TLR9 agonist ODN-CpG + TLR7/9 antagonist (B), TLR3 agonist PolyI:C + TLR7/9 antagonist (C), TLR4 agonist LPS + TLR7/9 antagonist (D). Data shown is 1 representative experiment out of 3 independent experiments.



Supplemental figure III:

Inhibition of TLR9 and TLR7 agonist induced IL-12 by dual antagonist of TLR7/9 in C57BL/6 mice. Mice (n=2/group) were injected s.c. with 5 mg/kg of antagonist in the left flank and 24 hr later 0.25 mg/kg of TLR9 agonist or 10 mg/kg of TLR7 agonist s.c. in the right flank. Two hours after agonist administration, blood was collected and serum IL-12 levels were measured by ELISA

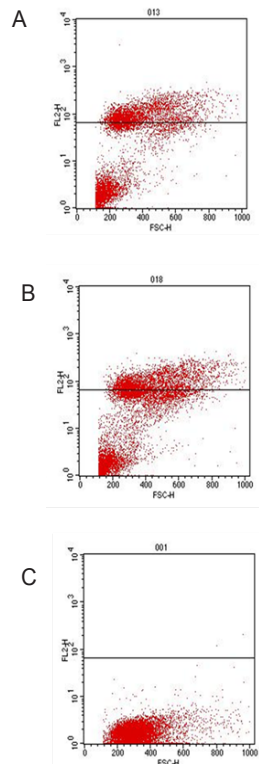


Supplemental figure IV:

Plasma IL10 levels in hypercholesterolemic ApoE3Leiden mice treated with or without TLR7/9 antagonist 14 days after cuff placement. Statistical analysis was performed by use of a non-parametric Mann-Whitney test, * = $P < 0.05$.

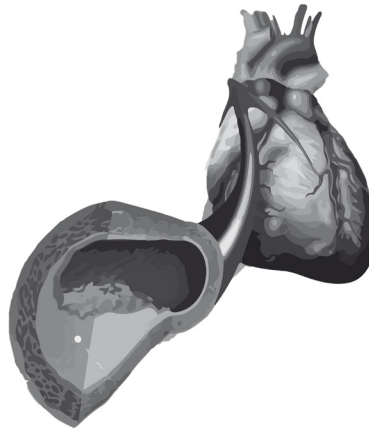
Supplemental figure V (right panel):

FACS analysis of CD36 expression on oxLDL stimulated macrophages. CD36 expression on macrophages stimulated for 24h with either oxLDL (A) and or with oxLDL in the presence of TLR7/9 antagonist (B) Isotype Control (C)





CHAPTER 6



Toll like receptors in vein graft remodeling: protective effects of TLR3 and downstream Interferon regulating factors.

de Vries M.R, Karper J.C*, van der Pouw Kraan T.C, Peters H.A.B, de Jong R.C.M, Hamming J.F, Jukema J.W, Horrevoets A, Quax P.H.*

** both authors contributed equally*

Manuscript in preparation

Abstract

As a part of the innate immunity, Toll like receptors (TLRs) are thought to be important in the inflammatory process of vein graft remodeling. TLR3 activates the MyD88 independent pathway via activation of TRIF and key interferon regulating factors, IRF3 and IRF7, resulting in induction of type I interferons. The aim of this study was to investigate the role of TLR3 pathway constituents on vein graft remodeling.

Methods and Results

Vein grafting was performed by interpositioning the caval vein of a donor mouse in the carotid artery of a receiver mouse and subsequently the vein grafts were harvested at specific time point for further analysis. Pathway analysis by gene set enrichment analysis revealed that in 14 and 28 days old vein grafts of hypercholesterolemic ApoE3Leiden mice the TLR pathway and the type I Interferon pathway belonged to the top 15 of significant regulated pathways. The importance of the type I Interferon pathway is further illustrated by the 2-fold increase in vein graft wall thickening in Tlr3^{-/-} mice compared to control mice (p<0.001). Also Irf3^{-/-} and Irf7^{-/-} mice showed increased vein graft wall thickening (Irf3^{-/-}; 39%, p=0.185, Irf7^{-/-}; 68% p=0.003). Also the outward remodeling increased compared to control mice, resulting in (Tlr3^{-/-}; 52%, p<0.001, Irf3^{-/-}; 26%, p=0.081, Irf7^{-/-}; 42%, p=0.049). Morphologic analysis revealed that Tlr3^{-/-}, Irf3^{-/-} and Irf7^{-/-} mice showed significant more influx of macrophages than the control mice. Expression of typical Type I interferons inducible genes were found decreased in all three strains. In contrast, TNF α and CCL2 were only significantly increased in the Tlr3^{-/-} mice.

Conclusions

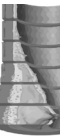
The TLR3 pathway regulates vein graft remodeling in a protective way since Tlr3^{-/-}, as well as the key downstream factors Irf3^{-/-} and Irf7^{-/-} vein grafts show increased vessel wall thickening and outward remodeling. This increased remodeling in the knockout mice is the result of a pro-inflammatory response as reflected by the increase in macrophages and pro-inflammatory cytokines in the vein graft wall.

Introduction

Autologous (saphenous) veins are commonly used as conduits to bypass occlusive atherosclerotic lesions in both coronary and femoral arteries. Unfortunately vein graft failure is a major drawback since, within 10 years, almost half of the patients may again require a form of revascularization. In the patho-physiological processes of vein graft failure, inflammation is considered to be an important accelerating factor 1-5. Toll like receptors (TLRs), part of the innate immune system, are important in inflammatory reactions via their recognition of exogenous pathogen associated molecular patterns (PAMPs) and endogenous damage associated molecular patterns (DAMPs). DAMPs are up regulated by cell death and tissue injury. Previously, we showed that cell death and tissue injury is part of the process of vein graft remodeling in murine vein grafts⁶. In agreement, DAMPs for TLR2 and TLR4, such as the extracellular matrix component EDA (alternatively spliced domain A of Fibronectin), Heat shock protein 60 (HSP60), extracellular matrix protein Biglycan and chromatin protein, high-mobility group protein B1 (HMGB1), are abundantly present in remodeled vein grafts⁷. Furthermore, TLR4 is functionally involved in intimal hyperplasia formation, accelerated atherosclerosis and vein graft remodeling⁷.

The role of other TLRs in vein graft development is currently unknown. Since TLRs have vessel- specific profiles that further vary due to changes in cellular activation and differentiation, and other local processes⁸, it is of particular interest to investigate their role in vein graft remodeling. The Toll like receptor (TLR) family consists of at least 13 members. All TLRs, except TLR3, signal via the myeloid differentiation primary response gene 88 (MyD88 pathway), which drives the induction of the transcription factor nuclear factor kappa-light-chain-enhancer of activated B cells (NFκB) resulting in induction of pro-inflammatory cytokines⁹. TLR3 signals via a MyD88- independent pathway with a central role for the adapter TIR-domain-containing adapter-inducing interferon-β (TRIF) and interferon regulatory factor (IRF)3 and IRF7 resulting in induction of type I interferons (IFNs) (Figure 1).

Interestingly, an unexpected protective role for TLR3 was found on neointima and atherosclerosis formation by Cole et al.¹⁰. Others however, found that TLR3 augments the inflammatory response to nucleic acids. TLR3 ligation also impaired endothelial function and specific deletion of TLR3 in immune cells resulted in reduced aortic inflammation and atherosclerotic burden¹¹⁻¹⁴. One should appreciate that the response to TLR3 stimulation is not uniform, and differs in specific tissue microenvironments⁸. TLR3 responsive genes, Type I IFNs and IFN-inducible genes are involved in bridging innate and adaptive immunity and induction of co-stimulation¹⁵. In viral infections, downstream TLR3 transcription factors IRF3 and IRF7 are the most important factors that control the expression of type I IFNs. IRF3 signaling results in early induction of the *Ifnb* gene, whereas IRF7 has a pivotal role in the induction of all type I IFN genes¹⁶. The role of Type I interferon (inducible) genes in vascular remodeling however, is unclear. Like most TLRs, TLR4 activation leads to an inflammatory profile resulting in augmentation of lesion formation and remodeling^{17, 18}. TLR4 signaling however depend on both the MyD88 and TRIF pathways for proper functioning^{9, 19}. Upon activation, TLR4 can be internalized into the endosome after which activation of the TRIF pathway follows. This indicates that not only different effects of TLRs are critical in vascular disease but also the importance of the underlying pathways as well as



the presence and/or quantity of endogenous ligands. Therefore it would be important to see if and how TLR3 influences vein graft remodeling. In this study we explored the role the TLR3 pathway by performing vein graft surgery in mice that are deficient in TLR3 and downstream factors IRF3 and IRF7 in comparison with TLR4 and TLR2 deficient mice without further exogenous ligand stimulation.

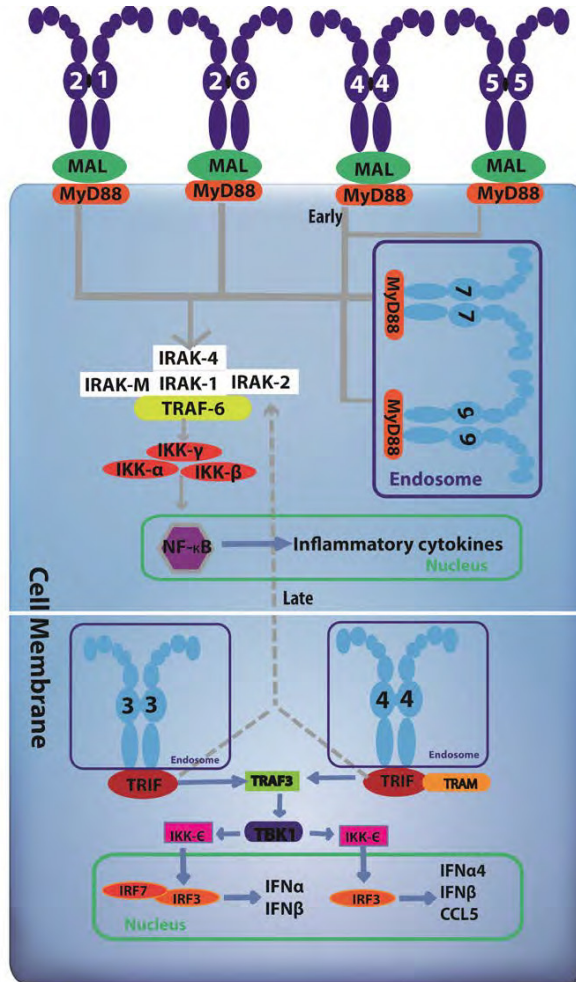


Figure 1. TLR signaling pathways. TLRs signal via specific pathways using transcription factors nuclear factor $\text{NF}\kappa\text{B}$ in the myeloid differentiation factor 88 (MyD88) route and interferon regulating factors IRF3 and IRF7 in the TIR-domain containing adaptor inducing interferon- β (TRIF) signaling route. MyD88 activation occurs upon cell surface signaling (TLR1, TLR2, TLR4, TLR6) using MyD88 adaptor-like (MAL) as an adaptor or via endosomal (TLR7, TLR9) signaling via III receptor-associated kinases, IRAK4, IRAK-M, IRAK1, IRAK2 in interaction with TNF receptor associated factor-6 (TRAF-6). This complex activates an inhibitor of κB kinase (IKK) complex that upon phosphorylation activates nuclear $\text{NF}\kappa\text{B}$ activation resulting in transcription of pro-inflammatory cytokines. TRIF signaling occurs via IRF3, specifically upon TLR3 activation also via IRF7, resulting in activation of Type I IFNs. TRIF signaling can also activate a late activation of $\text{NF}\kappa\text{B}$ as shown by the dotted line.

MATERIALS AND METHODS

Mice

This study was performed in compliance with Dutch government guidelines and the Directive 2010/63/EU of the European Parliament. All animal experiments were approved by the animal welfare committee of the Leiden University Medical Center. For the experiments 10-16 weeks old male mice were used. ApoE3Leiden mice (fed a high cholesterol diet (AB diets)) were bred in the local animal facility. As did the Tlr2^{-/-} and Tlr4^{-/-} that were kindly provided by Dr. Akira (Osaka University, Japan) and the Irf3^{-/-} and Irf7^{-/-} that were kindly provided by Dr. Taniguchi (University of Tokyo, Japan). Control C57BL/6 mice and Tlr3^{-/-} were purchased from Charles River Laboratories.

Vein graft surgery

Vein graft surgery was performed by donor caval vein interpositioning (caval vein of approximately 2 mm length) in the carotid artery of recipient mice as reported previously⁵. Before surgery, mice were anesthetized with midazolam (5 mg/kg, Roche Diagnostics), medetomidine (0.5 mg/kg, Orion) and fentanyl (0.05 mg/kg, Janssen Pharmaceutical). After the procedure the mice were antagonized with atipamezol (2.5 mg/kg, Orion) and fluminasenil (0.5 mg/kg Fresenius Kabi). Buprenorphine (0.1 mg/kg, MSD Animal Health) was given after surgery to relieve pain.

Whole-genome expression

In ApoE3L mice vein graft surgery was performed and mice were sacrificed at time point 3, 7, 14 and 28 days after surgery. From 3-4 mice per time point vein grafts were collected and total RNA was extracted using RNeasy fibrous tissue minikit (Qiagen). RNA integrity was checked by NanoDrop 1000 Spectrophotometer (NanoDrop Technologies) and 2100 Bioanalyzer (Agilent Technologies). For whole-genome expression profiling, amplified biotinylated RNA was generated using the Illumina TotalPrep RNA Amplification Kit. For array analysis, MouseWG-6 v2.0 Expression Beadchips (Illumina) were used. Expression levels were Log₂-transformed and after quantile normalization, transcripts showing background intensity were removed from the analysis. Gene expression levels at the different time points were expressed relative to average t0 levels generating ratios for 23.067 regulated genes.

RNA isolation, cDNA synthesis and RT-PCR

Total RNA was isolated from 10 (20µm thick) paraffin sections of vein grafts 28d after surgery (n=6/strain). RNA was isolated according manufacturers protocol (FFPE RNA isolation kit, Qiagen). Quantitative PCR (Q-PCR) analysis of 84 type I Interferon response-related genes was performed using a RT2 ProfilerPCRArray (SA Biosciences) as per the manufacturer's protocol. The complete list of the genes analyzed is available at http://www.sabiosciences.com/rt_pcr_product/HTML/PAMM-016Z.html. Prior to RT2 profiler array FPPE RNA was reverse transcribed using the RT² First Strand Kit (SA Biosciences). RNA for single Q-PCR was reverse transcribed using a High Capacity RNA-to-cDNA kit (Applied Biosystems). Commercially available TaqMan gene expression assays for hypoxanthine phosphoribosyl transferase (HPRT1), and selected genes were used (Applied Biosystems). All Q-PCRs were performed on the ABI

7500 Fast system. The 2-ΔΔCt method was used to analyze the relative changes in gene expression.



GSEA analysis

Gene set enrichment analysis (GSEA) was performed with the curated gene sets from Kegg, Biocarta, the Reactome and published studies, resulting in a total of 1564 gene sets. For each gene set (pathway) an enrichment score (ES) is calculated²⁰ representing the difference between expected and observed ranking which correlates with the phenotype of the vein grafts at the different time points.

Histological and immunohistochemical assessment of vein grafts

Vein grafts were harvested after perfusion fixation with 4% formaldehyde, fixated for 4 hours and paraffin-embedded. Six consecutive sections (with 150 μm interspace) per vein graft were routinely stained with hematoxylin-phloxine-saffron (HPS) for histological and morphometric analysis (Qwin, Leica). Vein graft thickening or vessel wall area was defined as the area between lumen and adventitia and determined by subtracting the luminal area from the total vessel wall area. Picrosirius red staining was used to visualize collagen content. Antibodies directed at smooth muscle cell actin, TLR3 (Sigma), CD45 (BD Pharmingen) TLR2, IRF3, IRF7 (Abcam), Mac-3 and TLR4 (Santa Cruz) were used for immunohistochemical stainings. For each antibody, isotype-matched antibodies were used as negative controls and staining was absent these sections (data not shown). SMC actin and Sirius red stained sections were quantified by computer assisted analysis (Qwin, Leica). The immuno-positive area measured is expressed as a percentage of the vessel wall area⁵. Vein graft segments were analyzed for influx of leukocytes (CD45) or macrophages (Mac-3) by scoring cells in 6 consecutive sections per mouse in a semi-quantitative manner. 1: < 25 positive cells / section, 2: 25-50 positive cells / section, 3: >50 positive cells.

Statistical analysis

Results are expressed as mean \pm SEM. Data, except for the GSEA, were analyzed by the non-parametric Kruskal-Wallis or Mann-Whitney test using GraphPad Prism. Probability-values <0.05 were regarded significant. GSEA; by permuting the phenotype labels for the ES, a statistical significance (nominal P value) for the ES is provided. An adjustment for the gene set size generated the normalized enrichment score (NES). To correct for multiple testing the proportion of false positives is calculated to provide the false discovery rate (FDR) corresponding to each NES. A combined P-value <0.05 and FDR q-value < 0.05 was considered significant.

Results

TLR pathway and type I Interferon pathway are strongly regulated during vein graft development

To obtain an overview on how TLRs are regulated during vein graft remodeling we analyzed expression of TLRs in hypercholesterolemic ApoE3Leiden mice with help of mRNA array analysis. Most TLRs showed significant up regulation at most time points compared to untreated caval veins (t0) (Figure 2A). Interestingly, TLR3 did not show any regulation in time whereas TLR4 was only significantly up regulated at t3. TLR5 was the only down regulated TLR. We further analyzed whether IRFs were regulated since these are the most prominent transcription factors downstream TLR3. Most IRFs showed regulation as illustrated by Figure 2B; especially IRF 7 was strongly up regulated. To better understand the biologic role of genes regulated in time during vein graft development, we performed pathway analysis by GSEA on 1564 available gene sets. We identified 176 significant up

regulated curated gene sets at t14 compared to uninjured caval veins (t0) whereas 52 gene sets were down regulated at t14. At t28 120 gene sets were significant up regulated and 108 gene sets were down regulated compared to t0. Within the top 15 of significant curated gene sets on both time points besides the expected extracellular matrix organization gene sets, TLR and Type I IFN gene sets can be found in Table 1 illustrating that both pathways are involved in vein graft development.

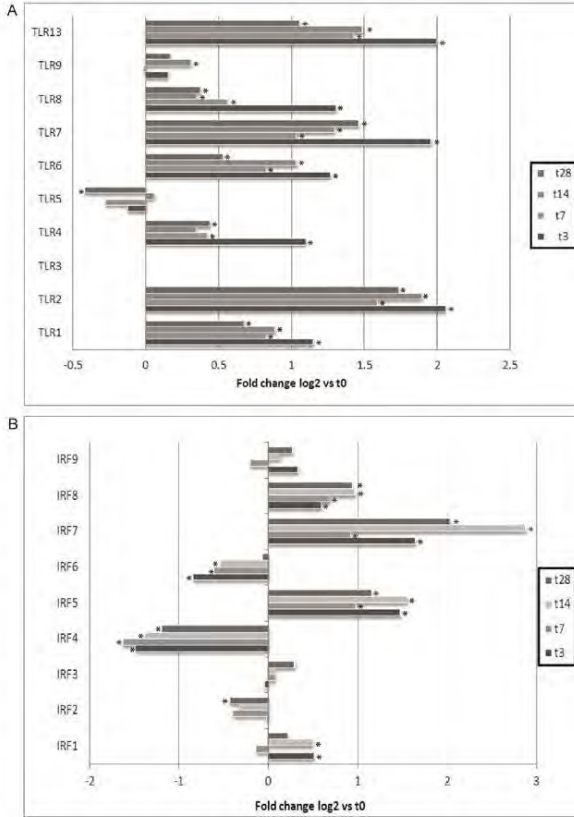


Figure 2. Regulation of TLRs and IRFs during vein graft remodeling. Array analysis of vein grafts in hypercholesterolemic ApoE3Leiden mice was performed on t3, t7, t14 and t28 in comparison to non-injured caval veins (t0). A. Most TLRs show up regulation at all the timepoints. TLR3 is not regulated in time. TLR4 is only significantly regulated at t3 and TLR5 is significantly down regulated at t28. B. IRFs show a diverse pattern in regulation; especially IRF7 is significantly up regulated, whereas IRF3 shows little regulation.

TLR3 deficiency results in enhanced vein graft thickening and outward remodeling

Since TLRs have vessel-specific profiles we first evaluated the expression of TLR3 in native caval veins and 28 day old vein grafts of C57BL/6 mice. Immunohistochemical staining of TLR3 (Figure 3A) revealed that most native caval vein SMCs as well as endothelial cells stained negative for TLR3 (in contrast to the surrounding adipose tissue). In 28 day old C57BL/6 vein graft segments (n=6) almost all inflammatory cells, adventitial fibroblasts and endothelium were found positive whereas SMCs showed diverse staining (Figure 3A). To investigate whether TLR3 might be involved in vein graft remodeling Tlr3-/- (n=9) and control mice (n=10) underwent vein graft surgery. No differences in weight were found between the groups pre- and post-surgery (data not shown). Interestingly, 28 days after surgery Tlr3-/- mice had developed a 2-fold increase in vein graft wall thickness compared to the control mice (figure 3B, E). This was accompanied by a significant increase in total vessel area (figure 3C). Do to this compensatory outward remodeling the lumen area did not deviate between the two groups (figure 3D). Next, we focused on the cellular composition



of the vein grafts. Analyzing the influx of inflammatory cells we detected significant more leukocytes in the Tlr3^{-/-} mice compared to the control group (Figure 3F). Since macrophages are a well-known source of TLRs we also looked at the influx of macrophages. Macrophage numbers were increased in the vein graft wall of the Tlr3^{-/-} mice (Figure 3G). A non-significant increase in SMC positive area was found in the knockout mice. When corrected for the vessel wall thickness (expressed as percentage SMCs in the vessel wall) there was no difference anymore between the Tlr3^{-/-} and control mice (figure 3H, I). A comparable effect was seen with the collagen content; a significant increase in collagen area was measured but corrected for vessel wall area the difference between the groups did not hold (Figure 3J, K).

NAME	SIZE	ES	NES	NOM p-val	FDR q-val
REACTOME_EXTRACELLULAR_MATRIX_ORGANIZATION	71	-0.725713	-2.504256	0	0
REACTOME_COLLAGEN_FORMATION	53	-0.737586	-2.436463	0	0
PID_INTEGRIN1_PATHWAY	63	-0.699737	-2.37663	0	0
KEGG_ECM_RECEPTOR_INTERACTION	74	-0.672714	-2.34805	0	0
KEGG_TOLL_LIKE_RECEPTOR_SIGNALING_PATHWAY	80	-0.647886	-2.318911	0	0
PID_SYNDECAN_1_PATHWAY	42	-0.73605	-2.309036	0	0
MONO_3H_LPS_INDUCED_20FOLD_ATHEROSTUDY	93	-0.630018	-2.299182	0	0
PID_TCR_PATHWAY	58	-0.675494	-2.259791	0	0
PID_INTEGRIN3_PATHWAY	37	-0.725231	-2.216987	0	0
PID_AVB3_INTEGRIN_PATHWAY	68	-0.631874	-2.189979	0	0
PID_CD8TCRPATHWAY	45	-0.673567	-2.189249	0	0
TYPE_I_IFN-INDUCED_GENES_(5-FOLD_BAECHLER)	47	-0.68511	-2.172356	0	0
KEGG_LEISHMANIA_INFECTION	46	-0.68335	-2.16871	0	0
KEGG_CYTOSOLIC_DNA_SENSING_PATHWAY	39	-0.698551	-2.167908	0	0
KEGG_NOD_LIKE_RECEPTOR_SIGNALING_PATHWAY	45	-0.665029	-2.143358	0	2.21E-04
PID_IL12_2PATHWAY	49	-0.653573	-2.139058	0	2.07E-04
KEGG_HEMATOPOIETIC_CELL_LINEAGE	53	-0.648938	-2.130527	0	1.95E-04
REACTOME_PEPTIDE_LIGAND_BINDING_RECEPTORS	77	-0.601486	-2.128913	0	1.84E-04
PID_INTEGRIN_A4B1_PATHWAY	32	-0.704845	-2.123901	0	1.74E-04
PID_UPA_UPAR_PATHWAY	32	-0.701829	-2.109648	0	1.68E-04
SIGN_2-FOLD_UP_IN_NON-CLASSICAL_MONOCYTES_VS_CLASSICAL_MONOCYTES	95	-0.571637	-2.105883	0	1.58E-04
KEGG_NATURAL_KILLER_CELL_MEDIATED_CYTOTOXICITY	70	-0.610491	-2.105352	0	1.51E-04
PID_SYNDECAN_4_PATHWAY	27	-0.735015	-2.095614	0	2.18E-04
REACTOME_GENERATION_OF_SECOND_MESSENGER_MOLECULES	19	-0.808632	-2.093359	0	2.78E-04
KEGG_CYTOKINE_CYTOKINE_RECEPTOR_INTERACTION	149	-0.537514	-2.089821	0	3.96E-04
REACTOME_CHEMOKINE_RECEPTORS_BIND_CHEMOKINES	30	-0.70502	-2.079377	0	5.10E-04
REACTOME_INTERFERON_ALPHA_BETA_SIGNALING	37	-0.674003	-2.078566	0	4.91E-04
PID_P53DOWNSTREAMPATHWAY	94	-0.574843	-2.076997	0	5.95E-04
PID_CXCR4_PATHWAY	85	-0.577559	-2.076992	0	5.74E-04
KEGG_CHEMOKINE_SIGNALING_PATHWAY	130	-0.530859	-2.058034	0	7.77E-04
SIG_REGULATION_OF_THE_ACTIN_CYTOSKELETON_BY_RHO_GTPASES	28	-0.717051	-2.052555	0	7.52E-04
SIGN_2-FOLD_UP_IN_CLASSICAL_MONOCYTES_VS_NON_CLASSICAL_MONOCYTES	147	-0.528166	-2.051414	0	8.88E-04
REACTOME_INTEGRIN_CELL_SURFACE_INTERACTIONS	70	-0.579167	-2.050619	0	8.61E-04
PID_INTEGRIN_A9B1_PATHWAY	22	-0.740254	-2.032393	0	0.001131
REACTOME_PLATELET_ACTIVATION_SIGNALING_AND_AGGREGATION	163	-0.51108	-2.025506	0	0.001245
KEGG_T_CELL_RECEPTOR_SIGNALING_PATHWAY	88	-0.560399	-2.024553	0	0.001303
KEGG_FOCAL_ADHESION	167	-0.505448	-2.019699	0	0.001407
REACTOME_SIGNALING_BY_ILS	86	-0.571797	-2.010214	0	0.001457
REACTOME_TOLL_RECEPTOR_CASCADES	97	-0.54668	-2.00807	0	0.00142
REACTOME_INTERFERON_SIGNALING	106	-0.540974	-2.004522	0	0.001426

Table 1. Top 40 of significantly regulated gene sets in vein grafts of hypercholesterolemic ApoE3Leiden mice 28 days after surgery as analyzed by gene set enrichment analysis (GSEA) with curated gene sets from Kegg, Biocarta, the Reactome and published studies. In red, relevant pathways regarding TLR signaling are shown.

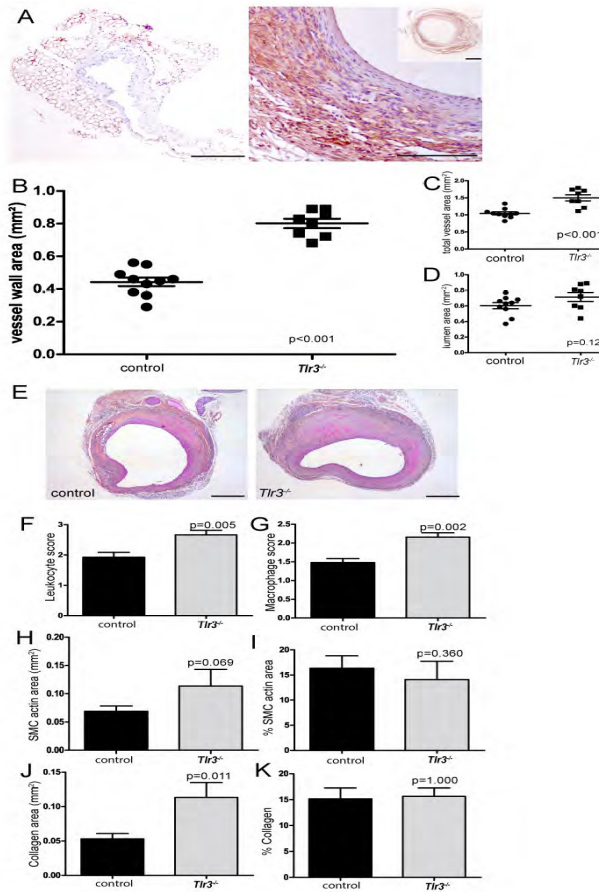
Deficiency of downstream TLR3 factors IRF3 and IRF7 results in aggravated vein graft remodeling.

IRF3 and IRF7 are key regulators of type I IFNs gene expression elicited by virus activated TLR3 signaling. Here we explored the role of these IRFs in vein graft remodeling. To see whether IRF3 and IRF7 are expressed by vascular tissues, we stained caval veins and vein grafts of C57BL/6 mice for both factors. Both cytoplasmic as well as nuclear staining was seen indicating that latent and active forms of IRF3 and IRF7 are available. IRF3 and IRF7 are constitutively expressed by SMC and endothelial cells in caval veins (left panels) and mature vein grafts (right panels). In the vein grafts inflammatory cells also stained positive for both factors. SMCs of remodeled vein grafts showed more intense staining of IRF7 than IRF3. Placement of vein grafts in IRF3^{-/-} mice (n=9) resulted in a trend towards increased

vein graft wall thickening compared to control mice (n=7) although non-significant (p=0.185). Interestingly, IRF7^{-/-} mice (n=8) showed a significant (p=0.003), 68% increase in size compared to controls (Figure 4C, F). Total vessel wall area, as an indicator for outward remodeling, was increased in the IRF7^{-/-} mice (p=0.049) whereas the IRF3^{-/-} showed a non-significant trend (p=0.081) in figure 2D. The lumen in all three groups was not significantly different (Figure 4E). Analysis of the inflammatory aspects of the vein grafts revealed that, in contrast to the Tlr3^{-/-} mice, both the IRF3^{-/-} and IRF7^{-/-} mice showed no significant differences in number of leukocytes compared to the control group (Figure 4G). The macrophage score however was in both the IRF3^{-/-} (p= 0.059) and IRF7^{-/-} (p=0.038) mice increased compared to the control group (Figure 4H). Again as seen in the Tlr3^{-/-} mice no differences in absolute area of SMCs and collagen between the three groups, except for the percentage collagen in the vessel wall which was significantly decreased in IRF7^{-/-} mice (Figure 4I-L).

Figure 3. Deficiency of TLR3 ameliorates vein graft remodeling.

A. TLR3 staining is absent in the vessel wall of native caval veins in C57BL/6 mice except for the surrounding fat tissue (left panel). 28 days after surgery intense TLR3 staining could be observed in the adventitia of vein grafts (C57BL/6) in fibroblasts and inflammatory cells, whereas SMCs in the vessel wall showed a patchy distribution (right panel), inset; overview of vein graft. B. Vein graft surgeries were performed in Tlr3^{-/-} mice (n=9) and control mice (n=10). Tlr3^{-/-} mice showed a 2-fold increase in vessel wall area, 28 days after surgery, compared to the control mice. C. Outward remodeling as scored by the total vessel wall area (D) graph representing the luminal area. E. shows representative photographs of control C57BL/6 and Tlr3^{-/-} mice indicating the differences in vein graft size between the strains. F. The number of infiltrating leukocytes were significantly increased in Tlr3^{-/-} mice (semi-quantitative scored in arbitrary units, 1; <25 cells, 2; 50-100 cells, 3>100 cells). This also accounts for the number of infiltrating macrophages (G) semi-quantitative scored in arbitrary units, 1; <25 cells, 2; 50-100 cells, 3>100 cells. H. Quantitative analysis of the SMCs content (expressed in mm²) did not reveal significant differences between the groups. I. The relative percentage SMCs in the vein graft segments was also not significantly different between the control and Tlr3^{-/-} mice J. Quantitative analysis of the Sirius red staining revealed an increased collagen content in the Tlr3^{-/-} vein grafts. However, when expressed as the relative percentage collagen in the vein grafts, no differences were observed between the groups (K).



A. TLR3 staining is absent in the vessel wall of native caval veins in C57BL/6 mice except for the surrounding fat tissue (left panel). 28 days after surgery intense TLR3 staining could be observed in the adventitia of vein grafts (C57BL/6) in fibroblasts and inflammatory cells, whereas SMCs in the vessel wall showed a patchy distribution (right panel), inset; overview of vein graft. B. Vein graft surgeries were performed in Tlr3^{-/-} mice (n=9) and control mice (n=10). Tlr3^{-/-} mice showed a 2-fold increase in vessel wall area, 28 days after surgery, compared to the control mice. C. Outward remodeling as scored by the total vessel wall area (D) graph representing the luminal area. E. shows representative photographs of control C57BL/6 and Tlr3^{-/-} mice indicating the differences in vein graft size between the strains. F. The number of infiltrating leukocytes were significantly increased in Tlr3^{-/-} mice (semi-quantitative scored in arbitrary units, 1; <25 cells, 2; 50-100 cells, 3>100 cells). This also accounts for the number of infiltrating macrophages (G) semi-quantitative scored in arbitrary units, 1; <25 cells, 2; 50-100 cells, 3>100 cells. H. Quantitative analysis of the SMCs content (expressed in mm²) did not reveal significant differences between the groups. I. The relative percentage SMCs in the vein graft segments was also not significantly different between the control and Tlr3^{-/-} mice J. Quantitative analysis of the Sirius red staining revealed an increased collagen content in the Tlr3^{-/-} vein grafts. However, when expressed as the relative percentage collagen in the vein grafts, no differences were observed between the groups (K).



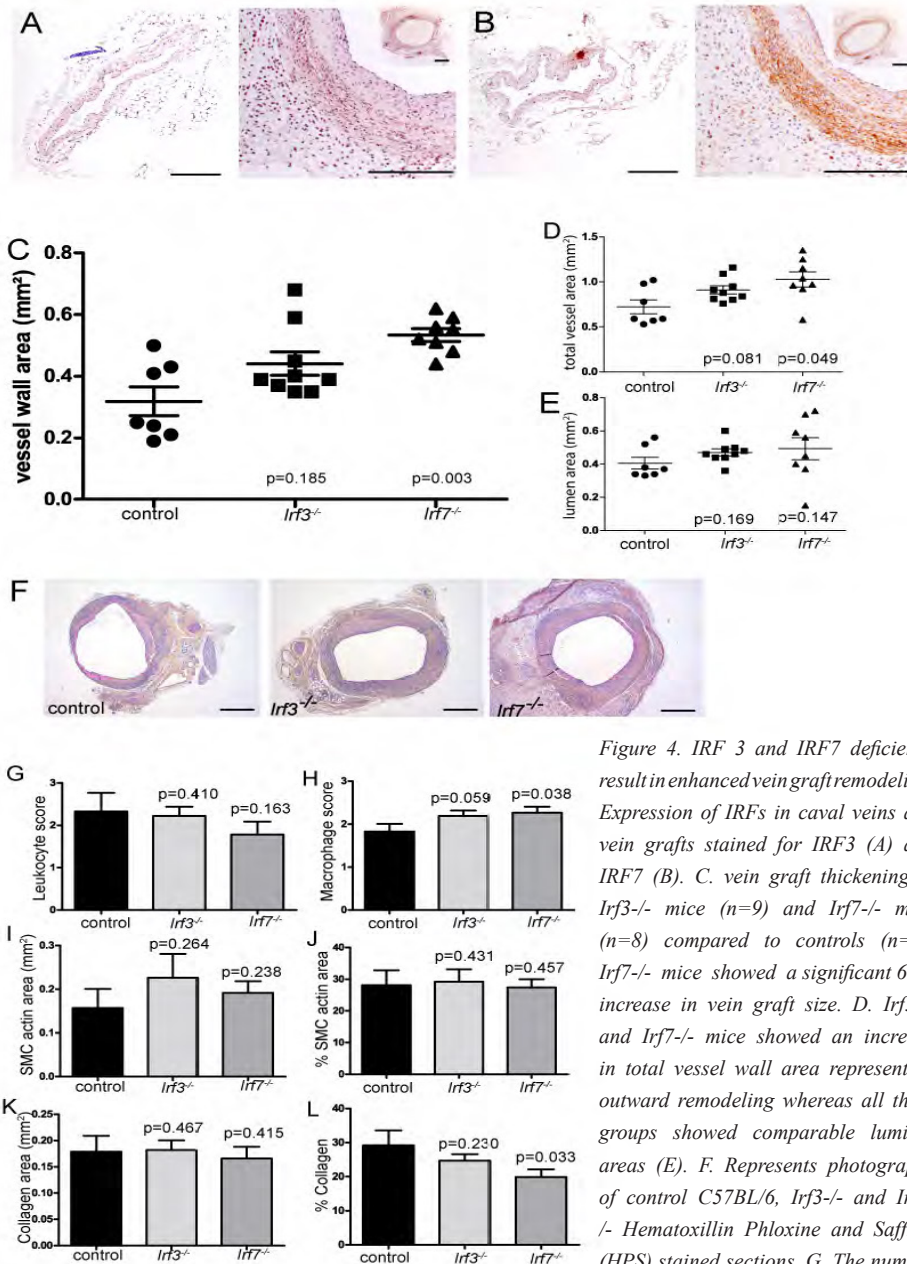


Figure 4. IRF 3 and IRF7 deficiency result in enhanced vein graft remodeling. Expression of IRFs in caval veins and vein grafts stained for IRF3 (A) and IRF7 (B). C. vein graft thickening in *lrf3*^{-/-} mice (n=9) and *lrf7*^{-/-} mice (n=8) compared to controls (n=7). *lrf7*^{-/-} mice showed a significant 68% increase in vein graft size. D. *lrf3*^{-/-} and *lrf7*^{-/-} mice showed an increase in total vessel wall area representing outward remodeling whereas all three groups showed comparable luminal areas (E). F. Represents photographs of control C57BL/6, *lrf3*^{-/-} and *lrf7*^{-/-} Hematoxyllin Phloxine and Saffron (HPS) stained sections. G. The number of infiltrating leukocytes was not significantly different in all groups (semi-quantitative scored in arbitrary units, 1; <25 cells, 2; 50-100 cells, 3>100 cells). H. The number of infiltrating macrophages was significantly increased in *lrf3*^{-/-} and *lrf7*^{-/-} vein grafts (semi-quantitative scored in arbitrary units, 1; <25 cells, 2; 50-100 cells, 3>100 cells). I. Quantification of the SMC content expressed in absolute numbers (mm²) or percentage (J) did not deviate between the groups. J. Quantitative analysis of the collagen content as measured by Sirius red staining, did not deviate between the groups. Whereas the relative percentage collagen in the *lrf7*^{-/-} vein grafts was significant decreased (K).



Deficiency of TLR4 deteriorates vein graft thickening

Besides the well-known MyD88-dependent signaling pathway resulting in activated (pro-inflammatory) genes⁹, TLR4 can signal via downstream pathway factors such as TRIF and IRF3 similar to TLR3, resulting in activation of the *Ifnb* gene. To investigate how the TLR4 pathway is involved in vein graft remodeling we included TLR4 deficient mice in our study. Although we previously showed the inhibiting effects of TLR4 deficiency on vein graft remodeling, that was studied in congenic BALB/c C3H-Tlr4LPS-d mice⁷. It is known that BALB/c mice show a T helper

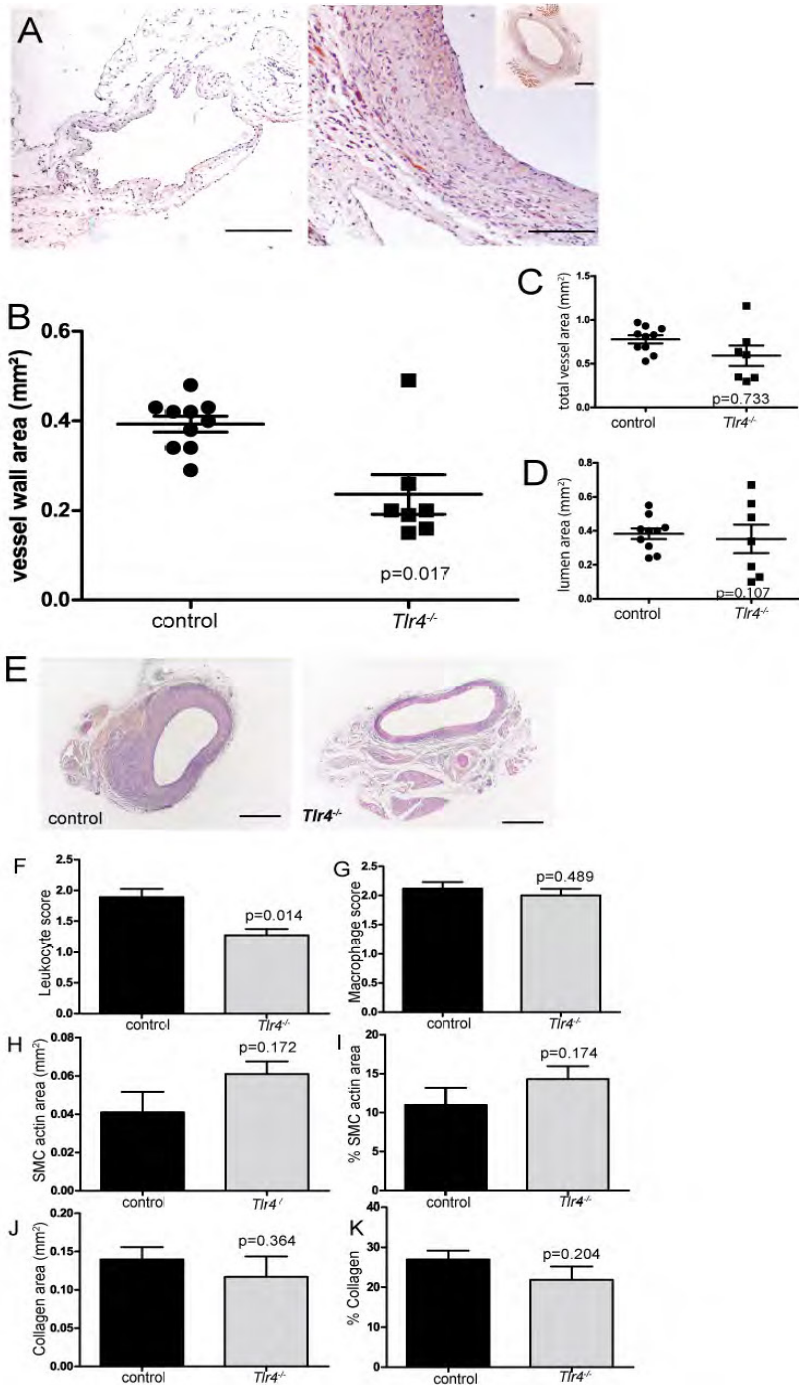
2-like immune response whereas the C57BL/6 mice express a pro-inflammatory Th1-like profile²¹. To enable a fair comparison of the effects of TLR4 deficiency with those of the other TLR and IRF deficient strains and not to linger in Th1/Th2 differences, we performed vein graft surgeries in C57BL/6 mice deficient for TLR4 (n=7) and littermate control mice (n=10). Both groups showed no differences in weight pre- and 28 days post-surgery (data not shown). TLR4 expression was first examined in caval veins and vein grafts in C57BL/6 mice (Figure 5A). Vein graft SMCs as well as endothelial cells and fibroblasts in the adventitia showed pronounced expression of TLR4 whereas native caval veins showed hardly any TLR4 staining. TLR4 deficiency on a C57BL/6 background resulted, in agreement with the C3H-Tlr4LPS-d mice⁷, in a significant 40% decrease in vessel wall area. No significant differences in outward remodeling and lumen area were detected between the groups (Figure 5B-E). The number of CD45 positive cells was significantly decreased in the Tlr4^{-/-} mice whereas no significant difference in macrophage counts could be detected (Figure 5F, G). Additional morphologic quantification revealed that the absolute area and percentage SMCs in the vessel wall did not differ between the Tlr4^{-/-} and control mice (figure 5H, I) nor did the collagen area and percentage collagen (Figure 5J, K)

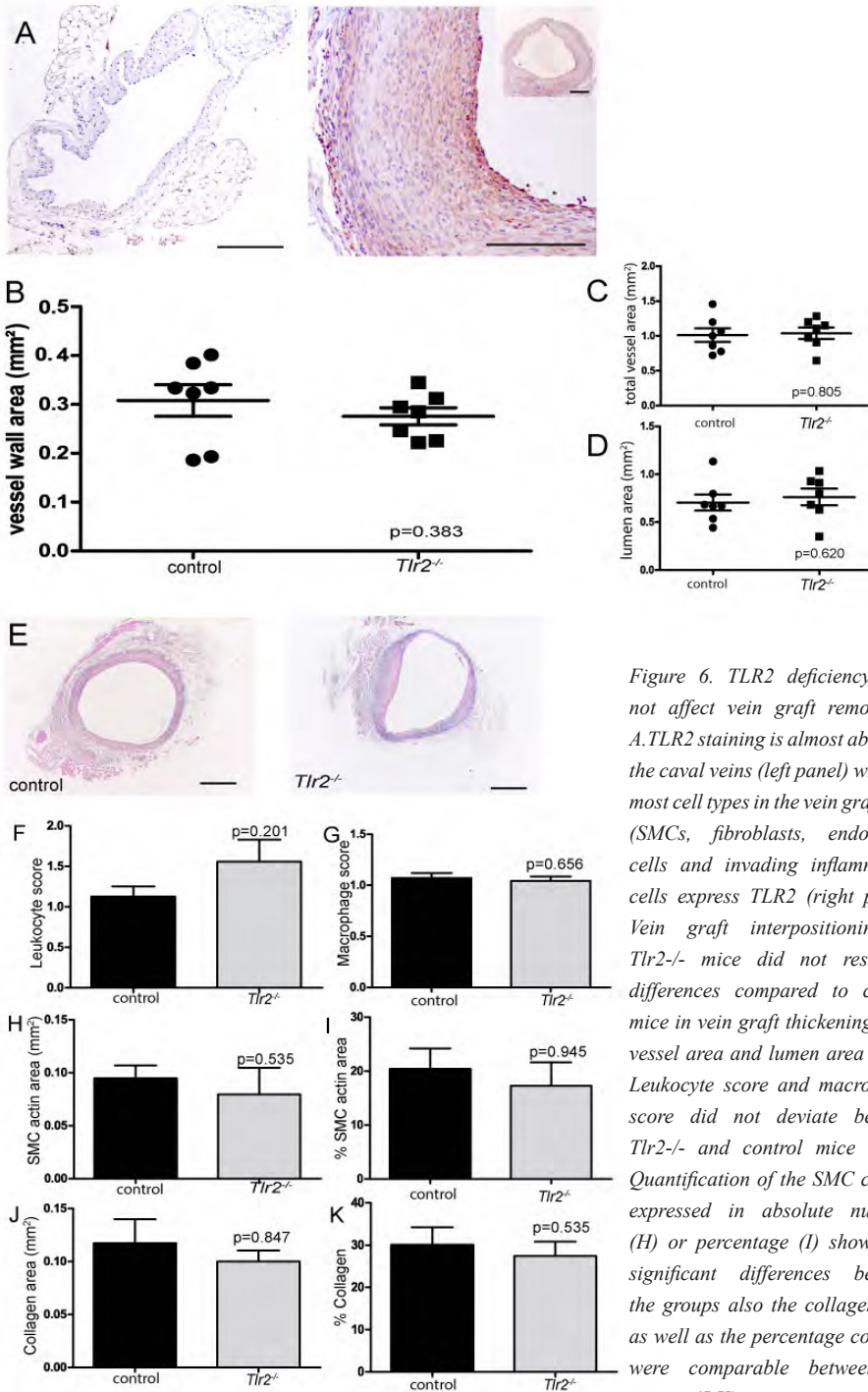
TLR2 does not seem to be crucial in vein graft development

Since the Tlr4^{-/-} mice demonstrated complete opposing remodeling to the Tlr3^{-/-} mice, we wondered if signaling via the MyD88 pathway was primarily responsible for the decrease in vein graft remodeling. Therefore we performed vein graft surgeries in mice that solely signal via the MyD88 pathway: the Tlr2^{-/-} mice. First, we examined the expression of TLR2 in the vein graft segments. Hardly any TLR2 was detectable in caval veins, whereas clear staining of TLR2 was found in infiltrating inflammatory cells, SMCs and endothelial cells in the vein grafts (figure 6A). Next, we performed vein graft surgery on Tlr2^{-/-} and C57BL/6 littermate control mice (n=7). No differences in weight were found pre- and 28 days post-surgery between the two groups (data not shown). Surprisingly, no difference in vessel wall area could be detected between the two groups (Figure 6B, E). Also total vessel area/outward remodeling and lumen area did not deviate either between the groups (Figure 6C and 5D). Leukocyte and macrophage numbers were equal between the groups (Figure 6F, G) while quantification of the smooth muscle cells (SMCs) area as well as percentage in the vessel wall revealed no significant differences between the Tlr2^{-/-} and control mice (figure 6H, I) nor did the area or percentage collagen (Figure 6J, K) deviated between the groups.

Figure 5 (next page). TLR4 deficiency results in decreased vein graft thickening and vascular inflammation. A. In caval veins TLR4 staining was restricted to a few cells, mainly SMCs (left panel). The majority of the SMCs in the vein grafts stained positive as did the inflammatory cells (right panel). B. A significant increase in vein graft thickening was seen in the Tlr4^{-/-} mice. In contrast both total vessel area and lumen area did not deviate between the Tlr4^{-/-} and control mice (C, D). E. representative photographs of vein grafts in Tlr4^{-/-} mice (n=7) and control mice

(n=10), HPS staining. The number of leukocytes was significantly increased in *Tlr4*^{-/-} mice whereas the macrophage score was not different from that of the control mice (F, G). Analysis of the area and percentage SMCs and collagen revealed no significant differences between the groups (H-K).





Type I interferon response genes involved in outward vein graft remodeling

We hypothesized that the outward vein graft remodeling in the TLR3, IRF3 and IRF7 deficient mice were the result of type I interferon (inducible) gene expression profiles. To test this hypothesis we performed a specific RT2 profiler array with 84 type I interferon response genes on pools of Tlr2^{-/-}, Tlr3^{-/-}, Tlr4^{-/-}, Irf3^{-/-}, Irf7^{-/-} and control C57BL/6 vein grafts. A low number of genes were found up regulated in the various knockout mice (Figure 7A). Deficiency of TLR3, IRF3 and IRF7, but unexpectedly also TLR2 deficiency, resulted in a (non-significant) decrease in specific IFN inducible genes such as Ifit1, Ifit3 and Isg15. Also IRF7 and Il6 were decreased expressed in these knockout mice as shown in figure 7B. Remarkably, Tlr4^{-/-} mice hardly expressed regulation of any of these genes.

To assess the effect of TLR and IRF deficiency on inflammatory cytokine expression we explored the gene expression of CCL2, TNF α and Il10 in the various knockout mice. RNA levels of CCL2 (Figure 7C) and TNF α (Figure 7D) were significantly increased in the Tlr3^{-/-} mice. Il10 was up regulated to a lesser extent although non-significant in the Tlr3^{-/-} mice as well as in the Tlr2^{-/-} mice (Figure 7E).

A

Gene Symbol	TLR2 ^{-/-}	TLR4 ^{-/-}	TLR3 ^{-/-}	IRF3 ^{-/-}	IRF7 ^{-/-}
Crp	3.62	3.33	2.66	2.52	6.17
H2-BI	2.56	<2	3.15	3.60	3.79
H2-M10.1	2.56	<2	17.44	3.39	2.62
Met	4.13	<2	2.33	2.13	4.10
MGDC	2.56	<2	3.15	<2	2.02
Ifne	7.75	<2	2.98	<2	5.36
Ifna2	2.56	<2	2.77	<2	2.23
Ifna4	2.60	<2	4.02	2.18	<2
Myd88	<2	<2	4.00	<2	<2
Gbp1	<2	<2	9.48	<2	<2
Il10	<2	<2	2.20	<2	<2
Irf1	<2	<2	3.80	<2	<2
Irf2	<2	<2	2.04	<2	<2
Casp1	<2	<2	2.42	<2	<2
Nos2	<2	<2	3.43	<2	<2
Psme2	<2	<2	2.58	<2	<2
Stat1	<2	<2	2.20	<2	<2
Vegfa	<2	<2	2.87	<2	<2
Sh2d1a	<2	<2	<2	2.57	<2
Ccl5	<2	<2	<2	3.89	<2
Cav1	<2	<2	<2	2.04	<2

B

Gene Symbol	TLR2 ^{-/-}	TLR4 ^{-/-}	TLR3 ^{-/-}	IRF3 ^{-/-}	IRF7 ^{-/-}
Ccl2	-3.13	<2	<2	<2	<2
Cxcl10	-4.91	<2	<2	<2	-9.07
Ifi1	-2.84	<2	-2.09	-3.86	-9.97
Ifi2	-2.32	<2	<2	-3.73	-8.12
Ifi3	-2.35	<2	-2.01	-5.31	-10.27
Il6	-3.97	<2	-3.22	-6.34	<2
Isg15	-2.65	<2	-2.27	-4.01	-8.08
Oas1a	-2.11	<2	<2	<2	-6.86
Oas1b	<2	<2	<2	<2	-4.08
Tlr7	-2.38	<2	<2	<2	<2
Mal	<2	-2.09	-3.39	<2	-2.04
Bst2	<2	<2	-2.03	<2	-2.04
Ifnz	<2	<2	-9.13	<2	<2
Irf7	<2	<2	-2.39	-5.37	-159.22
Sh2d1a	<2	<2	-2.19	<2	-4.63
Tlr3	<2	<2	-3.41	<2	<2
Tlr7	<2	<2	-2.55	<2	<2
Tlr9	<2	<2	<2	<2	-3.15
Ddx58	<2	<2	<2	-2.01	-2.88
If204	<2	<2	<2	-2.04	<2
Ifih1	<2	<2	<2	-3.15	<2
Ifitm2	<2	<2	<2	-2.01	<2
Mx1	<2	<2	<2	-2.28	-20.99
Mx2	<2	<2	<2	-2.87	-5.48
Nos2	<2	<2	<2	-2.12	<2
Oas2	<2	<2	<2	-6.06	-11.47
Stat1	<2	<2	<2	<2	-2.59
Stat2	<2	<2	<2	-2.10	-2.80
Timp1	<2	<2	<2	-3.31	<2
Ccl5	<2	<2	<2	<2	-2.62
Cd69	<2	<2	<2	<2	-7.36
Cd70	<2	<2	<2	<2	-4.44
Ifi2ak2	<2	<2	<2	<2	-2.07
Gbp1	<2	<2	<2	<2	-2.29
H2-K1	<2	<2	<2	<2	-2.67
H2-T10	<2	<2	<2	<2	-2.96
Ifih1	<2	<2	<2	<2	-3.95
Socs1	<2	<2	<2	<2	-2.35
Tap1	<2	<2	<2	<2	-2.74

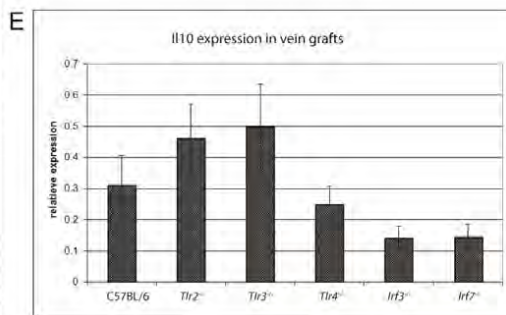
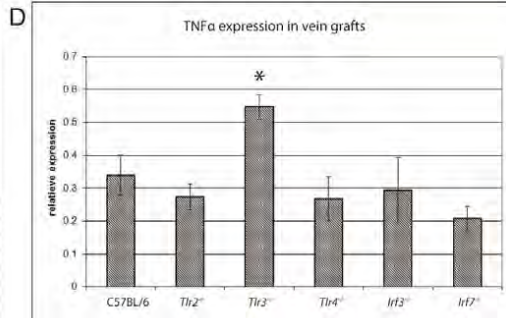
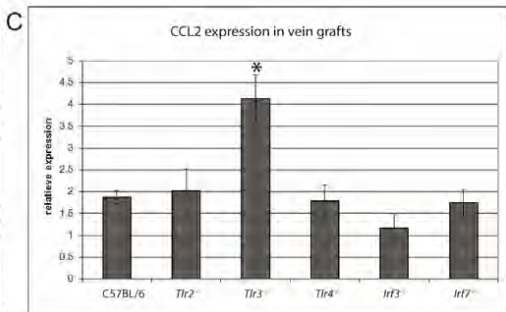


Figure 7 (previous page). Deficiencies of TLR and IRF differentially regulate type I interferon (inducible) genes and inflammatory cytokines. mRNA of vein graft of TLR2, TLR3, TLR4, IRF3 and IRF7 deficient mice were analyzed with reverse-transcription real-time PCR normalized to housekeeping genes A. RT2 profiler array of Type I IFNs on pools of TLR and IRF deficient vein grafts; genes are shown that are up regulated more than 2-fold in one of the strains. B. Type I IFNs RT2 profiler array; genes are shown that are down regulated more than 2-fold. Inflammatory cytokines CCL2 (C), TNF α (D) and Il10 (E), data are expressed as fold induction.

* $p < 0.05$.

Discussion

Although there is evidence of exogenous pathogens in vascular lesions²², it seems unlikely that these account for the complete repertoire of TLR activation. DAMP mediated activation of TLRs is thought to be an important process that drives immune-activated diseases such as cardiovascular diseases, rheumatoid arthritis and lupus²³⁻²⁵. We previously demonstrated the presence of several TLR DAMPS in remodeled vein grafts⁷. Cavasanni et al. showed that RNA

from necrotic cells could serve as ligand for TLR3 independent of viral stimuli²⁶. Here we

focused on the effects of TLR activation upon tissue damage and activation as a result of the engraftment procedure, flow disturbances and subsequent arterIALIZATION phase. mRNA array analysis revealed that both TLRs and IRFs are highly regulated during vein graft remodeling indicating that both pathways are substantially involved in vein graft development. This is further fueled by GSEA pathway analysis which showed that TLR and Type I IFN gene sets belonged to the top 15 of significantly regulated gene sets.

A prominent role for type I IFN genes in vein graft remodeling is suggested by the increased vein graft thickening and outward remodeling as seen in the Tlr3^{-/-} mice and the Irf7^{-/-} mice whereas, the Irf3^{-/-} mice showed near significant outward remodeling. This was accompanied by down regulation of typical type I IFN inducible genes in the vein grafts and pro-inflammatory responses in the vein grafts of Tlr3^{-/-} mice. Type I IFNs contribute to disease progression in auto-immune diseases by increased pro-inflammatory responses²⁷⁻²⁹. In animal models of cardiovascular diseases, inhibition of IFN β results in pro-inflammatory responses in the monocytic lineage^{30, 31}. This is in line with the increased influx of macrophages in these knockout strains suggesting that pro-inflammatory responses are responsible for the observed outward remodeling.

In contrast to the Tlr3^{-/-} mice, gene expression of pro-inflammatory cytokines in the Irf3^{-/-} and Irf7^{-/-} mice were not affected. Compensatory mechanisms by other TLRs in the Tlr3^{-/-} mice are a possible explanation for the increased expression of CCL2 and TNF α , especially since MyD88 gene transcription was found to be increased in Tlr3^{-/-} vein grafts. The main function of IRF3 and IRF7 is transcription of type I IFNs, therefore limited effect of IRFs on other genes such as pro-inflammatory cytokines are expected⁹. IRF7 is an inducer of a positive feedback loop of enhanced activation of type I IFNs-(TLR3)-IRF7^{16, 32}, this may explain the stronger reduction of type I Interferon (inducible) genes in the Irf7^{-/-} mice and subsequent effects on vein graft thickening and outward remodeling in comparison to the Irf3^{-/-} mice. Vein graft thickening was found impaired in the Tlr4^{-/-} mice. This was accompanied by a reduction in leukocytes but not the macrophages in the vessel wall. Reduced inflammatory responses and reduced vascular burden match the findings observed



in other TLR4 deficient murine models^{7, 33, 34}. TLR4 signaling to induce pro-inflammatory cytokines occurs initially via the MyD88 signaling pathway¹⁹. TLR4 was only significant up regulated at t3 in the array analysis. These results match the findings observed in the 28 day old Tlr4^{-/-} vein grafts that regulation of Type I IFN (inducible) genes was not detectable, nor regulation of MyD88 or pro-inflammatory cytokines suggesting that TLR4 is an early effector in vein graft remodeling. The fact that the remodeling was reduced after 28 days in Tlr4^{-/-} mice and no effects on type I IFN gene expression is observed suggests that in vein graft remodeling TLR4 signaling is rather an early response and associated with MyD88 signaling as described previously¹⁹ and not linked to the TRIF mediated, IRF3 associated type I IFN inducible genes. The latter pathway is linked to a late activation response that is observed after internalization of TLR4. TLR4 and TLR2 share common features such as the MyD88 signaling route as well as endogenous ligands such as HMGB1, Biglycan and HSP60 that were found to be expressed in remodeled vein grafts⁷. In contrast to the Tlr4^{-/-} mice, vein graft remodeling was not affected in Tlr2^{-/-} mice. Neither the cellular composition nor inflammatory cytokine expression was affected. This effect of limited responses without exogenous stimulation was also observed by Schoneveld et al. in a model of arterial remodeling, although stimulation of TLR2 with PAM3Cys clearly increased vascular burden³⁵. Remarkably, Tlr2^{-/-} vein grafts showed down regulation of some typical type I IFN inducible genes e.g. IFIT 1-3, Isg15 and Oas1a whereas IFN α 2 and IFN α 4 were up regulated. To our knowledge no direct links between TLR2 and Type I IFNs are reported, however, Liu et al. showed an indirect link: they showed that TLR2 can inhibit TLR7/9-dependent induction of type I IFNs via IRAK1 depletion³⁶, demonstrating that indirect effectuation of Type I IFNs by TLR2 is possible. Whether this particular pathway is applicable to our experiments seems unlikely since we did not observe regulation of TLR7, TLR9 or MyD88 in the Tlr2^{-/-} vein grafts at the 28 day time point.

Collectively, we here demonstrate that besides the MyD88 dependent pathways, the TRIF dependent pathway and downstream type I IFNs are of importance in vein graft remodeling. In particular our finding of increased vein graft thickening and remodeling in the Irf7^{-/-} mice gives food for thought to the discussion on the role of TLR pathways in vascular diseases. These data confirm once more that depending on the microenvironment and especially the contribution of immune cells to the vessel wall, TLRs exert different sets of pro-inflammatory mediators that ultimately determine the extent of vascular remodeling.

Acknowledgements

We thank Dr Akira for kindly providing the Tlr2^{-/-} and Tlr4^{-/-} mice and Dr Taniguchi for kindly providing the Irf3^{-/-} and Irf7^{-/-} mice.

Sources of Funding

This work was supported by the Dutch Top Institute Pharma (project D1-101; J.C. Karper) and the Research Program of the BioMedical Materials Institute (H.A.B. Peters).

Reference List

1. Ozaki CK. Cytokines and the early vein graft: strategies to enhance durability. *J Vasc Surg* 2007 June;45 Suppl A:A92-A98.
2. Owens CD, Rybicki FJ, Wake N, Schanzer A, Mitsouras D, Gerhard-Herman MD, Conte MS. Early remodeling of lower extremity vein grafts: inflammation influences biomechanical adaptation. *J Vasc Surg*

2008 June;47(6):1235-42.

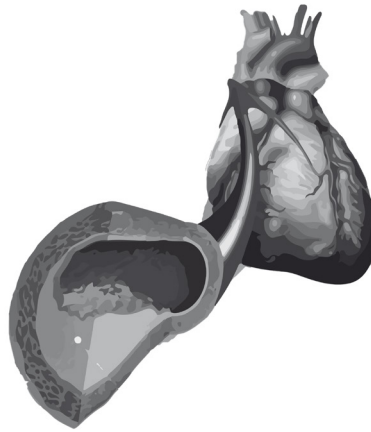
3. Eefting D, Bot I, de Vries MR, Schepers A, van Bockel JH, van Berkel TJ, Biessen EA, Quax PH. Local lentiviral short hairpin RNA silencing of CCR2 inhibits vein graft thickening in hypercholesterolemic apolipoprotein E3-Leiden mice. *J Vasc Surg* 2009 July;50(1):152-60.
4. Schepers A, Eefting D, Bonta PI, Grimbergen JM, de Vries MR, van W, V, de Vries CJ, Egashira K, van Bockel JH, Quax PH. Anti-MCP-1 gene therapy inhibits vascular smooth muscle cells proliferation and attenuates vein graft thickening both in vitro and in vivo. *Arterioscler Thromb Vasc Biol* 2006 September;26(9):2063-9.
5. de Vries MR, Wezel A, Schepers A, van Santbrink PJ, Woodruff TM, Niessen HW, Hamming JF, Kuiper J, Bot I, Quax PH. Complement Factor C5a as Mast cell Activator mediates Vascular Remodeling in Vein Graft Disease. *Cardiovasc Res* 2012 October 14.
6. Lardenoye JH, de Vries MR, Lowik CW, Xu Q, Dhore CR, Cleutjens JP, van Hinsbergh VW, van Bockel JH, Quax PH. Accelerated atherosclerosis and calcification in vein grafts: a study in APOE*3 Leiden transgenic mice. *Circ Res* 2002 October 4;91(7):577-84.
7. Karper JC, de Vries MR, van den Brand BT, Hoefler IE, Fischer JW, Jukema JW, Niessen HW, Quax PH. Toll-like receptor 4 is involved in human and mouse vein graft remodeling, and local gene silencing reduces vein graft disease in hypercholesterolemic APOE*3Leiden mice. *Arterioscler Thromb Vasc Biol* 2011 May;31(5):1033-40.
8. Pryshchep O, Ma-Krupa W, Younge BR, Goronzy JJ, Weyand CM. Vessel-specific Toll-like receptor profiles in human medium and large arteries. *Circulation* 2008 September 16;118(12):1276-84.
9. Kawai T, Akira S. The role of pattern-recognition receptors in innate immunity: update on Toll-like receptors. *Nat Immunol* 2010 May;11(5):373-84.
10. Cole JE, Navin TJ, Cross AJ, Goddard ME, Alexopoulou L, Mitra AT, Davies AH, Flavell RA, Feldmann M, Monaco C. Unexpected protective role for Toll-like receptor 3 in the arterial wall. *Proc Natl Acad Sci U S A* 2011 February 8;108(6):2372-7.
11. (11) Ahmad U, Ali R, Lebastchi AH, Qin L, Lo SF, Yakimov AO, Khan SF, Choy JC, Geirsson A, Pober JS, Tellides G. IFN-gamma primes intact human coronary arteries and cultured coronary smooth muscle cells to double-stranded RNA- and self-RNA-induced inflammatory responses by upregulating TLR3 and melanoma differentiation-associated gene 5. *J Immunol* 2010 July 15;185(2):1283-94.
12. Zimmer S, Steinmetz M, Asdonk T, Motz I, Coch C, Hartmann E, Barchet W, Wassmann S, Hartmann G, Nickenig G. Activation of endothelial toll-like receptor 3 impairs endothelial function. *Circ Res* 2011 May 27;108(11):1358-66.
13. Lundberg AM, Ketelhuth DF, Johansson ME, Gerdes N, Liu S, Yamamoto M, Akira S, Hansson GK. Toll-like receptor 3 and 4 signalling through the TRIF and TRAM adaptors in haematopoietic cells promotes atherosclerosis. *Cardiovasc Res* 2013 March 18.
14. Richards MR, Black AS, Bonnet DJ, Barish GD, Woo CW, Tabas I, Curtiss LK, Tobias PS. The LPS2 mutation in TRIF is atheroprotective in hyperlipidemic low density lipoprotein receptor knockout mice. *Innate Immun* 2013 February;19(1):20-9.
15. Gonzalez-Navajas JM, Lee J, David M, Raz E. Immunomodulatory functions of type I interferons. *Nat Rev Immunol* 2012 February;12(2):125-35.
16. Honda K, Taniguchi T. IRFs: master regulators of signalling by Toll-like receptors and cytosolic pattern-recognition receptors. *Nat Rev Immunol* 2006September;6(9):644-58.
17. Vallejo JG. Role of toll-like receptors in cardiovascular diseases. *Clin Sci (Lond)*2011 July;121(1):1-10.
18. Seneviratne AN, Sivagurunathan B, Monaco C. Toll-like receptors and macrophage activation in atherosclerosis. *Clin Chim Acta* 2012 January 18;413(1-2):3-14.
19. Kawai T, Akira S. Toll-like receptors and their crosstalk with other innate receptors in infection and immunity. *Immunity* 2011 May 27;34(5):637-50.



20. van der Pouw Kraan TC, van der Laan AM, Piek JJ, Horrevoets AJ. Surfing the data tsunami, a bioinformatic dissection of the proangiogenic monocyte. *Vascul Pharmacol* 2012 May;56(5-6):297-305.
21. Schulte S, Sukhova GK, Libby P. Genetically programmed biases in Th1 and Th2 immune responses modulate atherogenesis. *Am J Pathol* 2008 June;172(6):1500-8.
22. Rosenfeld ME, Campbell LA. Pathogens and atherosclerosis: update on the potential contribution of multiple infectious organisms to the pathogenesis of atherosclerosis. *Thromb Haemost* 2011 November;106(5):858-67
23. Yu L, Wang L, Chen S. Endogenous toll-like receptor ligands and their biological significance. *J Cell Mol Med* 2010 November;14(11):2592-603.
24. Goh FG, Midwood KS. Intrinsic danger: activation of Toll-like receptors in rheumatoid arthritis. *Rheumatology (Oxford)* 2012 January;51(1):7-23.
25. Seneviratne AN, Sivagurunathan B, Monaco C. Toll-like receptors and macrophage activation in atherosclerosis. *Clin Chim Acta* 2012 January 18;413(1-2):3-14.
26. Cavassani KA, Ishii M, Wen H, Schaller MA, Lincoln PM, Lukacs NW, Hogaboam CM, Kunkel SL. TLR3 is an endogenous sensor of tissue necrosis during acute inflammatory events. *J Exp Med* 2008 October 27;205(11):2609-21.
27. Schirmer SH, Fledderus JO, Bot PT, Moerland PD, Hofer IE, Baan J, Jr., Henriques JP, van der Schaaf RJ, Vis MM, Horrevoets AJ, Piek JJ, van RN. Interferon-beta signaling is enhanced in patients with insufficient coronary collateral artery development and inhibits arteriogenesis in mice. *Circ Res* 2008 May 23;102(10):1286-94.
28. Axtell RC, Raman C. Janus-like effects of type I interferon in autoimmune diseases. *Immunol Rev* 2012 July;248(1):23-35.
29. Gonzalez-Navajas JM, Lee J, David M, Raz E. Immunomodulatory functions of type I interferons. *Nat Rev Immunol* 2012 February;12(2):125-35.
30. Goossens P, Gijbels MJ, Zerneck A, Eijgelaar W, Vergouwe MN, van dM, I, Vanderlocht J, Beckers L, Buurman WA, Daemen MJ, Kalin U, Weber C, Lutgens E, de Winther MP. Myeloid type I interferon signaling promotes atherosclerosis by stimulating macrophage recruitment to lesions. *Cell Metab* 2010 August 4;12(2):142-53.
31. Schirmer SH, Bot PT, Fledderus JO, van der Laan AM, Volger OL, Laufs U, Bohm M, de Vries CJ, Horrevoets AJ, Piek JJ, Hofer IE, van RN. Blocking interferon {beta} stimulates vascular smooth muscle cell proliferation and arteriogenesis. *J Biol Chem* 2010 November 5;285(45):34677-85.
32. Honda K, Yanai H, Negishi H, Asagiri M, Sato M, Mizutani T, Shimada N, Ohba Y, Takaoka A, Yoshida N, Taniguchi T. IRF-7 is the master regulator of type-I interferon-dependent immune responses. *Nature* 2005 April 7;434(7034):772-7.
33. Michelsen KS, Wong MH, Shah PK, Zhang W, Yano J, Doherty TM, Akira S, Rajavashisth TB, Arditi M. Lack of Toll-like receptor 4 or myeloid differentiation factor 88 reduces atherosclerosis and alters plaque phenotype in mice deficient in apolipoprotein E. *Proc Natl Acad Sci U S A* 2004 July 20;101(29):10679-84.
34. Hollestelle SC, de Vries MR, Van Keulen JK, Schoneveld AH, Vink A, StrijderCF, Van Middelaar BJ, Pasterkamp G, Quax PH, de Kleijn DP. Toll-like receptor 4 is involved in outward arterial remodeling. *Circulation* 2004 January 27;109(3):393-8.
35. Schoneveld AH, Oude Nijhuis MM, van MB, Laman JD, de Kleijn DP, Pasterkamp G. Toll-like receptor 2 stimulation induces intimal hyperplasia and atherosclerotic lesion development. *Cardiovasc Res* 2005 April 1;66(1):162-9.
36. Liu YC, Simmons DP, Li X, Abbott DW, Boom WH, Harding CV. TLR2 signaling depletes IRAK1 and inhibits induction of type I IFN by TLR7/9. *J Immunol* 2012 February 1;188(3):1019-26.



CHAPTER 7



TLR accessory molecule RP105 (CD180) is involved in post-interventional vascular remodeling and soluble RP105 modulates neointima formation

Karper JC, Ewing MM, de Vries MR, de Jager SC, Peters EA, de Boer HC, van Zonneveld AJ, Kuiper J, Huizinga EG, Brondijk TH, Jukema JW, Quax PH

PLoS One. 2013;8(7):e67923.

Abstract

Background: RP105 (CD180) is TLR4 homologue lacking the intracellular TLR4 signaling domain and acts a TLR accessory molecule and physiological inhibitor of TLR4-signaling. The role of RP105 in vascular remodeling, in particular post-interventional remodeling is unknown.

Methods and Results TLR4 and RP105 are expressed on vascular smooth muscle cells (VSMC) as well as in the media of murine femoral artery segments as detected by qPCR and immunohistochemistry. Furthermore, the response to the TLR4 ligand LPS was stronger in VSMC from RP105^{-/-} mice resulting in a higher proliferation rate. In RP105^{-/-} mice femoral artery cuff placement resulted in an increase in neointima formation as compared to WT mice (4982±974µm² vs.1947±278µm²,p=0.0014). Local LPS application augmented neointima formation in both groups, but in RP105^{-/-} mice this effect was more pronounced (10316±1243µm² vs.4208±555µm²,p=0.0002), suggesting a functional role for RP105. For additional functional studies, the extracellular domain of murine RP105 was expressed with or without its adaptor protein MD1 and purified. SEC-MALSanalysis showed a functional 2:2 homodimer formation of the RP105-MD1 complex. This protein complex was able to block the TLR4 response in whole blood ex-vivo. In vivo gene transfer of plasmid vectors encoding the extracellular part of RP105 and its adaptor protein MD1 were performed to initiate a stable endogenous soluble protein production. Expression of soluble RP105-MD1 resulted in a significant reduction in neointima formation in hypercholesterolemic mice (2500±573 vs.6581±1894 µm²,p<0.05), whereas expression of the single factors RP105 or MD1 had no effect .

Conclusion RP105 is a potent inhibitor of post-interventional neointima formation.

Introduction

In interventional cardiology restenosis remains a critical determinant of long-term efficacy of Percutaneous Coronary Interventions (PCI). Neointima formation is a common feature of restenosis and atherosclerosis and is characterized by proliferation and migration of vascular smooth muscle cells (VSMC) and extracellular matrix formation^{1, 2}. These processes are strongly mediated by inflammation and influx of inflammatory cells in the affected vessel wall³. Under hypercholesterolemic conditions this is accompanied by lipid accumulation in the vessel wall, thereby initiating a process of accelerated atherosclerosis. Previously, we and others described an important causal role for Toll Like Receptor 4 (TLR4) in neointima formation. Furthermore, TLR4 activation by local application of LPS had a stimulatory effect on neointima formation and accelerated atherosclerosis development⁴⁻⁶. LPS initiates TLR4 activation and the resulting inflammatory reaction causes a release of many pro-inflammatory cytokines that will affect the pathophysiological process of neointima formation strongly^{7, 8}. TLR4 is expressed on VSMC and is involved in their proliferation⁹. Previously, we were able to detect co-localization between endogenous TLR4 ligands (HSP60 and fibronectin-EDA) and TLR4 during vascular remodeling^{4, 6}.

TLR4 is a pattern recognition receptor (PRR) of the innate immune system and is expressed by both immune and non-immune cells. It is the most robust and complex signaling TLR and can be activated by an array of ligands, including damage associated molecular patterns (DAMPs), which can for instance be degradation products of endogenous matrix molecules, necrotic cells, oxidized molecules and inflammation-specific molecules¹⁰. Activation of TLR4 by binding of LPS and or other ligands that become available after cell stress or tissue damage^{11, 12} is dependent on the presence of MD2, a TLR accessory molecule.

It is becoming more and more clear that accessory molecules play a key role in the complex TLR-signaling. Accessory molecules can be divided into molecules that reside in the endoplasmic reticulum, molecules that directly interact with TLR ligands or regulatory molecules present on the cell surface such as RP105 (CD180)¹³. RP105 is reported to be a physiological TLR4 inhibitor on myeloid cells.

In the presence of RP105 on myeloid cells activation of the TLR4 signaling pathway is directly reduced making RP105 one of the most important accessory molecules acting as a regulator of TLR4 signaling. Structurally, RP105 is highly homologous to TLR4, but lacks the intracellular Toll Interleukin Receptor (TIR) domain. TLR4 activation in cellular immunity, induced by e.g. its ligand LPS, is negatively regulated by RP105¹⁴⁻¹⁶. RP105 forms a complex with MD1, a MD2 homolog, in an unusual 2:2 homodimer^{17, 18}. This orientation is opposite to that of known ligand-induced TLR-homodimers. The functional consequence of this unusual dimer configuration is still under debate^{17, 18}. RP105/MD1 is thought to bind LPS and other TLR4 ligands, therefore RP105 is linked to several inflammatory processes including autoimmune diseases^{16, 19, 20}. So far, the involvement and possible causal role of RP105 in vascular remodeling and other cardiovascular related events is unknown.

In the current study we demonstrate a functional role for RP105 in vascular remodeling during neointimal formation by the use knockout mice, cultured VSMC, purified proteins and by in vivo gene transfer mediated overexpression of soluble RP105 (solRP105) protein combined with the MD1 accessory protein.



Material and methods:

Cell culture and cell culture immunostaining

Murine VSMCs explanted from aortas were cultured and incubated overnight with either PBS or LPS (1ng/ml or 10ng/ml). Cells were either cultured for RNA isolation or were cultured on glass coverslips and fixed. The latter was followed by blocking with PBS, 3% BSA, 2% FCS for one hour at room temperature. After blocking, primary antibodies and isotype controls were incubated for one hour followed by washing and incubation with labeled secondary antibodies for one hour in the dark. TLR4 presence was demonstrated using TLR4 antibody (rabbit anti-human, Santa Cruz). RP105 was stained with RP105 antibody (rat anti-mouse, Abcam, United Kindom). A ZEISS 510 microscope was used for analysis and confocal microscopy.

Macrophages

Macrophages were derived from bone marrow from tibia and femur and seeded at a density of 500.000 cells/well in 6-wells plates and cultured for 7 days in RPMI GlutaMax (Gibco) supplemented with 100U/ml penicillin/streptavidin, 25% Fetal Calf Serum (FCS) and 20mcg/ml M-CSF (Myltec Biotechnologies) as described previously²¹.

Dendritic cells

Dendritic cells were derived from bone marrow from tibia and femur and seeded at a density of 1.500.000 cells/well in 6-wells plates and cultured for 10 days in RPMI Glutamin (Gibco) supplemented with 100U/ml penicillin/streptavidin, 10% Fetal Calf Serum (FCS) and 20mcg/ml GM-CSF (Myltec Biotechnologies). as described previously²². Cells were cultured in the presence of 1ng/ml LPS.

RT-PCR

From VSMCs, total RNA was isolated using Tri-Reagent (Sigma-Aldrich) according to the manufacturer's protocol. The expression levels of TLR4 and RP105 were analyzed by real time polymerase chain reaction (RT-PCR) (Taqman, Applied Bioscience) on non-stimulated VSMCs and VSMCs stimulated with LPS overnight. The relative mRNA expression levels were determined using GAPDH as housekeeping gene and the $2^{-[\Delta\Delta C(T)]}$ method. Values were expressed as fold of unstimulated controls.

SMC Proliferation Assay

Murine SMCs, explanted from aortas, were subsequently cultured, characterized, and proliferation was measured using the ³H-Thymidine incorporation method as described previously²¹. Briefly, cells were seeded in a 24 well disk at a density of at least 100.000 cells per cm². Next, cells were made quiescent for 48 hours in serum free medium followed by stimulation with LPS in full medium containing 10% FCS. Methyl-³H-thymidine incorporation (Amersham, 0.25μCi per well) over a 16 hours period was measured by liquid- scintillation counting and compared to non stimulated control cells of WT and RP105^{-/-} VSMC in serum free medium. All experiments were done in triplicates.

Animals

Animal experiments were approved by the Institutional Committee for Animal Welfare of the Leiden University Medical Center (LUMC) and were performed according the regulatory

guidelines. 10 week old male wild type (WT, C57/B6) and 10 week old male RP105^{-/-} animals (C57/B6 background, backcrossed for more than 10 generations) bred in our laboratory, were used. RP105^{-/-} mice were provided by K.Miyake, Tokyo University, Japan and described previously²². 10 week old male hypercholesteremic ApoE3Leiden mice were used to study the effect of soluble RP105 overexpression. ApoE3Leiden mice received a western-type diet that started 3 weeks before surgery and continued during the experiment. One week before surgery cholesterol levels in serum were determined (Roche Diagnostics, The Netherlands). All mice received water and food ad libitum.

Murine model for neointima formation

Non-constricted polyethylene cuffs were placed around the femoral arteries as described previously²³. Mice were killed 3 weeks after cuff placement. The hypercholesterolemic mice were sacrificed after two weeks, since at this time point first signs of accelerated atherosclerosis and foam cells formation becomes detectable. For local TLR4 stimulation, TLR4 ligand LPS (1 µg/µL) (from Escherichia coli 055:B5, Sigma Aldrich, The Netherlands) was dissolved in pluronic gel (F-127, Sigma Aldrich, The Netherlands) and administered inside the cuff⁴.

Purification of solRP105 and solRP105-MD1

Plasmid Constructs

The extracellular domain of mouse RP105 comprising residues Thr21-Ala630 was inserted into a pUPE expression vector (U-Protein Express BV, Utrecht) that includes an N-terminal (His)6-(StrepII)3-TEV-tag. Mouse MD1 without its native signal sequence; residues Asp20-Ser162, was cloned into a pUPE expression vector that includes an N-terminal (His)6-tag. Both vectors include the human cystatin-S signal peptide for efficient secretion and expression is controlled by the CMV-promoter. The cloning procedure introduces a triple-alanine sequence at the C-terminus of both proteins.

Protein expression and purification

Expression vectors encoding solRP105 and MD1 were transfected transiently, either individually or in combination, in HEK293-EBNA1-S cells. Culture supernatant was harvested 6 days post-transfection. Supernatant was concentrated 10-fold using a Quixstand hollow fiber system (GE Healthcare) prior to diafiltration into 50 mM Tris-Cl, pH8.0, 300 mM NaCl. RP105 and RP105-MD1 complex were purified using Ni-Sepharose/Streptactin-Sepharose tandem-affinity-purification and eluted in 50 mM Tris-Cl, pH8.0, 300 mM NaCl supplemented with 5 mM desthiobiotin. MD1 was purified by Ni-Sepharose affinity purification in 50 mM Tris-Cl pH8.0, 300 mM NaCl supplemented with 250 mM imidazole followed by dialysis to buffer without imidazole. N-glycosylation of SDS-denatured MD1 was analysed by cleavage with PNGase (Roche) according to the manufacturer's protocol. Protein quality was further assessed by size-exclusion chromatography on a Superdex 200 PC3.2/30 column (GE Healthcare) using 50 mM Tris-Cl, pH8.0, 300 mM NaCl as the running buffer at 0.05 ml/min. The molecular weight of the solRP105-MD1 complex was determined by size exclusion chromatography with multi-angle light scattering (SEC-MALS) using a WTC-030S5 column (Wyatt technologies) and 50 mM Tris-Cl, pH8.0, 300 mM NaCl as the running buffer at 0.5 ml/min. Molecular weight was calculated by ASTRA software version 5.3.4.18 Wyatt technologies).



In vivo overexpression of soluble RP105

In vivo overexpression of soluble RP105 (solRP105) was achieved by gene-transfer of the expression plasmids encoding the extracellular domain of RP105, MD1 or both plasmids together. A Luciferase encoding plasmid was used as control. Electroporation mediated gene transfer was performed 3 days before cuff placement by injecting 50 µg of each plasmid per leg, either Luciferase, solRP105, MD1 or MD1 plus solRP105, into the calf muscles of both legs, followed by electroporation (8 pulses of 10 ms, field strength of 200 V/cm [Sq Wave Electroporator ECM 830, BTX] using Caliper Electrodes). Calf muscles were primed with an intramuscular injection containing 30 µL of hyaluronidase (0.45 U/µL, Sigma) one hour before electroporation as described previously²⁴.

Whole blood assay

Blood from three C57/B6 mice was collected (180µl blood with 20µl heparin) and incubated with either solRP105 purified protein (7.5µg/ml, MW=74706), solRP105-MD1 purified protein complex (9µg/ml, MW=90975) or PBS. Blood was stimulated overnight with 100ng/ml LPS and subsequently the cytokine TNFα was measured by ELISA (BD biosciences).

Morphological Quantification

Mice were sacrificed 21d (or as stated otherwise) after surgery for histological analysis. Arterial segments were harvested after perfusion fixation (100 mm Hg) with 4% formaldehyde, fixed overnight and paraffin-embedded using an automated tissue processor (Leica, Germany). Cross-sections were made throughout the embedded cuffed arteries. Six representative sections per vessel segment were stained with Elastin von Giesson and Haematoxylin-Phloxine- Saffron (HPS) for histological and morphometric analysis (QWin, Leica, Germany). Neointima formation was defined as the area between lumen and the internal elastic lamina.

Immunohistochemistry on vessels

Paraffin embedded sections (5µm) were de-paraffinized in xylene. Peroxidase activity was blocked by incubation in 0.3% (v/v) H₂O₂ in methanol for 20 min. Antigen retrieval was performed and tissue sections were pre-incubated with 5% bovine serum albumin (BSA), followed by overnight incubation with detecting antibody for either RP105 antibody (rat anti mouse, Abcam, United Kingdom) or CD45 (rat-anti mouse). After washing in PBS, sections were incubated for 1h with a secondary antibody, washed in PBS, incubated for 1h with AB complex (Vector laboratories, The Netherlands) and visualized with Novared (Vector laboratories) or DAB (Dako, Denmark). Slides were counterstained with haematoxylin. Immunopositive areas of leukocytes were calculated as percentage of total either media or neointima area in cross-sections by morphometry (Qwin, Leica, Germany). To confirm the specificity of the IHC staining, parallel sections were incubated with 1% PBS/BSA alone without adding the primary antibody or with IgG isotype control or without first antibody. Sections were incubated with the secondary antibody, AB complex and were visualized with Novared. Controls were all negative.

Statistics

For the animal experiments, values are presented as mean ± standard error of the mean (SEM). Statistical significance was calculated in SPSS for Windows 17.0. Differences

between groups were determined using a non-parametric Mann-Whitney test or One-Way ANOVA. In vitro data was statistically analyzed with a Student's-T-test.



Results

RP105 and TLR4 are both expressed by VSMC

Both TLR4 and RP105 mRNA are expressed in VSMC and as expected overnight incubation with LPS decreased mRNA expression for both TLR4 as described previously on leukocytes^{25,26} as well as RP105 (Figure 1A-B). TLR4 and RP105 protein was detected by immunohistochemistry (IHC) and was also decreased after overnight LPS incubation (Figure 1C-D). In non-stimulated cells co-localization between TLR4 and RP105 was sporadically detected (Figure 1E and Supplementary Figure 1). To detect RP105 expression in the vessel wall IHC was performed on cross sections of murine femoral arteries. RP105 was expressed particularly in the media that consists of VSMC (Figure 1F). Furthermore, RP105^{-/-} VSMC showed an increase in proliferation-index (fold of proliferation increase compared to unstimulated controls) compared to wild type controls upon LPS stimulation (Figure 1G).

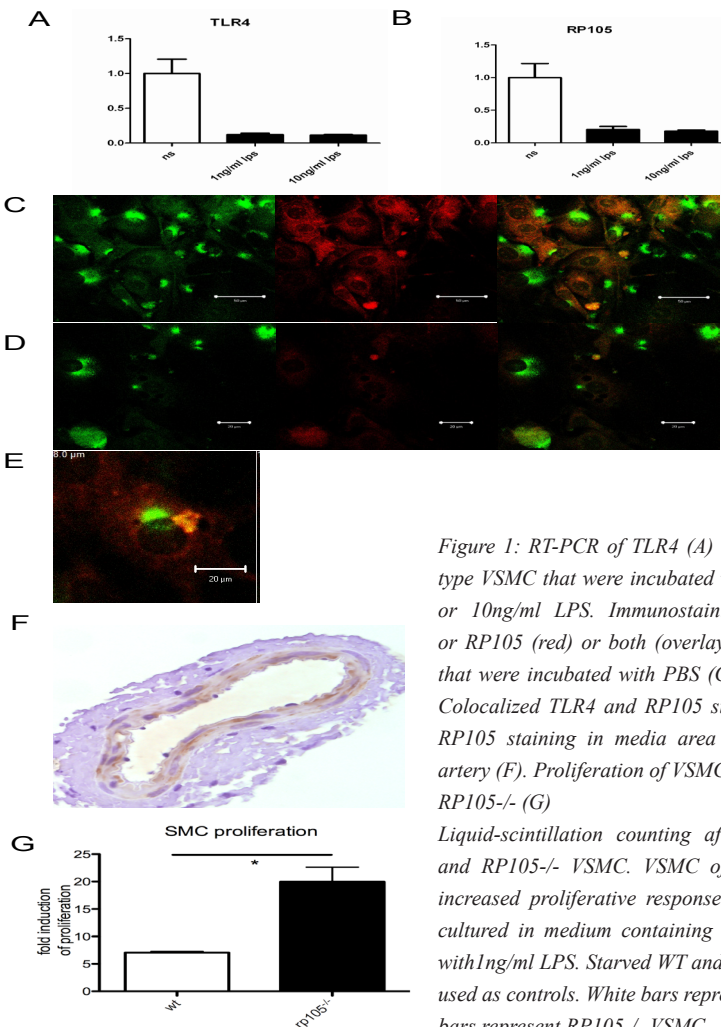
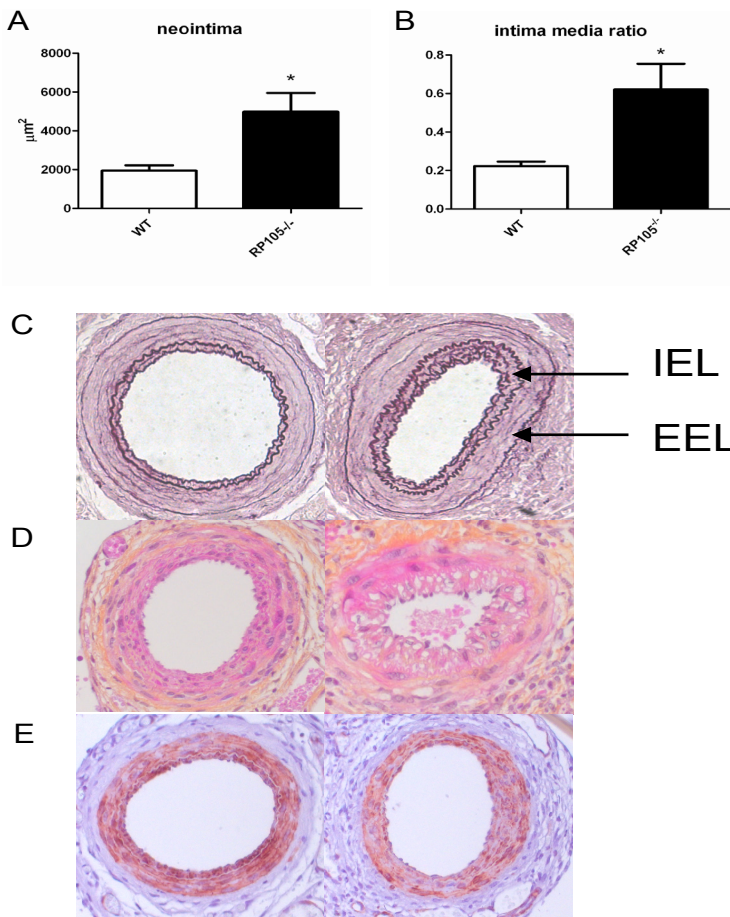


Figure 1: RT-PCR of TLR4 (A) or RP105 (B) on wild type VSMC that were incubated with PBS, 1ng/ml LPS or 10ng/ml LPS. Immunostaining of TLR4 (green) or RP105 (red) or both (overlay) on wild type VSMC that were incubated with PBS (C) or 1ng/ml LPS. (D) Colocalized TLR4 and RP105 staining on VSMC (E). RP105 staining in media area of a murine femoral artery (F). Proliferation of VSMC of WT and RP105^{-/-} (G)

Liquid-scintillation counting after 16 hours of WT and RP105^{-/-} VSMC. VSMC show a RP105^{-/-}-an increased proliferative response to LPS. VSMC were cultured in medium containing 10%FCS or 10%FCS with 1ng/ml LPS. Starved WT and RP105^{-/-} VSMC were used as controls. White bars represent WT VSMC, black bars represent RP105^{-/-} VSMC.

RP105 is present in the arterial wall and is protective in neointima formation

Cuff placement induces a mild vascular injury that is driven by a damage induced inflammatory response and can be detected as intimal thickening. Studies to determine the functional role of RP105 in restenosis were initiated. Femoral cuff placement to induce neointima formation was performed in RP105^{-/-} and control wild type (WT) mice. The neointima consists dominantly of VSMC as can be appreciated in (Figure 2AB). Quantification of the neointima revealed that RP105 deficiency resulted in enhanced neointima formation compared to WT mice (4982±974μm² (n=8) vs 1947±278μm² (n=10), p=0.0014) (figure 2B). The stronger neointima formation in the RP105^{-/-} caused a difference in intima/media ratio (0.62±0.13 vs. 0.22±0.02, P=0.0009) (figure 2C). No significant difference was seen in media area size (not shown).



*Figure 2: Neointima formation after femoral artery cuff placement in RP105^{-/-} and wild type mice. Areas of femoral arterial sections were quantified by using 6 sequential sections per segment and are expressed in micrometers squared (mean±SEM). Increased neointima formation in RP105^{-/-} mice compared to WT (wild type) controls (A). Increased intima/media ratio in RP105^{-/-} mice compared to WT controls (B). Representative pictures of Elastin von Giesson(C) HPS (D) and alpha-smooth muscle cell actin (E) of RP105^{-/-} and WT controls. * = P<0.05 Arrows indicate the Internal Elastic Lamina (IEL) and the External Elastic Lamina (EEL)*



LPS induced increased neointima formation and caused outward remodeling in RP105 deficient mice.

To initiate a stronger TLR4-driven vascular remodeling, the experiment presented above was repeated with local application of the TLR4 ligand LPS (1 $\mu\text{g}/\mu\text{L}$ in pluronic gel) around the cuffed artery. Local LPS application caused augmented neointima formation in both groups (RP105^{-/-} (n=9) vs WT (n=8)) and again significantly stronger neointima formation in RP105^{-/-} mice (10316 \pm 1243 μm^2 vs. 4208 \pm 555 μm^2 , p=0.0002) (figure 3A). Intima/media ratio after LPS application increased in both groups (1.05 \pm 0.12 vs. 0.52 \pm 0.07 p= 0.0037) (figure 3B). Previously, we showed that TLR4 induced neointima formation via local LPS application caused outward remodeling^{4, 18}. Therefore, we compared the total vessel wall areas of both groups to study the outward remodeling response. Outward remodeling in the RP105^{-/-} mice (33315 \pm 3945 μm^2 vs. 21401 \pm 1140 μm^2 , p=0.027) (figure 3C) was significantly stronger compared to the controls.

Previously, RP105-mediated suppression of TLR4 signaling by plasmid overexpression in HEK-293 cells was shown *in vitro*¹⁵. So far we found negative effects of RP105 deficiency on vascular remodeling and therefore we hypothesized that RP105, by regulating TLR signaling, might have therapeutic potential in post-interventional vascular remodeling. Therefore we produced soluble RP105 protein, characterized it and tested its therapeutic potential.

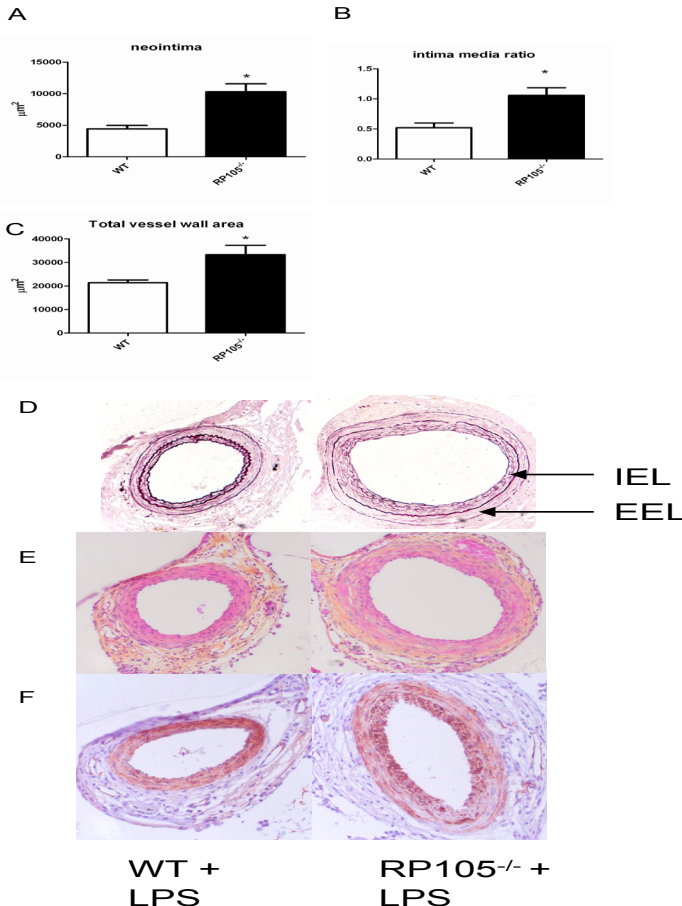


Figure 3 Neointima formation after femoral artery cuff placement with LPS in RP105^{-/-} and wild type mice. Areas of femoral arterial sections were quantified by using 6 sequential sections per segment and are expressed in micrometers squared (mean \pm SEM).

Increased neointima formation in RP105^{-/-} mice compared to WT controls after local LPS application (A). Increased intima/media ratio in RP105^{-/-} mice compared to WT controls after local LPS application (B). Increased outward remodeling in RP105^{-/-} mice compared to WT controls after local LPS application (C) Representative pictures of Elastin von Giesson (D), HPS (E) and alpha-smooth muscle cell actin (F) of RP105^{-/-} and WT controls. * = P<0.05. Arrows indicate the Internal Elastic Lamina (IEL) and the External Elastic Lamina (EEL)

Soluble RP105 protein – characterization SDS-PAGE analysis of the purified proteins, shows that the solRP105-MD1 complex and MD1 preparations are >95% pure, whereas the solRP105 preparation shows some impurities (Figure 4A). solRP105 has the expected molecular weight of ~90 kD whereas MD1 shows as a double band at approximately 23 and 26 kD (Figure 4A). Deglycosylation of denatured MD1 shows that the two bands in the MD1 preparation are due to differential glycosylation of the two N-glycosylation sites at positions Asn96 and Asn156 (Figure 4B). During size-exclusion chromatography, the solRP105-MD1 complex shows a single peak with an elution volume that is consistent with a hetero-tetrameric RP105₂MD1₂ complex, as was observed in the recently published crystal structures of the RP105-MD1 complex (16, 18). solRP105 shows a broad peak that is indicative of aggregation with a peak maximum at an elution volume that is consistent with monomeric RP105 (Figure 4C). The molecular weight of the complex was determined more accurately using SEC-MALS and yielding a value of 208±11 kD, which is in good agreement with the expected molecular weight of 214 kD for fully glycosylated RP105₂MD1₂ complex.

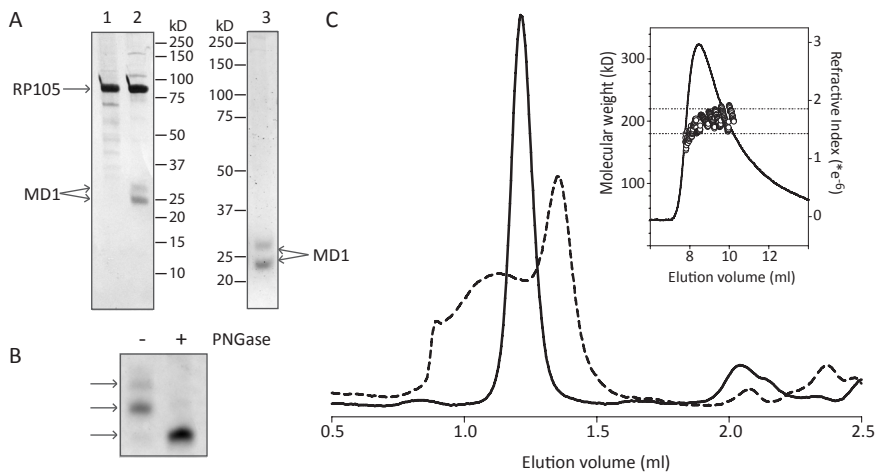


Figure 4: Purification and analysis of RP105, MD1 and RP105-MD1 complex. RP105 (lane 1) and RP105-MD1 complex (lane 2) purified by nickel- and streptactin- tandem affinity purification and analysed by SDS-PAGE (10%) and subsequent silverstaining. Lane 3 shows MD1 purified by nickel-affinity purification and analysed by SDS-PAGE (12%) and subsequent Coomassie staining (A). SDS-PAGE analysis of PNGase deglycosylation of SDS denatured MD1 (B). Size exclusion chromatography (Superdex200 PC3.2/30) of the purified RP105 (dashed line) and RP105-MD1 complex (solid line). Molecular weight determination of the RP105-MD1 complex using SEC-MALS (inset). The dashed horizontal lines indicate a molecular weight of 180 kD and 220 kD, respectively (C).

Soluble RP105 protein – functionality

We were able to show the increased TLR4 mediated inflammatory response in RP105 deficient myeloid cells (Supplementary Figure 2). To see whether solRP105 or solRP105-MD1 could have effects on cytokine production by these circulating cells we performed an *ex vivo* whole blood stimulation assay in the presence of these proteins. Blood was incubated



with LPS in the presence of solRP105, solRP105-MD1 complex or PBS and TNF was after measured after overnight LPS stimulation. solRP105-MD1 showed a marked decrease in TNF α production compared to controls (Figure 5).

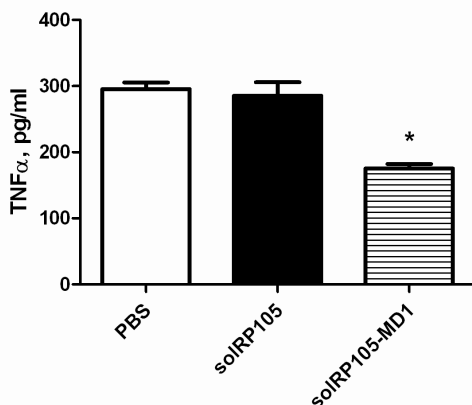


Figure 5 Whole blood stimulation. Blood stimulated with LPS and PBS or combined with purified solRP105 protein or purified solRP105-MD1 protein. Supernatant from triplicates was used for TNF α measurement. * = $P < 0.05$

solRP105-MD1 reduced neointima formation.

To see whether solRP105 could be a functional inhibitor of neointima formation in a more humanized model with mild foam cell formation in the neointima we applied our cuff model in ApoE3Leiden mice. Since RP105 also had strong effects on macrophages¹⁵ important in foam cell formation²³ and the above described effects on VSMC proliferation we hypothesized that overexpression of the soluble form of the RP105 receptor, either alone or in complex with MD1, could have potential therapeutic benefits to reduce restenosis. Plasmids encoding solRP105, MD1 or luciferase (control) were injected in calf muscles followed by electroporation into the muscle cells 3 days before cuff placement in transgenic ApoE3Leiden mice that develop a diet induced hypercholesterolemia. This resulted in systemic overexpression of the recombinant proteins, as we have demonstrated previously^{8, 27, 28}. Overexpression of both solRP105 and MD1 proteins combined caused a significant reduction in neointima formation compared to luciferase control (2500 ± 573 vs. $6581 \pm 1894 \mu\text{m}^2$, $P < 0.05$) and a more beneficial intima media ratio (Figure 6A-D), whereas overexpression of either solRP105 or MD1 did not affect neointima formation

Discussion

To our knowledge, the present study is the first to describe a role of RP105 in vascular disease. RP105 is expressed in cultured VSMC, as well as in the media. Furthermore, RP105 deficient mice develop less neointima after vascular injury and in these mice lacking the inhibitor TLR4 inhibitor R105, TLR4 activation via LPS clearly enhanced vascular remodeling more profoundly. Finally we demonstrated that overexpression of a soluble RP105/MD1 protein complex strongly reduced neointima formation.

RP105 can be distinguished from other endogenous TLR regulators by being an extracellular TLR4 structural homolog with contrasting capabilities like the inhibitory effects on myeloid cells and activation of B cells¹³. Our study shows that RP105 protein is also expressed by vascular smooth muscle cells (VSMC). Others have shown RP105 presence on smooth muscle cells of the airway²⁹. Additionally, we found via immunostaining as well as via RT-

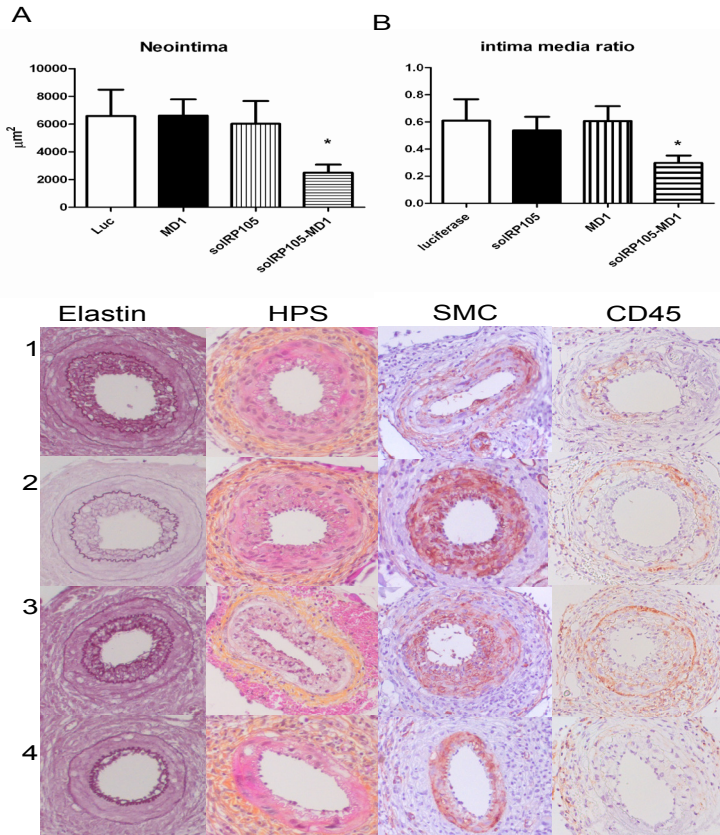


Figure 6: Neointima formation after femoral artery cuff placement with LPS in hypercholesterolemic APOE3Leiden mice. Areas of femoral arterial sections were quantified by using 6 sequential sections per segment and are expressed in micrometers squared (mean±SEM). Decreased neointima formation in mice that had overexpression of solRP105-MD1 (A). Intima Media ratio (B) Pictures of Elastin von Giesson (C) HPS (D) alpha-smooth muscle cell actin (E) and CD45 (F) of Luc(1) solRP105 (2) MD1 (3) solRP105-MD1 (4) * = $P < 0.05$

PCR that the expression of both receptors is down regulated upon overnight incubation with LPS as can be appreciated in figure 1. This is in line with previous observations in monocytes/macrophages exposed to LPS, which show reduced responses to second stimulation with LPS. Furthermore, after an initial LPS stimulation, TLR4 mRNA expression was significantly decreased within a few hours and remained suppressed over 24h. TLR4 presence at the cells surface rapidly decreased within 1 hour, with a gradual decrease after that²⁶. In patients a similar situation can be observed where a reduction in TLR4 expression can be appreciated on monocytes at the end of cardiopulmonary bypass procedures²⁵. While TLR4 might be down-regulated as a protective response, RP105 may just follow TLR4 expression as RP105 expression mimics that of TLR4 in human and mouse myeloid cells¹⁵. RP105 deficiency on VSMC caused an increase in proliferation upon incubation with TLR4 ligand LPS. A stimulating effect of TLR4 on VSMC proliferation was published previously⁹. This points towards a functional role of RP105 in vascular remodeling via its TLR4 inhibitory function, via its effects on VSMC in the pathophysiological process of neointima formation, as a common feature of restenosis. Femoral cuff placement in mice allows employing of a



mild mechanically-induced inflammatory-based neointima formation. Lesions in mice consist primarily of VSMC and application of this model to RP105^{-/-} and WT control mice leads to an increase in neointima formation in the RP105^{-/-} mice. This underscores the suggestion that RP105 is also functionally involved in the inhibition of post-interventional neointima formation, a process known to be regulated by TLR4 activation and may play a role in the pathophysiological process of restenosis.

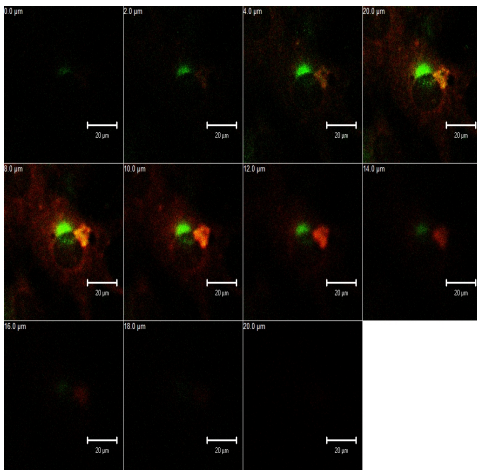
The influence of inflammation on restenosis is most prominent in the early phase after intervention. Interestingly, TLR4 was previously described to be involved in cardiovascular remodeling^{5, 6, 30} and local application of LPS causes a strong increase in neointima formation after cuff placement⁴. RP105 deficient mice have a stronger pro-inflammatory response upon systemically delivered TLR4 ligand LPS¹⁴. In figure 3 we show that short term activation of TLR4 directly after cuff placement via local application of LPS causes a strong increase in neointima formation. As a result, the vessel seems to respond by compensatory outward remodeling to secure the vessel patency³¹. In TLR4-deficient mice this response is inhibited upon local LPS application⁴. Due to a more prominent TLR4 activation in RP105^{-/-} mice we see that these mice have an increase in outward remodeling. So far a protective role for RP105 on post-interventional remodeling is appreciated. This indicates potential for new strategies to use RP105 in a therapeutic approach. Therefore we focused on the development of recombinant protein expression. Divanovic et al showed that the extracellular region of RP105 is functional only when co-expressed with MD1¹⁵. Similar to TLR4 surface expression that is dependent on MD2, RP105 surface expression was shown to be dependent on MD1³². While we could express the soluble ectodomain of RP105 in the absence of MD1, we find that MD1 is necessary to prevent its aggregation. Monomeric RP105 protein is not capable of inhibiting the LPS response on whole blood while the RP105-MD1 complex did inhibit LPS induced TNF α production, a factor known to be important in neointima formation⁷. The exact mechanism of how RP105-MD1 regulates TLR4 signaling is still under discussion. However, it is suggested that the complex formation is crucial, since monomeric RP105 is highly unstable. It has been shown that RP105-MD1 interacts directly with TLR4-MD2¹⁵. The unusual 2:2 homodimer of the RP105-MD1 complex suggests two possible mechanisms for inhibition of TLR4-MD2¹⁸; either (i) a lateral binding of TLR4-MD2 to the RP105-MD1 complex which would involve direct MD1-MD2 interactions or, (ii) the formation of quasi-symmetrical TLR4-MD2/RP105-MD1 complexes reminiscent of the usual ligand-induced TLR homodimers. In both scenarios RP105-MD1 could block TLR4 homodimer formation and possibly prevent/destabilize LPS binding to MD2¹⁸. However, the second mechanism was considered to be more plausible since it explains the regulation of the LPS response by RP105-MD1 regardless of LPS binding¹⁸. To set more focus on the therapeutic potential we initiated experiments to study the therapeutic potential of RP105 in a more humanized model having vessel damage combined with a diet induced hypercholesterolemia, i.e. cuff induced neointimal formation in hypercholesterolemic ApoE3*Leiden mice. No effect was seen of gene transfer of vectors expressing MD1 as a single factor. The absence of an effect of MD1 expression, as was also previously shown in vitro¹⁵, demonstrates that the mechanism that leads to reduction in TLR4 signaling does not rely on MD1-MD2 interactions, thus the above-discussed scenario 1 is unlikely. Overexpression of solRP105 alone as a single factor did not alter neointima formation suggesting that the endogenously produced MD1 is not sufficient to stabilize RP105 by formation of complexes as is required in vitro (Figure 4). Combined overexpression of both proteins, however, resulted in the formation of a functional complex and led to a strong

decrease in neointima formation. The soluble RP105/MD1 complex may act as a decoy receptor and as such have a therapeutic potential.

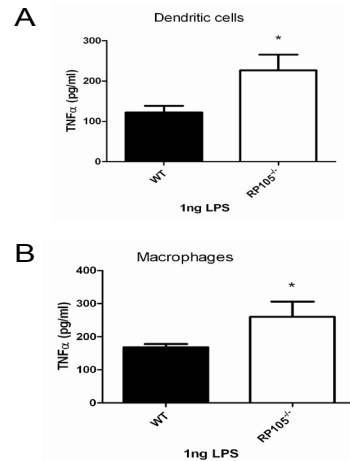
Apparently, overexpression in vivo of solRP105 with MD1 at the site of production is essential to form a stable and effective RP105-MD1 complex for functional inhibition of neointimal formation. These results are also supportive for the quasi-symmetrical working mechanism of RP105-MD1, the above-discussed second scenario of RP105 mediated TLR4 inhibition. In summary, we demonstrate the presence of RP105 on cultured VSMC and in VSMC in vivo in media and neointima and the increased restenosis in RP105^{-/-} mice indicate RP105 as a mediator of restenosis, probably as an inhibitor of TLR4. Furthermore, solRP105 significantly modulates the strong TLR4 driven vascular remodeling. Thus RP105 is an interesting new factor involved in the complex regulation of vascular remodeling and can be used to develop novel therapeutic strategies to inhibit neointima formation.

Acknowledgements: The authors thank K. Miyake for kindly providing the RP105^{-/-} mice. This study was (partly) performed within the framework of the Dutch Top Institute Pharma project D1-101. This project has been supported by the Foundation “De Drie Lichten” in the Netherlands.

Conflict of Interest: none



Supplementary Figure 1. Colocalized TLR4 and RP105 staining on VSMC shown by confocal microscopy.



Supplementary Figure 2 TNF α levels produced upon LPS stimulation by dendritic cells (A) and macrophages (B) from WT and RP105^{-/-} mice. * = P<0.05



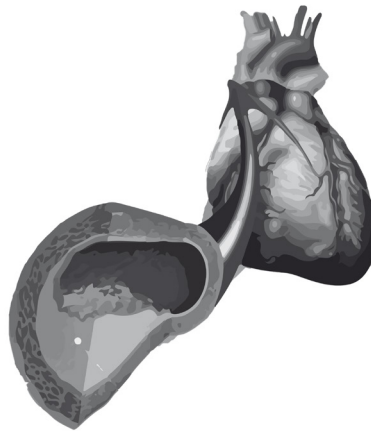
Reference List

1. Jukema JW, Ahmed TA, Verschuren JJ, Quax PH. Restenosis after PCI. Part 2:prevention and therapy. *Nat Rev Cardiol* 2012;9(2):79-90.
2. Jukema JW, Verschuren JJ, Ahmed TA, Quax PH. Restenosis after PCI. Part 1:pathophysiology and risk factors. *Nat Rev Cardiol* 2012;9(1):53-62
3. Monraats PS, Pires NM, Agema WR, Zwinderman AH, Schepers A, de Maat MP, Doevendans PA, de Winter RJ, Tio RA, Waltenberger J, Frants RR, Quax PH, van Vlijmen BJ, Atsma DE, van der Laarse A, van der Wall EE, Jukema JW. Genetic inflammatory factors predict restenosis after percutaneous coronary interventions. *Circulation* 2005;112(16):2417-25.
4. Hollestelle SC, De Vries MR, Van Keulen JK, Schoneveld AH, Vink A, Strijder CF, Van Middelaar BJ, Pasterkamp G, Quax PH, de Kleijn DP. Toll-like receptor 4 is involved in outward arterial remodeling. *Circulation* 2004;109(3):393-8.
5. Vink A, Schoneveld AH, van der Meer JJ, Van Middelaar BJ, Sluijter JP, Smeets MB, Quax PH, Lim SK, Borst C, Pasterkamp G, de Kleijn DP. In vivo evidence for a role of toll-like receptor 4 in the development of intimal lesions. *Circulation* 2002;106(15):1985-90.
6. Karper JC, De Vries MR, van den Brand BT, Hoefler IE, Fischer JW, Jukema JW, Niessen HW, Quax PH. Toll-like receptor 4 is involved in human and mouse vein graft remodeling, and local gene silencing reduces vein graft disease in hypercholesterolemic APOE*3Leiden mice. *Arterioscler Thromb Vasc Biol* 2011;31(5):1033-40.
7. Monraats PS, Pires NM, Schepers A, Agema WR, Boesten LS, De Vries MR, Zwinderman AH, de Maat MP, Doevendans PA, de Winter RJ, Tio RA, Waltenberger J, 't Hart LM, Frants RR, Quax PH, van Vlijmen BJ, Havekes LM, van der Laarse A, van der Wall EE, Jukema JW. Tumor necrosis factor-alpha plays an important role in restenosis development. *FASEB J* 2005;19(14):1998-2004
8. Schepers A, Eefting D, Bonta PI, Grimbergen JM, De Vries MR, van W, V, de Vries CJ, Egashira K, van Bockel JH, Quax PH. Anti-MCP-1 gene therapy inhibits vascular smooth muscle cells proliferation and attenuates vein graft thickening both in vitro and in vivo. *Arterioscler Thromb Vasc Biol* 2006;26(9):2063-9.
9. de Graaf R, Kloppenburg G, Kitslaar PJ, Bruggeman CA, Stassen F. Human heat shock protein 60 stimulates vascular smooth muscle cell proliferation through Toll-like receptors 2 and 4. *Microbes Infect* 2006;8(7):1859-65.
10. Kawai T, Akira S. The role of pattern-recognition receptors in innate immunity:update on Toll-like receptors. *Nat Immunol* 2010;11(5):373-84.
11. Kim HM, Park BS, Kim JI, Kim SE, Lee J, Oh SC, Enkhbayar P, Matsushima N, Lee H, Yoo OJ, Lee JO. Crystal structure of the TLR4-MD-2 complex with bound endotoxin antagonist Eritoran. *Cell* 2007;130(5):906-17.
12. Shimamoto A, Chong AJ, Yada M, Shomura S, Takayama H, Fleisig AJ, Agnew ML, Hampton CR, Rothnie CL, Spring DJ, Pohlman TH, Shimp H, Verrier ED. Inhibition of Toll-like receptor 4 with eritoran attenuates myocardial ischemia- reperfusion injury. *Circulation* 2006;114(1 Suppl):I270-I274.
13. Akashi-Takamura S, Miyake K. TLR accessory molecules. *Curr Opin Immunol*2008;20(4):420-5.
14. Divanovic S, Trompette A, Atabani SF, Madan R, Golenbock DT, Visintin A, Finberg RW, Tarakhovskiy A, Vogel SN, Belkaid Y, Kurt-Jones EA, Karp CL. Inhibition ofTLR-4/MD-2 signaling by RP105/MD-1. *J Endotoxin Res* 2005;11(6):363-8.
15. Divanovic S, Trompette A, Atabani SF, Madan R, Golenbock DT, Visintin A, Finberg RW, Tarakhovskiy A, Vogel SN, Belkaid Y, Kurt-Jones EA, Karp CL. Negative regulation of Toll-like receptor 4 signaling by the Toll-like receptor homolog RP105. *Nat Immunol* 2005;6(6):571-8.
16. Divanovic S, Trompette A, Petiniot LK, Allen JL, Flick LM, Belkaid Y, Madan R, Haky JJ, Karp CL. Regulation of TLR4 signaling and the host interface with pathogens and danger: the role of RP105. *J Leukoc Biol* 2007;82(2):265-71.



17. Ohto U, Miyake K, Shimizu T. Crystal Structures of Mouse and Human RP105/MD-1 Complexes Reveal Unique Dimer Organization of the Toll-Like Receptor Family. *J Mol Biol.* 2011;413(4):815-25.
18. Yoon SI, Hong M, Wilson IA. An unusual dimeric structure and assembly for TLR4 regulator RP105-MD-1. *Nat Struct Mol Biol* 2011;18(9):1028-35.
19. Freudenberg J, Lee AT, Siminovitch KA, Amos CI, Ballard D, Li W, Gregersen PK. Locus category based analysis of a large genome-wide association study of rheumatoid arthritis. *Hum Mol Genet* 2010;19(19):3863-72.
20. Tada Y, Koarada S, Morito F, Mitamura M, Inoue H, Suematsu R, Ohta A, Miyake K, Nagasawa K. Toll-like receptor homolog RP105 modulates the antigen-presenting cell function and regulates the development of collagen-induced arthritis. *Arthritis Res Ther* 2008;10(5):R121.
21. Arkenbout EK, de Waard V, van Bragt M., van Achterberg TA, Grimbergen JM, Pichon B, Pannekoek H, de Vries CJ. Protective function of transcription factor TR3 orphan receptor in atherosclerosis: decreased lesion formation in carotid artery ligation model in TR3 transgenic mice. *Circulation* 2002;106(12):1530-5
22. Miyake K, Yamashita Y, Ogata M, Sudo T, Kimoto M. RP105, a novel B cell surface molecule implicated in B cell activation, is a member of the leucine-rich repeat protein family. *J Immunol* 1995;154(7):3333-40
23. Lardenoye JH, Delsing DJ, De Vries MR, Deckers MM, Princen HM, Havekes LM, van Hinsbergh VW, van Bockel JH, Quax PH. Accelerated atherosclerosis by placement of a perivascular cuff and a cholesterol-rich diet in ApoE*3Leiden transgenic mice. *Circ Res* 2000;87(3):248-53.
24. McMahon JM, Signori E, Wells KE, Fazio VM, Wells DJ. Optimisation of electrotransfer of plasmid into skeletal muscle by pretreatment with hyaluronidase -- increased expression with reduced muscle damage. *Gene Ther* 2001;8(16):1264-70.
25. Hadley JS, Wang JE, Michaels LC, Dempsey CM, Foster SJ, Thiemermann C, Hinds CJ. Alterations in inflammatory capacity and TLR expression on monocytes and neutrophils after cardiopulmonary bypass. *Shock* 2007;27(5):466-73.
26. Nomura F, Akashi S, Sakao Y, Sato S, Kawai T, Matsumoto M, Nakanishi K, Kimoto M, Miyake K, Takeda K, Akira S. Cutting edge: endotoxin tolerance in mouse peritoneal macrophages correlates with down-regulation of surface toll-like receptor 4 expression. *J Immunol* 2000;164(7):3476-9.
27. Eefting D, Schepers A, De Vries MR, Pires NM, Grimbergen JM, Lagerweij T, Nagelkerken LM, Monraats PS, Jukema JW, van Bockel JH, Quax PH. The effect of interleukin-10 knock-out and overexpression on neointima formation in hypercholesterolemic APOE*3-Leiden mice. *Atherosclerosis* 2007;193(2):335-42
28. Eefting D, Seghers L, Grimbergen JM, De Vries MR, de Boer HC, Lardenoye JW, Jukema JW, van Bockel JH, Quax PH. A novel urokinase receptor-targeted inhibitor for plasmin and matrix metalloproteinases suppresses vein graft disease. *Cardiovasc Res* 2010;88(2):367-75.
29. Zhang Y, Xu CB, Cardell LO. Long-term exposure to IL-1beta enhances Toll-IL-1 receptor-mediated inflammatory signaling in murine airway hyperresponsiveness. *Eur Cytokine Netw* 2009;20(3):148-56.
30. Timmers L, Sluijter JP, Van Keulen JK, Hoefler IE, Nederhoff MG, Goumans MJ, Doevendans PA, van Echteld CJ, Joles JA, Quax PH, Piek JJ, Pasterkamp G, de Kleijn DP. Toll-like receptor 4 mediates maladaptive left ventricular remodeling and impairs cardiac function after myocardial infarction. *Circ Res* 2008;102(2):257-64.
31. Ward MR, Pasterkamp G, Yeung AC, Borst C. Arterial remodeling. Mechanisms and clinical implications. *Circulation* 2000;102(10):1186-91.
32. Miyake K, Shimazu R, Kondo J, Niki T, Akashi S, Ogata H, Yamashita Y, Miura Y, Kimoto M. Mouse MD-1, a molecule that is physically associated with RP105 and positively regulates its expression. *J Immunol* 1998;161(3):1348-5

CHAPTER 8



RP105 deficiency aggravates cardiac dysfunction after myocardial infarction in mice

Karper J.C, Louwe M.C*, de Vries M.R, Bastiaansen A.J.N.M, van der Hoorn J.W.A, Willems van Dijk K, Rensen P.C.N, Steendijk P, Smit J.W.A, Quax P.H.A*

** both authors contributed equally*

Manuscript under revision

Abstract

Background: Toll-like receptor-4 (TLR4), a receptor of the innate immune system, is suggested to have detrimental effects on cardiac function after myocardial infarction (MI). RP105 (CD180) is a TLR4 homolog lacking the intracellular signalling domain that competitively inhibits TLR4-signalling. Thus, we hypothesized that RP105 deficiency, by amplifying TLR4 signalling, would lead to aggravated cardiac dysfunction after MI.

Methods and Results: First, whole blood from RP105^{-/-} and wild-type (WT) male C57Bl/6N mice was stimulated with LPS, which induced a strong inflammatory TNF α response in RP105^{-/-} mice. Then, baseline heart function was assessed by left ventricular pressure-volume relationships which were not different between RP105^{-/-} and WT mice. Permanent ligation of the left anterior descending coronary artery was performed to induce MI. Infarct sizes were analysed by (immuno)histology and did not differ. Fifteen days post MI heart function was assessed and RP105^{-/-} mice had significantly higher heart rate (+21%, $P<0.01$), end systolic volume index (+57%, $P<0.05$), end systolic pressure (+22%, $P<0.05$) and lower relaxation time constant tau (-12%, $P<0.05$), and a tendency for increased end diastolic volume index (+42%, $P<0.06$), compared to WT mice. In the area adjacent to the infarct zone, compared to the healthy myocardium, levels of RP105, TLR4 and the endogenous TLR4 ligand fibronectin-EDA were increased as well as the number of macrophages, however this was not different between both groups.

Conclusion: Deficiency of the endogenous TLR4 inhibitor RP105 leads to an enhanced inflammatory status and more pronounced cardiac dilatation after induction of MI, underscoring the role of the TLR4 pathway in post-infarction remodelling.

Introduction

Cardiovascular diseases remain the leading cause of death in the western countries, which is mainly accounted for by the high incidence of myocardial infarction (MI). Although survival after MI has improved significantly due to novel medical strategies and interventions, the incidence and prevalence of MI related morbidity is increasing which is mainly due to development of congestive heart failure (CHF) [1, 2]. CHF is the result of a remodelling response of the ventricle upon reduced contraction capacity after cardiac damage such as MI [2]. During the last decades the immune system was demonstrated to play a major role in myocardial repair and remodelling. Evidence accumulates that prolongation of the post-infarction inflammatory response leads to increased remodelling and thereby CHF progression [3-5]. Therefore, new strategies to intervene in the pathogenesis of CHF may be worthwhile, which can be achieved by immediate anticipation and tackling of the inflammatory- and matrix degeneration processes that have been initiated by the immune system [6].

Toll like receptors (TLR) are part of the innate immune system and are capable of recognizing Pathogen Associated Molecular Patterns (PAMPS) as well as Damage Associated Molecular Patterns (DAMPs). PAMPs are parts of exogenous pathogens such as bacteria while DAMPs, like fibronectin-EDA or Heat Shock Protein, may become available after cell stress or tissue damage/injury without the involvement of exogenous pathogens [7]. They have been widely associated with atherosclerotic plaque formation, restenosis and vein graft failure; all processes that may initiate ischemia or MI, resulting in cardiac remodelling [8-10]. One of the most studied TLRs is TLR4, which is present on circulating cells and cardiomyocytes. Cardiac expression of TLR4 was shown to be upregulated in cardiomyopathy [11]. In preclinical studies TLR4 was shown to play an important role in myocardial infarct healing, LV remodelling and functional impairment following MI [12]. Additionally, intervention with a specific TLR4 antagonist Eritoran was demonstrated to be protective against remodelling [13].

TLR-signalling is mainly regulated by accessory molecules [14], and no role for these accessory molecules in cardiac remodelling has been defined yet. RadioProtective105 (RP105), one of these molecules, resides on the cell surface and has a high extracellular structural similarity to TLR4 (Fig. 1) [15]. In addition, like TLR4, whose signalling depends on association with the extracellular accessory protein MD-2, RP105 surface expression depends on co-expression of the MD2 homolog: MD1. However, in contrast to TLR4, RP105 lacks the intracellular Toll Interleukin Receptor (TIR) domain that is essential to initiate cellular activation. As such RP105 is an inhibitor of the TLR4 signaling pathway [16, 17]. Whereas no direct ligands have been found for RP105, strong indications exist that it can bind TLR4 ligands, thereby influencing TLR4 signalling and dampening the inflammatory responses induced by TLR4 activation.

As TLR4 activation has been shown to enhance cardiac remodelling after MI, we hypothesized that RP105 deficiency would aggravate these effects, through reduced inhibition (thus by stimulation) of TLR4 signalling. In this study we demonstrate that RP105 deficiency indeed has a functional role in cardiac remodeling, since systolic and diastolic cardiac function indices are affected after myocardial infarction.



Material and methods

2.1 Animals and experimental design

Studies were performed with 10-12 week old, male RP105-deficient (RP105^{-/-}) mice bred in our animal facility and wild-type (WT) mice (Charles River, Maastricht, The Netherlands), both on a C57Bl/6N background. Animals were housed in a temperature and humidity-controlled room on a 12:12-h light-dark cycle with ad libitum access to water and normal chow diet. Body weights were measured weekly (RP105^{-/-} day 0: 28.6±1.6, day 15: 27.3±1.8 g; WT day 0: 24.4±1.4 g, day 15: 23.6±1.5 g). MI was induced by coronary ligation (see below) at day 0 in RP105^{-/-} (n=12) and WT (n=12) mice. Subsequently, cardiac function assessments by pressure-volume loops (PV-loops) were performed at day 15. To obtain baseline cardiac function, additional PV-loop measurements were performed in a separate group of animals (RP105^{-/-}, n=4; WT, n=4) without MI. After PV-loop measurements the mice were sacrificed and hearts were isolated for further examination. The protocol was approved by the Animal Ethics Committee from the Leiden University Medical Center and conformed to the Guide for Care and Use of Laboratory Animals (NIH publication No.85-23, Revised 1996).

2.2 Whole blood TNF α stimulation assay

In order to investigate the inflammatory response at baseline of the different groups, venous blood via a tail vein cut was collected in a separate batch of mice and suspended 1:25 with RPMI 1640 (Gibco 52400-025) supplemented with non-essential amino acids (PAA M11-003) and glutamax (Gibco 35050). Blood from both WT en RP105^{-/-} mice was incubated overnight at 37°C in absence and presence of LPS in the concentrations 25 ng/mL and 50 ng/mL. Subsequently, TNF α levels were measured by ELISA (BD Biosciences, Erembodegem, Belgium).

2.3 Induction of myocardial infarctions

Mice were anesthetized by an intraperitoneal injection of a mixture of dormicum (0.7 mg/kg BW), dexdomitor (7.2 mg/kg BW) and fentanyl (0.07 mg/kg BW). Body temperature was maintained at 37°C using a temperature-controlled, automatic heating pad. Mice were artificially ventilated using a dedicated mouse ventilator (model 845, Harvard Apparatus, Holliston, MA). The left anterior descending coronary artery (LAD) was ligated with a 7-0 ethilon suture (Johnson and Johnson, New Brunswick, NJ), just distal to the left atrial appendage. Ischemia was visually confirmed by bleaching of the LV. The thorax was closed and the mice received an intraperitoneal injection of anexasate (0.5 mg/kg BW), antisedan (2.5 mg/kg BW), naloxon (1.2 mg/kg BW) to antagonize the anesthesia. Analgesic temgesic (1.5 μ g in 50 μ L PBS) was administered subcutaneously. Thereafter, the mice were allowed to recover on a temperature-controlled heating pad.

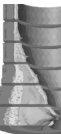
2.4 Hemodynamic measurements

Thirteen days after induction of the MI, transthoracic, cardiac echocardiography was performed using a VisualSonics Vevo 770 with a 30 MHz ultrasound transducer (VisualSonics, Toronto, Canada) as described earlier [18]. The following parameters were obtained: heart rate (HR), stroke volume (SV), cardiac output (CO), end-diastolic volume (EDV) end-systolic volume (ESV), ejection fraction (EF), fractional area change (FAC) and area change. Briefly, mice were anesthetized with 3% isoflurane, and placed supine on a temperature-controlled animal

platform. Parasternal long axis and short axis images were recorded in all animals. Analysis of the data was performed with software provided by VisualSonics. Subsequently, 2 days later (at day 15 post MI), LV function was assessed by invasive PV-loops as described earlier [18]. Mice were anesthetized with a starting dose of 4% isoflurane and a maintenance dose of 1.5% isoflurane. After intubation mice were ventilated and the jugular vein was cannulated for infusion of hypertonic saline to determine parallel conductance. Via the right carotid artery a 1.2F PV catheter (FTS-1212B-4518, Scisense Inc., London, Ontario, Canada) was placed into the LV. The catheter was connected to a Scisense ADV signal processor (Scisense Inc) to generate high-fidelity pressure and volume signals. Positioning of the catheter was guided by online pressure and volume signals. On-line display and acquisition of the signals (2000 samples/s) was performed with a PowerLab 8/30 data acquisition system and LabChart Pro software (AD Instruments GmbH, Spechbach, Germany). Off-line data analysis was performed with custom-made software (CircLab, P. Steendijk). Conversion of conductance data to absolute volumes was based on matching conductance derived volumes with echocardiographically determined EDV and ESV the same mouse two days earlier. The following parameters were measured: heart rate (HR), stroke volume (SV), cardiac output (CO), end-diastolic volume (EDV) end-systolic volume (ESV), ejection fraction (EF), end-diastolic pressure (EDP) and end-systolic pressure (ESP). Stroke work (SW) was determined as the area of the PV-loop and the maximal and minimal rate of LV pressure change, dP/dt_{MAX} and dP/dt_{MIN} , were obtained. Effective arterial elastance (EA) was calculated as ESP/SV . Relaxation time tau was calculated as the time-constant of mono-exponential pressure decay during isovolumic relaxation. The end-systolic pressure-volume relationship (ESPVR) was determined by a single-beat method as previously described and validated [19]. Subsequently, the ESPVR was quantified by its slope, end-systolic elastance E_{es} , and the volume intercept at 70 mmHg ESV_{70} . The end-diastolic pressure-volume relationship (EDPVR) was estimated using a single-beat approach as described previously [20]. Briefly, the filling phase pressure-volume data (from the point with minimal pressure to the point with maximal volume) were fitted with an exponential relation to determine the stiffness constant KED ($P = A \cdot \exp(KED \cdot V)$). Alternatively, we applied a linear fit to determine end-diastolic elastance E_{ed} ($P = P_0 + E_{ed} \cdot V$) and the pressure-intercept at 2 μ L/g, EDV_2

2.5 Myocardial (immuno)histochemistry

Hearts were fixed overnight in para-formaldehyde and cut into five 1 mm-thick slices, perpendicular to the long axis of the heart. These slices were flat-embedded in paraffin and 5 μ m-thick sections were prepared. To delineate LV area and infarct area the lower 3 sections were stained for collagen with Sirius Red. Total LV wall area (including septum, but excluding lumen) and infarct area were measured with cell[^]D imaging software (Olympus Soft Imaging Solutions). The infarct area was expressed as percentage (vol/vol) of the LV wall volume. Additionally, sections were immunohistochemically stained for macrophages (rat anti-mouse MAC-3, 1:200; BD Biosciences, Erembodegem, Belgium) to count the infiltrating macrophages into the myocardium, TLR4 (rabbit anti-human TLR4, 1:150 SantaCruz, Heidelberg, Germany) to observe presence of TLR4 in the different areas of the myocardium, RP105 (rabbit anti-human, 1:250 SantaCruz, Heidelberg, Germany) to verify the presence of the accessory molecule in WT mice, and fibronectin-EDA (mouse anti-human 1:800, Abcam, Cambridge, United Kingdom) whose presence precedes that of collagen and serves as an endogenous ligand for TLR4 and is frequently induced upon tissue injury and is known to play a role in cardiac remodeling. Images were scored by an observer blinded for



the study groups. Per image three specific areas of the myocardium were distinguished: the infarcted area, the border zone and the remote, undamaged, healthy myocardium. MAC-3 staining was analyzed by counting the number of macrophages in three consecutive fields of view per specific area. For TLR4, RP105 and fibronectin-EDA stainings were scored in a semi-quantitative manner, using zero staining as grade 0, mild to moderate staining as grade 1 and a profound staining as grade 2.

2.6 Statistical methods

Significance of differences between the groups was calculated non-parametrically using a Mann-Whitney U-test. Difference in survival rate after MI was calculated using a chi-squared test. P-values <0.05 were considered statistically significant. SPSS 17.0 for Windows (SPSS, Chicago, USA) was used for statistical analysis. Values are presented as means ± SD.

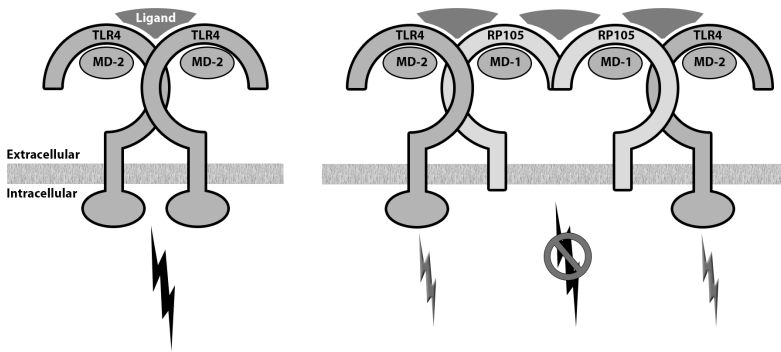


Fig. 1. Schematic model of the TLR4-MD2 and RP105-MD1 complex. Activation of the TLR4-MD2 heterodimer by ligand binding results in activation of the intracellular signaling domain thereby initiating a downstream signaling cascade (left panel). The formation of the unusual 2:2 homodimer by TLR4-MD2 and RP105-MD1 alters the TLR4 signaling cascade, whereas RP105 dimerization by itself has no signaling capacity at all as it lacks the intracellular Toll Interleukin Receptor (TIR) domain (right panel). Adapted from Otho et al. [27]

Table 1. Effect of RP105 deficiency TLR4 mediated inflammatory response.

LPS dose (ng/mL)	TNFα (ng/mL)	TNFα (ng/mL)
	WT	RP105 ^{-/-}
25	20.0±4.1 ng/mL	108±24 ng/mL*
50	28.7±7.0 ng/mL	128±25 ng/mL*

Blood samples of WT and RP105^{-/-} mice were diluted 1:25 with RPMI 1640, and incubated overnight with 25 or 50 ng/mL LPS. Subsequently TNFα levels were measured and expressed as ng/mL. Values represent means ± SD; n=5 per group. * P<0.01

3. Results

3.1 Increased inflammatory response in RP105^{-/-} mice after TLR4 stimulation by LPS

To demonstrate whether an increased TLR4 mediated inflammatory response is present in RP105^{-/-} mice as compared to WT mice, an ex vivo whole blood stimulation assay was performed in the presence and absence of LPS. After an overnight LPS stimulation with 25 ng/mL and 50 ng/mL LPS, TNF α levels were markedly increased in RP105^{-/-} mice compared to WT mice for both concentrations, whereas no significant difference was observed under non-stimulated conditions (Table 1).

3.2 RP105 deficiency does not affect baseline cardiac function

To determine possible differences in baseline cardiac function between WT and RP105^{-/-} mice, echocardiography and pressure-volume loops were measured in animals without MI. Since body weight differed between the groups (25.7 ± 0.7 g in WT vs. 28.9 ± 2.7 g in RP105^{-/-}, $P=0.036$) all volumetric parameters were corrected for body weight. Results for the main PV loop-derived parameters show no significant differences between the WT and the RP105^{-/-} mice (see online data supplement table). These findings indicate that RP105 deficiency per se does not influence basal cardiac function.

3.3 RP105 deficiency promotes cardiac dilatation after myocardial infarction

To investigate whether RP105 deficiency influences cardiac function after MI, the LAD was permanently ligated in 12 WT and 12 RP105^{-/-} mice. No significant difference in survival rates was observed (92% in WT vs. 75% in RP105^{-/-}, $P=0.273$), suggesting that both strains were equally able to cope with the severe cardiac damage.

Fifteen days after induction of the MI, functional parameters were obtained by intraventricular PV-loop measurements. The results of these analyses are summarized in Table 2. Based on mean values for end-diastolic and end-systolic pressures and volumes, average PV-loops were created for both groups (Fig. 2).

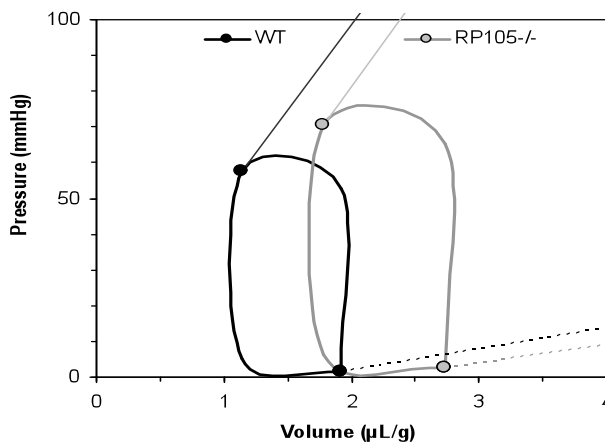


Fig. 2. Pressure-volume loops after myocardial infarction. WT and RP105^{-/-} mice underwent ligation of the LAD, and 15 days post myocardial infarction pressure-volume loops were recorded in each mouse. Average pressure-volume loops and pressure-volume relations, corrected for body weight, are shown per group; $n=8$ per group.



Corresponding end-diastolic and end-systolic PV-relations were added, based on mean EES and EED values. These measurements revealed that RP105 deficiency significantly affected heart function after MI. Compared with WT mice, RP105^{-/-} mice showed significantly higher heart rate (+21% P=0.003), end-systolic volume index (+42%, P=0.038), end-systolic pressure (+22%, P=0.021) and lower Tau (-12%, P=0.046). Furthermore a clear tendency for a higher end-diastolic volume (+35%, P=0.058) and higher -dP/dtMIN (+24%, P=0.093) was observed. Taken together, RP105^{-/-} mice showed more prominent cardiac dilatation after MI, but general hemodynamics appeared to be relatively unaffected at this stage.

3.4 RP105 deficiency does not influence infarct size

Then it was investigated whether the enhanced dilatation of the RP105^{-/-} mice could be secondary to an increased myocardial infarct size. Directly after the PV-loop measurements, 15 days after MI, mice were sacrificed and hearts were isolated. Fig. 3 shows representative Sirius Red stained cross sections of the infarcted heart. No differences in total LV area were observed ($27 \times 10^6 \pm 4 \times 10^6 \mu\text{M}$ in WT vs $31 \times 10^6 \pm 3 \times 10^6 \mu\text{M}$ in RP105^{-/-}, P=0.11) whereas the infarct area comprised $12 \pm 5\%$ of the total LV in the WT animals versus $16 \pm 10\%$ in the RP105^{-/-} mice (P=0.53).

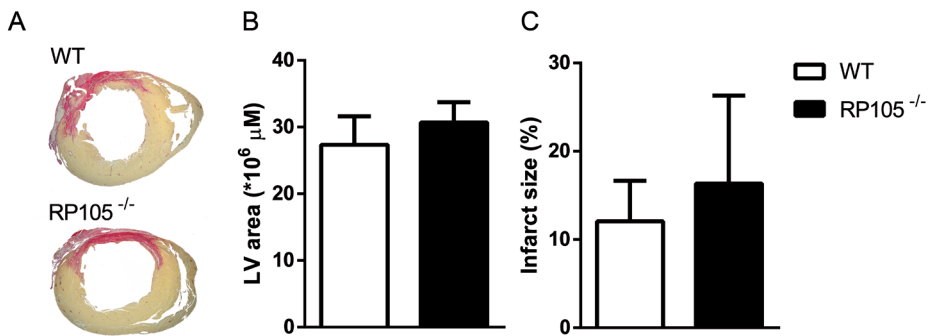


Fig. 3. Left ventricular area and myocardial infarct size in WT and RP105^{-/-} mice. Infarct size was measured by Sirius red staining in the two groups of mice and quantified as the area occupied by collagen. Representative cross sections, after Sirius Red staining, are shown above the corresponding bars for myocardial infarct size. Each bar represent mean ± SD; n= 8-10 per group.

3.5 Structural analysis of the myocardium and infarct area

To investigate potential underlying mechanisms causing the observed differences in cardiac function after MI, (immune)histochemical analyses on the myocardium of both groups were performed. We focused on inflammatory components in specific areas of the myocardium: the infarcted area, the border zone and the remote ‘undamaged/healthy’ myocardium. Fig. 4 shows representative images of the different stainings for Sirius Red, TLR4, EDA, MAC-3 and RP105. All stainings showed little to no response in the undamaged myocardium remote from the infarct area. An upregulation of TLR4, fibronectin-EDA staining and the number of macrophages (Fig. 5) were observed in the area adjacent to the infarcted zone. As expected the infarcted area consisted mainly of collagen (scar tissue) and macrophages. No differences in staining patterns were observed between WT and RP105^{-/-} mice.

Table 2. Effect of RP105 deficiency on cardiac function after a myocardial infarction.

	WT	RP105 ^{-/-}	P value
<i>General</i>			
HR (beats/min)	446±19	538±44	0.003
SV (μL/g)	0.8±0.3	0.9±0.4	0.490
CO ((mL/g)/min)	0.4±0.1	0.5±0.2	0.300
SW (mmHg.(μL/g))	42±14	57±44	0.916
Ea (mmHg/(μL/g))	0.2±0.1	0.1±0.1	0.223
Ees/Ea	0.7±0.3	0.6±0.3	0.395
<i>Systolic</i>			
ESP (mmHg)	58±9	70±9	0.021
ESV (μL/g)	1.1±0.7	1.8±0.7	0.038
EF (%)	43±16	35±10	0.372
dP/dtMax (mmHg/ms)	5±2	6±2	0.462
Ees (mmHg/(μL/g))	48±10	49±27	0.955
<i>Diastolic</i>			
EDP (mmHg)	1±2	2±2	0.293
EDV (μL/g)	1.9±0.6	2.7±0.9	0.058
Tau (ms)	11.9±0.9	10.4±1.5	0.046
-dP/dtMin (mmHg/ms)	4±0.8	5±2	0.093
Eed (mmHg/(μL/g))	6±4	5±3	0.721
Ked (1/(μL/g))	0.2±0.1	0.1±0.0	0.114

HR, heart rate; SV, stroke volume; CO, cardiac output; SW, stroke work; Ea, arterial elastance (afterload); Ees/Ea, ventricular arterial coupling; ESP, end systolic pressure; ESV, end systolic volume; EF, ejection fraction; dP/dtMax, maximal rate of pressure increase; Ees, end systolic elastance (slope of ESPVR); EDP, end diastolic pressure; EDV, end diastolic volume; Tau, relaxation time constant; -dP/dtMin, maximal rate of pressure decline; Eed, diastolic stiffness (slope of EDPVR); KED, diastolic stiffness constant. Values represent means ± SD; n=8 per group.

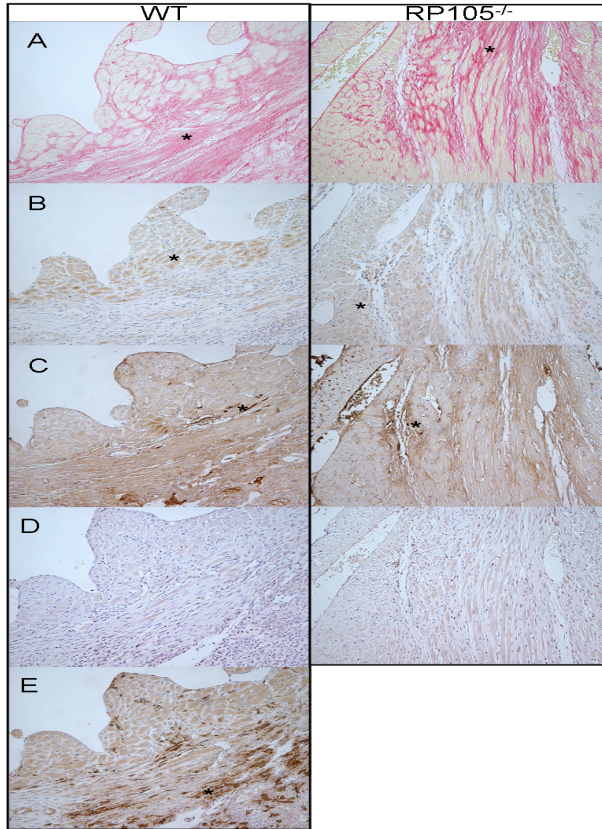


Fig. 4. Typical examples of (immuno)histological stainings for WT mouse (left panel) and RP105^{-/-} mouse (right panel), 200x magnification. Images are shown of (A) Sirius Red staining indicating the collagen in the tissue adjacent to the MI area (*), (B) TLR4 staining in tissue adjacent to the MI area (*), (C) EDA staining in tissue adjacent to the MI area (*), (D) MAC-3 (macrophages) and (E) RP105 staining in tissue adjacent to the MI area (*). All images were photographed in sections adjacent to the infarcted area. No differences were observed for Sirius Red, TLR4, EDA or MAC-3 staining between the two groups.

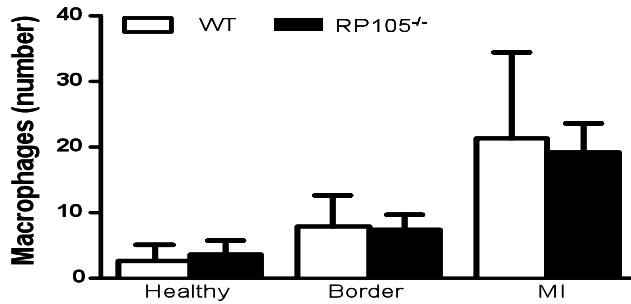


Fig. 5. Amount of macrophages per specific area of the myocardium in WT and RP105^{-/-} mice. the infarcted area, the border zone and the remote 'undamaged/healthy' myocardium Per image three specific areas of the myocardium were distinguished per image; the infarcted area, the border zone and the remote, undamaged, healthy myocardium. The number of macrophages was in three consecutive fields of view per specific area. Each bar represent mean \pm SD; n= 8-10 per group.

4. Discussion

The innate immune system, and especially TLRs, plays a pivotal role in the remodeling process that is initiated after an MI. Since the role of TLR accessory molecules and especially the negative regulator of TLR4, RP105, in cardiovascular disease is still largely unknown, we investigated its role in post MI cardiac function and remodeling. Our results show, for the first time, that deficiency of the TLR accessory molecule RP105, results in hampered post MI repair and subsequently increased cardiac volumes indicated by the right shifted pv-loop that corresponds to pv loops found in dilated cardiomyopathy. This causal involvement of RP105 in the post MI inflammatory processes provides new opportunities for therapeutic approaches to reduce cardiac remodeling and thereby improving cardiac function after a myocardial event.

RP105 was originally identified as a B-cell specific molecule, but turned out to be also present on myeloid cells including macrophages and dendritic cells [16, 21]. Since the expression of RP105 mirrors that of TLR4, and TLR4 is an important player in the pathophysiology of cardiovascular disease processes, we hypothesized that RP105 might be an essential regulator in cardiovascular diseases. In this study we demonstrate that after an MI, RP105 deficiency results in an increased ESV and EDV which is associated with a more dilated left ventricle. Since infarct size was similar in both groups, this effect suggests that the unaffected healthy myocardium of RP105^{-/-} mice is less able to preserve cardiac function after MI as compared to WT mice.

After MI, loss of function in the infarct zone may be compensated by the unaffected myocardium, for example by hypertrophy, or by invoking the Frank-Starling mechanism via cardiac dilatation. In addition, cardiac output may be maintained by increased heart rate. No significant differences in cardiac output were observed between the two groups, but the RP105^{-/-} mice showed a more pronounced dilatation and higher heart rate. This suggests that the intrinsic myocardial function in the undamaged myocardium was less in these mice, requiring more pronounced compensatory responses.



This conclusion is supported by the results regarding the ESPVR as shown in Fig. 2. The figure illustrates that the differences between the groups do not merely reflect altered loading conditions, but changes in intrinsic LV function as well, reflected by a rightward shift of the ESPRV. Interestingly, in contrast to the ESPVR which indicates a depressed systolic LV function, the downward shift of the EDPVR points towards an improved diastolic function in line with the positive effects on Tau, dp/dt_{MIN} and Ked.

Although macrophages in the infarcted zone are essential for the removal of necrotic tissue [22] they may also contribute to cardiac dysfunction by adherence to cardiomyocytes [23]. However, as both WT and RP105^{-/-} animals show a comparable density of macrophages in the border and infarcted areas, this cannot explain the differences in cardiac function.

Another factor that may contribute to the observed LV dilatation could be the availability of ligands for TLR4. Previously we showed presence of TLR4 and the endogenous TLR4 ligand fibronectin-EDA after myocardial infarction resulting in deteriorating effects on cardiac remodeling [12, 24]. Similarly, in this study we observed an upregulation of fibronectin-EDA in WT mice when the damaged myocardium is compared to the undamaged myocardium. This was similar in the RP105 deficient animals showing equal fibronectin-EDA expression. We thereby demonstrated that RP105 does not influence local endogenous TLR ligand fibronectin-EDA expression.

In the current study we did not observe any effects of RP105 deficiency on histologic parameters. This could be explained by the lack of RP105 expression in the myocardium, since RP105 is known to be present on antigen presenting cells (APC) [16] but not on cardiomyocytes. APCs are well known to be involved in the cardiac remodeling process

Alternatively it could be that RP105 has no direct signaling capacities. Since RP105 has no direct signaling function, but rather acts as a potent inhibitor of TLR4 signaling, it is more likely that the effects of RP105 deficiency are due to enhanced TLR4 signaling. In line with previously published results of Divanovic et al. [16, 25] we were able to demonstrate an enhanced inflammatory response in whole blood in RP105^{-/-} mice. Ex vivo stimulation of whole blood samples of RP105^{-/-} mice by the TLR4 ligand LPS resulted in strong upregulation of TNF α levels compared to the controls (Table 1), a difference in TNF α levels that was not observed under unstimulated conditions. This supports the hypothesis that the TLR4 mediated inflammatory response is enhanced by RP105 deficiency.

RP105 alters TLR4 signaling via the RP105-MD1 complex which forms an unusual 2:2 homodimer. Two possible mechanisms for signaling inhibition effects on TLR4-MD2 were suggested previously; a lateral binding of TLR4-MD2 to the RP105-MD1 complex or the formation of TLR4-MD2/RP105-MD1 complexes reminiscent of the usual ligand-induced TLR homodimers [26]. Therefore the final effects of same amount of endogenous ligands activating TLR signaling, and thereby initiating cardiac remodeling, may have been increased due to the lack of RP105. While TLR4 expression in the myocardium was also comparable in both groups, this supports the hypothesis that RP105 does not cause its effects in remodeling directly via endogenous ligand or modulation of TLR4 receptor expression but probably via its previously described alternation of TLR4 signalling. By demonstrating that deficiency of the TLR accessory molecule RP105 affects the remodelling process, we reveal that a non-signalling extracellular receptor may be a potential target in the prevention of cardiac remodelling.

In summary, this study provides the first evidence that RP105 is involved in mechanisms

underlying the TLR4 pathway induced post-infarction healing process. We show that RP105 deficiency has deleterious effects on cardiac function after a MI compared to WT mice with similar infarct size. These results underscore the role of the TLR4-pathway in post-infarction remodelling and as a result modulating RP105 may be an interesting new therapeutic strategy. To elucidate the exact mechanism further investigations are necessary.

1. Kannel WB, Sorlie P, McNamara PM. Prognosis after initial myocardial infarction: the Framingham study. *Am J Cardiol* 1979;44:53-9.
2. Lewis EF, Moye LA, Rouleau JL, Sacks FM, Arnold JM, Warnica JW et al. Predictors of late development of heart failure in stable survivors of myocardial infarction: the CARE study. *J Am Coll Cardiol* 2003;42:1446-53.
3. Frangiannis NG, Smith CW, Entman ML. The inflammatory response in myocardial infarction. *Cardiovasc Res* 2002;53:31-47.
4. Frangiannis NG. The immune system and cardiac repair. *Pharmacol Res* 2008;58:88-111.
5. Frangiannis NG. Regulation of the inflammatory response in cardiac repair. *Circ Res* 2012;110:159-73.
6. McMurray JJ, Adamopoulos S, Anker SD, Auricchio A, Bohm M, Dickstein K et al. ESC Guidelines for the diagnosis and treatment of acute and chronic heart failure 2012: The Task Force for the Diagnosis and Treatment of Acute and Chronic Heart Failure 2012 of the European Society of Cardiology. Developed in collaboration with the Heart Failure Association (HFA) of the ESC. *Eur Heart J* 2012;33:1787-847.
7. Kawai T, Akira S. The role of pattern-recognition receptors in innate immunity: update on Toll-like receptors. *Nat Immunol* 2010;11:373-84.
8. Hansson GK, Hermansson A. The immune system in atherosclerosis. *Nat Immunol* 2011;12:204-12.
9. Karper JC, De Vries MR, van den Brand BT, Hoefler IE, Fischer JW, Jukema JW et al. Toll-like receptor 4 is involved in human and mouse vein graft remodeling, and local gene silencing reduces vein graft disease in hypercholesterolemic APOE*3Leiden mice. *Arterioscler Thromb Vasc Biol* 2011;31:1033-40.
10. Vink A, Schoneveld AH, van der Meer JJ, Van Middelaar BJ, Sluijter JP, Smeets MB et al. In vivo evidence for a role of toll-like receptor 4 in the development of intimal lesions. *Circulation* 2002;106:1985-90.
11. Frantz S, Kobzik L, Kim YD, Fukazawa R, Medzhitov R, Lee RT et al. Toll4 (TLR4) expression in cardiac myocytes in normal and failing myocardium. *J Clin Invest* 1999;104:271-80.
12. Timmers L, Sluijter JP, van Keulen JK, Hoefler IE, Nederhoff MG, Goumans MJ et al. Toll-like receptor 4 mediates maladaptive left ventricular remodeling and impairs cardiac function after myocardial infarction. *Circ Res* 2008;102:257-64.
13. Shimamoto A, Chong AJ, Yada M, Shomura S, Takayama H, Fleisig AJ et al. Inhibition of Toll-like receptor 4 with eritoran attenuates myocardial ischemia-reperfusion injury. *Circulation* 2006;114:I270-I274.
14. Akashi-Takamura S, Miyake K. TLR accessory molecules. *Curr Opin Immunol* 2008;20:420-5.
15. Miyake K, Yamashita Y, Ogata M, Sudo T, Kimoto M. RP105, a novel B cell surface molecule implicated in B cell activation, is a member of the leucine-rich repeat protein family. *J Immunol* 1995;154:3333-40.
16. Divanovic S, Trompette A, Atabani SF, Madan R, Golenbock DT, Visintin A et al. Negative regulation of Toll-like receptor 4 signaling by the Toll-like receptor homolog RP105. *Nat Immunol* 2005;6:571-8.
17. Divanovic S, Trompette A, Petiniot LK, Allen JL, Flick LM, Belkaid Y et al. Regulation of TLR4 signaling and the host interface with pathogens and danger: the role of RP105. *J Leukoc Biol* 2007;82:265-71.
18. Louwe MC, van der Hoorn JW, van den Berg SA, Jukema JW, Romijn JA, Willems van DK et al. Gender-dependent effects of high-fat lard diet on cardiac function in C57Bl/6J mice. *Appl Physiol Nutr Metab* 2012;37:214-24.
19. Ten Brinke EA, Klautz RJ, Verwey HF, van der Wall EE, Dion RA, Steendijk P. Single-beat estimation of the left ventricular end-systolic pressure-volume relationship in patients with heart failure. *Acta Physiol (Oxf)*. 2010; 198: 37-46.



20. Ten Brinke EA, Burkhoff D, Klautz RJ, Tschöpe C, Schalij MJ, Bax JJ, van der Wall EE, Dion RA, Steendijk P. Single-beat estimation of the left ventricular end-diastolic pressure-volume relationship in patients with heart failure. *Heart* 2010; 96: 213-219.
21. Miyake K, Yamashita Y, Hitoshi Y, Takatsu K, Kimoto M. Murine B cell proliferation and protection from apoptosis with an antibody against a 105-kD molecule: unresponsiveness of X-linked immunodeficient B cells. *J Exp Med* 1994;180:1217-24.
22. Lambert JM, Lopez EF, Lindsey ML. Macrophage roles following myocardial infarction. *Int J Cardiol* 2008;130:147-58.
23. Simms MG, Walley KR. Activated macrophages decrease rat cardiac myocyte contractility: importance of ICAM-1-dependent adhesion. *Am J Physiol* 1999;277:H253-H260.
24. Arslan F, Smeets MB, Riem Vis PW, Karper JC, Quax PH, Bongartz LG et al. Lack of fibronectin-EDA promotes survival and prevents adverse remodeling and heart function deterioration after myocardial infarction. *Circ Res* 2011;108:582-92.
25. Divanovic S, Trompette A, Atabani SF, Madan R, Golenbock DT, Visintin A et al. Inhibition of TLR-4/MD-2 signaling by RP105/MD-1. *J Endotoxin Res* 2005;11:363-8.
26. Yoon SI, Hong M, Wilson IA. An unusual dimeric structure and assembly for TLR4 regulator RP105-MD-1. *Nat Struct Mol Biol* 2011;18:1028-35.
27. Ohto U, Miyake K, Shimizu T. Crystal structures of mouse and human RP105/MD-1 complexes reveal unique dimer organization of the toll-like receptor family. *J Mol Biol* 2011;413:815-25.



Online data supplement table

Table 1. Baseline cardiac function of WT and RP105^{-/-} mice.

	WT	RP105 ^{-/-}	P value
<i>General</i>			
HR (beats/min)	587 ± 51	545 ± 79	1.000
SV (μL/g)	0.7±0.3	0.8±0.3	1.000
CO ((mL/g)/min)	0.4 ± 0.1	0.4 ± 0.2	0.886
SW (mmHg.(μL/g))	69±20	71±19	1.000
Ea (mmHg/(μL/g))	0.2±0.1	0.2±0.1	0.486
Ees/Ea	1.0±0.1	0.9±0.1	0.343
<i>Systolic</i>			
ESP (mmHg)	96 ± 14	90 ± 17	0.686
ESV (μL/g)	1.0 ± 0.3	0.9 ± 0.2	0.686
EF (%)	42.3 ± 5.7	45 ± 10.4	0.686
dP/dtMax (mmHg/ms)	8.9±1.8	8.0±1.4	0.686
Ees (mmHg/(μL/g))	138±57	116±66	0.686
<i>Diastolic</i>			
EDP (mmHg)	6 ± 5	3 ± 3	0.686
EDV (μL/g)	1.7 ± 0.6	1.7 ± 0.4	1.000
Tau (ms)	10±3	9±1	1.000
-dP/dtMin (mmHg/ms)	8±2	7±1	1.000
Eed (mmHg/(μL/g))	6±1	8±4	1.000
Ked (1/(μL/g))	0.16±0.03	0.09±0.0	0.500

HR, heart rate; SV, stroke volume; CO, cardiac output; SW, stroke work; Ea, arterial elastance (afterload); Ees/Ea, ventricular arterial coupling; ESP, end systolic pressure; ESV, end systolic volume; EF, ejection fraction; dP/dtMax, maximal rate of pressure increase; Ees, end systolic elastance (slope of ESPVR); EDP, end diastolic pressure; EDV, end diastolic volume; Tau, relaxation time constant; -dP/dtMin, maximal rate of pressure decline; Eed, diastolic stiffness (slope of EDPVR); KED, diastolic stiffness constant. Values represent means ± SD; n=8 per group.



22

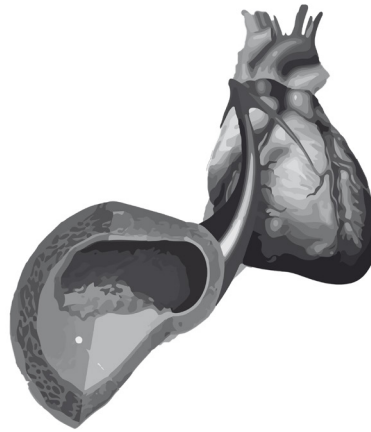
22

22

22

22

CHAPTER 9



An unexpected intriguing effect of TLR regulator RP105 (CD180) on atherosclerosis formation with alterations on B cell activation

Karper J.C, de Jager S.C.A*, Ewing M.M, de Vries M.R, Bot I, van Santbrink P.J, Redeker A, Mallat Z, Binder C.J, Arens R, Jukema J.W, Kuiper J, Quax P.H.A*

** both authors contributed equally*

Arterioscler Thromb Vasc Biol. 2013 Dec;33(12):2810-7



Abstract

Objective In atherosclerosis Toll like Receptors are traditionally linked to effects on tissue macrophages or foam cells. RP105, a structural TLR4 homolog, is an important regulator of TLR signaling. The effects of RP105 on TLR signaling vary for different leukocyte subsets known to be involved in atherosclerosis making it unique in its role of either suppressing (in myeloid cells) or enhancing (in B cells) TLR regulated inflammation in different cell types. We aimed to identify a role of TLR accessory molecule RP105 on circulating cells in atherosclerotic plaque formation.

Approach and results Irradiated LDLr^{-/-} mice received RP105^{-/-} or wild-type bone marrow. RP105^{-/-} chimeras displayed a 57% reduced plaque burden. Interestingly, total and activated B-cell numbers were significantly reduced in RP105^{-/-} chimeras. Activation of B1 B-cells was unaltered, suggesting that RP105 deficiency only affected inflammatory B2 B-cells. IgM levels were unaltered but anti-oxLDL and anti-MDA-LDL IgG2c antibody levels were significantly lower in RP105^{-/-} chimeras, confirming effects on B2 B-cells rather than B1 B-cells. Moreover BAFF expression was reduced in spleens of RP105^{-/-} chimeras.

Conclusion RP105 deficiency on circulating cells results in an intriguing unexpected TLR-associated mechanisms that decrease atherosclerotic lesion formation with alterations on pro-inflammatory B2 B-cells.

Introduction

Atherosclerosis is characterized by infiltration of circulating leukocytes into the intimal area that initiate a local inflammatory response and subsequent atherosclerotic lesion formation¹. Currently, different subtypes of leukocytes are linked to atherosclerotic lesion formation and progression. Both macrophages and T cells are well known contributors to atherosclerosis, but also dendritic cells (DCs), mast cells and B cells were more recently shown to be involved^{2, 3}.

Toll Like Receptors (TLR) are major contributors to cardiovascular disease development⁴⁻⁸, as they initiate inflammatory responses in both immune and non-immune cells by recognizing pathogen and damage associated molecular patterns (PAMPs and DAMPs respectively) that can be up regulated upon e.g. tissue damage or cell stress⁹⁻¹¹. In atherosclerosis TLR function is traditionally linked to its effect on tissue macrophages or foam cells. This mechanism is however not fully elucidated^{12, 13}. Mice deficient for TLR4 or its downstream adaptor protein Myd88 have reduced atherosclerosis formation^{14, 15}. TLR activation and signaling is strongly regulated by a number of accessory molecules¹⁶. Activation of TLR4 is dependent on the presence of MD2 which is capable of binding LPS and a variety of other known endogenous ligands^{17, 18}. Next to MD2, RP105 (CD180) is an important accessory molecules acting as a regulator of TLR signalling¹⁹⁻²¹. RP105 consists of the same extracellular domain as TLR4, but lacks the Toll like Interleukin Receptor (TIR) domain that regulates downstream signaling and has an, for TLR family members, atypical dimeric structure²². Interestingly the role of RP105 in modulating inflammatory responses depends on the cell type making it unique in its role of either enhancing or suppressing TLR regulated inflammation in different cell types²³. While it functions as an inhibitor of TLR4 signaling in myeloid cells such as DCs and macrophages, it enhances TLR4-induced activation in B cells^{24, 25}. Both myeloid cells as well as B and T cells are considered to play a major role in atherosclerosis and these cell types can all be influenced directly or indirectly via TLR signaling and regulation². Unlike myeloid cells, B cells do not express MD2, representing a major difference between their respective TLR4 pathways²⁵⁻²⁷. In MD2 deficient B cells, the RP105/MD1 complex was shown to function as MD2 on these cells²⁵. RP105 cell surface expression is strongly influenced by MD1, a structural homolog of MD2 and capable of binding lipids in its cavity^{28, 29}. A recent paper by Allen et al. suggested a mechanistic role for BAFF expression in B cell proliferation of RP105^{-/-} mice³⁰. Direct and indirect effects of TLR signaling on adaptive immunity players such as T- and B cells could play an important role in enhanced stimulation atherosclerosis development besides their traditional role on myeloid cells³¹. The TLR regulator RP105 may play a very important role in the complex TLR pathway mediated atherosclerosis formation by its unique function on different cell types²³.

In this study, we investigated the contribution of RP105 deficiency in atherosclerosis by repopulating lethally irradiated LDLr^{-/-} mice with either wild-type or RP105^{-/-} bone marrow and observed that RP105 deficiency led to an unexpected decrease in atherosclerotic plaque formation indicating a novel route via which the TLR signaling pathway affects atherosclerosis.

Material and Methods

For a detailed description of all materials and methods used, see the supplemental material, available online at <http://atvb.ahajournals.org>.



Results:

RP105 deficiency ameliorates atherosclerosis

To assess the role of RP105 in atherosclerosis, we generated bone marrow chimeras by transplantation of RP105^{-/-} or wild type (WT) bone marrow cells in LDLR^{-/-} mice. Animals were allowed to recover for 6 weeks and were subsequently fed a high fat, high cholesterol diet (Western Type Diet (WTD), 0.25% cholesterol and 15% cacao butter (SDS, Sussex, UK)). RP105 deficiency was assessed by flow cytometry on CD19⁺ B cells, CD11c⁺ Dendritic cells and CD11b⁺ monocytes isolated from spleen (Supplemental figure 1) Susceptibility to atherosclerosis in the proximal aortic root of LDLR^{-/-} mice reconstituted with either WT or RP105^{-/-} bone marrow was analyzed after 9 weeks WTD feeding. Cryostat sections of the proximal aortic root showed reduced Oil-red O staining in the RP105^{-/-} chimera transplanted group as compared to the WT transplanted controls. (Figure 1A,B). Lesion burden in the proximal aortic root was significantly decreased in the RP105^{-/-} chimeras ($230 \pm 26 \times 10^3 \mu\text{m}^2$ vs $131 \pm 15 \times 10^3 \mu\text{m}^2$, $p=0.004$) indicating decreased atherosclerosis formation in these mice (Figure 1C). No differences in bodyweight (supplemental figure 2) or cholesterol levels (supplemental figure 2) were observed between the WT and the RP105^{-/-} chimeras.

Plaque composition

Next to the observed effects on lesion size we also assessed plaque composition. Intimal macrophage area was significantly decreased in RP105^{-/-} chimeras ($57.2 \pm 8.8 \times 10^3 \mu\text{m}^2$ vs $25.6 \pm 6.5 \times 10^3 \mu\text{m}^2$, $p=0.007$, Figure 1D).

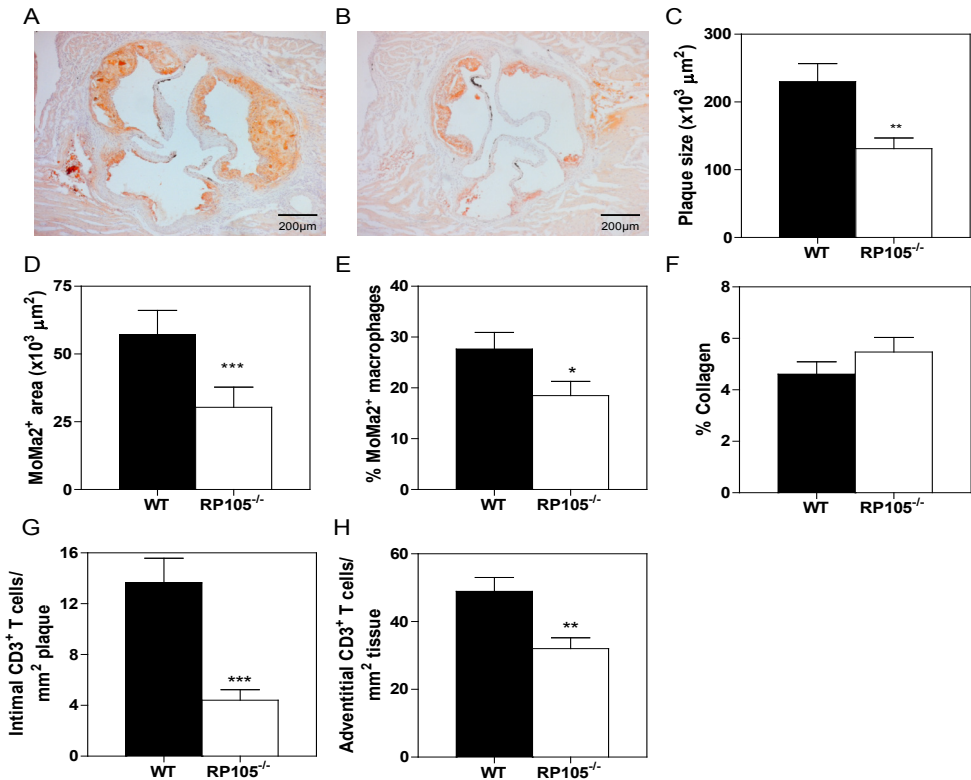


Figure 1. Atherosclerotic lesion formation is attenuated in RP105^{-/-} chimeras. Hematopoietic deficiency of RP105 in atherosclerosis and atherosclerotic plaque composition. LDLr^{-/-} mice were irradiated and subsequently received bone marrow from either RP105^{-/-} or wild type (WT) control mice. After recovery LDLr^{-/-} mice received a high-fat diet for 9 weeks. A, Atherosclerotic plaques were quantified in the aortic root after Oil Red O staining. Representative pictures of Oil Red O-stained plaques from WT (A) and RP105^{-/-} chimeras (B). Intimal lesion area was significantly decreased in RP105^{-/-} chimeras (C). Macrophages, collagen content and T cells were visualized by MoMa, Trichrome or CD3 respectively. Macrophage content (MoMa⁺ intimal area (D) and relative macrophage content (E). Collagen content (F) and T cell infiltration (intimal (G) and adventitial (H)). Image acquisition was performed on a Leica DMRE microscope with Leica DC 500 camera at 50x magnification (5x/0.15 objective). T cells were counted manually at 1000x magnification (110x/1.30 oil objective). Black bars represent WT chimeras, white bars represent RP105^{-/-} chimeras, n=16, *p<0.05, **p<0.01, ***p<0.001.

Even when correcting the macrophage area for total intimal area we still observed a significant 33% decrease (27.6 ± 3.2 vs $18.5 \pm 0.9\%$, $p=0.039$, Figure 1E and supplemental figure 2). Collagen content in the plaque was not affected (WT vs RP105^{-/-}; 4.6 ± 0.4 vs. $5.1 \pm 0.04\%$, $p=0.39$, Figure 1F and supplemental figure 2). Immunohistochemical analysis of CD3 expression as a T-cell marker revealed that T-cell numbers were significantly reduced in the intimal (13.6 ± 1.9 cells vs 4.4 ± 0.8 cells, $p<0.0001$, Figure 1G and supplemental figure 2) and perivascular area (48.9 ± 15.9 cells vs 32.0 ± 12.4 cells, $p=0.0037$, Figure 1H) of the proximal aortic root in the RP105^{-/-} chimeras.

Decreased B-cell activation in RP105^{-/-} chimeras

RP105 deficiency is known to result in an increase of pro-inflammatory cytokine production by cultured myeloid cells upon LPS administration. Myeloid cells are known to be important in atherosclerosis development and contain multiple TLRs. Therefore we analyzed the activation status of splenic DC and macrophages in both chimera groups. No difference in activation status of DC, (MHC-II and CD40 expression)(Figure 2A), macrophages (CD40 expression) (figure 2B) or CD4 and CD8 T cells (Figure 2C-D) was found between the chimera groups. Since RP105 was originally described to be highly expressed on B cells, we also investigated B cells activation. Less IgM⁺ B cells were detected in the RP105^{-/-} chimeras. Concomitantly, a decreased percentage of CD86⁺ B cells was found, indicative of a decreased number of activated B2-cells in the RP105^{-/-} chimeras (Figure 2E). Subtype analysis showed no difference in B1-cell number or activation status (Figure 2F).

Proliferation of splenocytes by LPS is reduced in RP105^{-/-} chimeras

Splenocytes from both chimera groups were stimulated ex vivo with 10 or 100ng/ml LPS and proliferation was assessed by [³H]-Thymidine incorporation. Splenocytes from the RP105^{-/-} chimeras showed a lower degree of proliferation to LPS (proliferation index 1.9 ± 0.5 vs. 3.0 ± 1.6 to 10ng/ml LPS and 2.2 ± 0.6 vs. 6.6 ± 3.0 to 100ng/ml LPS, $p<0.05$) (figure 3A).

RP105 deficient B cells have reduced proliferation and are less activated upon TLR4 stimulation

In order to establish if the observed effect on splenocyte proliferation could be B-cell related, we isolated CD19⁺ B cells from WT and RP105^{-/-} mice and exposed these cells to LPS and anti-CD40mAb to stimulate B-cell surface receptors. In agreement with earlier observations, RP105 deficient cells were less responsive to LPS (proliferation index: 22.6 ± 3.7



vs. 58.2 ± 7.2 to 100 ng LPS , $p=0.0001$ and 85.7 ± 4.7 vs. 129.7 ± 12.8 to $1 \mu\text{g LPS}$, $p=0.0007$), but not to anti-CD40mAb stimulation (135.0 ± 0.6 vs. 114.7 ± 18.0 , $p=0.12$, figure 3B).

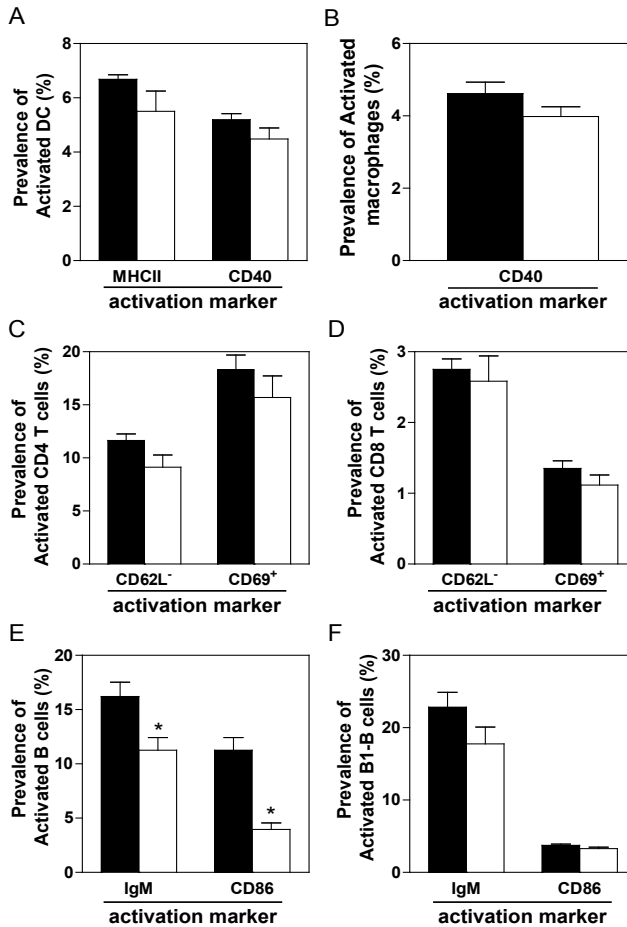


Figure 2. Decreased B Cell activation in the spleen of RP105^{-/-} chimeras. Splenocytes from LDLr^{-/-} chimeras were harvested and analyzed for cell subtype and activation status by flowcytometry. Activation status of CD11c⁺ DCs (identified by high MHCII expression or CD40 expression) (A) and F4/80⁺ macrophages (identified by CD40 expression) (B). No difference in CD4⁺ or CD8⁺ T cell activation was observed. Activated CD4⁺ (C) and CD8⁺ T (D) cell subsets identified by low CD62L or high CD69 expression. B cells were selected as CD19 positive cells. Percentage of IgM/CD19 and CD86/CD19 positive cells (E). Percentage of B1-cells expressing IgM or CD86 (F). Black bars represent WT chimeras, white bars represent RP105^{-/-} chimeras, n=6, *p<0.05.

The observed decrease in proliferation may reflect altered cell survival, cell cycle progression or both. Cell cycle progression was then assessed by monitoring CFSE dilution. Loss of CFSE fluorescence, indicative of cell division, was measured by flow cytometry on day 3 and was strongly reduced in the RP105^{-/-} B cells upon LPS stimulation, but not upon anti-CD40mAb, indicating a TLR4-specific induction of cell cycle arrest (Figure 3C). B cells from RP105^{-/-} mice also produced less IL-6 (supplemental figure 1) and showed less phenotypical activation (CD86 and CD25) upon TLR4 but not CD40 activation (supplemental figure 3)

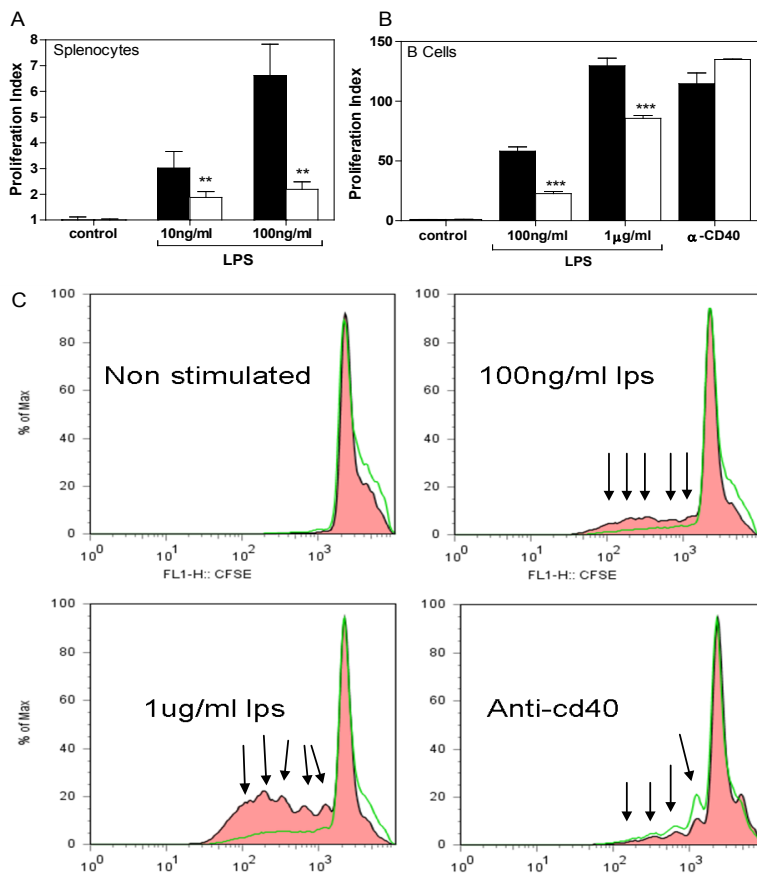


Figure 3. Reduced proliferative response to LPS by RP105^{-/-} splenocytes of chimeras.

Splenocytes derived from LDLR^{-/-} chimeras at sacrifice were with LPS (10 and 100ng/ml) incorporated with 3H-thymidine stimulated. Proliferative response of splenocytes from chimeras to LPS (A) Black bars represent WT chimeras, white bars represent RP105^{-/-} chimeras, n=6, average of 4 experiments, **p<0.01.

Reduced proliferative response to LPS by RP105^{-/-} B cells.

CD19⁺ cells from WT or RP105^{-/-} were stimulated with 100ng/ml LPS, 1μg/ml LPS or αCD40mAb. Proliferative response to LPS, and to αCD40mAb (B). Black bars represent WT B cells, white bars represent RP105^{-/-} B cells, average of 3 experiments n=4 mice per experiment, ***p<0.001. To count the amount of cell divisions and the amount of cells dividing, B cells were incorporated with CFSE. Loss of CFSE fluorescence (indicating cell division progression) by B cells from RP105^{-/-} (green line) and WT (filled histogram) mice (C).

Together, these results indicate that RP105 modulates B-cell function through cell surface receptor TLR4 but not CD40.

Altered levels of IgG but not IgM specific antibodies

Plasma IgM and IgG antibody titers against oxLDL and MDA-LDL were determined at sacrifice. Ox-LDL IgG and IgG2c and MDA-LDL specific IgG2c isotype antibodies were

significantly reduced in the RP105^{-/-} chimeras (Figure 4A/C/E). The exact role of IgG isotype antibodies is however still under debate³² Interestingly we did not observe differences in oxLDL or malondialdehyde-modified LDL (MDA-LDL) specific IgM production, indicating effects of RP105 predominately on B2 but not B1a cells. (Figure 4B/D). Phosphocholine (PC)-specific IgM T15/EO6, which is a B1a-cell derived natural antibody was also not different between the chimera groups, supporting the hypothesis that B1a IgM production was not altered and in line with the finding that B1-cell number and activation was not affected (figure 4F).

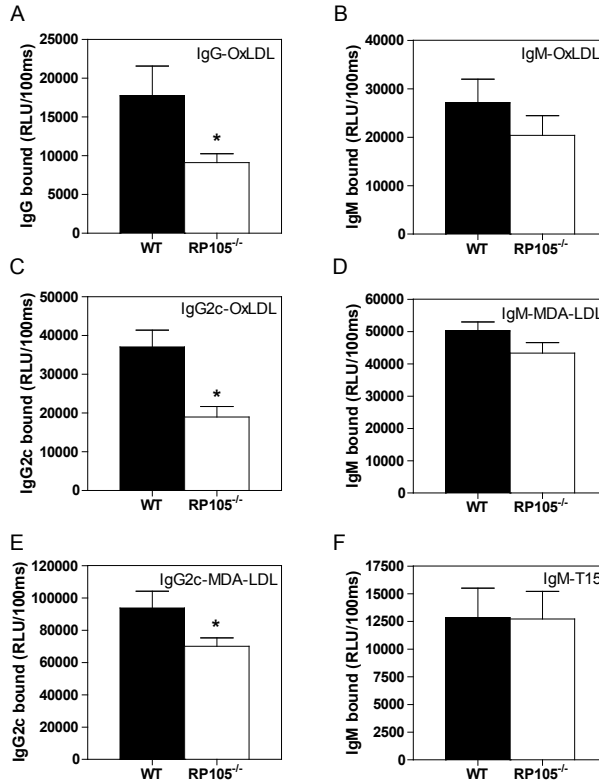


Figure 4. Reduced oxLDL and MDA-LDL IgG(2c) titers in RP105^{-/-} chimeras.

Antibody titers were measured in plasma by chemiluminescent ELISA. Blood was harvested at sacrifice of the chimera hypercholesterolemic LDLr^{-/-} mice. Total IgG against cu-oxLDL (A), IgG2c against cu-oxLDL (B), IgG2c against MDA-LDL (C), Total IgM against cu-oxLDL (D), total IgM against MDA-LDL (E) and PC-specific IgM T15/EO6 (F). Black bars represent WT chimeras, white bars represent RP105^{-/-} chimeras and data is presented as Reflective Light Units (RLU), WT n=10, RP105^{-/-} n=15, *p<0.05.

Decreased cytokine expression in spleens of RP105^{-/-} chimeras.

In atherosclerosis increased expression of cytokines in the plaque usually parallels that in splenocytes³³. mRNA levels of IL6, IP-10, IL12 and IL10 were significantly reduced in spleens of the RP105^{-/-} compared to WT chimeras (Figure 5A-D). Even more interesting we found a reduced expression of B-cell activating factor (BAFF) in the spleens of the RP105^{-/-} chimeras (Figure 5E). These reductions were representative since total numbers and percentages of different leukocyte cell types in the spleen were not different between

the groups (supplemental table 1). Interestingly basal BAFF expression in splenocytes of normal WT or RP105^{-/-} mice is much lower compared to the chimera groups receiving a western type diet. Moreover full body RP105 knockout mice on a normal diet show a trend towards higher instead of lower BAFF expression in the splenocytes (P=0.08) compared to WT mice (supplemental figure 4).

Discussion

In the present study we show that deficiency of the TLR regulator RP105 on circulating cells in LDLr^{-/-} mice results in an unexpected 57% reduction in atherosclerotic lesion formation. This finding is quite intriguing since the hypothesis thus far was that TLR4 activation on macrophages stimulates atherosclerotic lesion development, and consequently that in the absence of the TLR4 inhibitor RP105 atherosclerotic lesion development would be enhanced. Here we show for the first time an unexpected regulation of atherosclerosis formation via TLR regulator RP105 with effects on inflammatory B2 B cells and BAFF expression but not on myeloid cells. Hereby it shows a novel manner of TLR pathway mediated atherosclerosis formation via B cell activation that was stronger than the TLR4 modulation by RP105 on macrophages.

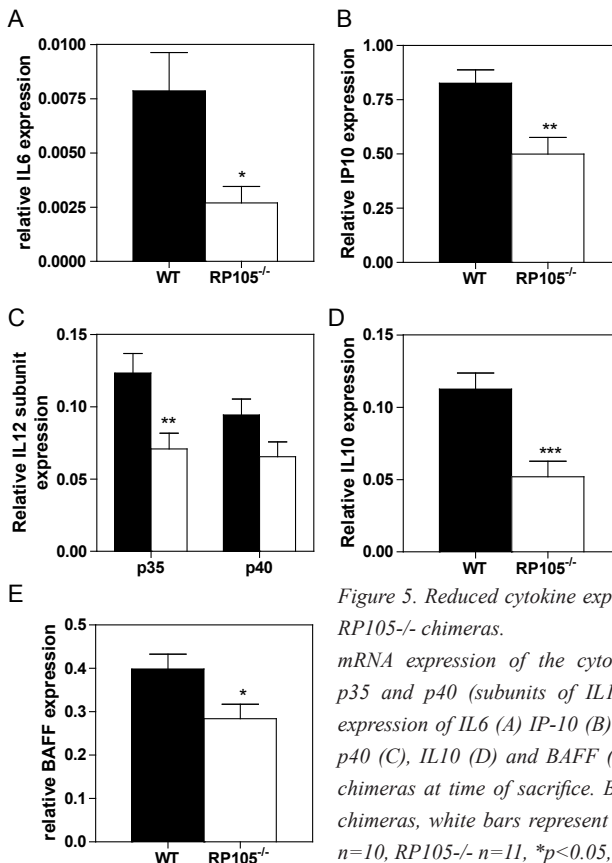


Figure 5. Reduced cytokine expression in the spleens of RP105^{-/-} chimeras.

mRNA expression of the cytokines IL6, IP10, IL10, p35 and p40 (subunits of IL12) in spleens. Relative expression of IL6 (A) IP-10 (B) IL-12 subunits p35 and p40 (C), IL10 (D) and BAFF (E) in WT and RP105^{-/-} chimeras at time of sacrifice. Black bars represent WT chimeras, white bars represent RP105^{-/-} chimeras, WT n=10, RP105^{-/-} n=11, *p<0.05, **p<0.01, ***p<0.001.



In atherosclerosis TLR function is traditionally linked to its effect on tissue macrophages or foam cells. This mechanism is however not fully elucidated. The modulating capacities of RP105 on inflammatory responses depend on the cell type making it unique in its role of either enhancing or suppressing TLR regulated inflammation in different cell types. In our experiments we could notice effects on inflammatory B2 B cells and BAFF expression but not on myeloid cells. Although currently the role of B cells in atherosclerosis receives much attention, several issues of controversy exist³². Interestingly the crosstalk between TLR and B cell receptor signals plays a crucial role in B cell responses to pathogens¹³. B cells are considered to play a major role in the pathophysiology of autoimmune diseases³⁴ and during the last decade a number of studies have also indicated an important role for TLRs in autoimmunity³⁵. Interestingly, patients with autoimmune-like diseases such as systemic lupus erythematosus (SLE) or rheumatoid arthritis (RA) have an increased risk of atherosclerotic plaque development³⁶. B cells can affect atherosclerosis development via antibody production to modified LDL³⁷. Besides their important role in antibody production, B cells are also capable of producing cytokines and thereby can have an additional effector role to their regulating role in inflammation. The cytokine producing effector B cells are most likely derived from B2 subtype mature follicular B cells, while B1 cells are IgM antibody producing cells³⁸.

We now demonstrate that RP105 deficiency on hematopoietic cells reduced atherosclerotic plaque formation with reduced B cell numbers and considerably less activated B cells in the RP105^{-/-} mice, as indicated by less CD19⁺ IgM⁺ CD86⁺ cells. CD86 is a B7 family member and important for co-stimulation of other cells like T cells³⁹. The effect of RP105 deficiency on cell number and activation was not observed on B cell subtype B1 cells (CD4⁻, CD5⁺) and we did consequently not observe effects on the levels of IgM antibodies, which are mainly produced by these cells. Our *in vitro* studies confirmed that RP105 affects B2 B cells via modulation of the TLR4 response. LPS, as a TLR4 cell surface stimulator, but not anti-CD40, as a CD40 cell surface stimulator, caused multiple effects on B cells. The function of RP105 is complex since it has a divergent role on myeloid and B cells¹⁶. The differential effects of RP105 on myeloid and B cells may be related to the lack of MD2 in B cells^{25, 27} and the capability of RP105 to directly cause B-cell activation⁴⁰. Previously, Ait-Oufella and co-workers showed that the atheroprotective effect of CD20⁺ B cell depletion may be due to effects on T cell activation. They showed this mainly depended on reduction in IgG-type antibodies and not in IgM-isotype antibody titers⁴¹. In addition Kyaw and co-authors showed that B2 B cells may enhance atherosclerosis without presence of other inflammatory cells and independent of antibody levels⁴². Both depletion studies noticed a decrease in macrophages in the plaque while Ait-Oufella et al, also observed a reduction in T-cell accumulation⁴¹. Our data is in agreement with both studies showing a decrease in both T cells and macrophages in the plaque. More recent studies on the mechanism of B cell mediated atherosclerotic plaque formation demonstrated a role for B cell activating factor (BAFF) receptor. BAFF is required for B cell maturation and supports the survival of self reactive B cells⁴³. BAFF receptor deficiency in bone marrow cells resulted in reduced B2 B cells and attenuated atherosclerotic lesion development⁴⁴. Depletion of B2 B cells in BAFF receptor knockout mice inhibited lesion development by ameliorating vascular inflammation⁴⁵. In agreement with these observations, we now found reduced expression of BAFF and B2 B cell responses in the RP105^{-/-} chimeras that had less plaque formation. Recently modulation of B cell proliferation by RP105 was mechanistically related to BAFF expression³⁰. In agreement we found an increase of BAFF expression in

splenocytes of full body WT and full body RP105^{-/-} mice on a normal diet. Interestingly both chimera groups on a western type diet showed actually much higher BAFF expression. In the chimeras however BAFF expression in splenocytes of RP105^{-/-} chimeras was significantly lower to WT chimera mice. in splenocytes This data suggests an association of BAFF expression with RP105 which may play an important role in effects seen on atherosclerosis in the RP105^{-/-} chimeric LDR^{-/-}.

Additionally we found a decrease in mRNA expression of cytokines/chemokines such as IP-10 in the spleens of the RP105^{-/-} chimeras. In atherosclerosis increased expression of cytokines in the plaque usually parallels that in splenocytes and since IP-10 is an important T-cell attractant this may partly explain differences in T-cell numbers in the plaque of the RP105^{-/-} chimeras^{33, 46}. In contrast hypercholesterolemic mice lacking B cells showed an increase in atherosclerosis, an effect attributed to the loss of protective natural IgM antibodies^{33, 46-49}, the opposite effect of the discussed studies that depleted B cells via anti-CD20 administration^{41, 42}. Lifelong deficiency in B cells will certainly influence (long lived) plasma cell formation and antibody production by these cells, and may very well explain the different findings in these studies. Specific depletion by anti-CD20 will spare CD20 deficient long-lived plasma cells. Interestingly autoimmune disease patients treated with anti-CD20 humanized antibody (Rituximab) show extended periods of clinical remission without reductions in antibody titers⁵⁰. Particularly in autoimmune settings B cells can actively promote atherosclerosis⁵¹. Using Rituximab would however be a difficult therapy for CVD patients since statins may impair its effect by inducing conformational changes on CD20⁵². This would make new therapeutic targets on B cells such as RP105 even more interesting. In addition SLE patients with a history of CVD showed elevated titers of oxLDL and malondialdehyde-modified LDL (MDA-LDL) specific IgG antibodies compared with other SLE patients without CVD or population controls⁵³. In the RP105^{-/-} chimeras we also found a reduction in IgG2c titers against oxLDL and MDA-LDL while IgM levels against oxLDL or MDA-LDA were not altered. IgM titers specifically derived from B1a B cells were also not altered, thus confirming our results on B1 B cell number and activation and thereby indicating the cell specific effects of RP105 via TLR signaling on inflammatory type B2 B cells.

Recently new data suggests that RP105 is expressed in epididymal white adipose tissue on stromal vascular fractions and has an important role in the induction of adipose tissue inflammation. High fat diet induced obesity, adipose tissue inflammation and insulin resistance are hampered in RP105^{-/-} mice. On long term these processes are associated with hypertension, diabetes and coronary disease⁵⁴. In our study we did not use full body knockout mice but performed bone marrow transfer to LDLR^{-/-} mice. At sacrifice we did not observe any difference in body mass of LDLR^{-/-} on a high fat diet that received RP105^{-/-} bone marrow cells compared to mice that received WT bone marrow. Therefore effects of insulin resistance are not likely to be involved in the effects on atherosclerotic lesion formation we observed here. Nevertheless, the protective effects of RP105 deficiency on atherosclerosis in our study combined with previously published attenuation of obesity and insulin resistance by RP105 deficiency definitely point out the potential of RP105 as therapeutic target for disease processes that are considered to be responsible for the highest morbidity and mortality numbers in the western world.

In conclusion RP105 is an important TLR regulator that influences atherosclerotic plaque formation with strong effects on B2 B cells and BAFF expression without directly affecting myeloid subsets. This may have strong implications for the role of TLR signaling in athero-



sclerosis and development of novel therapeutic approaches.

Acknowledgements

The authors thank K. Miyake for kindly providing the RP105^{-/-} mice. The authors have no conflicting financial interests. This work was performed within the framework of the Dutch Top Institute Pharma (project: D1-101 JCK. SdJ. JK, PQ).

Disclosures:

None

Reference List

1. Libby P, Ridker PM, Hansson GK. Inflammation in atherosclerosis: from pathophysiology to practice. *J Am Coll Cardiol* 2009;54:2129-38.
2. Hansson GK, Hermansson A. The immune system in atherosclerosis. *Nat Immunol* 2011;12:204-12.
3. Bot I, de Jager SC, Zerneck A, Lindstedt KA, van Berkel TJ, Weber C, Biessen EA. Perivascular mast cells promote atherogenesis and induce plaque destabilization in apolipoprotein E-deficient mice *Circulation* 2007;115:2516-25.
4. Edfeldt K, Swedenborg J, Hansson GK, Yan ZQ. Expression of toll-like receptors in human atherosclerotic lesions: a possible pathway for plaque activation. *Circulation* 2002;105:1158-61.
5. Hollestelle SC, De Vries MR, Van Keulen JK, Schoneveld AH, Vink A, Strijder CF, Van Middelaar BJ, Pasterkamp G, Quax PH, de Kleijn DP. Toll-like receptor 4 is involved in outward arterial remodeling. *Circulation* 2004;109:393-8.
6. Karper JC, De Vries MR, van den Brand BT, Hoefler IE, Fischer JW, Jukema JW, Niessen HW, Quax PH. Toll-like receptor 4 is involved in human and mouse vein graft remodeling, and local gene silencing reduces vein graft disease in hypercholesterolemic APOE*3Leiden mice. *Arterioscler Thromb Vasc Biol* 2011;31:1033-40.
7. Karper JC, Ewing MM, Habets KL, De Vries MR, Peters EA, van Oeveren-Rietdijk AM, de Boer HC, Hamming JF, Kuiper J, Kandimalla ER, La MN, Jukema JW, Quax PH. Blocking toll-like receptors 7 and 9 reduces postinterventional remodeling via reduced macrophage activation, foam cell formation, and migration. *Arterioscler Thromb Vasc Biol* 2012;32:e72-e80.
8. Vink A, Schoneveld AH, van der Meer JJ, Van Middelaar BJ, Sluijter JP, Smeets MB, Quax PH, Lim SK, Borst C, Pasterkamp G, de Kleijn DP. In vivo evidence for a role of toll-like receptor 4 in the development of intimal lesions. *Circulation* 2002;106:1985-90.
9. Akira S, Takeda K, Kaisho T. Toll-like receptors: critical proteins linking innate and acquired immunity. *Nat Immunol* 2001;2:675-80.
10. Kawai T, Akira S. The role of pattern-recognition receptors in innate immunity: update on Toll-like receptors. *Nat Immunol* 2010;11:373-84.
11. Arslan F, Smeets MB, Riem Vis PW, Karper JC, Quax PH, Bongartz LG, Peters JH, Hoefler IE, Doevendans PA, Pasterkamp G, de Kleijn DP. Lack of fibronectin-EDA promotes survival and prevents adverse remodeling and heart function deterioration after myocardial infarction *Circ Res* 2011;108:582-92.
12. Seneviratne AN, Sivagurunathan B, Monaco C. Toll-like receptors and macrophage activation in atherosclerosis. *Clin Chim Acta* 2012;413:3-14.
13. Rawlings DJ, Schwartz MA, Jackson SW, Meyer-Bahlburg A. Integration of B cell responses through Toll-like receptors and antigen receptors. *Nat Rev Immunol* 2012;12:282-94.
14. Michelsen KS, Wong MH, Shah PK, Zhang W, Yano J, Doherty TM, Akira S, Rajavashisth TB, Ardit M. Lack of Toll-like receptor 4 or myeloid differentiation factor 88 reduces atherosclerosis and alters plaque phenotype in mice deficient in apolipoprotein E. *Proc Natl Acad Sci U S A* 2004 20;101:10679-84.

15. Bjorkbacka H, Kunjathoor VV, Moore KJ, Koehn S, Ordija CM, Lee MA, Means T, Halmen K, Luster AD, Golenbock DT, Freeman MW. Reduced atherosclerosis in MyD88-null mice links elevated serum cholesterol levels to activation of innate immunity signaling pathways. *Nat Med* 2004;10:416-21.
16. Akashi-Takamura S, Miyake K. TLR accessory molecules. *Curr Opin Immunol* 2008;20:420-5.
17. Shimamoto A, Chong AJ, Yada M, Shomura S, Takayama H, Fleisig AJ, Agnew ML, Hampton CR, Rothnie CL, Spring DJ, Pohlman TH, Shimp H, Verrier ED. Inhibition of Toll-like receptor 4 with eritoran attenuates myocardial ischemia-reperfusion injury. *Circulation* 2006;114:I270-I274.
18. Kim HM, Park BS, Kim JI, Kim SE, Lee J, Oh SC, Enkhbayar P, Matsushima N, Lee H, Yoo OJ, Lee JO. Crystal structure of the TLR4-MD-2 complex with bound endotoxin antagonist Eritoran. *Cell* 2007;130:906-17.
19. Divanovic S, Trompette A, Petiniot LK, Allen JL, Flick LM, Belkaid Y, Madan R, Haky JJ, Karp CL. Regulation of TLR4 signaling and the host interface with pathogens and danger: the role of RP105. *J Leukoc Biol* 2007;82:265-71.
20. Miyake K, Yamashita Y, Ogata M, Sudo T, Kimoto M. RP105, a novel B cell surface molecule implicated in B cell activation, is a member of the leucine-rich repeat protein family. *J Immunol* 1995;154:3333-40.
21. Miyake K, Ogata H, Nagai Y, Akashi S, Kimoto M. Innate recognition of lipopolysaccharide by Toll-like receptor 4/MD-2 and RP105/MD-1. *J Endotoxin Res* 2000;6:389-91.
22. Yoon SI, Hong M, Wilson IA. An unusual dimeric structure and assembly for TLR4 regulator RP105-MD-1. *Nat Struct Mol Biol* 2011;18:1028-35.
23. Lee CC, Avalos AM, Ploegh HL. Accessory molecules for Toll-like receptors and their function. *Nat Rev Immunol* 2012;12:168-79.
24. Divanovic S, Trompette A, Atabani SF, Madan R, Golenbock DT, Visintin A, Finberg RW, Tarakhovskiy A, Vogel SN, Belkaid Y, Kurt-Jones EA, Karp CL. Negative regulation of Toll-like receptor 4 signaling by the Toll-like receptor homolog RP105. *Nat Immunol* 2005;6:571-8.
25. Ogata H, Su I, Miyake K, Nagai Y, Akashi S, Mecklenbrauker I, Rajewsky K, Kimoto M, Tarakhovskiy A. The toll-like receptor protein RP105 regulates lipopolysaccharide signaling in B cells. *J Exp Med* 2000;192:23-9.
26. Nagai Y, Shimazu R, Ogata H, Akashi S, Sudo K, Yamasaki H, Hayashi S, Iwakura Y, Kimoto M, Miyake K. Requirement for MD-1 in cell surface expression of RP105/CD180 and B-cell responsiveness to lipopolysaccharide. *Blood* 2002;99:1699-705.
27. Akashi S, Shimazu R, Ogata H, Nagai Y, Takeda K, Kimoto M, Miyake K. Cutting edge: cell surface expression and lipopolysaccharide signaling via the toll-like receptor 4-MD-2 complex on mouse peritoneal macrophages. *J Immunol* 2000;164:3471-5.
28. Harada H, Ohto U, Satow Y. Crystal structure of mouse MD-1 with endogenous phospholipid bound in its cavity. *J Mol Biol* 2010;400:838-46.
29. Miyake K, Shimazu R, Kondo J, Niki T, Akashi S, Ogata H, Yamashita Y, Miura Y, Kimoto M. Mouse MD-1, a molecule that is physically associated with RP105 and positively regulates its expression. *J Immunol* 1998;161:1348-53.
30. Allen JL, Flick LM, Divanovic S, Jackson SW, Bram R, Rawlings DJ, Finkelman FD, Karp CL. Cutting edge: regulation of TLR4-driven B cell proliferation by RP105 is not B cell autonomous *J Immunol* 2012;188:2065-9.
31. Schnare M, Barton GM, Holt AC, Takeda K, Akira S, Medzhitov R. Toll-like receptors control activation of adaptive immune responses. *Nat Immunol* 2001;2:947-50.
32. Nilsson J, Fredrikson GN. The B cell in atherosclerosis: teaming up with the bad guys? *Clin Chem* 2010;56:1789-91.
33. Tedgui A, Mallat Z. Cytokines in atherosclerosis: pathogenic and regulatory pathways. *Physiol Rev* 2006;86:515-81.



34. Pillai S, Mattoo H, Cariappa A. B cells and autoimmunity. *Curr Opin Immunol* 2011;23:721-31.
35. Midwood KS, Piccinini AM, Sacre S. Targeting Toll-like receptors in autoimmunity. *Curr Drug Targets* 2009;10:1139-55.
36. Bernatsky S, Boivin JF, Joseph L, Manzi S, Ginzler E, Gladman DD, Urowitz M, Fortin PR, Petri M, Barr S, Gordon C, Bae SC, Isenberg D, Zoma A, Aranow C, Dooley MA, Nived O, Sturfelt G, Steinsson K, Alarcon G, Senecal JL, Zummer M, Hanly J, Ensworth S, Pope J, Edworthy S, Rahman A, Sibley J, El-Gabalawy H, McCarthy T, St PY, Clarke A, Ramsey-Goldman R. Mortality in systemic lupus erythematosus. *Arthritis Rheum* 2006;54:2550-7.
37. Kyaw T, Tay C, Krishnamurthi S, Kanellakis P, Agrotis A, Tipping P, Bobik A, Toh BH. B1a B lymphocytes are atheroprotective by secreting natural IgM that increases IgM deposits and reduces necrotic cores in atherosclerotic lesions. *Circ Res* 2011;109:830-40.
38. Lund FE. Cytokine-producing B lymphocytes-key regulators of immunity. *Curr Opin Immunol* 2008;20:332-8.
39. Harris NL, Ronchese F. The role of B7 costimulation in T-cell immunity. *Immunol Cell Biol* 1999;77:304-11.
40. Yazawa N, Fujimoto M, Sato S, Miyake K, Asano N, Nagai Y, Takeuchi O, Takeda K, Okochi H, Akira S, Tedder TF, Tamaki K. CD19 regulates innate immunity by the toll-like receptor RP105 signaling in B lymphocytes. *Blood* 2003;102:1374-80.
41. Ait-Oufella H, Herbin O, Bouaziz JD, Binder CJ, Uyttenhove C, Laurans L, Taleb S, Van VE, Esposito B, Vilar J, Sirvent J, Van SJ, Tedgui A, Tedder TF, Mallat Z. B cell depletion reduces the development of atherosclerosis in mice. *J Exp Med* 2010;207:1579-87.
42. Kyaw T, Tay C, Khan A, Dumouchel V, Cao A, To K, Kehry M, Dunn R, Agrotis A, Tipping P, Bobik A, Toh BH. Conventional B2 B cell depletion ameliorates whereas its adoptive transfer aggravates atherosclerosis. *J Immunol* 2010;185:4410-9.
43. MacKay F, Schneider P. Cracking the BAFF code *Nat Rev Immunol* 2009;9:491-502.
44. Sage AP, Tsiantoulas D, Baker L, Harrison J, Masters L, Murphy D, Loinard C, Binder CJ, Mallat Z. BAFF receptor deficiency reduces the development of atherosclerosis in mice--brief report *Arterioscler Thromb Vasc Biol* 2012;32:1573-6.
45. Kyaw T, Tay C, Hosseini H, Kanellakis P, Gadowski T, MacKay F, Tipping P, Bobik A, Toh BH. Depletion of B2 but not B1a B cells in BAFF receptor-deficient ApoE mice attenuates atherosclerosis by potentially ameliorating arterial inflammation *PLoS One* 2012;7:e29371.
46. van Wanrooij EJ, de Jager SC, van ET, de VP, Birch HL, Owen DA, Watson RJ, Biessen EA, Chapman GA, van Berkel TJ, Kuiper J. CXCR3 antagonist NBI-74330 attenuates atherosclerotic plaque formation in LDL receptor-deficient mice. *Arterioscler Thromb Vasc Biol* 2008;28:251-7.
47. Major AS, Fazio S, Linton MF. B-lymphocyte deficiency increases atherosclerosis in LDL receptor-null mice. *Arterioscler Thromb Vasc Biol* 2002;22:1892-8.
48. Caligiuri G, Nicoletti A, Poirier B, Hansson GK. Protective immunity against atherosclerosis carried by B cells of hypercholesterolemic mice. *J Clin Invest* 2002;109:745-53.
49. Lewis MJ, Malik TH, Ehrenstein MR, Boyle JJ, Botto M, Haskard DO. Immunoglobulin M is required for protection against atherosclerosis in low-density lipoprotein receptor-deficient mice. *Circulation* 2009;120:417-26.
50. Sanz I, Anolik JH, Looney RJ. B cell depletion therapy in autoimmune diseases. *Front Biosci* 2007;12:2546-67.
51. Zhao M, Wigren M, Duner P, Kolbus D, Olofsson KE, Bjorkbacka H, Nilsson J, Fredrikson GN. FcγRIIB inhibits the development of atherosclerosis in low-density lipoprotein receptor-deficient mice. *J Immunol* 2010;184:2253-60.
52. Winiarska M, Bil J, Wilczek E, Wilczynski GM, Lekka M, Engelberts PJ, Mackus WJ, Gorska E, Bojarski

L, Stoklosa T, Nowis D, Kurzaj Z, Makowski M, Glodkowska E, Issat T, Mrowka P, Lasek W, Dabrowska-Iwanicka A, Basak GW, Wasik M, Warzocha K, Sinski M, Gaciong Z, Jakobisiak M, Parren PW, Golab J. Statins impair antitumor effects of rituximab by inducing conformational changes of CD20. *PLoS Med* 2008;5:e64.

53. Svenungsson E, Jensen-Urstad K, Heimburger M, Silveira A, Hamsten A, de FU, Witztum JL, Frostegard J. Risk factors for cardiovascular disease in systemic lupus erythematosus. *Circulation* 2001;104:1887-93.
54. Nagai, Y., Y. Watanabe, and K. Takatsu, The TLR family protein RP105/MD-1 complex: A new player in obesity and adipose tissue inflammation. *Adipocyte*, 2013. 2(2): p. 61-6.

Significance

This is the first paper to provide evidence of RP105 involvement in atherosclerotic plaque formation with effects on B2-cells and BAFF expression. We show a previously unknown involvement of TLR signaling in B-cell regulation in atherosclerosis indicating a novel route via which the TLR signaling pathway affects atherosclerosis. These effects seem to be more pronounced than effects of RP105 deficiency on TLR signaling on monocytes/macrophages, a process thought to enhance atherosclerosis. This makes RP105 an interesting new therapeutic target and our findings not only identify a novel mediator of atherosclerotic plaque formation but may have strong implications for the understanding the underlying mechanism of TLR signaling in atherosclerosis and consequently the development of novel therapeutic approaches. This might even contribute to the explanation why patients with autoimmune diseases are prone to develop more atherosclerosis as in autoimmune settings B cells can actively promote atherosclerosis



Online supplement: Material and methods

Animals

LDLreceptor (LDLr)^{-/-} and RP105^{-/-} mice (on C57BL/6 background) were obtained from the local animal breeding facility. WT controls were obtained from Charles River. All experimental protocols were approved by the ethics committee for animal experiments of Leiden University Medical Center.

Bone marrow transplantation

To induce bone marrow aplasia, male LDLr^{-/-} recipient mice were exposed to a single dose of 9 Gy (0.19 Gy/min, 200 kV, 4 mA) total body irradiation using an Andrex Smart 225 Röntgen source (YXLON International) with a 6-mm aluminum filter 1 day before the transplantation. Bone marrow was isolated by flushing the femurs and tibias of RP105^{-/-} and WT mice with PBS. Subsequently, the cell suspension was gently filtered through a 70µm cell strainer to obtain a single cell suspension (70µm pores, BD Bioscience). Irradiated recipients received 0.5×10⁷ bone marrow cells by tail vein injection. Drinking water was supplied with antibiotics (83 mg/liter ciprofloxacin and 67 mg/liter polymyxin B sulfate) and 6.5 g/liter sucrose for the first three weeks after irradiation. Thereafter animals received normal drinking water ad libitum. After a six week recovery period, animals were placed on a Western-type diet containing 0.25% cholesterol and 15% cacao butter (SDS) diet for 9 wk and subsequently sacrificed. N=17 WT, N=18 RP105^{-/-}, male mice, 12 weeks of age at start of the experiment.

Flow Cytometry

Spleens were harvested and single-cell suspensions of splenocytes were prepared by gently mincing the spleen through a cell strainer (70µm pores, BD Bioscience). Splenocytes were incubated at 4°C with erythrocyte lysis buffer (155mM NH₄CL in 10mM Tris/HCL, pH 7.2) for 5 minutes. Cells were centrifuged for 5 minutes at 1500 rpm, resuspended in lysis buffer to remove residual erythrocytes. Cells were washed twice with PBS. Cell suspensions were incubated with 1% normal mouse serum in PBS and stained for the surface markers CD4, CD5, CD8, CD19, CD11c, CD40, CD62L, CD69, F4/80, IgM, MHCII (eBioscience, Vienna, Austria), at a concentration of 0.25 µg Ab/200,000 cells.^{1,2,3,4} Subsequently cells were subjected to flow cytometric analysis (FACSCANTO, BD Biosciences). FACS data were analyzed with CELLQuest software (BD Biosciences).

RT-PCR

Total RNA was isolated from the spleens of the WT and RP105^{-/-} chimeras using Tri-Reagent (Sigma-Aldrich) according to the manufacturer's protocol. The expression levels of IL6, IP10, IL10, p35 and p40 (subunits of IL12) and BAFF were analyzed by real time polymerase chain reaction (RT-PCR) (Taqman, Applied Bioscience). The relative mRNA expression levels were determined using HPRT and RPL27 as housekeeping gene and the 2^[-ΔΔC(T)] method.

Splenocyte proliferation

Splenocytes were isolated by gently squeezing the spleen over a cell strainer (70µm pores, BD Bioscience). Cells were resuspended in RPMI 1640 (supplemented with 10% FCS, 20mM L-glutamine, 100U/ml penicillin and 100 µg/mL streptomycin) and seeded at a

density of 2×10^5 cells/well in a 96 wells plate. Cells were stimulated with 10 or 100 ng/ml LPS. Cells were incubated with $0.5 \mu\text{Ci}$ [^3H]Thymidine during the last 16 hours of 3 days in culture. To quantify thymidine incorporation the cells was washed with PBS and lysed with 0.1M NaOH and cell-associated radioactivity was determined by liquid scintillation counting.

B-cell proliferation

Single-cell suspensions of splenocytes were obtained by mincing through cell strainers, and erythrocytes were lysed with ammonium chloride solution. B cells were positively enriched by using CD19 MACS microbeads and the MACS system, according to the manufacturer's guidelines (Miltenyi Biotec, Germany). The purity of the isolated cells was verified by flow cytometric analysis ($>95\%$ CD19). Purified B cells were cultured in IMDM medium (Invitrogen Life Technologies, Gaithersburg, MD) supplemented with 10% heat-inactivated FCS, L-glutamine, gentamicin, and $5 \times 10^5 \text{ M}$ 2-ME. B cells were seeded at 2×10^5 cells/well in a final volume of $200 \mu\text{l}$ in 96-well flat-bottom plates and incubated for the indicated time periods at 37°C in a humidified atmosphere containing 5% CO_2 . Cells were stimulated with various concentrations of either LPS (Sigma-Aldrich, St. Louis, MO) or anti-CD40 mAb (BD Pharmingen, USA).

Cell cycle analysis

Cell cycle progression was analyzed by flow cytometry using CFSE. B cells (1×10^7) were washed three times with PBS, and subsequently CFSE was added to a final concentration of $5 \mu\text{M}$ in PBS. After 10 min at 37°C , labeling was stopped by adding 10% FCS-containing IMDM and cells were washed twice. CFSE-labeled cells were cultured, as described above, with $1 \mu\text{g/ml}$ LPS or anti-CD40 for 3 days.

ELISA assays

ELISA assays were performed with cell free supernatant using commercial available kits following the instructions of the manufacturer (BD Biosciences). Specific antibody titers to given antigens in plasma were determined by chemiluminescent ELISA, as previously described^{32, 33}

Histological analysis

Cryostat sections of the aortic root ($10 \mu\text{m}$) were collected and stained with Oil-red-O to determine lesion size. Macrophages were visualized immunohistochemically with an antibody directed against a macrophage specific antigen (MOMA-2, monoclonal rat IgG2b, dilution 1:50; Serotec, Oxford, UK). Goat anti-rat IgG-AP (dilution 1:100; Sigma, St. Louis, MO) was used as secondary antibody and NBT-BCIP (Dako, Glostrup, Denmark) as enzyme substrates. Masson's trichrome staining (Sigma) was used to visualize collagen (blue staining). T cells were visualized immunohistochemically with an antibody directed against CD3 (CD3). Goat anti-rabbit (dilution 1:100; Sigma-Aldrich) was used as secondary antibody and Novared (Dako) as enzyme substrates. Histological analysis was performed at room temperature, by an independent operator (blinded to specimen identity) using Leica DMRE Microscope equipped with a Leica DC 500 camera and with Qwin quantification software (Leica, Rijswijk, the Netherlands).



Statistics

Data are expressed as mean±SEM. A two-tailed Student's T-test was used to compare individual groups. Nonparametric data were analyzed using a Mann-Whitney U test. A level of $P < 0.05$ was considered significant.

1. de Jager SC, Bot I, Kraaijeveld AO, Korporaal SJ, Bot M, van Santbrink PJ, van Berkel TJ, Kuiper J, Biessen EA., Leukocyte-specific CCL3 deficiency inhibits atherosclerotic lesion development by affecting neutrophil accumulation., *Arterioscler Thromb Vasc Biol.* 2013 Mar;33(3):e75-83.

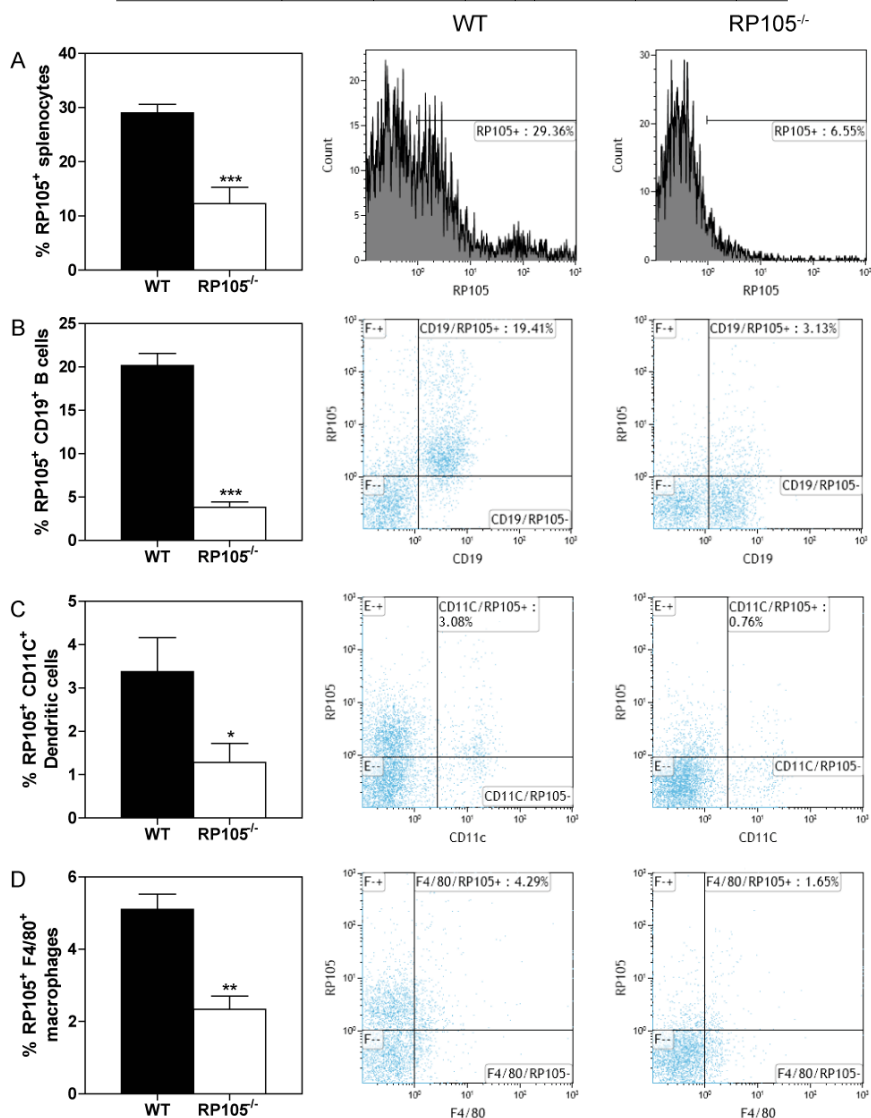
2. Bastiaansen AJ, Ewing MM, de Boer HC, van der Pouw Kraan TC, de Vries MR, Peters EA, Welten SM, Arens R, Moore SM, Faber JE, Jukema JW, Hamming JF, Nossent AY, Quax PH. Lysine acetyltransferase PCAF is a key regulator of arteriogenesis. *Arterioscler Thromb Vasc Biol.* 2013 Aug;33(8):1902-10.

3. Ewing MM, Karper JC, Abdul S, de Jong RC, Peters HA, de Vries MR, Redeker A, Kuiper J, Toes RE, Arens R, Jukema JW, Quax PH. T-cell co-stimulation by CD28-CD80/86 and its negative regulator CTLA-4 strongly influence accelerated atherosclerosis development. *Int J Cardiol.* 2013 Jan 22. doi:pii: S0167-5273(12)01729-9. 10.1016/j.ijcard.2012.12.085. [Epub ahead of print]

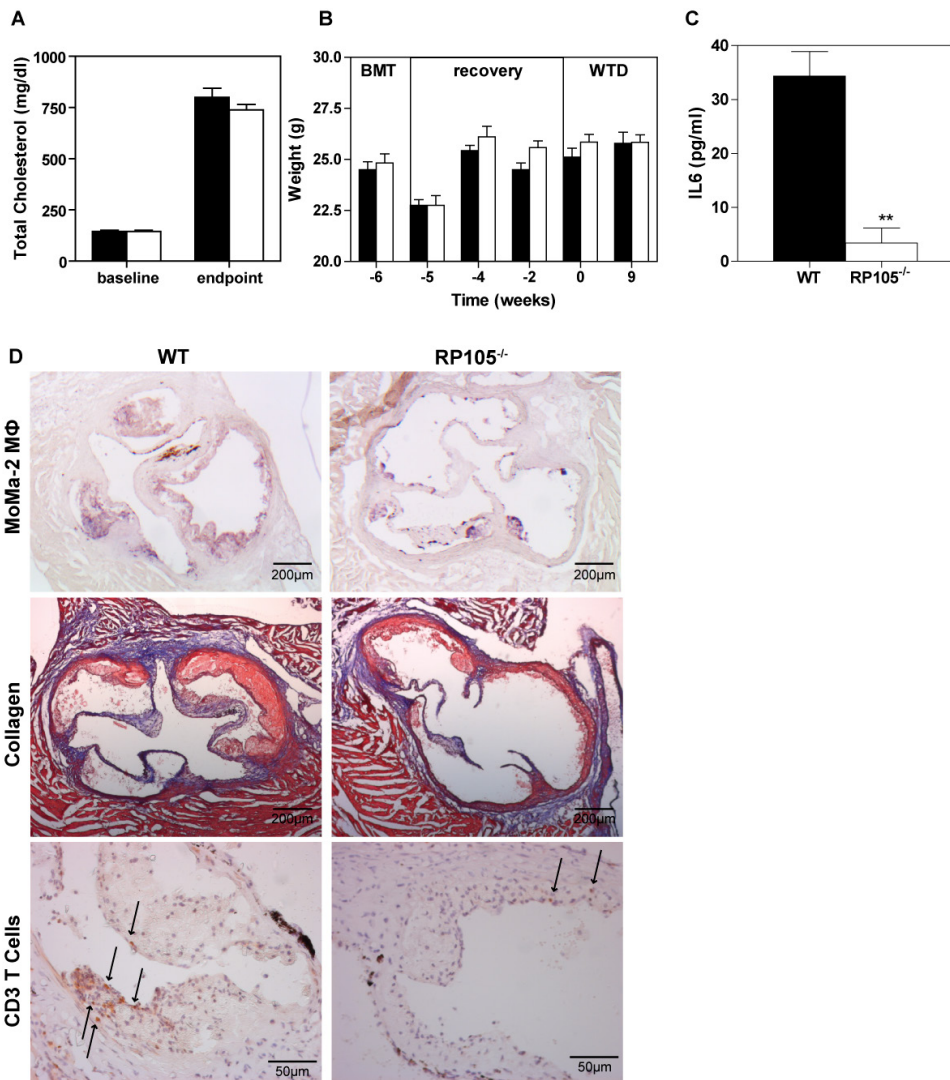
4. H. Zola, B. Swart, I. Nicholson, E. Voss. Leukocyte and stromal cell molecules. The CD markers. Wiley, New York (2007)

Supplemental table 1: Cellular composition of the spleens of WT and RP105^{-/-} chimeras

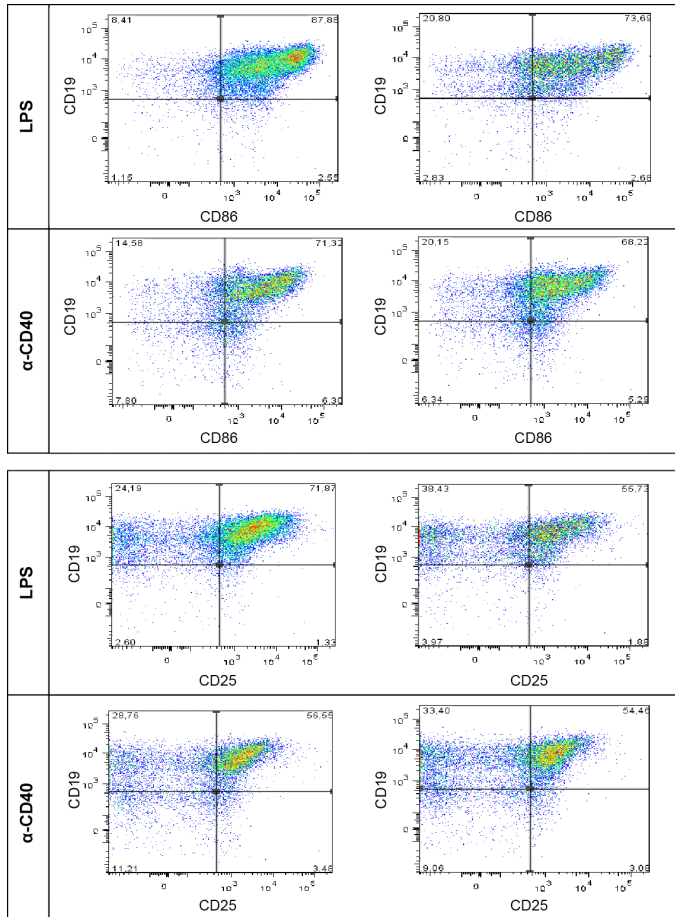
	Percentage			Absolute counts		
	WT	RP105 ^{-/-}	p	WT	RP105 ^{-/-}	p
CD19 B cell	24.2 ± 3.6	25.5 ± 3.0	0.51	49.2 ± 16.5	65.0 ± 18.6	0.15
CD4 T cell	22.6 ± 2.7	20.0 ± 5.5	0.34	45.0 ± 11.9	45.4 ± 20.4	0.97
CD8 T cell	15.7 ± 1.9	13.7 ± 5.7	0.42	31.0 ± 6.0	32.0 ± 9.5	0.83
CD11c DC	12.7 ± 0.9	12.7 ± 1.0	0.95	25.4 ± 6.7	31.9 ± 8.3	0.17
F4/80 Macrophage	7.8 ± 1.1	7.3 ± 1.3	0.51	15.8 ± 5.1	18.7 ± 6.3	0.40



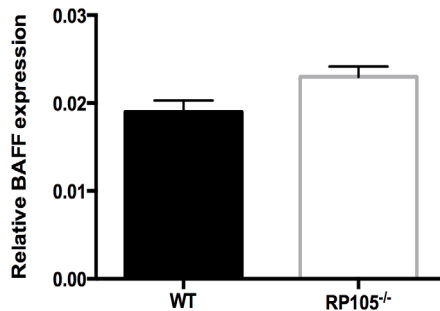
RP105 expression levels on total splenocytes (A), CD19⁺ B Cells (B), CD11c⁺ Dendritic Cells (C) and F4/80⁺ macrophages (D) in WT and RP105^{-/-} LDLR^{-/-} chimeras (A). Black bars represent WT chimeras, white bars represent RP105^{-/-} chimeras. **p*<0.05, ***p*<0.01, ****p*<0.001. *n*=6 mice per group.



Supplemental figure 2 Cholesterol levels (A) and bodyweight (B) for the WT and the RP105^{-/-} LDLR^{-/-} chimeras. IL6 production by B cells from RP105^{-/-} and WT mice stimulated with LPS (C). Representative pictures of MoMa2 macrophage, collagen and CD3 T Cell staining in 5 WT and RP105^{-/-} chimeras (D). Black bars represent WT chimeras, white bars represent RP105^{-/-} chimeras. ***p*<0.01. Average of 3 experiments *n*=4 mice per experiment.

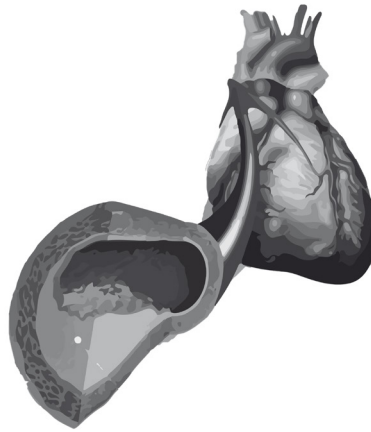


Number of activated B cells from RP105^{-/-} and WT mice stimulated with either LPS or anti-CD40. B cell activation measured by the number of CD19/CD86 and CD19/CD25 positive cells. After LPS stimulation; CD19/CD86 cells: 87.6% (WT) vs 73.6% (RP105^{-/-}) positive cells. CD19/CD25 cells: 71.8% (WT) vs. 55.7% (RP105^{-/-}) positive cells after LPS stimulation. After anti-CD40 stimulation; CD19/CD86: 71.3% (WT) vs 68.2% (RP105^{-/-}) positive cells. CD19/CD25: 56.5% (WT) vs 54.4% (RP105^{-/-}) positive cells.



Relative BAFF expression in splenocytes from WT and RP105^{-/-} mice. (N=5 per group, p=0.08)

CHAPTER 10



Summary and general discussion



Summary and general discussion:

Background

Atherosclerosis, restenosis and cardiac remodeling after myocardial infarction can cause serious clinical problems that greatly contribute to both high morbidity and mortality. In all these processes, the inflammatory responses caused by activation of the immune system play a very prominent role. This thesis elaborates on the role of specific components of the immune system and the therapeutic possibilities that lay hidden therein. This was done by focussing on the pathophysiological process in which Damage Associated Molecular Patterns (DAMPs) are released upon cell stress and cell death or other tissue damage, and may play an important role via different mechanisms. The data in this thesis illustrates specific involvement of DAMPs recognizing factors such as Toll-like Receptors in vascular remodeling and the therapeutic potential that lies within these findings.

This thesis

Overall, the aim of this thesis was to investigate the non-pathogenic-induced inflammatory response in cardiovascular remodeling with a specific focus on DAMPs and Toll Like Receptors. **Chapter 1** provides a general introduction on vascular remodeling, involvement of the immune system and Toll Like Receptor signalling.

In this thesis we investigate the pathophysiological processes of vascular remodeling in a pre-clinical setting. Explorations of these processes require good models that allow involvement of e.g. hypercholesterolemia and damage caused by intervention, to mimic the clinical setting. This is discussed in **Chapter 2** that focus on the various available animal models that can be used to study the process of restenosis. Furthermore, it examines the potential of local therapy to reduce adverse systemic side effects. These models can also be used to discover and study potential biomarkers.

Chapter 3 zooms in on these potential future biomarkers for restenosis. Biomarkers may provide tools to monitor disease initiation or progression. The fact that the problems of vascular remodeling and restenosis continue to exist, emphasizes the need for specific biomarkers to detect pathogenic vascular remodeling, upon which adequate treatment can be initiated. The immunogenic reactions leading to cardiovascular remodeling and atherosclerosis development are rather complex and therefore require more specific biomarkers to adequately evaluate these processes. We discuss a number of possible biomarkers selected due to their involvement in the pathophysiological process of restenosis. In this process DAMPs, released after cell stress or death or by other forms of tissue damage, seem to play an important role and may be recognized by various components of the immune system. Examples of DAMPs that can serve as potential biomarkers are Annexin A5, HMGB1, HSP60, Tenascin C and Fibronectin-EDA. These DAMPs can be found locally in the damaged vessel wall and are known to trigger the immune response directly e.g. via TLR signalling. In particular intervention procedures such as PCI may cause cell and tissue damage that will lead to enhanced expression of a wide variety of these DAMPs. A distinction in potential biomarkers was made between circulating, local and circulating cell-bound markers. Via better understanding of the underlying pathophysiological process a more specific biomarker selection can take place, which will increase the reliability and applicability of these markers. TLR 4 is considered to be an important DAMP recognizer. In **Chapter 4** we have in addition to previous studies, focused on the possible involvement of Toll-like receptor 4 (TLR4) on intimal hyperplasia formation, remodeling and atherosclerosis formation in vein grafts. TLRs

as Pattern Recognition Receptors (PRR) are important receptors of a large variety of DAMPs. We showed that reperfusion of venous segments, of both murine and human origin, gives an increase in the expression of TLR4. This was studied *ex vivo* (in case of the human segments) and *in vivo* using a mouse vein grafting model. Furthermore, the functional involvement of TLR4 on intimal hyperplasia and remodeling in vein grafts was demonstrated in mice. In addition, it was shown that a fair number of DAMPs, known to act as endogenous ligands for TLR4, are present during the remodeling process in the vessel wall of the vein grafts. It is thought that their presence is caused by the vascular injury induced by the intervention and vascular distension of the venous segment positioned in the arterial circuit, for they are not detected in healthy undamaged vessels. These ligands can activate TLR4, and so further enhance the inflammatory response. Finally we provided evidence, via application of local gene silencing in hypercholesterolemic mice, that TLR4 can be a local therapeutic target to reduce vein graft thickening and remodeling. Other TLRs may also be involved in these processes and thereby interesting local therapeutic targets. Some however are located intracellular and it unknown if and how they are involved.

In **Chapter 5**, we showed validation of a new TLR7 and TLR9 antagonist that did not affect other TLRs. TLR7 and 9 were unknown to be involved in vascular remodeling and are traditionally linked to inflammation initiated by viral components such as CpG. Our TLR7/9 blocking compound was capable of inhibiting restenosis and accelerated atherosclerosis in hypercholesterolemic mice. Intracellular TLRs such as TLR7 and TLR9 recognize DAMPs in the form of self DNA and / or RNA fragments that are frequently released from cells that underwent increased cell stress or damage. In this way, these TLRs cause an inflammatory reaction in response to released endogenous ligands. The antagonist reduced restenosis by minimalizing the infiltration of macrophages, reduced foam cell formation and increased production of anti-inflammatory cytokine IL10. Furthermore HMGB1, which can be up regulated via TLR9 activation and serves as an enhancer of TLR7 and TLR9 activation was reduced in the vessel wall of mice treated with the antagonist. These data suggests that this could be a potential future therapy used for the inhibition of post-interventional restenosis. Another intracellular and nucleic acid recognizing TLR is TLR3. **Chapter 6** focused on the effects of TLR3 and downstream signalling mediators on vein graft remodeling. Pathway analysis showed that the TLR and type 1 Interferon pathway belonged to the top 15 of regulated pathways in vein graft remodeling. TLR3 is the only TLR that solely signals through the myd88-independent pathway that causes up regulation of type 1 interferons. Therefore TLR3 and important downstream Interferon Regulating Factors (IRF) were studied using the same vein graft model. Here TLR3 showed protective effects on vein graft remodeling with a decrease of inflammatory cell influx into the vessel wall compared to TLR3^{-/-} mice. Interestingly TLRs that are traditionally linked to vascular inflammation such as TLR2 or TLR4 do not have these protective effects and TLR4 even enhances the vascular remodeling process, which was also previously shown in Chapter 5. Furthermore IRF7 also showed strong protective effects on remodeling by decreasing inflammatory cell influx. Since no exogenous ligands were used in these studies the data shown in this chapter provides evidence that the TLR3 pathway is involved in damage-associated vascular remodeling with effects that are uncommon for TLR signalling in vascular remodeling. Recently we know that TLR signalling is strongly influenced by co-factors that function as accessory molecules.

Chapter 7 examined the role of the TLR accessory molecule RP105 in the arterial restenosis process. RP105 is a receptor homologous to TLR4, but lacks the intracellular portion of the protein and is therefore unable to instigate an intracellular signalling cascade by itself. This



chapter described the presence of RP105 on smooth muscle cells and functional effects on restenosis for the first time. Analysis of the crystal structure showed that RP105 only forms a stable protein in the presence of MD1 and that compared to other TLRs, this complex thereby formed an unusual protein structure. In addition, we were able by means of ex-vivo whole blood stimulation to demonstrate that a soluble form of RP105 combined with the accessory molecule MD1 is able to inhibit the TLR4-induced inflammation, and that over-expression of this complex in vivo can inhibit restenosis.

Chapter 8 described the effects of RP105 absence on cardiac function after myocardial infarction. Here we showed that RP105 deficiency had no effect on infarct size and no significant differences in cardiac output 15 days post-infarction. RP105^{-/-} mice however had a marked left ventricular dilatation and showed an elevated heart rate. This suggests that the intrinsic myocardial function of the intact heart muscle was decreased in these mice, and therefore a more pronounced need for a post-infarction compensatory response. This conclusion was supported by the results with respect to the pressure-volume curves. Interestingly, in contrast to indications of a depressed systolic function, the diastolic function seemed to be improved. Therefore RP105^{-/-} mice have a more prominent cardiac dilation after MI, but displayed relatively good hemodynamic parameters by adequate compensation. In **chapter 9**, we studied the effects of RP105 on atherosclerotic plaque formation in order to understand the role of RP105 in the development of atherosclerosis without the strong cellular damage induced by PCI or infarction. This chapter described an effect of TLR-regulator RP105 on atherosclerosis formation. Previously we described a strong increase in remodeling in post-interventional remodeling processes such as restenosis and myocardial remodeling after infarction in RP105-deficient mice. In this chapter however we noticed an intriguing unexpected effect since atherosclerosis formation was hampered in irradiated hypercholesterolemic mice that had received RP105 deficient bone marrow. These effects could be partly explained by effects noticed on B cell activation and antibody production. For the first time, a direct link between TLR involvement in atherosclerosis and B cell activation was shown that was not caused by the traditional affiliated TLR cells of the innate immune system such as the monocytes/macrophages. Moreover, these results may be important for patients with autoimmune disorders such as SLE and Rheumatoid Arthritis (RA), in which B cells play an important pathological role in disease progression. These patients also have an increased risk of developing heart and vascular disease, thus further emphasizing the important role of the immune system in atherosclerosis.

Supplemental material to chapter 2

Rheumatoid Arthritis (RA) is considered an autoimmune disease for which a variety of new drugs have been developed such as Abatacept. Abatacept is a soluble CTLA4 Ig fusion protein that acts by blocking T-cell activation via interfering with CD28-CD80/86 the co-stimulation complex of T cells. This paper offers a closer look at the involvement of T cells in the restenosis process and in particular the role of co-stimulation. Reduced neointima formation was observed in mice that have no T cells (CD4^{-/-} mice), or that have a disturbed T cell co-stimulation pathway (CD80^{-/-}CD86^{-/-} mice). In hypercholesterolemic animals, administration of Abatacept led to a reduced neointima formation and inhibition of accelerated atherosclerosis. This shows that inhibition of the T cell co-stimulation had a protective effect on vascular remodeling even after vascular interventions and could be a potentially beneficial side effect for RA patients. During these kind of inflammatory processes many cells are activated or are dying via apoptosis or necrosis. Cells that undergo apoptosis, cell death

or cells that are activated by an inflammatory reaction all express phosphatidylserine (PS) on their outer cell surface. Annexin A5 binds to PS and can also be used to demonstrate the presence of PS in atherosclerotic plaques. The paper describes the possibilities to use Annexin A5 as a therapeutic and as a risk marker of arterial restenosis. In physiological conditions, PS remains on the inside of the cellular membrane. When PS appears at the outer cell surface it supports platelet binding and activation. This makes PS an interesting functional DAMP and therefore a potential therapeutic target. We show that single nucleotide polymorphisms of Annexin A5 could be related to an increased risk of restenosis in patients. Administration of Annexin A5 to hypercholesterolemic mice has demonstrated that there is a reduced leukocyte adhesion, less inflammatory activity, and also less atherosclerosis formation in the Annexin A5 treated mice after femoral artery cuff placement. Blocking of a DAMP such as PS thus gives promising results in reducing vascular remodelling by interfering in the DAMP-induced inflammatory response.

Discussion

The aim of this thesis was to gain insight into the involvement of the immune system in the pathophysiological mechanism of vascular remodeling in order to be able to point out new potential therapeutic targets. The focus was in particular on the involvement of Damage Associated Molecular Patterns (DAMPs), Toll Like Receptors and final application of immunomodulation to inhibit adverse remodeling. The results presented in this thesis allow us to better understand how vascular remodeling is mediated by inflammation and how targeted immunomodulation may have beneficial effects. However, it will take some time before this pre-clinical work will be effectively applicable to daily clinical practice, partly because immunomodulation may have downside effects such as a decreased resistance to pathogens. Therefore it is necessary to apply immunomodulation that is specifically directed against a target, which is only possible if there is a proper understanding of the underlying pathophysiological mechanism. The discoveries from pre-clinical studies unravel these mechanisms and thereby allow us to design novel safe and effective therapies. Nevertheless one can only speculate on the future success of these findings for clinical application. However the involvement of TLRs and presence of DAMPs as demonstrated in this thesis offer a huge therapeutic potential that may even go beyond the process of vascular remodeling. Interestingly DAMPs and TLRs are considered to be involved in other diseases as well such as cancer and autoimmune diseases. Recently a phase 2 study was successfully completed with our TLR7/9 antagonist for the treatment of psoriasis. On the other hand, one should consider that apart from beneficial effects on vascular remodeling it is still possible that these therapies will initiate or worsen other diseases. Furthermore one should take into account that individual TLRs may have different effects. Our finding that TLR3 has an opposite effect on vein graft remodeling compared to TLR4, although they share an important signalling pathway, is a nice example. Additionally the discovery of various co-factors involved in TLR signalling, such as RP105, have made the understanding and interpretation of TLR signalling even more complex. Yet these cofactors offer interesting possibilities for therapeutic intervention since they regulate TLR signalling. Modulation of the co-factors may therefore keep a proper immune balance instead of shutting down a full TLR signalling route. Once again, as we show for RP105, the specific underlying disease mechanism should be taken into account to understand the results in different models of vascular remodeling. Future experiments have to be performed to understand and clarify these intriguing but complex findings. Finally it is interesting to focus on DAMPs. If DAMPs present in the plaque, will



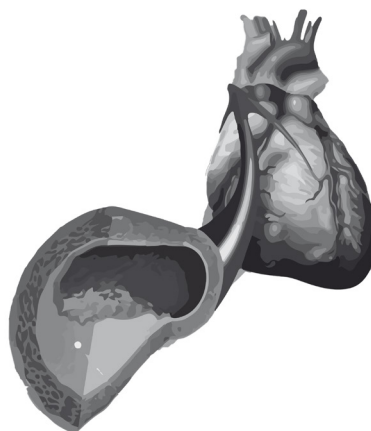
also be released in the circulation and can be detected in plasma, their levels may be related to a particular risk profile and thereby not only function as therapeutic target but as biomarker as well. Especially DAMPs are excellent candidates for both indications since they are only released in response to tissue or cellular damage.

Before the results presented in this thesis will lead to adequate therapies to counteract adverse vascular remodelling, additional research has to be performed focused on effectiveness and safety.

Conclusion:

Endogenous activation of the immune system plays an important role in the post-interventional vascular remodeling process. The release of DAMPs after vascular damage cause activation of Toll-like receptors leading to an inflammatory response that contributes significantly to the remodeling process. Multiple DAMPs such as HMGB1 are absent before the intervention however they were found highly up regulated locally in the vessel wall after intervention indicating a specific relation with the intervention procedure. The presence and involvement of a variety of Toll Like Receptors in different models of vascular remodeling is interesting since these receptors are considered to be important recognizers of the DAMPs locally found in the vessel wall. Different intracellular signalling pathways and TLR accessory molecules seem to mediate the outcome of the specific DAMP-TLR interactions on vascular remodeling majorly. Protective effects of TLR3 and different outcomes of RP105 deficiency on vascular remodeling processes indicate the complexity of the underlying pathophysiological processes. These results can be partly explained by downstream TLR signalling and involvement of specific cell subtypes. The exploration of these underlying mechanisms offers new opportunities for biomarker selection and therapy development. A good biomarker predicts the amount of damage by the intervention, restenosis risk, disease progression or can monitor therapy efficacy. Especially for therapies targeted against TLRs one should weigh the risks and benefits since these receptors are considered to be involved in many other disease processes and important for host defence against exogenous derived pathogens. Nevertheless specifically targeted immunomodulation has the potential of inhibiting the pathophysiological remodeling process in a convenient and controlled manner.

CHAPTER 11



Nederlandse samenvatting



Nederlandse samenvatting:

Achtergrond

Atherosclerose, restenose en remodeling na myocardinfarct veroorzaken ernstige klinische problemen die sterk bijdragen aan zowel een hoge morbiditeit als mortaliteit. In al deze processen spelen ontstekingsreacties, veroorzaakt door activering van het immuunsysteem, een zeer belangrijke rol. Dit proefschrift gaat in op de rol van specifieke onderdelen van het immuunsysteem en de therapeutische mogelijkheden die hierin verborgen liggen. Er is gefocust op de pathofysiologische processen waarin Schade Geassocieerde Moleculaire Patronen (DAMPs= damage associated molecular pattern) vrijkomen bij cel-stress en celdood of andere weefselschade, waardoor ze via verschillende mechanismen een belangrijke rol kunnen spelen. De studies in dit proefschrift illustreren ook specifieke betrokkenheid van DAMPs herkende factoren zoals Toll-like Receptoren in vasculaire remodeling en hun therapeutisch potentieel.

Dit proefschrift

In het algemeen is het doel van dit proefschrift om de niet-pathogene-geïnduceerde ontstekingsreactie in cardiovasculaire remodeling te onderzoeken met een specifieke focus op DAMPs en Toll like Receptoren. **Hoofdstuk 1** geeft een algemene inleiding op vasculaire remodeling, betrokkenheid van het immuunsysteem en Toll Like Receptor signalering.

In dit proefschrift onderzoeken we de pathofysiologische processen van vasculaire remodeling in een preklinische setting. Verkenningen van deze processen vereisen goede modellen die betrokkenheid toestaan van bijvoorbeeld hypercholesterolemie en schade als gevolg van de interventie procedure, om de klinische setting adequaat na te bootsen.

In **hoofdstuk 2** wordt ingegaan op de verschillende beschikbare diermodellen die gebruikt kunnen worden om het proces van restenose na te bootsen. Bovendien wordt het potentieel van lokale therapie besproken waarmee nadelige bijwerkingen van systemische therapie verminderd kunnen worden. Deze modellen kunnen ook gebruikt worden om potentiële biomarkers te ontdekken en te bestuderen

Hoofdstuk 3 richt zich op deze mogelijk toekomstige biomarkers voor restenose. Biomarkers kunnen tools bieden om de ziekte initiatie of progressie te volgen. Het feit dat de problemen van vasculaire remodeling en restenose nog steeds bestaan benadrukt de noodzaak van specifieke biomarker-selectie om zo pathogene vasculaire remodeling tijdig te detecteren zodat adequate behandeling kan worden ingezet. De immunogene reacties die leiden tot cardiaalremodeling en tot het ontwikkelen van atherosclerose, zijn tamelijk complex en vragen om meer specifieke biomarkers waarmee deze processen adequaat geëvalueerd kunnen worden. Een aantal mogelijke biomarkers, geselecteerd vanwege hun betrokkenheid bij het pathofysiologische proces van restenose, zijn uitgelicht en besproken. Daarbij lijken DAMPs, vrijgegeven na celspanning, celdood of andere vormen van weefselbeschadiging een belangrijke rol te spelen en worden ze herkend door verschillende componenten van het immuunsysteem. Voorbeelden van DAMPs die kunnen dienen als potentiële biomarkers zijn annexine A5, HMGB1, HSP60, Tenascin C en fibronectine-EDA. Deze DAMPs kunnen lokaal worden gevonden in de beschadigde vaatwand en staan bekend de immunrespons direct aan te kunnen zwengelen, bijvoorbeeld via TLR-signalering. Vooral interventieprocedures zoals Percutane Coronaire Interventie (PCI) kunnen cel en weefselschade geven die leiden tot expressie van een groot aantal van deze DAMPs. In potentiële biomarkers werd onderscheid gemaakt tussen circulerende, lokale en circulerende cel-gebonden markers. Door een

beter begrijpen van het onderliggende pathofysiologische proces kan een meer specifieke biomarkerselectie plaatsvinden, die de betrouwbaarheid en toepasbaarheid van deze markers doet toenemen. TLR4 wordt gezien als een belangrijke DAMP herkenner.

In **hoofdstuk 4** hebben we ons, in aanvulling op eerdere studies, gericht op de mogelijke betrokkenheid van Toll-like receptor 4 (TLR4) op intima hyperplasie vorming, remodeling en atherosclerose vorming in veneuze bypasses. TLRs als Pattern Recognition Receptors (PRR) zijn belangrijke receptoren van een zeer uiteenlopend aantal DAMPs. We tonen aan dat reperfusie van veneuze segmenten, van zowel muis als humane oorsprong, een verhoging geeft van de expressie van TLR4. Dit is onderzocht ex vivo in humane veneuze vaatsegmenten en in vivo in een veneuze bypass muis model. Bovendien is de functionele betrokkenheid van TLR4 aangetoond op intimale hyperplasie en remodeling in bypasses in muizen. Tevens is aangetoond dat een behoorlijk aantal DAMPs, bekend als endogene liganden voor TLR4, aanwezig zijn in de vaatwand van de veneuze grafts gedurende het remodelingsproces. De gedachte is dat de aanwezigheid van deze DAMPs wordt veroorzaakt door vasculaire schade geïnitieerd door chirurgische interventie en vaatstress door de hogere bloeddruk van het arteriële circuit. Dit wordt ondersteund doordat zij niet in gezonde onbeschadigde vaten worden gedetecteerd. Deze liganden kunnen TLR4 activeren en dus verdere versterking van de ontstekingsreactie initiëren. Tot slot hebben we het bewijs geleverd, via de toepassing van lokale gen uitschakeling in hypercholesterolemische muizen, dat TLR4 een lokaal therapeutisch doel kan zijn waarmee vaatwandverdikking en remodeling zijn te verminderen. Andere TLRs zijn mogelijk ook bij deze processen betrokken en daarmee interessante therapeutisch targets. Sommige zitten echter in de cel en het is onduidelijk of en hoe ze hierbij betrokken te zijn.

In **hoofdstuk 5**, tonen we de validatie van een nieuwe TLR7/TLR9 antagonist aan, die geen invloed heeft op andere TLRs. TLR7 en 9 zijn niet bekend betrokken te hebben bij vasculaire remodeling maar zijn traditioneel verbonden met ontstekingen, geïnitieerd door virale componenten zoals CpG. In hypercholesterolemische muizen zien we dat de TLR7/9 blokkerende verbinding restenose en versnelde atherosclerose kan remmen. Intracellulaire TLRs, zoals TLR7 en TLR9, herkennen DAMPs in de vorm van eigen DNA en / of RNA-fragmenten, die vaak worden vrijgemaakt uit cellen die onder verhoogde celstress staan of schade hebben opgelopen. Deze TLRs veroorzaken een ontsteking in reactie op deze vrijgegeven endogene liganden. De antagonist vermindert restenose via het minimaliseren van de infiltratie van macrofagen, verminderde vorming van schuimcellen en een verhoogde productie van het anti-inflammatoire cytokine IL10. Bovendien is de hoeveelheid van HMGB1, die als een versterker van TLR7 en TLR9 activatie kan dienen, vermindert in de vaatwand van muizen behandeld met de antagonist. Deze hoeveelheid kan tevens worden geregeld via TLR9 activatie. De resultaten suggereren dat dit een potentiële toekomstige therapie voor de remming van restenose na interventie zou kunnen worden. Een andere intracellulaire en nucleïne zuur herkende TLR is TLR3. **Hoofdstuk 6** richt zich op de effecten van TLR3 en lager gelegen signalerings mediators op veneuze graft remodeling. Pathway-analyse toont aan dat de TLR en type 1 interferon pathway tot de top 15 van gereguleerde pathways in veneuze graft remodeling behoren. TLR3 is de enige TLR die uitsluitend signaleert via de MyD88-onafhankelijke pathway, die regulering van type 1 interferonen veroorzaakt. Om deze reden zijn TLR3 en belangrijke downstream Interferon Regulerende Factoren (IRF) onderzocht met behulp van hetzelfde bypass model. TLR3 toont aan een beschermend effect te hebben op bypass remodeling met afname van de instroom van inflammatoire cellen in de vaatwand ten opzichte van TLR3^{-/-} muizen. Interessant genoeg laten TLRs die traditioneel



verbonden zijn met vasculaire ontsteking, zoals TLR2 of TLR4, zien niet deze beschermende effecten te hebben. TLR4 verbetert zelfs het vasculaire remodeling proces, zoals in hoofdstuk 4 ook is aangetoond. Verder heeft IRF7 ook sterke beschermende effecten op de remodeling door het verlagen van inflammatoire cel instroom. Aangezien er geen exogene liganden zijn gebruikt in deze studies, levert dit onderzoek bewijs dat het TLR3 pathway betrokken is bij schade-geassocieerde vasculaire remodeling, met effecten die ongewoon zijn voor de eerder bekende TLR signalering in vasculaire remodeling.

Sinds kort weten we dat TLR signalering sterk wordt beïnvloed door co-factoren die werken als hulpmolecuul in de TLR signalering. In **hoofdstuk 7** wordt de rol van het TLR hulpmolecuul RP105 beschreven in het arteriële restenose proces. RP105 is een receptor homoloog aan TLR4, maar mist het intracellulaire gedeelte van het eiwit en is daarom niet in staat om een intracellulaire signalering cascade uit zichzelf aan te zetten. Voor de eerste keer wordt de aanwezigheid van RP105 op gladde spiercellen beschreven en zijn de functionele effecten op restenose aangetoond. Uit analyse van de kristalstructuur blijkt dat RP105 slechts een stabiel eiwit vormt in aanwezigheid van MD1. Dit is in vergelijking met andere TLRs een ongewoon complex. Bovendien hebben we door middel van ex-vivo volbloed stimulatie kunnen aantonen dat een oplosbare vorm van RP105 in combinatie met het accessoire molecuul MD1 de TLR4-geïnduceerde ontstekingsreactie kan remmen en overexpressie van dit eiwit in vivo restenose kan doen verminderen.

In **hoofdstuk 8** wordt gekeken naar het effect van RP105 deficiëntie op de hartfunctie na een myocard infarct. Hier tonen we aan dat RP105 deficiëntie geen effect heeft op infarctgrootte en geen significante verschillen laat zien in hartminuutvolume 15 dagen na het infarct. RP105^{-/-} muizen tonen echter een duidelijke linker ventriculaire dilatatie en een verhoogde hartslag. Dit suggereert dat de intrinsieke myocardiale functie van de intacte hartspier verminderd is bij deze muizen en er derhalve een meer uitgesproken behoefte is aan een compenserende respons post-infarct. Deze conclusie wordt ondersteund door de resultaten van de druk-volume curven. Interessant is dat in tegenstelling tot vermeldingen van een verminderde systolische functie de diastolische functie lijkt te verbeteren. RP105^{-/-} muizen hebben derhalve een prominentere cardiale dilatatie na myocard infarct, maar relatief goede hemodynamische parameters door adequate compensatie mechanismen.

In **hoofdstuk 9** hebben we de effecten van RP105 onderzocht op atherosclerotische plaquevorming om inzicht te krijgen in de ontwikkeling van atherosclerose onder invloed van RP105 zonder de aanwezigheid van sterke cellulaire schade veroorzaakt door bijvoorbeeld een PCI of infarct. Eerder hebben we een sterke toename in remodeling in post-interventionele remodeling processen beschreven zoals restenose en myocard remodeling na infarct in RP105-deficiënte muizen. Echter, we hebben hier een intrigerend onverwacht effect bemerkt waarbij atherosclerose vorming wordt geremd in bestraalde hypercholesterolemische muizen, die RP105 deficiënt beenmerg hebben ontvangen. Deze resultaten kunnen deels worden verklaard door de effecten op B cel activatie en antilichaam productie. Voor het eerst is een direct verband aangetoond tussen TLR betrokkenheid bij atherosclerose en B cel activatie, die niet werd veroorzaakt door de traditionele gelieerde TLR cellen van het aangeboren immuunsysteem, zoals monocyt / macrofagen. Bovendien kunnen deze resultaten belangrijk zijn voor patiënten met auto-immuunziekten zoals SLE en reumatoïde artritis (RA), waarbij B-cellen een belangrijke pathologische rol spelen in de ziekteprogressie. Deze patiënten hebben ook een verhoogd risico op hart-en vaatziekten, waarbij meer nadruk komt te liggen op de belangrijke rol van het immuunsysteem bij atherosclerose vorming.

Aanvullend materiaal bij hoofdstuk 2

Reumatoïde artritis (RA) wordt beschouwd als een auto-immuunziekte waarvoor een verscheidenheid van nieuwe geneesmiddelen wordt ontwikkeld, zoals Abatacept. Abatacept is een oplosbaar CTLA4-Ig fusie-eiwit dat werkt door het blokkeren van T-celactivering via inmenging in de CD28-CD80/86 co-stimulatie van T-cellen. Dit artikel geeft inzicht in de betrokkenheid van T-cellen binnen het restenose-proces en in het bijzonder de rol van co-stimulatie. Verminderde neointima vorming is waargenomen bij muizen die geen T-cellen (CD4^{-/-} muizen) hebben en- of een verstoorde T-cel co-stimulatie aanwezig is (CD80^{-/-} CD86^{-/-} muizen). In hypercholesterolemische dieren leidt toediening van Abatacept tot een verminderde neointimavorming en remming van versnelde atherosclerose. Dit toont aan dat de remming van de T-cel co-stimulatie een beschermend effect heeft op vasculaire remodeling, zelfs na vasculaire interventies en dit kan potentieel gunstig bijeffect hebben voor RA patiënten.

Tijdens dergelijke ontstekingsprocessen worden er veel cellen geactiveerd of gaan cellen dood via apoptose of necrose. Cellen die apoptose of necrose ondergaan of cellen die worden geactiveerd door een ontstekingsreactie laten allen expliciete aanwezigheid van fosfatidylserine (PS) op hun celoppervlak zien. Annexine A5 bindt aan PS en kan ook worden gebruikt om de aanwezigheid van PS aan te tonen in atherosclerotische plaques. In dit artikel worden de mogelijkheden beschreven om annexine A5 te gebruiken als therapeutische- en als een risicofactor van arteriële restenose. In fysiologische omstandigheden blijft PS aan de binnenkant van het celmembraan zitten. Indien PS verschijnt aan het buitenoppervlak van de cel dan ondersteunt het de binding en activering van bloedplaatjes. Dit maakt PS tot een interessante functionele DAMP en daarmee een potentieel therapeutisch doelwit. We laten zien dat bepaalde single nucleotide polymorfismen (SNPs) van annexine A5 kunnen worden gerelateerd aan een verhoogd risico op restenose bij patiënten. Toediening van Annexine A5 aan hypercholesterolemische muizen heeft aangetoond dat er een verlaagde leukocyt adhesie is, er een verminderde ontstekingsactiviteit is en ook minder atherosclerose vorming optreedt in de annexine A5 behandelde muizen na plaatsing een femorale arteriële cuff. Het blokkeren van een DAMP, zoals PS, geeft dus veelbelovende resultaten in het verminderen van vasculaire remodeling door zich te mengen in de DAMP-geïnduceerde ontstekingsreactie.

Discussie

Doel van dit proefschrift was om beter inzicht te krijgen in de betrokkenheid van het immuunsysteem in het pathofysiologisch mechanisme van vasculaire remodelling om zo nieuwe potentiële therapeutisch targets aan te kunnen wijzen. De focus lag hierbij met name op de betrokkenheid van DAMPs, Toll Like Receptoren en de uiteindelijke toepassing van immunomodulatie om de ongunstige remodeling te remmen. Met de resultaten in dit proefschrift begrijpen we beter hoe vasculaire remodeling door ontsteking wordt beïnvloed en hoe hierop gerichte behandelingen gunstige effecten kunnen hebben. Diverse voorbeelden zijn hiervan in dit proefschrift terug te vinden. Het zal echter nog wel enige tijd duren voordat dit pre-klinische werk daadwerkelijk toegepast zal kunnen worden in de dagelijkse praktijk, mede omdat immunomodulatie ook zijn keerzijde kent in de vorm van een afgenomen weerstand tegen pathogenen. Daarom zal men zeer specifieke immunomodulatie moeten toe passen wat alleen kan indien er goed begrip bestaat van het onderliggende pathofysiologisch mechanisme. Het pre-klinisch ontrafelen hiervan is dus van wezenlijk belang om nieuwe therapieën veilig en effectief te laten zijn. Over toekomstig succes in de kliniek kan op basis van dit proefschrift echter alleen worden gespeculeerd. De betrokkenheid van TLRs



en aanwezigheid van DAMPs zoals aangetoond in dit proefschrift bieden wel een enorm therapeutisch potentieel dat mogelijk verder reikt dan alleen vasculaire remodeling. In andere ziekteprocessen waarin het immuunsysteem belangrijk is zoals kanker en autoimmuun ziekten, lijken TLRs en DAMPs ook van groot belang. Zo is er recent een succesvolle fase 2 studie afgerond met de door ons gebruikte TLR7/9 antagonist voor de behandeling van psoriasis. Aan de andere kant is het mogelijk dat een gunstig effect op bijvoorbeeld vasculaire remodeling juist negatieve effecten heeft voor een andere ziekte door deze te initiëren of te verergeren. Ook zal men rekening moeten houden met de verschillende effecten van individuele TLRs. Zo is onze bevinding dat TLR3 een tegengesteld effect heeft op vein graft remodeling in vergelijking met TLR4. Daarnaast heeft de ontdekking van diverse cofactoren, zoals RP105, die de TLR signalering beïnvloeden, het begrip en interpretatie van TLR signalering een stuk complexer gemaakt. Toch bieden deze cofactoren juist interessante mogelijkheden voor therapie omdat hiermee niet een heel TLR systeem volledig wordt plat gelegd. Immunomodulatie via deze cofactoren kunnen er mogelijk voor zorgen dat ontstekingsprocessen via TLR signalering niet doorslaan en in balans blijven. Ook hier zal weer rekening gehouden moeten worden met het specifieke onderliggende proces zoals wij bijvoorbeeld voor RP105 laten zien. Hoe dit precies werkt is nog niet helemaal duidelijk en zal met toekomstige experimenten verder opgehelderd moeten worden. Verder is het voor de toekomst interessant om therapie juist op DAMPs te richten. Indien DAMPs, aanwezig in de plaque, ook circulerend vrijkomen en in plasma kunnen worden aangetoond kunnen ze mogelijk gerelateerd worden aan een bepaald risico en zouden ze naast therapeutisch target ook als biomarker kunnen gaan fungeren. Juist DAMPs zijn hiervoor interessant omdat ze alleen vrijkomen bij schade geïnduceerde processen.

Voordat de in dit proefschrift gevonden resultaten tot een adequate therapie leiden om ongunstige vasculaire remodeling tegen te gaan, dient er echter nog veel onderzoek naar effectiviteit en veilige toepassing te worden gedaan.

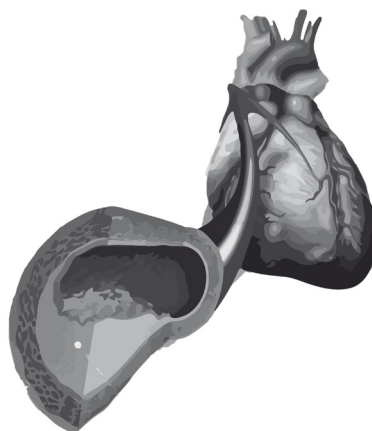
Conclusie:

Endogene activering van het immuunsysteem speelt een belangrijke rol in post-interventionele vasculaire remodeling. De afgifte van DAMPs na vasculaire schade veroorzaakt activering van Toll-like Receptoren hetgeen leidt tot een ontstekingsreactie die sterk bijdraagt aan het remodeling proces. Meerdere DAMPs, zoals HMGB1, zijn afwezig voor een vasculaire interventie procedure maar blijken lokaal verhoogd aanwezig te zijn in de vaatwand na een ingreep, wat wijst op een specifieke relatie met de interventie procedure. De aanwezigheid en betrokkenheid van diverse Toll Like Receptoren in verschillende modellen van vasculaire remodeling is interessant omdat deze receptoren belangrijk herkenneren zijn van lokale DAMPs in de vaatwand. Verschillende intracellulaire signalen en TLR accessoire moleculen lijken de uitkomst van de specifieke DAMP-TLR interacties op vasculaire remodeling in belangrijke mate te bepalen. Beschermende effecten van TLR3 en verschillende uitkomsten van RP105 deficiëntie op vasculaire remodeling geven de complexiteit van de onderliggende pathofysiologische processen weer. Deze resultaten kunnen deels worden verklaard door downstream TLR signalering en betrokkenheid van specifieke cel subtypes. De verkenning van deze onderliggende mechanismen biedt nieuwe kansen voor biomarker selectie en ontwikkeling van behandelingen. Een goede biomarker voorspelt de mate van schade door de interventie, restenose risico, ziekteprogressie en/of kan de effectiviteit van de therapie volgen. Met name bij therapieën, gericht tegen TLRs, moeten de risico's en voordelen goed worden afgewogen aangezien deze receptoren worden geacht betrokken te zijn bij vele ziekteprocessen

en belangrijk zijn voor afweermechanismen tegen exogene afgeleide pathogenen. Niettemin heeft specifieke immunomodulatie het potentieel het pathofysiologische remodelingsproces op een adequate en gecontroleerde manier te remmen.



CHAPTER 12



List of publications and curriculum vitae



List of publications

Full papers

1. TLR Accessory Molecule RP105 (CD180) Is Involved in Post-Interventional Vascular Remodeling and Soluble RP105 Modulates Neointima Formation. Karper JC, Ewing MM, de Vries MR, de Jager SC, Peters EA, de Boer HC, van Zonneveld AJ, Kuiper J, Huizinga EG, Brondijk TH, Jukema JW, Quax PH. *PLoS One*. 2013 Jul 2;8(7):e67923.
2. T-cell co-stimulation by CD28-CD80/86 and its negative regulator CTLA-4 strongly influence accelerated atherosclerosis development. Ewing MM, Karper JC, Abdul S, de Jong RC, Peters HA, de Vries MR, Redeker A, Kuiper J, Toes RE, Arens R, Jukema JW, Quax PH. *Int J Cardiol*. 2013 Jan 22.
3. Blocking toll-like receptors 7 and 9 reduces postinterventional remodeling via reduced macrophage activation, foam cell formation, and migration. Karper JC, Ewing MM, Habets KL, de Vries MR, Peters EA, van Oeveren-Rietdijk AM, de Boer HC, Hamming JF, Kuiper J, Kandimalla ER, La Monica N, Jukema JW, Quax PH. *Arterioscler Thromb Vasc Biol*. 2012 Aug;32(8):e72-80.
4. Annexin A5 prevents post-interventional accelerated atherosclerosis development in a dose-dependent fashion in mice. Ewing MM, Karper JC, Sampietro ML, de Vries MR, Pettersson K, Jukema JW, Quax PH. *Atherosclerosis*. 2012 Apr;221(2):333-40.
5. Future potential biomarkers for postinterventional restenosis and accelerated atherosclerosis. Karper JC, Ewing MM, Jukema JW, Quax PH. *Biomark Med*. 2012 Feb;6(1):53-66.
6. Lack of fibronectin-EDA promotes survival and prevents adverse remodeling and heart function deterioration after myocardial infarction. Arslan F, Smeets MB, Riem Vis PW, Karper JC, Quax PH, Bongartz LG, Peters JH, Hoefler IE, Doevendans PA, Pasterkamp G, de Kleijn DP. *Circ Res*. 2011 Mar 4;108(5):582-92.
7. Toll-like receptor 4 is involved in human and mouse vein graft remodeling, and local gene silencing reduces vein graft disease in hypercholesterolemic APOE*3Leiden mice. Karper JC, de Vries MR, van den Brand BT, Hoefler IE, Fischer JW, Jukema JW, Niessen HW, Quax PH. *Arterioscler Thromb Vasc Biol*. 2011 May;31(5):1033-40.
8. In vivo suppression of vein graft disease by nonviral, electroporation-mediated, gene transfer of tissue inhibitor of metalloproteinase-1 linked to the amino terminal fragment of urokinase (TIMP-1.ATF), a cell-surface directed matrix metalloproteinase inhibitor. Eefting D, de Vries MR, Grimbergen JM, Karper JC, van Bockel JH, Quax PH. *J Vasc Surg*. 2010 Feb;51(2):429-37.
9. Toll like receptors in vein graft remodeling: protective effects of TLR3 and downstream Interferon regulating factors. de Vries M.R, Karper J.C, van der Pouw Kraan T.C, Peters H.A.B, de Jong R.C.M, Hamming J.F, Jukema J.W, Horrevoets A, Quax P.H. Manuscript in preparation
10. An unexpected intriguing effect of TLR regulator RP105 (CD180) on atherosclerosis formation with alterations on B cell activation Karper J.C, de Jager S.C.A, Ewing M.M, de Vries M.R, Bot I, van Santbrink P.J, Redeker A, Mallat Z, Binder C.J, Arens R, Jukema J.W, Kuiper J, Quax P.H.A. *Arterioscler Thromb Vasc Biol*. 2013 Dec;33(12):2810-7
11. RP105 deficiency aggravates cardiac dysfunction after myocardial infarction in mice. Karper J.C, Louwe M.C, de Vries M.R, Bastiaansen A.J.N.M, van der Hoorn J.W.A, Willems van Dijk K, Rensen P.C.N, Steendijk P, Smit J.W.A, Quax P.H.A. Manuscript under revision
12. TLR4 Accessory Molecule RP105 (CD180) Regulates Arteriogenesis and Angiogenesis. Antonius J.N.M. Bastiaansen, Jacco C. Karper, Hetty C. de Boer, Sabine M.J. Welten, Rob C.M. de Jong, Erna A.B. Peters, Margreet R. de Vries, Annemarie M. van Oeveren-Rietdijk, A.J. van Zonneveld, Jaap F. Hamming, A. Yaël Nossent, Paul H.A. Quax. Submitted for publication
13. Optimizing Natural Occurring IgM Antibodies for Therapeutic Use: Inflammatory Vascular Disease Treatment with Anti-Phosphorylcholine IgG. M.M. Ewing, J.C. Karper, M.R. de Vries, M. Nordzell, S.A.P. Karabina, R. Atout, D. Sexton, H. Lettesjö, I. Dahlbom, O. Camber, J. Frostegård, J. Kuiper, E. Ninio, J.W. Jukema, K. Pettersson, P.H.A. Quax. Submitted for publication

14. The epigenetic factor PCAF regulates vascular inflammation and is essential for accelerated atherosclerosis development. Ewing MM, Karper JC, Peters HAB, Bastiaansen AJNM, de Vries MR, van den Elsen PJ, Gongora C, Maurice T, Jukema JW, Quax PHA. Submitted for publication

Bookchapters

Small animal models to study restenosis and effects of (local) drug therapy. Karper JC, Ewing MM, de Vries MR, Jukema JW, Quax PHA. Coronary stent restenosis. Editor: IC Tintoiu. Bucharest: The Publishing House of the Romanian Academy, 2011.



Curriculum vitae

The author of this thesis was born on March 5th 1984 in Zwolle, the Netherlands. He graduated from CSG Liudger (VWO) in Drachten in 2002. In September 2003 he started his medical study at the Leiden University Medical Center (LUMC) in Leiden, the Netherlands. During his study he worked as “Joshua” at the Thoracic Intensive Care Unit in the LUMC. In 2007 he did his science-internship under supervision of dr. J.H.N. Lindeman (vascular surgery) and prof.dr. R.C.M. Klautz (thoracic surgery) and obtained his doctoral exam. In 2008 he started his PhD training with the work described in this thesis under supervision of prof. dr. P.H.A. Quax and prof. dr. J.W. Jukema. For a 3-month period he worked in the lab of prof. dr. Z. Mallat and prof. dr. A.Tedgui in Paris, France. The author was selected to present his work at several congresses including the American Heart Association Scientific Sessions in 2009, 2010 and 2011 and received an ATVB young investigators travel award from the American Heart Association and a Dutch Atherosclerosis Fellowship award. He was selected to attend and present at the European Atherosclerosis Society Summer School on “Inflammation and Cardiovascular Disease“ Obergurgl, Tyrol, Austria. Furthermore he received personal grants from the Leiden University Fund, Foundation “De Drie Lichten” and the Michael van-Vloten Fund. Starting January 2012 he performed his medical rotations at the LUMC and his semi-arts period at the department of cardiology at the University Medical Center Groningen (UMCG) under supervision of prof. dr. M.P. van den Berg. November 2013 he received his medical degree with honours (cum laude) and started in December 2013 as AIOS Cardiology at the UMCG under supervision of dr. P.P. van Geel. He lives in Groningen, the Netherlands.



SUPPLEMENTAL MATERIAL TO CHAPTER 2

T-cell co-stimulation by CD28-CD80/86 and its negative regulator CTLA-4 strongly influence accelerated atherosclerosis development

Ewing MM, Karper JC, Abdul S, de Jong RC, Peters HA, de Vries MR, Redeker A, Kuiper J, Toes RE, Arens R, Jukema JW, Quax PH

Int J Cardiol. 2013 Jan 22.

Abstract

Objective T-cells are central to the immune response responsible for native atherosclerosis. The objective of this study is to investigate T-cell contribution to post-interventional accelerated atherosclerosis development, as well as the role of the CD28-CD80/86 co-stimulatory and Cytotoxic T-Lymphocyte Antigen (CTLA)-4 co-inhibitory pathways controlling T-cell activation status in this process.

Methods and Results The role of T-cells and the CD28-CD80/86 co-stimulatory and CTLA-4 co-inhibitory pathways were investigated in a femoral artery cuff mouse model for post-interventional remodeling, with notable intravascular CTLA-4+ T-cell infiltration. Reduced intimal lesions developed in CD4^{-/-} and CD80^{-/-}CD86^{-/-} mice compared to normal C57Bl/6J controls. Systemic abatacept-treatment, a soluble CTLA-4Ig fusion protein that prevents CD28-CD80/86 co-stimulatory T-cell activation, prevented intimal thickening by 58.5% (p=0.029).

Next, hypercholesterolemic ApoE3*Leiden mice received abatacept-treatment which reduced accelerated atherosclerosis development by 78.1% (p=0.040) and prevented CD4 T-cell activation, indicated by reduced splenic fractions of activated KLRG1⁺, PD1⁺, CD69⁺ and CTLA-4⁺ T-cells. This correlated with reduced plasma interferon- γ and elevated interleukin-10 levels. The role of CTLA-4 was confirmed using CTLA-4 blocking antibodies, which strongly increased vascular lesion size by 66.7% (p=0.008), compared to isotype-treated controls.

Conclusions T-cell CD28-CD80/86 co-stimulation is vital for post-interventional accelerated atherosclerosis development and is regulated by CTLA-4 co-inhibition, indicating promising clinical potential for prevention of post-interventional remodeling by abatacept.

Introduction

Atherosclerosis is a chronic inflammatory disease in which endothelial dysfunction leads to retention of oxidized low-density lipoprotein (oxLDL) cholesterol particles, attracting leukocytes and leading to a local inflammatory response[1-3]. T-cell subsets have been shown to play a vital role in this process[4, 5]. Unlike native atherosclerosis, their contribution to post-interventional remodeling and accelerated atherosclerosis development remains uninvestigated. Although local intimal hyperplasia consist predominately of smooth muscle cells (SMCs) and connective tissue[6], platelet and leukocyte (e.g. T-cells) adherence and activation have been shown to be driving factors behind this overshooting inflammatory healing response, leading to re-occlusion[7].

T-cell responses to immunogenic (neo) antigens such as oxLDL cholesterol are regulated by antigen recognition signals provided by peptide-MHC antigen complexes on antigen-presenting cells (APCs) that bind to the T-cell antigen receptor (TCR), which operates in concert with co-stimulatory signals. The dominant co-stimulatory receptor CD28 is constitutively expressed on resting T-cells, whereas Cytotoxic T-lymphocyte antigen (CTLA)-4 is a co-inhibitory receptor expressed on activated T-cells[8, 9]. Their ligands CD80 and CD86 are upregulated upon activation and predominantly expressed on dendritic cells, B cells, and monocytes/macrophages. CTLA-4 is homologous to CD28 and binds CD80-CD86 with much higher affinity than CD28[10]. During an ongoing immune response, CTLA-4 is upregulated and outcompetes CD28 leading to inhibition of T-cell proliferation and reduction of interleukin (IL)-2 production[11]. The importance of the CD28/CTLA-4 pathways has become evident by generating mice genetically deficient in CTLA-4, which develop fatal lymphoproliferative disease with progressive T-cell accumulation in peripheral lymphoid and solid organs[12, 13].

Upon stimulation, CD4⁺ T helper 1 (Th1) effector cells upregulate CD40 ligand and produce interferon (IFN)- γ , responsible for pro-atherogenic cellular chemotaxis and macrophage activation [3], leading to inflammation. Blocking of CD28-CD80/86 mediated co-stimulation by CTLA-4 domain-containing Ig fusion proteins (abatacept), capable of binding CD80/86 with high-affinity can downregulate T-cell proliferation[14] and production of tumor necrosis factor (TNF)- α , IL-2 and IFN- γ in vitro[15]. Abatacept displays little immunogenicity, with <3% of patients developing an antibody response towards abatacept[16] and is used to treat rheumatoid arthritis (RA) patients[17-19]. Although the T-cell[20, 21] and CD28-CD80/CD86 co-stimulation[5, 22] roles have been demonstrated in native atherosclerosis, their contribution to post-interventional remodeling and accelerated atherosclerosis development is unknown, as is the role of CTLA-4. We hypothesized that the CD28-CD80/86 pathway is instrumental in post-interventional T-cell-regulated arterial inflammation and that the co-inhibitory CTLA-4 pathway downregulates these T-cell responses limiting inflammatory-induced intimal thickening.

In the present study, we studied the role of CD4 T-cells and co-stimulatory cellular activation in post-interventional remodeling in both CD4^{-/-} and CD80^{-/-}CD86^{-/-} mice using a well-established mouse model[7, 23]. CTLA-4 contribution to this process is investigated by treating operated C57Bl/6 mice with abatacept. Next, CTLA-4 co-inhibition effects are investigated by studying post-interventional accelerated atherosclerosis development in hypercholesterolemic ApoE3*Leiden mice after both abatacept treatment and systemic CTLA-4 antibody blockade. Our results demonstrate that CD4 T-cells promote post-interventional atherosclerosis in a CD28-CD80/CD86-dependent fashion and that CD4 T-cell CTLA-4 co-inhibition regulates accelerated atherosclerosis development and bears

high potential for prevention of post-revascularization vascular remodeling.

Methods

The authors of this manuscript have certified that they comply with the Principles of Ethical Publishing in the International Journal of Cardiology[24].

Femoral arterial cuff mouse model

All experiments were approved by the Institutional Committee for Animal Welfare of the Leiden University Medical Center and the investigations are in conformation with the Guide for the Care and Use of Laboratory Animals published by the US National Institutes of Health (NIH Publication No. 85-23, revised 1996). We performed multiple *in vivo* studies in which wildtype (C57Bl/6) control, CD4^{-/-} and CD80^{-/-}CD86^{-/-} mice were subjected to femoral artery cuff placement to induce vascular injury and remodeling[7, 23]. Both during surgery and sacrifice, mice were anesthetized with a combination of IP injected Midazolam (5 mg/kg, Roche), Medetomidine (0.5 mg/kg, Orion) and Fentanyl (0.05 mg/kg, Janssen). This surgery produces concentric intimal lesions that affect vessel patency and consist predominately of SMCs and connective tissue and is strongly inflammation-dependent[6].

Abatacept treatment

Treatment with 10 mg/kg abatacept at the time of surgery through intraperitoneal injection, similarly to that used in clinical treatment of RA and in earlier murine studies was given to evaluate the role of the CD28-CD80/CD86 co-stimulatory pathway in this process.

Vascular wall lesion analysis

In these vascular segments, inflammatory cell adhesion, infiltration, intimal thickening and lesion composition were assessed using histology, morphometry and immunohistochemistry (IHC), as described previously[23]. Samples were stained with hematoxylin-phloxine-saffron and specific vessel wall composition was visualized for elastin, collagen and with antibodies against leukocytes, macrophages, vascular SMCs, CD3 and CD4 T-cells, matrix metalloproteinase-9 and CTLA-4. This analysis was repeated in operated hypercholesterolemic ApoE3*Leiden mice to assess accelerated atherosclerotic lesion phenotype.

Flow cytometry

Leukocyte subsets were characterized using flow cytometry in spleen and draining inguinal lymph nodes[25]. These were harvested and single-cell suspensions were prepared by mincing the tissue through a 70- μ m cell strainer. For cell surface staining, cells were resuspended in staining buffer and incubated with fluorescent conjugated antibodies. After washing and resuspension in staining buffer, cells were acquired using a BD LSRII flow cytometer and data was analyzed using FlowJo software. Cells were stained with fluorochrome-conjugated monoclonal antibodies specific for CD3, CD4, CD44, CD25, CD62L CD69, CD127, CTLA-4, and KLRG1 and staining for intracellular FoxP3 was performed using the FoxP3 staining set. 7-AAD was used to exclude dead cells.

Biochemical analysis

Plasma IFN- γ and IL-10 levels were determined using ELISA were performed according to the manufacturer's instructions and total plasma cholesterol was measured enzymatically.

Functional CTLA-4 blockade

CTLA-4 co-inhibition effects on accelerated atherosclerosis development was confirmed using anti-CTLA-4 blocking antibodies[11]. Anti-murine CTLA-4 IgG antibodies used in this study were isolated from supernatants from the 9H10 hybridoma line. Antibody concentration was performed using an artificial kidney and the concentrated antibodies were

protein G-purified. CTLA-4 blockade in ApoE3*Leiden mice was induced by injecting animals IP with 200 µg of anti-mouse CTLA-4 or control IgG once every 2 days, starting at the time of surgery.

All materials and methods are described in detail in the supplemental material.

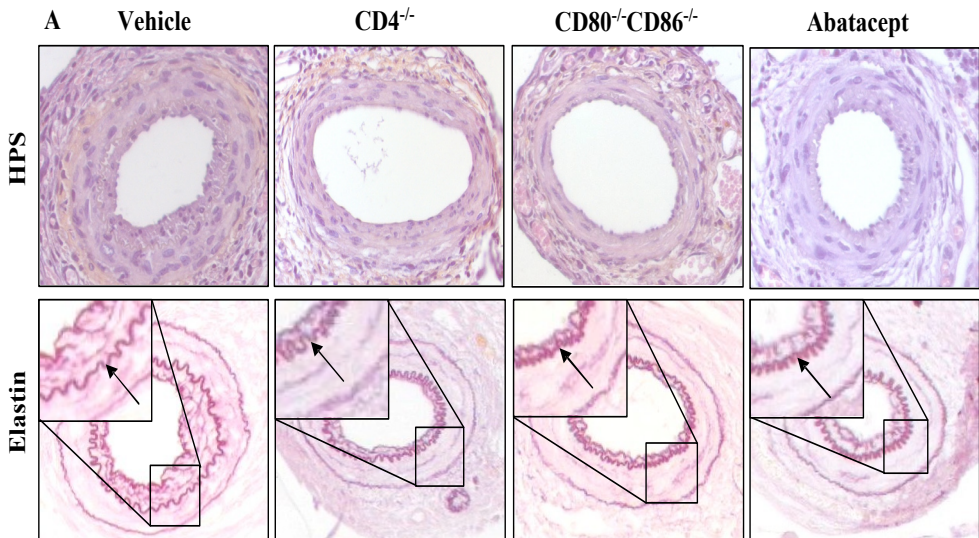
Results

CD4 T-cells and CD80/86 mediated-co-stimulation are critically involved in post-interventional vascular remodeling

To investigate the contribution of CD4 T-cells and the CD28/CTLA-4-CD80/86 pathways to vascular remodeling, we placed femoral artery cuffs in control, CD4^{-/-} and CD80^{-/-}CD86^{-/-} mice and animals receiving abatacept-treatment. Murine body weights were similar at surgery and sacrifice (table 1). 21d after surgery lesions were stained with hematoxylin-phloxine-saffron (HPS) to visualize overall vascular wall morphology (fig 1A), and revealed that untreated animals, compared to CD4^{-/-}, CD80^{-/-}CD86^{-/-} and abatacept-treated mice, developed concentric intimal thickening leading to luminal stenosis. Weigert's elastin staining was performed to allow morphometric analysis using the elastic laminae to assess vessel layer surface area and remodeling. Analysis showed that intimal thickening was reduced by 72.1% (p=0.006) in CD4^{-/-} mice, by 64.2% (p=0.015) in CD80^{-/-}CD86^{-/-} mice and by 58.5% (p=0.029) in abatacept-treated animals compared to controls (fig 1B).

Since the total surface area (µm²) of the media was similar in all groups (fig 1B), absence of CD4 T-cells and CD80/86 co-stimulatory molecules and abatacept-treatment led to reduced intima / media ratio with respectively 70.0% (p=0.011), 66.4% (p=0.005) and 55.3% (p=0.047, fig 1C). Additionally, the percentage luminal stenosis was reduced in these groups by 48.7% (p=0.042), 47.7% (p=0.031) and 49.9% (p=0.036) respectively (fig 1D). These results indicate a reduced inflammatory-driven remodeling process the injured arterial segments. The total vessel and luminal areas (µm²) were not different between all groups (fig 1A,C). These data indicate an important role of CD4 T-cells and the CD28/CTLA-4-CD80/CD86 co-stimulatory axis in post-interventional vascular remodeling.

Figure 1



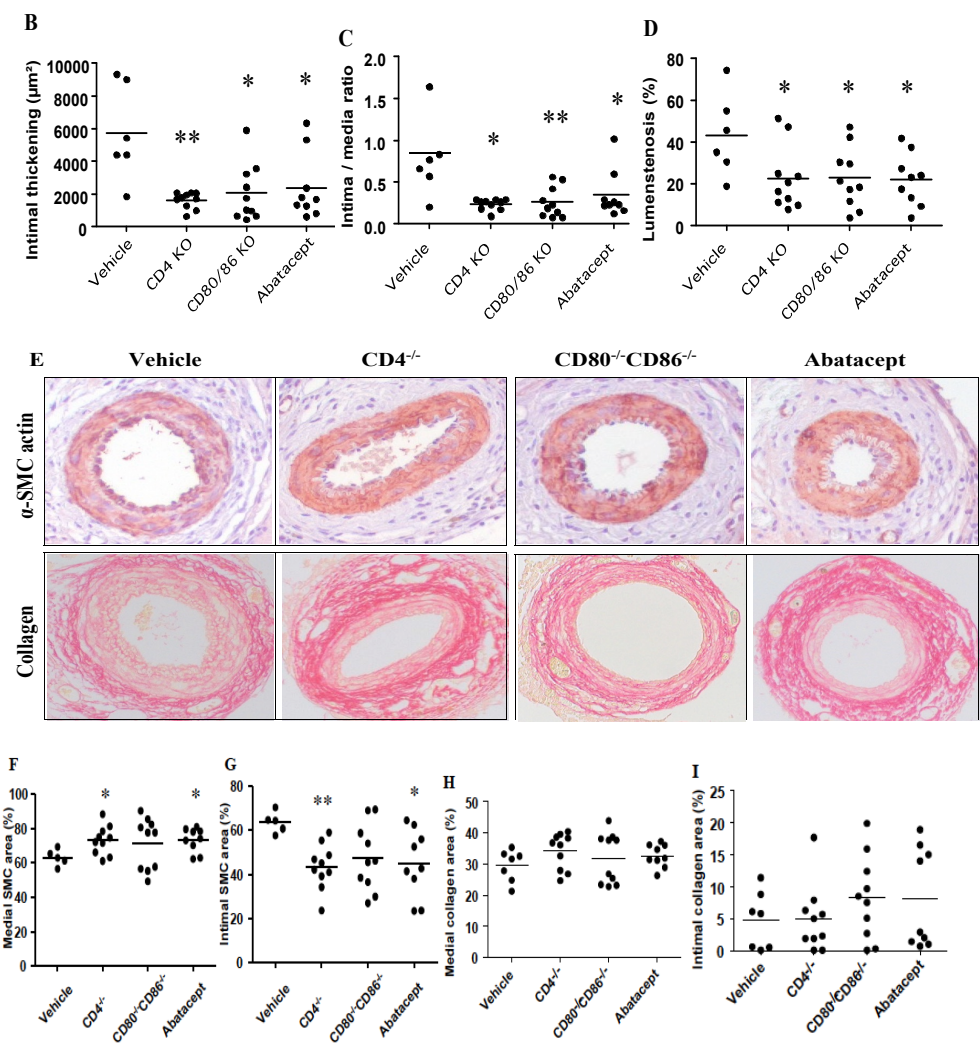
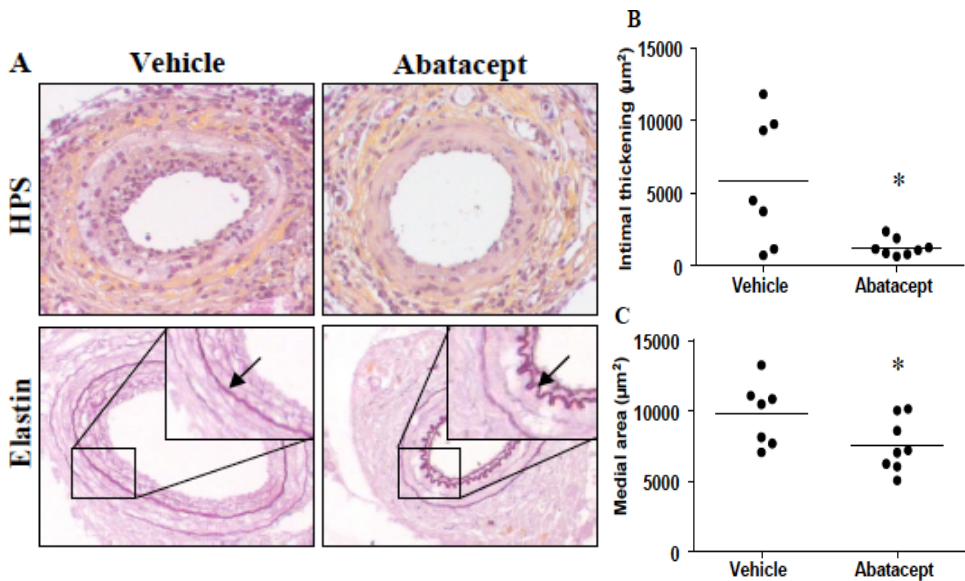


Figure 1. Reduced vascular remodeling in CD4^{-/-} and CD80^{-/-}CD86^{-/-} and abatacept-treated mice. Representative cross-sections of cuffed-femoral arteries of CD4^{-/-}CD80^{-/-}CD86^{-/-} and abatacept-treated mice (A) after 21d (hematoxylin-phloxine-saffron (HPS) and Weigert's elastin staining, 80x, arrows indicate internal elastic laminae). Quantification of intimal thickening (µm²) (B), intima / media ratio (C) and luminal stenosis (%) (D). Representative cross-sections of cuffed-femoral arteries of CD4^{-/-}CD80^{-/-}CD86^{-/-} and abatacept-treated mice (E) after 21d (α-SMC actin and Sirius Red collagen staining, 80x). Quantification of relative medial SMC (F) and collagen (G) areas (%) and intimal SMC (H) and collagen (I) areas (%). Horizontal bars indicate median values, n=10. * p<0.05, ** p<0.01.

CD4^{-/-}, CD80^{-/-}CD86^{-/-} and abatacept-treated mice display an altered lesion composition during post-interventional vascular remodeling

Lesion composition was analyzed using IHC, which showed larger relative areas (to the total vessel layer surface area) of α -SMC actin in the media by 15.8% ($p=0.028$) in CD4^{-/-} and 16.1% ($p=0.028$) in abatacept-treated mice (fig 1E), whilst α -SMC actin⁺ relative area in the intima was significantly decreased compared to controls by 31.6% ($p=0.001$) and 29.3% ($p=0.019$) respectively (fig 1G). Both medial (fig 1H) and intimal (fig 1I) relative collagen areas (%) were similar between groups, reflecting absolute α -SMC actin⁺ and collagen areas (μm^2) in the media (fig IIA,C). Total α -actin⁺ SMC area (μm^2) in the intima was only reduced in CD4^{-/-} mice by 59.7% ($p=0.008$) whilst collagen area (μm^2) remained unchanged (fig IIB,D) with limited CD45 leukocyte and CD4 T-cell infiltration in the vascular layers in control sections (fig IIE), indicating an indirect but clear effect of CD4 T-cells upon vascular SMC proliferation and migration.



legend figure 2; next page

Abatacept prevents accelerated atherosclerosis

The contribution of the CD28-CD80/CD86 co-stimulatory pathway to accelerated atherosclerosis development was tested in a preclinical model of accelerated atherosclerosis development in Western-type diet-fed hypercholesterolemic ApoE3*Leiden mice using abatacept as therapeutic intervention strategy. Plasma cholesterol concentrations (12.1 ± 3.1 mmol/L) were similar in all groups throughout this study (table 2). Vehicle and abatacept-treated ApoE3*Leiden mice were sacrificed 14d after arterial cuff placement and accelerated atherosclerotic lesions were stained with HPS to visualize overall vascular morphology (fig 2A). This revealed that vehicle-treated animals developed concentric intimal thickening and luminal stenosis, consisting of connective tissue with profound cellular infiltration which was absent in abatacept-treated mice. Quantitative analysis of cuffed arteries stained with Weigert's elastin identified reduced intimal thickening after abatacept treatment with 78.1% ($p=0.040$, fig 2B). Abatacept also decreased absolute medial surface area (μm^2) by 22.9%

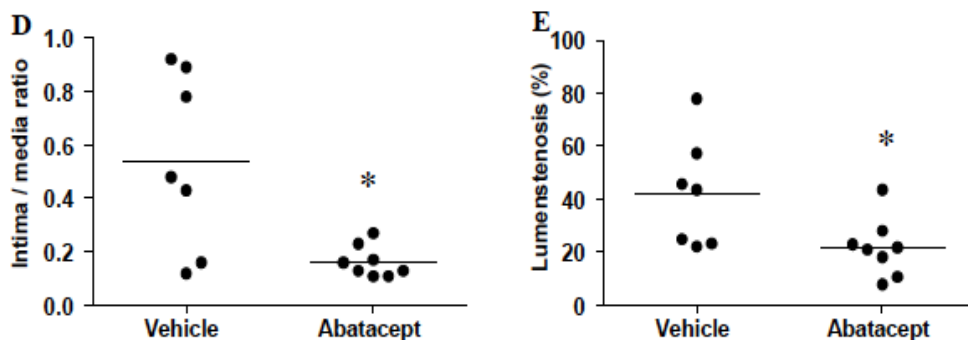


Figure 2. Abatacept prevents accelerated atherosclerosis in hypercholesterolemic mice. Representative cross-sections of cuffed-femoral arteries of hypercholesterolemic ApoE3*Leiden mice following vehicle or abatacept-treatment (A) after 14d (HPS and Weigert's elastin staining, 80x, arrows in inserts indicate internal elastic laminae). Quantification of intimal thickening (μm^2) (B), medial area (μm^2) (C), intima / media ratio (D) and luminal stenosis (%) (E). Horizontal bars indicate median values, $n=10$. * $p<0.05$.

($p=0.040$, fig 2C), and intima / media ratio by 69.5% ($p=0.037$, fig 2D). Furthermore, luminal stenosis percentage was reduced by 48.2% ($p=0.021$, fig 2E), identifying a potent role for CTLA-4 co-inhibition controlling inflammatory post-interventional vascular remodeling. The total vessel and luminal areas (μm^2) were similar in the abatacept-treated group, although a trend towards reduced total vessel area by 34.6% was observed ($p=0.094$) (fig IIIA, B).

Abatacept positively affects accelerated atherosclerotic lesion composition

Lesion composition was analyzed using IHC to allow arterial wall inflammatory phenotype assessment (fig 3A). Abatacept-treatment produced an altered lesion composition with a reduced inflammatory phenotype. Abatacept reduced leukocyte and macrophage/foam cell fractions (% of all cells) in the media by 64.0% ($p=0.043$, fig 3B) and 72.1% respectively ($p=0.003$, fig 3D) and intima by 73.9% ($p=0.009$, fig 3C) and 30.5% ($p=0.048$, fig 3E), respectively. Abatacept-treatment also led to a comparable medial ($p=0.602$, fig 3F) and 29.8% ($p=0.042$, fig 3G) increased intimal α -SMC actin surface area (%), although absolute intimal SMC area (μm^2) was not increased ($p=0.743$, fig IVA), similarly to the tunica media ($p=0.888$, fig IVB). Whereas limited CD3 T-cells and matrix metalloproteinase-9 expressing cells could be detected in the tunica intima (fig 3H, I), corresponding with a similar collagen quantity in the intima, abatacept reduced these cells in the tunica adventitia by 65.9% ($p<0.0001$, fig 3J) and 64.7% ($p<0.0001$, fig 3K) respectively. T-cell CTLA-4 and CD4 colocalized expression was identified using IHC in the injured arterial segments of vehicle-treated ApoE3*Leiden mice and was absent in uninjured arteries, but occurred 3d after surgery and could still be observed 14d after injury, indicating continuing local arterial T-cell activation throughout the remodeling process and accelerated atherosclerosis development (fig 3L).

Figure 3

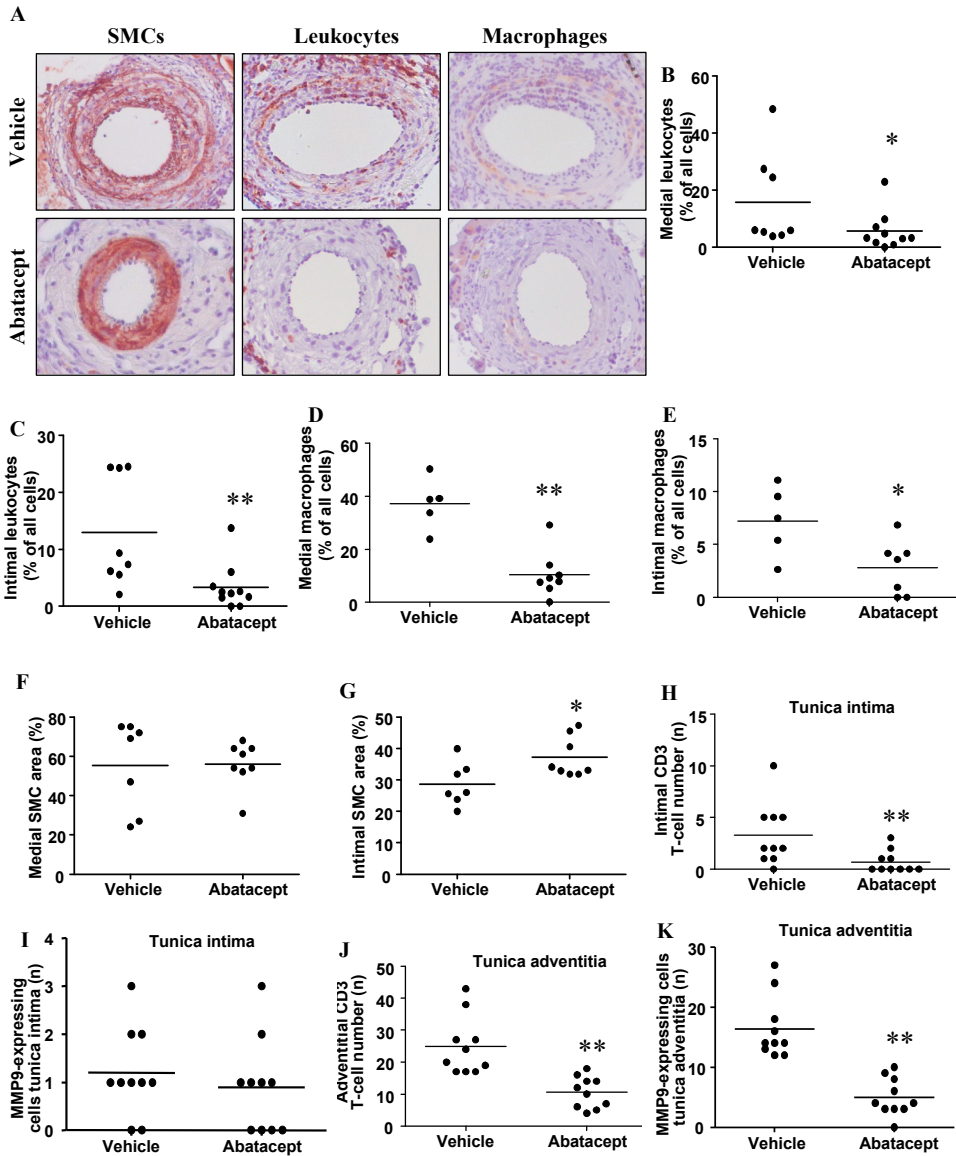
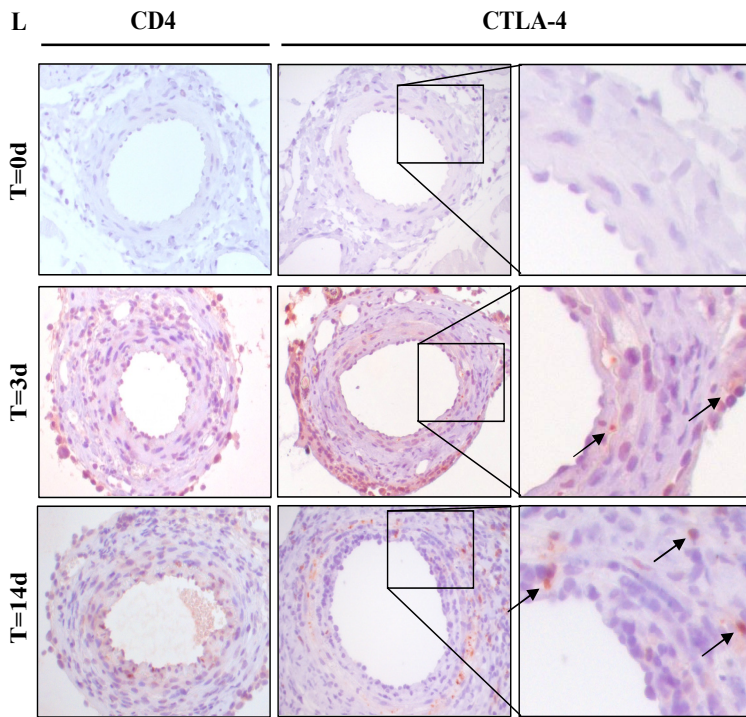


Figure 3 (next page). Abatacept positively affects accelerated atherosclerotic lesion composition.

Representative cross-sections of cuffed-femoral arteries of ApoE3*Leiden mice following vehicle or abatacept-treatment (A) after 14d (leukocyte, macrophage and α -SMC actin staining, 80x). Quantification of relative medial leukocyte (B), macrophage (D) and SMC (F) areas (%) and intimal leukocyte (C), macrophage (E) and SMC (G) areas (%) and intimal CD3 (n) (H) and MMP-9 (n) (I), as well as adventitial CD3 (n) (J) and MMP-9 cells (n) (K). Horizontal bars indicate median values, n=10. * $p < 0.05$, ** $p < 0.01$. (L) T-cell CTLA-4 and CD4 expression throughout the vessel wall of ApoE3*Leiden mice in time before and 3d and 14d after surgery (CTLA-4 and CD4 staining, 80x, arrows in inserts indicate positive staining).

Figure 3



Abatacept prevents systemic CD4 T-cell activation during accelerated atherosclerosis

To examine the role of CTLA-4 co-inhibition upon T-cell activation involved in accelerated atherosclerosis development, CD4 T-cell numbers and T-cell activation status were assessed. The markers Killer cell lectin-like receptor subfamily G member (KLRG)-1, Programmed Death (PD)-1, CD69 and CTLA-4 were used to analyze T-cell activation in the splenic reservoir and draining inguinal lymph nodes of mice 14d after surgery.

Absolute CD4 ($p=0.557$, fig 4A) splenic T-cell numbers were similar in vehicle and abatacept-treated mice, as were total splenic cell contents (absolute cells) and percentages CD4 T-cell fractions (fig VA,B). Abatacept reduced splenic CD4 T-cells fractions expressing CD69 by 61.9% ($p=0.008$, fig 4B), PD1 by 49.4% ($p=0.041$, fig 4C), KLRG1 by 47.4% ($p=0.032$, fig 4E), and CTLA-4 by 47.0% ($p=0.016$, fig 4F). These data indicate that abatacept strongly and consistently prevented systemic CD4 T-cell activation, thereby reducing accelerated atherosclerotic lesion formation. In contrast to the reduced severity of inflammatory vascular remodeling, co-inhibition with abatacept treatment also reduced fractions of CD4+CD25+FoxP3+ regulatory T-cells by 33.3% ($p=0.016$, fig 4H) in the spleen. No significant differences in the percentages of naive (CD62L+ CD44-), central-

memory (CD62L+ CD44+) or effector-memory (CD62L- CD44+) CD4 T-cell populations were observed ($p>0.05$, fig VC-F).

Contrary to significant reduction of activated CD4 T-cells in the spleen after abatacept-treatment, no evidence of T-cell activation in draining inguinal lymph nodes could be found (fig VIA-G), despite adequate cell number isolation for analysis.

Figure 4

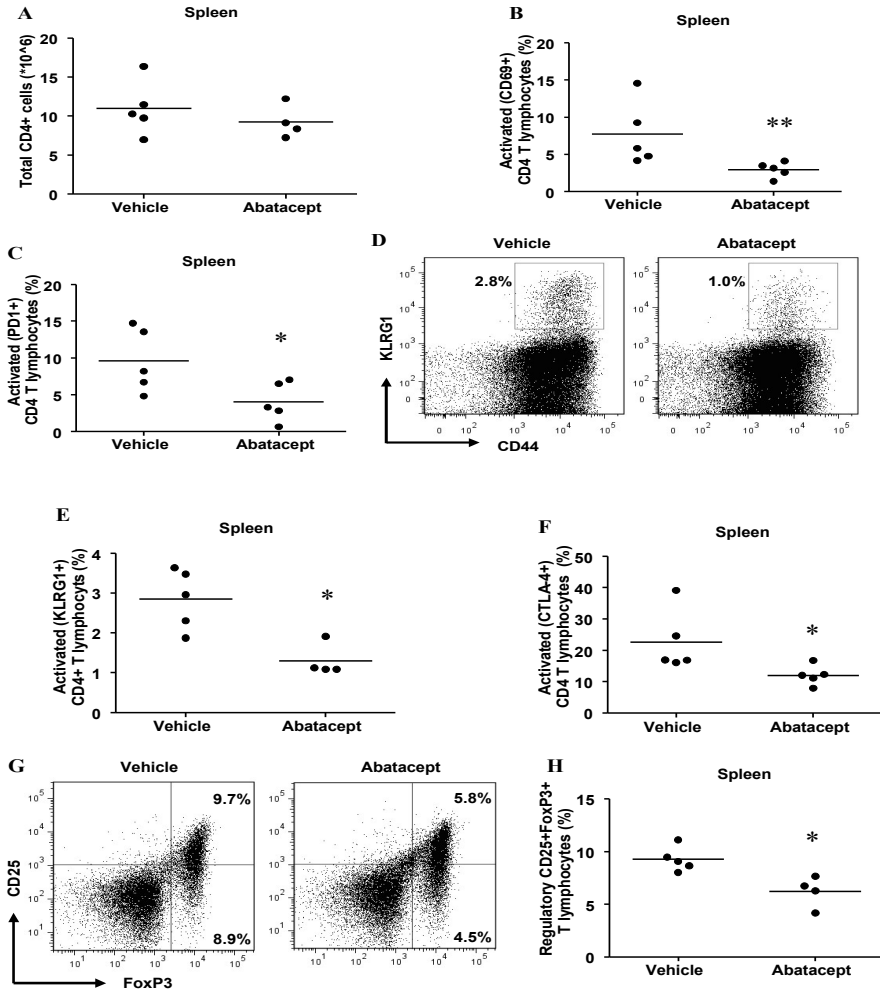


Figure 4. Abatacept prevents systemic CD4 T-cell activation in ApoE3*Leiden mice. Abatacept did not affect total CD4 splenic T-cell count (absolute cells) 14d after surgery (A). T-cells were analyzed using multiparametric flow cytometry and gated for 7AAD-, CD3+ and CD4+ markers and subsequently for either KLRG1+, PD1+, CD69+, CTLA-4+ or CD25+ and FoxP3+ expression and are displayed in dot plots (D and G). Abatacept reduced CD69+ (B), PD1+ (C), KLRG1+ (E) and CTLA-4+ (F) activated CD4 T-cell fractions (%), together with CD25+FoxP3+ regulatory (H) CD4 T-cell fractions (%). Horizontal bars indicate median values, $n=5$. * $p<0.05$, ** $p<0.01$.

Abatacept affects systemic cytokine levels during accelerated atherosclerosis

Contribution of activated T-cell fractions to vascular remodeling severity is supported by the positive correlation ($R^2=0.61$, $p=0.002$) between $KLRG1^+$ $CD4^+$ T-cells (%) and intimal thickening (μm^2) (fig 5A). Interestingly, the ratio between regulatory and effector helper T-cells remained unchanged in treated animals (fig 5B). Affected systemic $CD4$ T-cell activation in abatacept-treated mice was investigated by $\text{IFN-}\gamma$ and IL-10 measurements in plasma at 14d. Hypercholesterolemic control animals contained an elevated plasma concentration $\text{IFN-}\gamma$ of 43.2 ± 12.1 pg/ml, while abatacept-treatment reduced the $\text{IFN-}\gamma$ concentration to non-detectable levels ($p=0.00023$, fig 5C) after vascular injury. In contrast, plasma IL-10 was significantly elevated from 4.5 ± 2.0 pg/ml in controls to 23.7 ± 7.1 pg/ml ($p=0.012$, fig 5D) in abatacept-treated mice. Together, these cytokines indicate that abatacept reduced systemic inflammation.

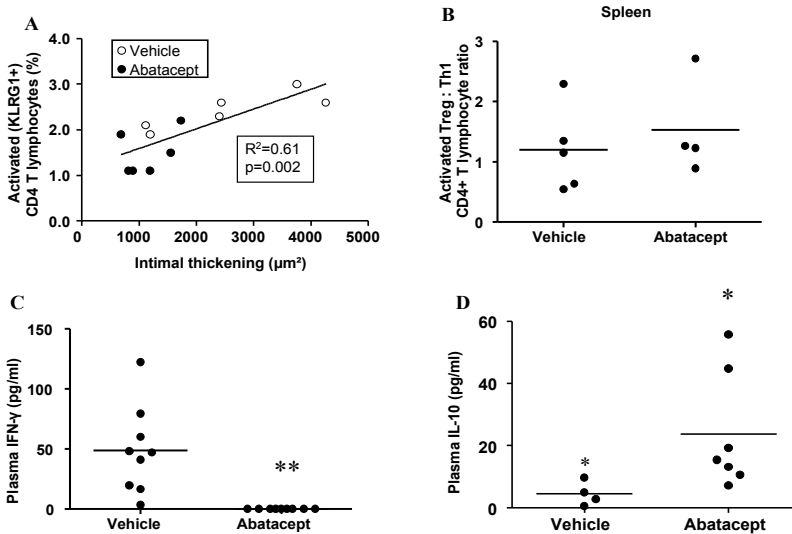


Figure 5. Profound $CD4$ T-cell contribution to post-interventional accelerated atherosclerosis development. (A) Positive correlation between $KLRG1^+$ $CD4$ T-cell fractions (%) and intimal thickening (μm^2) ($n=6$). Abatacept did not affect $CD4$ regulatory T-cell: effector T-cell ratio (B). Plasma $\text{IFN}\gamma$ (pg/ml) was reduced after 14d following abatacept-treatment (C), whilst plasma IL-10 (pg/ml) was upregulated (D). Horizontal bars indicate median values, $n=10$. n.d. non-detectable. * $p<0.05$, ** $p<0.01$.

CTLA-4 blockade exacerbates accelerated atherosclerosis development.

To confirm the anti-inflammatory role of CTLA-4 co-inhibition in accelerated atherosclerotic lesion development, we analyzed injured femoral lesions of mice undergoing CTLA-4 blockade using antibodies. HPS staining (fig 6A) revealed that CTLA-4 blocking provoked increased accelerated atherosclerosis development and decreased luminal patency. Weigert's elastin staining and morphometric vessel wall analysis confirmed increased intimal thickening by 66.7% compared to control mice receiving non-specific anti- β gal IgG ($p=0.008$, fig 6B). Due to a comparable medial area between groups, the intima / media ratio was increased by 69.3% ($p=0.010$, fig 6C). Finally, CTLA-4 blockade increased relative luminal stenosis by 86.3% ($p=0.004$, fig 6D) and compromised absolute luminal area by 56.9% ($p=0.010$, fig 6E).

Total vessel and medial areas (μm^2) were both not different between groups (fig VIIA,B). Together, these results indicate a strong increase of inflammatory induced post-interventional vascular remodeling during functional blockade of CTLA-4 function.

Accelerated atherosclerotic lesion phenotype is preserved during CTLA-4 blockade

Lesion composition was analyzed using IHC to assess arterial wall inflammatory phenotype (fig VIIIA). Although CTLA-4 blockade enhanced accelerated atherosclerosis development, no lesion composition differences were observed compared to controls. There were similar leukocyte and macrophage/foam cell fractions (% of all cells) in the media ($p=0.414$, fig VIIIB; $p=0.097$, fig VIIID, respectively) and intima ($p=0.142$, fig VIIIC; $p=0.769$, fig VIIIE, respectively). CTLA-4 blockade also led to a comparable medial ($p=0.728$, fig VIIIF) and intimal ($p=0.258$, fig VIIIG) α -SMC actin surface areas (%). IHC revealed that functional CTLA-4 blockade led to a significant increase of CD3+ T-cells (n) in both the tunica intima by 200.0% ($p=0.0001$, fig 6F) and in the tunica adventitia by 241.4% ($p=0.0003$, fig 6G) compared to controls.

Figure 6

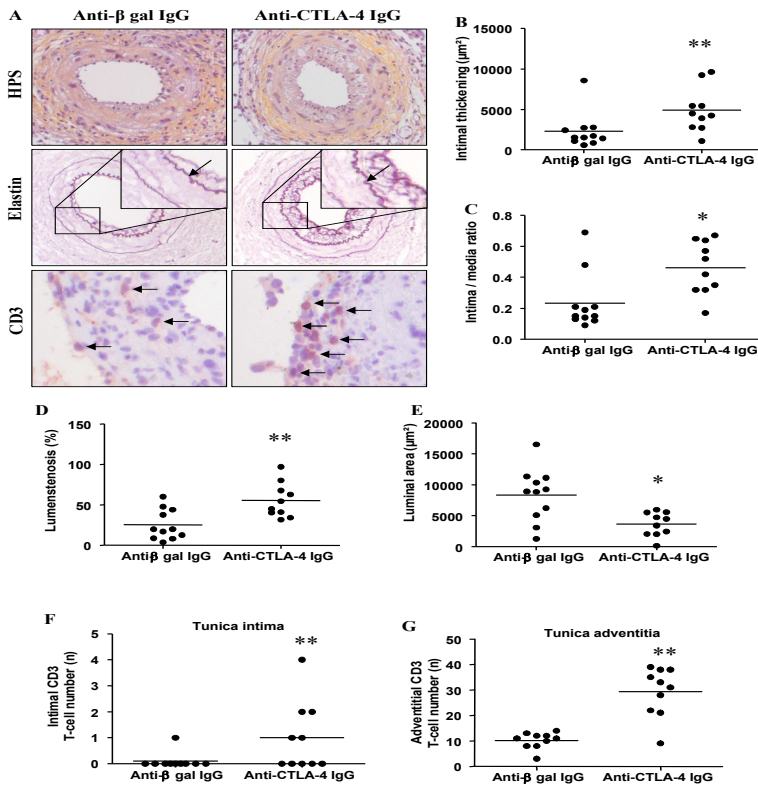


Figure 6. CTLA-4 blockade exacerbates accelerated atherosclerosis development. Representative cross-sections of cuffed-femoral arteries of hypercholesterolemic ApoE3*Leiden mice following isotype antibody or anti-CTLA-4 IgG-treatment (A) after 14d (HPS, Weigert's elastin and CD3 staining, 80-160x, arrows in inserts indicate internal elastic laminae and CD3+ T-cells). Quantification of intimal thickening (μm^2) (B), intima / media ratio (C), lumen stenosis (%) (D) and luminal area (μm^2) (E). Quantification of intimal CD3 (n) (F) and adventitial CD3 (n) (G) cells. Horizontal bars indicate median values, n=10. * $p < 0.05$, ** $p < 0.01$.

Discussion

This study demonstrates an important role for T-cell co-stimulation by CD28-CD80/CD86 and the negative regulator CTLA-4 in post-interventional intimal hyperplasia and accelerated atherosclerosis development. We show that CD4^{-/-} and CD80^{-/-}CD86^{-/-} mice develop significantly smaller SMC-rich lesions following vascular injury and that infiltrated T-cells express CTLA-4 early after surgery. Therapeutic inhibition of CD28-CD80/86 function by abatacept significantly prevented accelerated atherosclerosis development in hypercholesterolemic ApoE3*Leiden mice together with reduced IFN- γ plasma concentration (fig 5C), probably due to reduced CD4 T-cell activation. The role of CTLA-4 co-inhibition was confirmed using blocking antibodies which led to profound increased vascular lesion size.

The role of CD4 T-cells and CD80/86-mediated co-stimulation during native atherosclerosis development[26, 27] has been investigated, but their contribution to post-interventional vascular remodeling remained until this study unknown. In ApoE^{-/-} mice, T-cells have been shown to be important in early native atherosclerotic lesion progression, but not its initiation[27, 28]. We provide evidence for activated CD4 T-cell involvement in the early stage of vascular remodeling following intervention. As of yet, it remains to be investigated towards which antigen the T-cell response is raised. Nevertheless, this form of accelerated atherosclerosis develops within months and in a localized area, opening the perspective for (local) T-cell-directed treatment directly after percutaneous coronary interventions.

CTLA-4 is expressed on activated effector T-cells and constitutively on regulatory T-cells, while both CD80 and CD86 are primarily expressed on activated dendritic cells, B cells, monocytes/macrophages, which play an important role in native atherosclerosis development [4]. T-cell-mediated immune responses are initiated in lymphoid tissues where they are activated by APCs presenting two concomitant signals: an antigenic signal provoked by specific MHC-antigen peptide complexes that bind to the TCR and a co-stimulatory signal induced by CD80 and CD86 molecules that interact with CD28 expressed on all T-cells. Together, TCR and CD28 signals lead to an inflammatory and pro-atherogenic response. We show that abatacept-treatment was able to prevent this systemic activation by reducing the number of activated CD4 T-cells fractions in the spleen as evidenced by the activation markers KLRG1, PD1, CD69 and CTLA-4. Since vascular injury occurs locally, profound T-cell activation was expected to occur in draining lymph nodes. However, only low fractions of activated T-cells were identified in these lymph nodes (fig VIA-G) whilst analysis of splenic T-cell fractions revealed significant activation (fig 4A-F). We cannot exclude effects of abatacept in other lymph nodes, but these are unlikely to supersede the effects in the analyzed primary draining lymph nodes.

Although abatacept effects on accelerated atherosclerosis are mediated through systemically reduced T-cell activation, it is not clear to which extent effects on specific T-cell subsets contributed to the lesion development. Buono et al.[22] showed that CD80^{-/-}CD86^{-/-}LDL-receptor (r)^{-/-} mice developed decreased atherosclerotic lesions compared to LDL-r^{-/-} mice through reduced CD4 Th1 cell activation by CD80/86 on APCs. Unlike activated effector T-cells, regulatory CD25⁺ FoxP3⁺ T-cells constitutively express CTLA-4[29] and this is essential for their suppressive function[30, 31]. Ait-Oufella et al.[5] demonstrated the vital role of regulatory T-cells in native atherosclerosis development, using irradiated LDL-r^{-/-} mice receiving reconstituted bone-marrow from CD80^{-/-}CD86^{-/-} mice which developed increased atherosclerotic lesions through strongly reduced splenic fractions of regulatory CD25⁺FoxP3⁺ T-cells. Therefore, it is possible that abatacept, may have inhibitory effects

on accelerated atherosclerosis development through regulatory T-cell activation status modulation. However, Platt et al. showed that abatacept prevented effector T-cell activation, although effects on regulatory T-cell status in this murine arthritis model were not studied[14]. This study shows reduced fractions of both activated Th1 and regulatory T-cells in hypercholesterolemic ApoE3*Leiden mice receiving abatacept. Since the Th1: regulatory T-cell ratio remained unchanged (fig 5B), this strongly suggests that therapeutic effects of abatacept can primarily be attributed to directly reduced activation of Th1 T-cells and not to Th1 suppression through regulatory T-cells, reflected by an elevated concentration of IL-10 (fig 5D) in plasma (baseline 14.4 ± 2.3 pg/ml)[23] and reduced concentration of IFN- γ (fig 5C) (baseline 9.8 ± 4.6 pg/ml)[23], similarly to that observed following IL-12 vaccination by Hauer et al. which downregulated the Th1 immune response and led to attenuation of native atherosclerosis development[32].

These findings are based upon results from animal studies and cannot be automatically extrapolated to the clinical situation. However, they do provide further insight into the role of T-cell co-stimulatory pathways when viewed in the light of recent exiting data by Dumitriu et al.[33] concerning the role of CD28-/- activated T-cells and regulatory T-cells during acute coronary syndromes (ACS) in humans, as well as carotid stenosis[34], unstable angina[35, 36] and atherosclerosis development in both humans[37] and animals in general[38]. The function relevance of CTLA-4 expression for human peripheral T-cell has previously been shown by Hoff et al.[39] and Yi-qun et al.[40], in which CTLA-4 blockade was found to both determine CD28null T-cell and memory T-cell longevity and responsiveness (e.g. IL-2 production). The potential of co-stimulatory-based T-cell-directed intervention strategies in the clinical situation is further enhanced by the findings of Bluestone et al.[41] and Körmeny et al.[42], in which functional CTLA-4 blockade functionally affected circulating regulatory T-cells in patients undergoing kidney transplantation and peripheral Th cells in rheumatoid arthritis patients. This study demonstrated the effectiveness of modulation of co-stimulatory receptors against post-interventional atherosclerotic vascular remodeling in mice, thus greatly enhancing the potential of a similar therapeutic approach to improve the survival of ACS patients.

In conclusion, this study shows that T-cell co-stimulation through the CD28-CD80/86 pathway plays a vital role in post-interventional accelerated atherosclerosis development and is strongly negatively regulated by CTLA-4 co-inhibition. These results may have important clinical implications. Immune-mediated interventions directed towards therapeutically controlling the inflammatory T-cell response such as abatacept are widely applied in other immune (e.g. rheumatoid) disorders and could now be used in an early phase following interventions such as revascularization or bypass grafting procedures in patients to prevent subsequent vascular remodeling. This application could be accelerated by the availability of abatacept as a currently clinically approved T-cell specific therapeutic agent.

Disclosures None.

Reference List

1. Ross R. Atherosclerosis--an inflammatory disease. *N Engl J Med* 1999;340:115-26.
2. Hansson GK, Hermansson A. The immune system in atherosclerosis. *Nat Immunol* 2011;12:204-12.
3. Hansson GK. Inflammation, atherosclerosis, and coronary artery disease. *N Engl J Med* 2005;352:1685-95.
4. Weber C, Zernecke A, Libby P. The multifaceted contributions of leukocyte subsets to atherosclerosis: lessons from mouse models. *Nat Rev Immunol* 2008;8:802-15.

5. Ait-Oufella H, Salomon BL, Potteaux S, Robertson AK, Gourdy P, Zoll J et al. Natural regulatory T cells control the development of atherosclerosis in mice. *Nat Med* 2006;12:178-80.
6. Pires NM, Schepers A, van der Hoeven BL, de Vries MR, Boesten LS, Jukema JW et al. Histopathologic alterations following local delivery of dexamethasone to inhibit restenosis in murine arteries. *Cardiovasc Res* 2005;68:415-24.
7. Lardenoye JH, Delsing DJ, de Vries MR, Deckers MM, Princen HM, Havekes LM et al. Accelerated atherosclerosis by placement of a perivascular cuff and a cholesterol-rich diet in ApoE*3Leiden transgenic mice. *Circ Res* 2000;87:248-53.
8. Gotsman I, Sharpe AH, Lichtman AH. T-cell costimulation and coinhibition in atherosclerosis. *Circ Res* 2008;103:1220-31.
9. Alegre ML, Frauwirth KA, Thompson CB. T-cell regulation by CD28 and CTLA-4. *Nat Rev Immunol* 2001;1:220-8.
10. Maszyra F, Hoff H, Kunkel D, Radbruch A, Brunner-Weinzierl MC. Diversity of clonal T cell proliferation is mediated by differential expression of CD152 (CTLA-4) on the cell surface of activated individual T lymphocytes. *J Immunol* 2003;171:3459-66.
11. Krummel MF, Allison JP. CD28 and CTLA-4 have opposing effects on the response of T cells to stimulation. *J Exp Med* 1995;182:459-65.
12. Chambers CA, Sullivan TJ, Allison JP. Lymphoproliferation in CTLA-4-deficient mice is mediated by costimulation-dependent activation of CD4+ T cells. *Immunity* 1997;7:885-95.
13. Chambers CA, Cado D, Truong T, Allison JP. Thymocyte development is normal in CTLA-4-deficient mice. *Proc Natl Acad Sci U S A* 1997;94:9296-301.
14. Platt AM, Gibson VB, Patakas A, Benson RA, Nadler SG, Brewer JM et al. Abatacept limits breach of self-tolerance in a murine model of arthritis via effects on the generation of T follicular helper cells. *J Immunol* 2010;185:1558-67.
15. Webb LM, Walmsley MJ, Feldmann M. Prevention and amelioration of collagen-induced arthritis by blockade of the CD28 co-stimulatory pathway: requirement for both B7-1 and B7-2. *Eur J Immunol* 1996;26:2320-8.
16. Fiocco U, Sfriso P, Oliviero F, Pagnin E, Scagliori E, Campana C et al. Co-stimulatory modulation in rheumatoid arthritis: the role of (CTLA4-Ig) abatacept. *Autoimmun Rev* 2008;8:76-82.
17. Ruderman EM, Pope RM. The evolving clinical profile of abatacept (CTLA4-Ig): a novel co-stimulatory modulator for the treatment of rheumatoid arthritis. *Arthritis Res Ther* 2005;7 Suppl 2:S21-S25.
18. Ruderman EM, Pope RM. Drug Insight: abatacept for the treatment of rheumatoid arthritis. *Nat Clin Pract Rheumatol* 2006;2:654-60.
19. Kremer JM, Westhovens R, Leon M, Di GE, Alten R, Steinfeld S et al. Treatment of rheumatoid arthritis by selective inhibition of T-cell activation with fusion protein CTLA4Ig. *N Engl J Med* 2003;349:1907-15.
20. Mallat Z, Taleb S, Ait-Oufella H, Tedgui A. The role of adaptive T cell immunity in atherosclerosis. *J Lipid Res* 2009;50 Suppl:S364-S369.
21. Zhou X, Robertson AK, Hjerpe C, Hansson GK. Adoptive transfer of CD4+ T cells reactive to modified low-density lipoprotein aggravates atherosclerosis. *Arterioscler Thromb Vasc Biol* 2006;26:864-70.
22. Buono C, Pang H, Uchida Y, Libby P, Sharpe AH, Lichtman AH. B7-1/B7-2 costimulation regulates plaque antigen-specific T-cell responses and atherogenesis in low-density lipoprotein receptor-deficient mice. *Circulation* 2004;109:2009-15.
23. Ewing MM, de Vries MR, Nordzell M, Pettersson K, de Boer HC, van Zonneveld AJ et al. Annexin A5 therapy attenuates vascular inflammation and remodeling and improves endothelial function in mice. *Arterioscler Thromb Vasc Biol* 2011;31:95-101.
24. Coats AJ, Shewan LG. Statement on authorship and publishing ethics in the International Journal of Cardiology. *Int J Cardiol* 2011;153:239-40.

25. Arens R, Loewendorf A, Redeker A, Sierro S, Boon L, Klenerman P et al. Differential B7-CD28 costimulatory requirements for stable and inflationary mouse cytomegalovirus-specific memory CD8 T cell populations. *J Immunol* 2011;186:3874-81.
26. Mallat Z, Ait-Oufella H, Tedgui A. Regulatory T cell responses: potential role in the control of atherosclerosis. *Curr Opin Lipidol* 2005;16:518-24.
27. Zhou X, Robertson AK, Rudling M, Parini P, Hansson GK. Lesion development and response to immunization reveal a complex role for CD4 in atherosclerosis. *Circ Res* 2005;96:427-34.
28. Robertson AK, Hansson GK. T cells in atherogenesis: for better or for worse? *Arterioscler Thromb Vasc Biol* 2006;26:2421-32.
29. Vignali DA, Collison LW, Workman CJ. How regulatory T cells work. *Nat Rev Immunol* 2008;8:523-32.
30. Sakaguchi S. Naturally arising Foxp3-expressing CD25+CD4+ regulatory T cells in immunological tolerance to self and non-self. *Nat Immunol* 2005;6:345-52.
31. Salomon B, Lenschow DJ, Rhee L, Ashourian N, Singh B, Sharpe A et al. B7/CD28 costimulation is essential for the homeostasis of the CD4+CD25+ immunoregulatory T cells that control autoimmune diabetes. *Immunity* 2000;12:431-40.
32. Hauer AD, Uyttenhove C, de VP, Stroobant V, Renaud JC, van Berkel TJ et al. Blockade of interleukin-12 function by protein vaccination attenuates atherosclerosis. *Circulation* 2005;112:1054-62.
33. Dumitriu IE, Baruah P, Finlayson CJ, Loftus IM, Antunes RF, Lim P et al. High levels of costimulatory receptors OX40 and 4-1BB characterize CD4+CD28null T cells in patients with acute coronary syndrome. *Circ Res* 2012;110:857-69.
34. Ammirati E, Cianflone D, Banfi M, Vecchio V, Palini A, De MM et al. Circulating CD4+CD25hiCD127lo regulatory T-Cell levels do not reflect the extent or severity of carotid and coronary atherosclerosis. *Arterioscler Thromb Vasc Biol* 2010;30:1832-41.
35. Caligiuri G, Paulsson G, Nicoletti A, Maseri A, Hansson GK. Evidence for antigen-driven T-cell response in unstable angina. *Circulation* 2000;102:1114-9.
36. Liuzzo G, Goronzy JJ, Yang H, Kopecky SL, Holmes DR, Frye RL et al. Monoclonal T-cell proliferation and plaque instability in acute coronary syndromes. *Circulation* 2000;101:2883-8.
37. de Boer OJ, van der Meer JJ, Teeling P, van der Loos CM, van der Wal AC. Low numbers of FOXP3 positive regulatory T cells are present in all developmental stages of human atherosclerotic lesions. *PLoS One* 2007;2:e779.
38. Ammirati E, Cianflone D, Vecchio V, et al. Effector memory T cells are associated with atherosclerosis in humans and animal models. *J Am Heart Assoc.* 2012;1:27- 41.
39. Hoff H, Knieke K, Cabail Z, Hirseland H, Vratsanos G, Burmester GR et al. Surface CD152 (CTLA-4) expression and signaling dictates longevity of CD28null T cells. *J Immunol* 2009;182:5342-51.
40. Yi-qun Z, Lorre K, de BM, Ceuppens JL. B7-blocking agents, alone or in combination with cyclosporin A, induce antigen-specific anergy of human memory T cells. *J Immunol* 1997;158:4734-40.
41. Bluestone JA, Liu W, Yabu JM, Laszik ZG, Putnam A, Belingheri M et al. The effect of costimulatory and interleukin 2 receptor blockade on regulatory T cells in renal transplantation. *Am J Transplant* 2008;8:2086-96.
42. Kormendy D, Hoff H, Hoff P, Broker BM, Burmester GR, Brunner-Weinzierl MC. The impact of the CTLA-4/CD28 axis on the processes of Joint Inflammation in Rheumatoid Arthritis. *Arthritis Rheum* 2012.

Online supplements

T-cell co-stimulation by CD28-CD80/86 and its negative regulator CTLA-4 strongly influence accelerated atherosclerosis development

Materials and Methods

Mice

All experiments were approved by the Institutional Committee for Animal Welfare of the Leiden University Medical Center (LUMC). Male C57Bl/6J controls, CD4^{-/-} and CD80^{-/-}CD86^{-/-} mice on a C57Bl/6J background were purchased from the Jackson Laboratory (Bar Harbor) and transgenic male ApoE^{*3}-Leiden mice, backcrossed for more than 20 generations on a C57Bl/6J background, were bred in our own laboratory. All animals used for this experiment were 10-12 weeks at the start of a dietary run-in period or surgery and were weighed before and at the end of the experimental period.

Diets

C57Bl/6J controls, CD4^{-/-} and CD80^{-/-}CD86^{-/-} mice received chow diet and transgenic male ApoE^{*3}-Leiden mice were fed a Western-type diet containing 1% cholesterol and 0.05% cholate to induce hypercholesterolemia to desired levels in male ApoE^{*3}-Leiden mice (AB Diets). The Western-type diet was given three weeks prior to surgery and was continued throughout the experiment. All animals received food and water ad libitum during the entire experiment.

Treatment protocol

To investigate the role of CTLA-4 co-inhibition, C57Bl/6J control and ApoE^{*3}-Leiden animals were injected intraperitoneally (IP) with abatacept (Bristol-Myers Squibb B.V.) in a concentration of 10 mg/kg twice monthly (200 µl) or vehicle, starting at the time of surgery. CTLA-4 blockade in ApoE^{*3}-Leiden mice was induced by injecting animals IP with 200 µg of anti-mouse CTLA-4 IgG (clone 9H10[1]) or control IgG diluted in 200 µl sterile phosphate-buffered saline (PBS) once every 2 days, starting at the time of surgery.

Blocking CTLA-4 IgG antibody generation

Anti-murine CTLA-4 IgG antibodies used in this study were isolated from supernatants from the 9H10 hybridoma line[1], first using Iscove's Modified Dulbecco's Medium (IMDM) (Invitrogen) with 8% FCS and 1% glutamine, followed by GIBCO™ protein-free hybridoma medium (PFHM)-II (Invitrogen) throughout T75, T175 and roller bottle culture systems (Sigma-Aldrich Chemie B.V), maintained at 37°C with 5% CO₂. Antibody concentration was performed using an artificial kidney (Fresenius Medical Care). The concentrated antibodies were protein G-purified (GE Healthcare Bio-Sciences AB) and antibody concentrations were determined using a Nanodrop spectrophotometer and stored at 2 mg/ml in sterile PBS at -20°C for further use.

Femoral artery cuff mouse model

To investigate the role of CD4 T lymphocytes, CD28-CD80/CD86 co-stimulation and CTLA-4 co-inhibition, mice were subjected to arterial femoral arterial cuff placement to induce intimal thickening and accelerated atherosclerosis development[2-4]. In brief, mice were anesthetized before surgery with a combination of IP injected Midazolam (5 mg/kg, Roche), Medetomidine (0.5 mg/kg, Orion) and Fentanyl (0.05 mg/kg, Janssen). The right femoral artery was isolated and sheathed with a rigid non-constrictive polyethylene cuff (Portex, 0.40mm inner diameter, 0.80mm outer diameter and an approximate length of 2.0mm). Using two ligatures, the polyethylene cuff was held in place, after which the wound was closed using continuous sutures.

Either 14 days (ApoE3*Leiden mice) or 21 days (normocholesterolemic mice) after cuff placement, mice were anesthetized as before and euthanized. At sacrifice, venous blood was drawn in EDTA collection tubes (Sarstedt B.V) and subjected to centrifugation (6000 r.p.m. for 10 min at 4°C) to obtain plasma, which was stored at -20°C for further research. The spleen and draining inguinal lymph nodes were isolated and either snap frozen in liquid nitrogen for further analysis (stored at -80°C) or minced through a 70-µm cell strainer (BD Biosciences) to create single-cell suspensions and stored in 3% fetal calf serum-rich GIBCO™ RPMI 1640 medium (Invitrogen) on ice.

Next, the thorax was opened and mild pressure-perfusion (100mm Hg) with PBS for 4min by cardiac puncture in the left ventricle. After perfusion, the cuffed femoral artery was harvested, fixed overnight in 3.7% formaldehyde in water (w/v) and paraffin-embedded. Serial cross-sections (5 µm thick) were made from the entire length of the artery for analysis.

Biochemical analysis

Total plasma cholesterol (Roche Diagnostics, kit 1489437) concentration was measured enzymatically before randomization and at sacrifice. Plasma cholesterol concentrations (12.1±3.1 mmol/L) were similar in all groups throughout this study (p>0.15, table 2). To investigate effects of abatacept on systemic CD4 T-cell specific activation after surgery, interferon (IFN)-γ and interleukin-10 enzyme-linked immuno sorbent assays (ELISAs) were performed (BD Biosciences) according to the manufacturer's instructions.

Quantification of cuffed femoral artery lesions

Immunohistochemical (IHC) staining was performed using positive and negative tissue-specific controls as indicated by the antibody manufacturer. Samples were stained with hematoxylin-phloxine-saffron (HPS) and specific vessel wall composition was visualized

for elastin (Weigert's elastin staining), collagen (Sirius Red staining) and with antibodies against leukocytes (anti-CD45 antibodies 1:200, Pharmingen), macrophages (MAC3, 1:200, BD Biosciences), vascular SMCs (α -SMC actin 1:800, Dako), T-cells (anti-CD3, 1:100, AbD Serotec and anti-CD4, 1:250, Abcam), matrix metalloproteinase-9 (anti-MMP-9, 1:100, Santa Cruz), and CTLA-4 (anti-mouse CTLA-4, 1:200, Abbiotec), using hematoxylin for counterstaining to visualize all cells. The anti-CD4 antibody specificity for CD4 was confirmed on cuffed sections of CD4 knock-out mice (21d) (fig IIF).

Sections were deparaffinized by placement in xylene for 5 minutes, followed by ethanol 100% for 2 minutes, ethanol 70% for 2 minutes and ethanol 50% for 2 minutes and distilled water for 2 minutes. Sections underwent citrate buffer antigen retrieval (10mM sodium citrate, pH 6.0) for 10 minutes at 100°C, followed by 30 minutes cooling. PBS (1%) was used as a wash solution and for diluting antibodies. Novared (Vector laboratories) was used as staining vector according to the manufacturer's instructions. Sections were dehydrated by placement in ethanol 50% for 2 minutes, ethanol 70% for 2 minutes and ethanol 100% for 2 minutes, followed by xylene for 5 minutes. The slides were mounted with xylene-based pertex and 24x60 mm coverslips.

The number of leukocytes, macrophages and cells expressing CTLA-4 attached to the endothelium, within the neointimal tissue or infiltrated in the medial layer of the femoral arteries was quantified and is displayed as a percentage of the total number of present cells. The area containing vascular SMCs, collagen or macrophages was quantified using computer-assisted morphometric analysis (Qwin, Leica) and is expressed as a percentage of the total cross-sectional arterial wall layer area. All quantification in this study was performed on six equally spaced (150 μ m distance) serial stained perpendicular cross-sections throughout the entire length of the vessel and was performed by blinded observers.

Flow cytometry

Spleens and draining inguinal lymph nodes were harvested and single-cell suspensions were prepared by mincing the tissue through a 70- μ m cell strainer (BD Biosciences). Erythrocytes were lysed using hypotonic (0.82%) ammonium chloride buffer. For cell surface staining, cells were resuspended in staining buffer (PBS + 3%P PFCS + 0.05% sodium azide) and incubated with fluorescent conjugated antibodies at 4°C for 30 minutes in 96-well plates. After washing and resuspension in staining buffer, cells were acquired using a BD LSR II flow cytometer and data was analyzed using FlowJo software (version 7.4.6., Tree Star).

Cells were stained with fluorochrome-conjugated monoclonal antibodies specific for CD3, CD4, CD44, CD25, CD62L CD69, CD127, CTLA-4, and KLRG1. All antibodies were purchased from eBioscience or BD Biosciences. Staining for intracellular FoxP3 was performed using the FoxP3 staining set from eBioscience (1:200, APC). 7-AAD was used to exclude dead cells.

Statistical analysis

All data are presented as mean \pm standard error of the mean (SEM). Groups were compared using a Mann-Whitney sum test for non-parametric data. All statistical analyses were performed with SPSS 17.0 software for Windows or using Prism software. P-values <0.05 were regarded as statistically significant and are indicated with an asterisk (*).

Table 1. Murine body weights at surgery and sacrifice.

Group	Body weight (gram)	
	Surgery	Sacrifice
C57Bl/6J	22.6±0.4	24.8±0.4
CD4 ^{-/-}	26.7±0.4	29.0±0.4
CD80 ^{-/-}	24.1±1.1	26.0±1.0
Abatacept	23.7±0.4	25.9±0.3

Body weight (gram) of control, CD4^{-/-}, CD80^{-/-}/CD86^{-/-} and abatacept-treated (10 mg/kg/twice monthly) C57Bl/6J mice at surgery and sacrifice at day 21 (mean±SEM, n=10). No significant differences were observed.

Table 2. Murine body weights and plasma total cholesterol at surgery and sacrifice.

Group	Body weight (gram)		Total cholesterol (mmol/L)	
	Surgery	Sacrifice	Surgery	Sacrifice
Vehicle	29.0±0.6	29.4±0.7	11.3±0.4	7.9±0.6
Abatacept	29.4±0.7	29.9±0.7	11.5±1.0	10.4±2.4
Anti-β gal IgG	28.8±0.6	29.0±0.6	13.4±1.4	8.9±0.9
Anti-CTLA-4 IgG	30.4±0.7	30.1±0.8	12.3±0.9	8.1±1.5

Body weight (gram) and plasma total cholesterol (mmol/L) of vehicle, abatacept (10

Body weight (gram) and plasma total cholesterol (mmol/L) of vehicle, abatacept (10 mg/kg/twice monthly), isotype control antibody (anti-β gal IgG 200 μg every 2 days) or anti-mouse CTLA-4 IgG (200 μg every 2 days)-treated ApoE3*Leiden mice measured at surgery and sacrifice (14 days) (mean±SEM, n=10). No significant differences were observed.

Reference List

1. Krummel MF, Allison JP. CD28 and CTLA-4 have opposing effects on the response of T cells to stimulation. *J Exp Med* 1995;182:459-465.
2. Lardenoye JH, Delsing DJ, de Vries MR, Deckers MM, Princen HM, Havekes LM et al. Accelerated atherosclerosis by placement of a perivascular cuff and a cholesterol-rich diet in ApoE*3Leiden transgenic mice. *Circ Res* 2000;87:248-253.
3. Pires NM, Schepers A, van der Hoeven BL, de Vries MR, Boesten LS, Jukema JW et al. Histopathologic alterations following local delivery of dexamethasone to inhibit restenosis in murine arteries. *Cardiovasc Res* 2005;68:415-424.
4. Ewing MM, de Vries MR, Nordzell M, Pettersson K, de Boer HC, van Zonneveld AJ et al. Annexin A5 therapy attenuates vascular inflammation and remodeling and improves endothelial function in mice. *Arterioscler Thromb Vasc Biol* 2011;31:95-101

Figure I

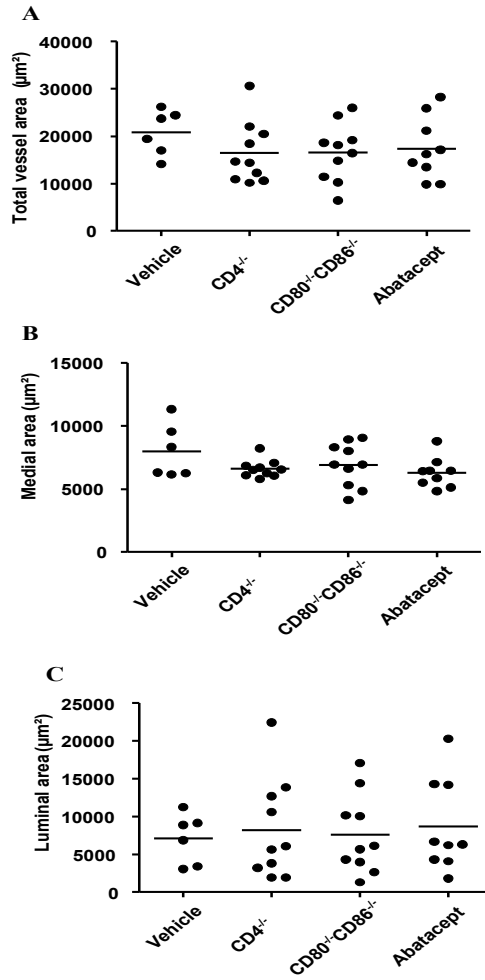


Figure I. Reduced vascular remodeling in CD4^{-/-} and CD80⁺CD86^{-/-} and abatacept-treated mice. Quantification of total vessel area (μm^2) (A), medial area (μm^2) (B) and luminal area (μm^2) (C) after 21 days. Horizontal bars indicate median values, n=10.

Figure II

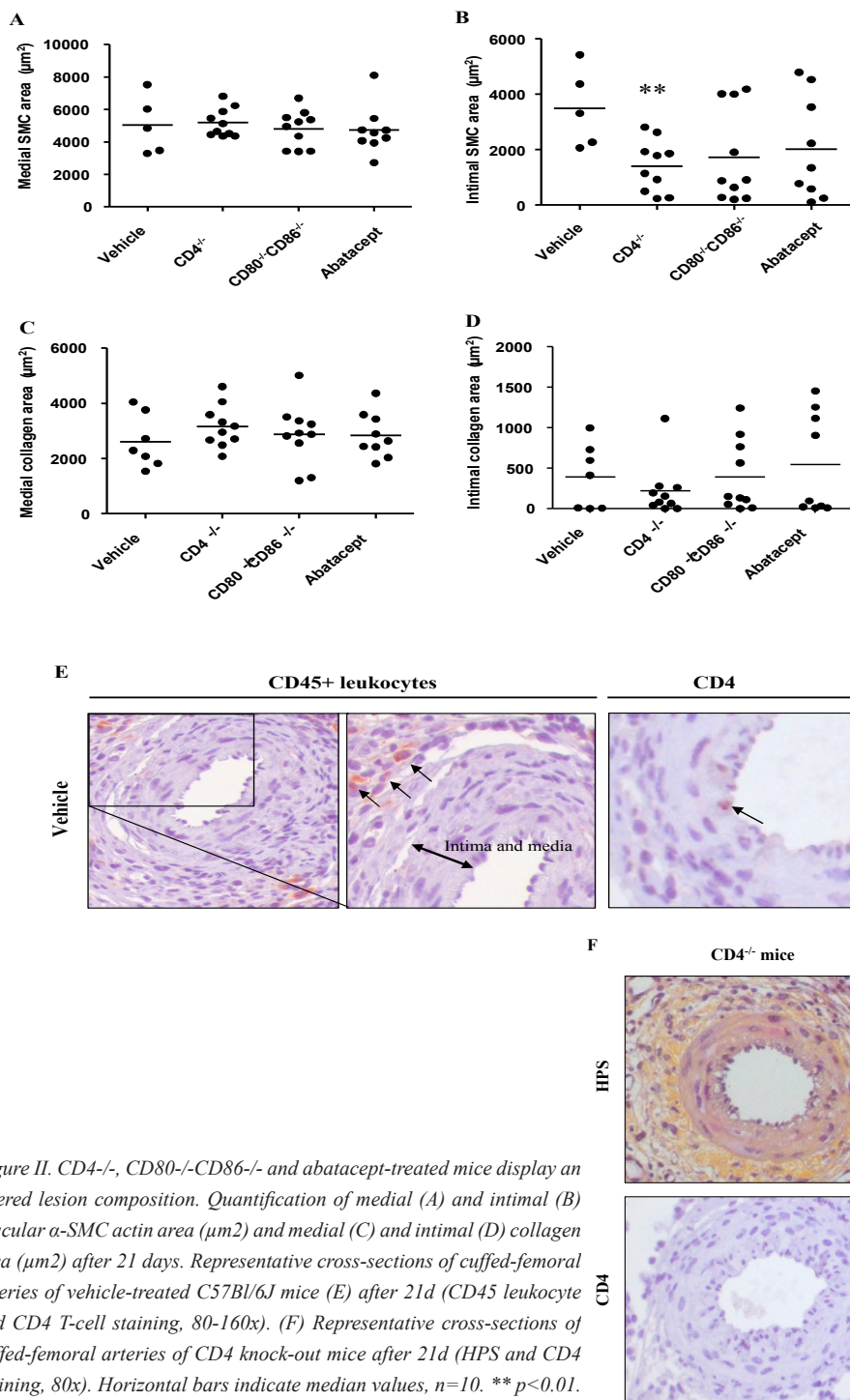


Figure II. CD4^{-/-}, CD80^{-/-}CD86^{-/-} and abatacept-treated mice display an altered lesion composition. Quantification of medial (A) and intimal (B) vascular α -SMC actin area (μm^2) and medial (C) and intimal (D) collagen area (μm^2) after 21 days. Representative cross-sections of cuffed-femoral arteries of vehicle-treated C57Bl/6J mice (E) after 21d (CD45 leukocyte and CD4 T-cell staining, 80-160x). (F) Representative cross-sections of cuffed-femoral arteries of CD4 knock-out mice after 21d (HPS and CD4 staining, 80x). Horizontal bars indicate median values, n=10. ** p<0.01.

Figure III

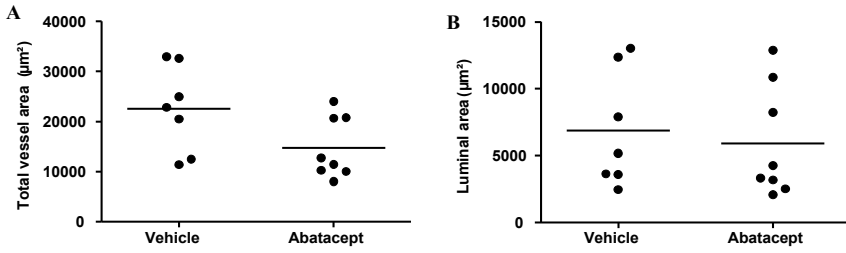


Figure III. Abatacept prevents accelerated atherosclerosis in hypercholesterolemic *ApoE3*Leiden* mice. Quantification of total vessel area (μm^2) (A) and luminal area (μm^2) (B) after day 14. Horizontal bars indicate median values, $n=10$.

Figure IV

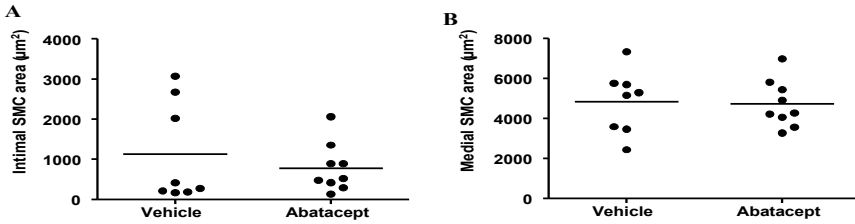


Figure IV. Abatacept positively affects accelerated atherosclerotic lesion composition. Quantification of total intimal (A) and medial (B) SMC areas (μm^2) after day 14. Horizontal bars indicate median values, $n=10$. * $p<0.05$, ** $p<0.01$.

Figure V

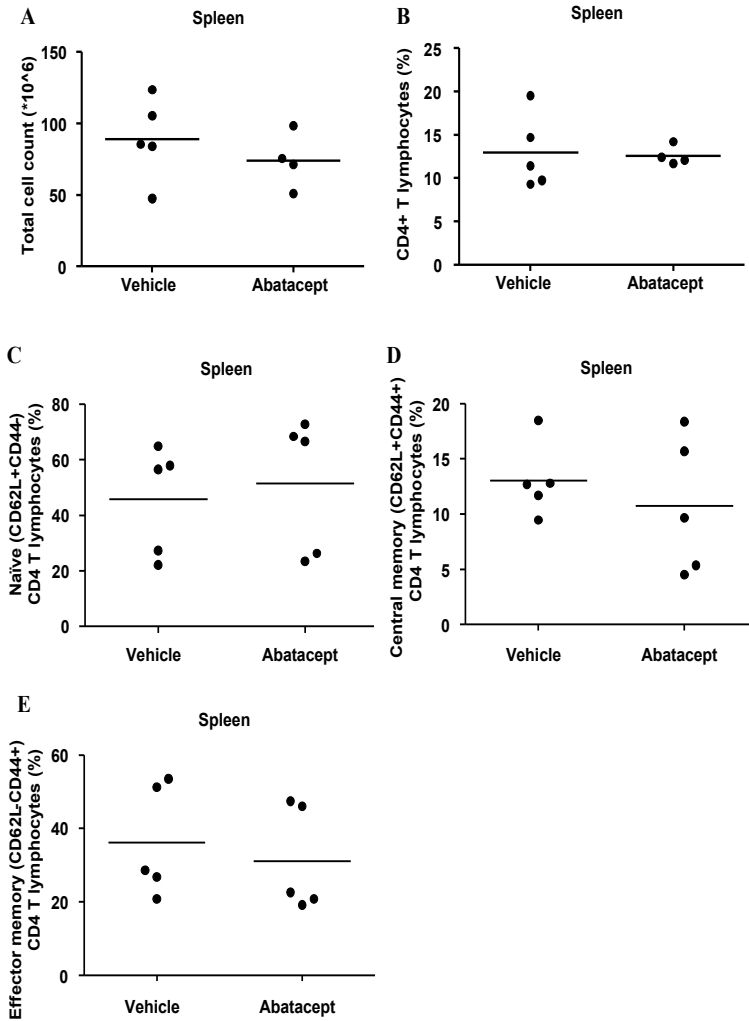


Figure V. Abatacept prevents systemic CD4 T-cell activation in ApoE3*Leiden mice. Quantification of splenic total cell count (*10⁶ cells) (A), CD4 T-cell fractions (%) (B), splenic naïve (CD62L+CD44-) (C) and activated central-memory (CD62L+CD44+) (D) and effector-memory (CD62L-CD44+) (E) CD3+CD4+ T-cells (%) 14 days after surgery. Horizontal bars indicate median values, n=5.

Figure VI

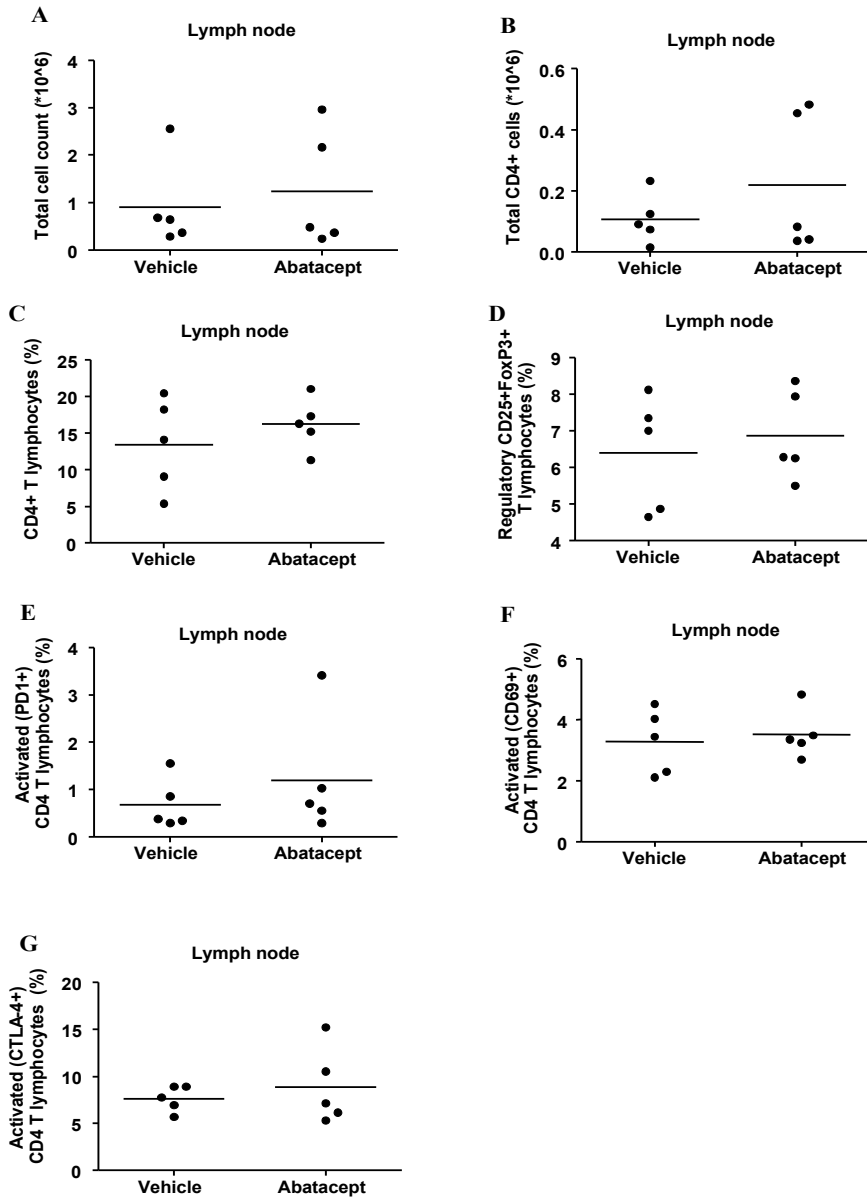


Figure VI. Abatacept does not affect draining inguinal lymph node T-cell activation status in hypercholesterolemic ApoE3*Leiden mice. Quantification of total cell count (*10⁶ cells) (A), total CD4 T-cells (*10⁶ cells) (B), CD4 T-cell fraction (%) (C), regulatory CD4+CD25+FoxP3+ T-cells (%) (D), activated PD1+ (E), CD69+ (F) and CTLA-4+ (G) CD4 T-cells (%) in draining inguinal lymph nodes, 14 days after surgery. Horizontal bars indicate median values, n=5.

Figure VII

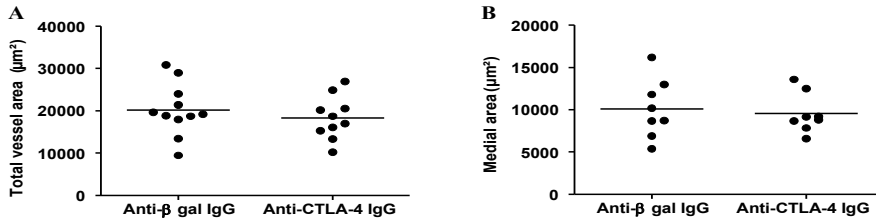


Figure VII. CTLA-4 blockade exacerbates accelerated atherosclerosis development in hypercholesterolemic ApoE3*Leiden mice. Quantification of total vessel area (μm^2) (A) and medial area (μm^2) (B), 14 days after surgery. Horizontal bars indicate median values, $n=10$.

Figure VIII

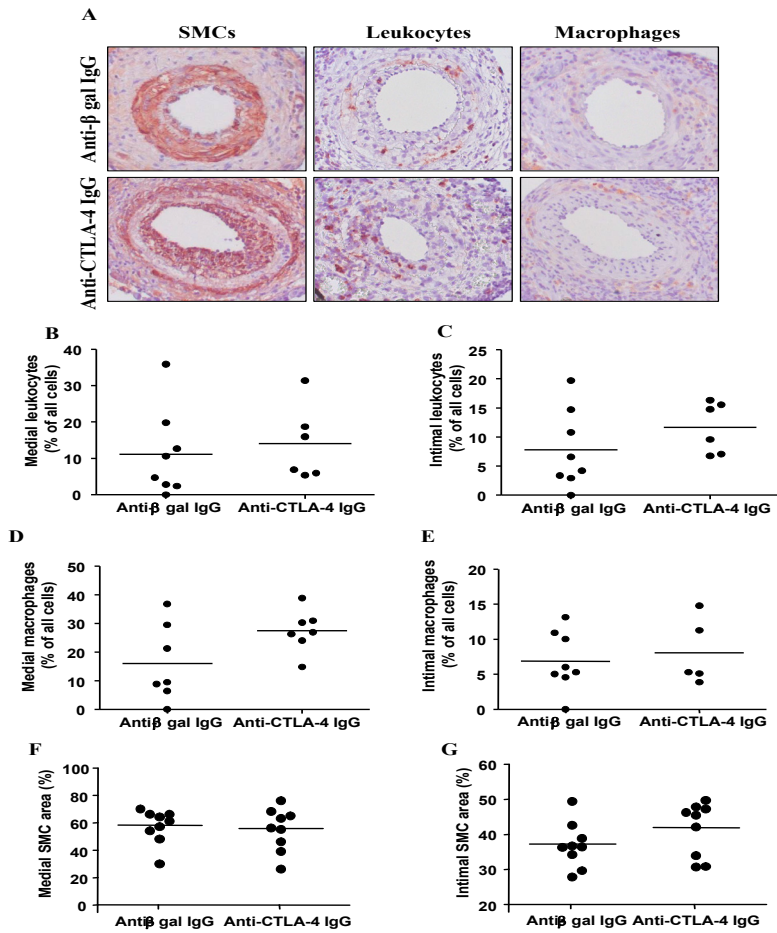


Figure VIII. Accelerated atherosclerotic lesion phenotype is preserved during CTLA-4 blockade. Representative cross-sections of cuffed-femoral arteries of ApoE3*Leiden mice following isotype antibody or anti-CTLA-4 IgG-treatment (A) after 14d (leukocyte, macrophage and α -SMC actin staining, 80x). Quantification of relative medial leukocyte (B), macrophage (D) and SMC (F) areas (%) and intimal leukocyte (C), macrophage (E) and SMC (G) areas (%) showed no significant differences. Horizontal bars indicate median values, n=10.

SUPPLEMENTAL
MATERIAL TO
CHAPTER 2

Annexin A5 prevents post-interventional accelerated atherosclerosis development in a dose-dependent fashion.

Ewing MM, Karper JC, Sampietro ML, de Vries MR, Pettersson K, Jukema JW, Quax PH

Atherosclerosis 2012;221:333-340.

Abstract

Background Activated cells in atherosclerotic lesions expose phosphatidylserine (PS) on their surface. Annexin A5 (AnxA5) binds to PS and is used for imaging atherosclerotic lesions. Recently, AnxA5 was shown to inhibit vascular inflammatory processes after vein grafting. Here, we report a therapeutic role for AnxA5 in post-interventional vascular remodeling in a mouse model mimicking percutaneous coronary intervention (PCI).

Methods and Results Associations between the rs4833229 (OR=1.29 (CI 95%), $p_{\text{allelic}}=0.011$) and rs6830321 (OR=1.35 (CI 95%), $p_{\text{allelic}}=0.003$) SNPs in the AnxA5 gene and increased restenosis-risk in patients undergoing PCI were found in the GENDER study. To evaluate AnxA5 effects on post-interventional vascular remodeling and accelerated atherosclerosis development in vivo, hypercholesterolemic ApoE^{-/-} mice underwent femoral arterial cuff placement to induce intimal thickening. Dose-dependent effects were investigated after 3 days (effects on inflammation and leukocyte recruitment) or 14 days (effects on remodeling) after cuff placement. Systemically administered AnxA5 in doses of 0.1, 0.3 and 1.0 mg/kg compared to vehicle reduced early leukocyte and macrophage adherence up to 48.3% ($p=0.001$) and diminished atherosclerosis development by 71.2% ($p=0.012$) with a reduction in macrophage/foam cell presence. Moreover, it reduced the expression of the endoplasmic reticulum stress marker GRP78/BiP, indicating lower inflammatory activity of the cells present.

Conclusions AnxA5 SNPs could serve as markers for restenosis after PCI and AnxA5 therapeutically prevents vascular remodeling in a dose-dependent fashion, together indicating clinical potential for AnxA5 against post-interventional remodeling.

Keywords

Atherosclerosis, restenosis, inflammation, annexin A5, genetics

Introduction

Post-interventional vascular remodeling and accelerated atherosclerosis development are important complications of revascularization strategies and limit treatment success rate (1). These features are elicited by endothelial and atherosclerotic plaque injury, triggering inflammatory activation and leukocyte recruitment to the injured arterial segment. These cells are the driving factors behind smooth muscle cell (SMC) proliferation and extracellular matrix deposition leading to intimal hyperplasia. Subendothelial retention and oxidation of low-density lipoprotein (LDL) cholesterol is central to the initial lesion formation in both native atherosclerosis and restenosis development (2,3). Recently, it was postulated that endoplasmic reticulum (ER) stress, leading to the unfolded protein response (UPR), is involved in the regulation of inflammation in activated vascular cells and the link between UPR and arterial inflammation is emerging as an important factor in (accelerated) atherosclerosis development (4-7).

AnxA5 is a member of the annexin family of proteins that calcium-dependently bind to negatively-charged phospholipid surfaces and was originally discovered as an anticoagulant and antithrombotic protein (8-11) and has been shown to inhibit the prothrombinase complex (12) and to down-regulate the surface expression of tissue factor (13). It is now known to have anti-inflammatory and anti-atherosclerotic properties (14,15) and to regulate interferon γ signalling (16). Viable cells express phosphatidylserine (PS) on their inner cellular membrane leaflet. When PS is externalized, it serves as an 'eat-me' signal. Annexin A5 (AnxA5) binds reversibly, specifically and with high affinity to PS (15). PS becomes externalized during apoptosis, which makes AnxA5 a powerful tool to detect apoptosis (and atherosclerosis) both in vitro and in vivo (17). PS is expressed in native atherosclerosis and after revascularisation procedures, and circulating AnxA5 binds with high affinity to these cells, and is therefore present in high concentrations in atherosclerotic plaques and injured vascular segments. PS externalization is normally thought to be associated to apoptosis, but can also be externalized in a controlled and reversible way in non-apoptotic cells (18,19).

Plasma levels of AnxA5 are inversely related to the severity of coronary stenosis and are indicative of the extent of atherosclerotic plaques (20), but are also elevated in subjects with left ventricular hypertrophy and following myocardial infarction (21,22). It was recently shown that systemically administered AnxA5 can prevent vein graft disease and vascular inflammation (23) and that the dimer of annexin A5, diannexin, can protect against renal ischemia-reperfusion injury and inflammatory cell infiltration into transplanted islet grafts (24,25). Patients with hypercholesterolemia and previous coronary heart disease (CHD) undergoing PCI for atherosclerosis are most at risk for inflammatory-driven post-interventional restenosis development. The risk for development of restenosis may partially be determined by genetic factors. It has been shown that genetic variations in genes encoding inflammatory factors (SNPs) can predict the risk for restenosis after percutaneous coronary intervention (PCI) (26). The effects of genetic variation in the AnxA5 gene on clinical restenosis after PCI or cardiovascular disease progression have thus far not been elucidated.

In the present study we investigated the association between AnxA5 SNPs and restenosis-risk in patients undergoing PCI, followed by in vivo evaluation of the therapeutic effectiveness of AnxA5 in a humanized mouse model for post-interventional vascular remodeling using ApoE3*Leiden mice. Our findings point to a potential diagnostic and therapeutic clinical role for AnxA5 against post-PCI vascular remodeling.

Materials and Methods

Association between single nucleotide polymorphisms (SNPs) in the AnxA5 gene, extracted from the GENDER genome wide association study (GWAS) dataset (27) and restenosis-risk following PCI was investigated.

We performed *in vivo* intervention studies in which hypercholesterolemic ApoE^{-/-} mice on a Western-type diet were subjected to femoral artery cuff placement to induce vascular injury and remodeling (28). Cuff placement leads to a localized vascular inflammation, which in turn produces concentric intimal lesions that can affect vessel patency. The lesions consist of SMCs, connective tissue and infiltrated leukocytes such as macrophages / foam cells and are strongly inflammation-dependent (29). In these vascular segments, inflammatory cell adhesion, infiltration, intimal thickening and lesion composition were assessed using histology, morphometry and immunohistochemistry (IHC), as described previously (29). Treatment with vehicle, 0.1, 0.3 and 1.0 mg/kg AnxA5 was given to operated ApoE^{-/-} mice. A three day protocol was used to evaluate effects on leukocyte recruitment, and a 14 day protocol to evaluate effects on vascular remodeling. All materials and methods are described in detail in the supplemental material.

Results

Annexin A5 SNP as risk marker for clinical restenosis

AnxA5 plasma levels are linked to the severity of coronary stenosis and AnxA5 is a marker of cardiovascular disease progress. These data indicate a potential role of AnxA5 in (post-interventional) accelerated atherosclerosis development. Therefore we investigated the association between AnxA5 SNPs and restenosis risk in patients undergoing PCI enrolled in the GENDER study, composed of 866 patients (295 cases that developed restenosis following PCI and 571 controls that did not develop restenosis). Clinical outcome was linked to genetic data obtained through a genome-wide association analysis.

The allelic association test identified two SNPs, rs4833229 and rs6830321, which are significantly associated with restenosis risk after PCI (**fig 1A**). Both SNPs increased the risk for restenosis (rs4833229, odds ratio (OR) =1.29, (95% confidence interval (CI) 1.06-1.58), $p_{\text{allelic}}=0.011$ and rs6830321, OR=1.35 (95% CI 1.10-1.64), $p_{\text{allelic}}=0.003$), even after adjustment for clinical risk factors, such as total occlusion, diabetes, smoking and residual stenosis (**table 1**). The minor allele frequencies for cases and controls from the GENDER population are 0.481 and 0.418 for rs4833229 and 0.510 and 0.436 for rs6830321 respectively, indicating they are present in a large proportion of the population. The AnxA5 gene linkage disequilibrium (LD) plot shows that rs4833229 and rs6830321 are in high LD ($r^2=0.91$, **fig 1B**). Haplotype analysis in the gene showed similar association results with restenosis as found in the single SNP analysis (haplotype ACAGTTGTT, frequency: 0.427, OR=1.275, $p=0.018$). These data link AnxA5 SNPs to restenosis-risk after PCI and suggest that AnxA5 genotype functions as risk marker for restenosis. We therefore further explored AnxA5's therapeutic potential using an *in vivo* model for restenosis and intimal hyperplasia.

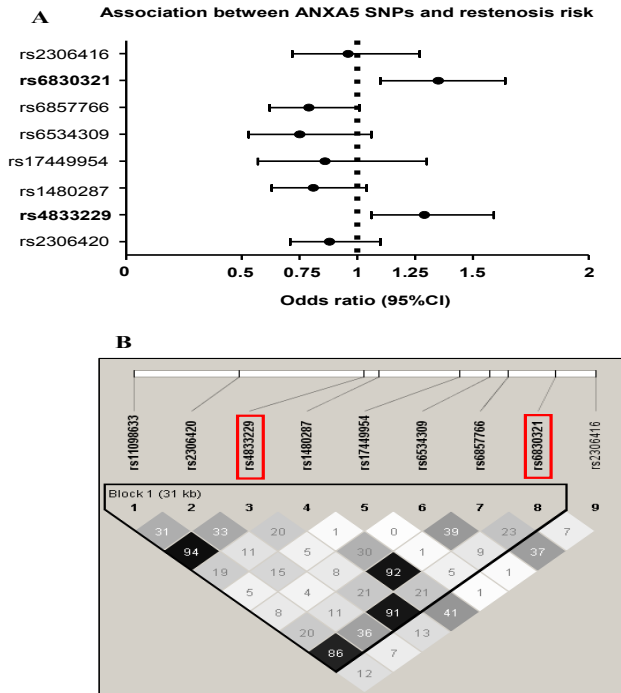


Figure 1. *AnxA5* is a genetic risk marker for clinical restenosis after PCI. Association results for the allelic test for eight SNPs in the *ANXA5* gene (A). LD plot shows that rs4833229 and rs6830321 SNPs are in high LD ($r^2 = 0.91$) (B).

Table 1

Association between restenosis risk and SNPs in the *ANXA5* gene.

SNP	Base position	Minor/major allele	MAF cases/controls	OR (95% CI)	p Value
rs2306420	122810925	T/C	0.283/0.309	0.88 (0.71–1.10)	0.2622
rs4833229	122820114	A/G	0.481/0.418	1.29 (1.06–1.58)	0.0114
rs1480287	122821231	A/G	0.481/0.215	0.81 (0.63–1.04)	0.0954
rs17449954	122827178	C/T	0.181/0.067	0.86 (0.57–1.30)	0.4705
rs6534309	122829379	C/T	0.058/0.108	0.75 (0.53–1.06)	0.1040
rs6857766	122830735	A/G	0.083/0.230	0.79 (0.62–1.01)	0.0636
rs6830321	122834205	T/C	0.510/0.436	1.35 (1.10–1.64)	0.0034
rs2306416	122837138	CT	0.139/0.145	0.96 (0.72–1.27)	0.7564

Allelic association results for 8 SNPs included in the annexin A5 gene in the GENDER study. Positions are based on hg18 build. Abbreviations: Chr, chromosome; MAF, minor allele frequency. ORs are computed for the minor allele from the two by two allele contingency table. Significant association was observed for SNPs rs4833229 and rs6830321 and restenosis-risk with SNPs displaying high linkage.

Annexin A5 dose-dependently prevents leukocyte recruitment after vascular injury

Effects of AnxA5 on leukocyte recruitment to injured arterial segments was investigated in the femoral artery cuff model in ApoE^{-/-} mice receiving daily vehicle or 0.1, 0.3 or 1.0 mg/kg AnxA5 through IP injection. Total plasma cholesterol was not affected by annexin A5

treatment (**supplementary table I**). Three days after cuff placement there is inflammation in the cuffed arteries, with leukocytes both adherent to the endothelial surface and with cells that have migrated into the media layer (**fig 2A**). Staining of arterial lesions at this time point revealed that 0.1, 0.3 and 1.0 mg/kg/d AnxA5-treated animals displayed a reduced percentage of endothelial leukocyte adhesion by 26.7% ($p=0.014$), 34.9% ($p=0.010$) and 48.3% ($p=0.001$) respectively (**fig 2B**). For monocytes/macrophages, this percentage was reduced by 40.0% ($p=0.029$), 66.9%, ($p=0.001$) and 45.0% ($p=0.037$) respectively (**fig 2C**). The percentage leukocyte infiltration into the media was reduced by all AnxA5 treatments by 49.4% ($p=0.008$), 53.3% ($p=0.006$) and 49.9% ($p=0.011$) respectively (**fig 2D**). The percentage medial macrophages was reduced by 61.2% ($p=0.025$) by 1.0 mg/kg AnxA5, the other dosages did not significantly affect monocyte/macrophage extravasation (**fig 2E**). Together, these data indicate an important role for AnxA5 in low dosages in the prevention of leukocyte recruitment to injured arterial segments.

Figure 2

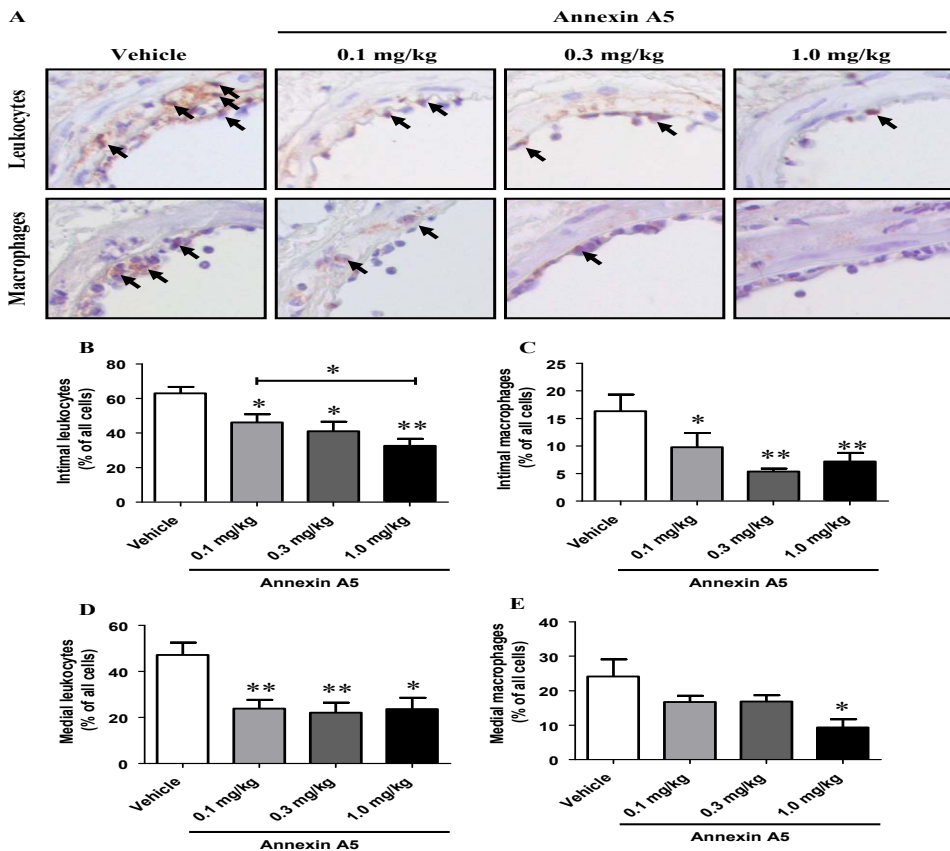


Figure 2. Annexin A5 dose-dependently prevents leukocyte recruitment after vascular injury. Representative cross-sections of cuffed-femoral arteries of *ApoE*^{-/-} mice treated with vehicle or 0.1, 0.3 or 1.0 mg/kg/d AnxA5 (leukocyte and macrophage staining, magnification 80x, arrows indicate positive staining) after 3d (A). Quantification of intimal adhering leukocytes (B) and macrophages (C) as percentage of all cells within the internal elastic lamina and medial infiltrated leukocytes (D) and macrophages (E) (%). Results indicated as mean±SEM, n=10. * $p<0.05$, ** $p<0.01$.

Annexin A5 dose-dependently prevents accelerated atherosclerosis development

The inflammation caused by cuff placement leads to an inflammation driven intimal hyperplasia. Therapeutic effectiveness of AnxA5 on (neo-)intima development was evaluated 14 days after cuff placement. Annexin A5 treatment did not affect plasma total cholesterol concentration (**supplementary table I**). Accelerated atherosclerotic lesion development was measured on sections stained with HPS and Weigert's elastin (**fig 3A**). Vehicle-treated animals developed intimal thickening, resulting in luminal stenosis. Quantitative analysis displayed reduced intimal thickening (expressed as μm^2 per cross-section) after 0.1, 0.3 and 1.0 mg/kg AnxA5-treatment by 54.6% ($p=0.041$), 71.2% ($p=0.012$) and 66.9% ($p=0.009$) respectively (**fig 3B**). Intimal thickening was 38.1% more reduced ($p=0.031$) by 0.3 compared to 0.1 mg/kg AnxA5.

AnxA5 (0.3 and 1.0 mg/kg) also decreased the absolute medial surface area (μm^2) by 30.1% ($p=0.012$) and 24.1% ($p=0.025$, **fig 3C**) and intima / media ratio by 62.3% ($p=0.004$) and 60.3% ($p=0.007$, **fig 3D**), although the lowest dose was ineffective. Furthermore, luminal stenosis (%) was reduced by 58.0% ($p=0.001$) and 58.8% ($p=0.0004$, **fig 3E**), identifying a potent role for AnxA5 in the control of inflammatory post-interventional vascular remodeling. Compared to 0.1 mg/kg, 0.3 mg/kg AnxA5 had increased protective effects on both the intima / media ratio (by 38.5%, $p=0.016$) and luminal stenosis percentage (by 33.2%, $p=0.042$). The total vessel wall diameter and luminal areas were both similar in all AnxA5 dosages, except for 1.0 mg/kg, which displayed 27.1% ($p=0.043$) reduced total vessel area (**supplementary fig IA, B**). IHC showed profound intravascular macrophages/foam cell areas, which co-localized with AnxA5 (**supplementary fig IIA, B**) staining at both 3d and 14d after surgery. AnxA5 in all dosages strongly reduced the accumulation of the percentage of macrophages/foam cell area (**fig 4A**) in the tunica media (**fig 4B**, $p=0.0002$, $p=0.028$ and $p=0.0005$ respectively) and in the tunica intima (**fig 4C**, $p=0.002$, $p=0.011$ and $p=0.002$ respectively) after 14d. The 78 kDa glucose regulated protein/BiP (GRP78) is an ER protein and associates permanently with mutant or defective incorrectly folded proteins, preventing their export from the ER lumen. ER stress including upregulation of GRP78 is present in unstable atherosclerotic lesions. We investigated if annexin A5 affected GRP78 expression in cuffed femoral arteries. AnxA5 in all dosages strongly reduced GRP78 BiP expressing cells in the media (**fig 4D**) by 50.2% ($p=0.006$), 66.3% ($p=0.0006$) and 68.0% ($p=0.004$) respectively, but not in the intima (**fig 4E**).



Figure 3

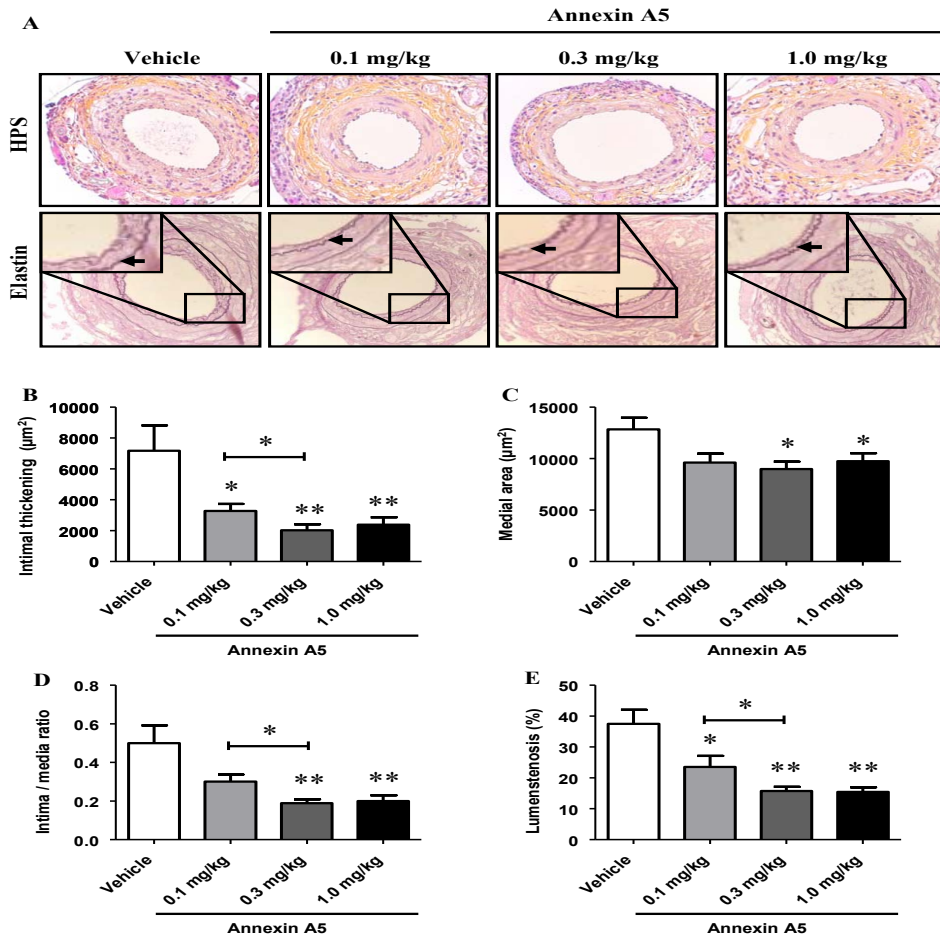
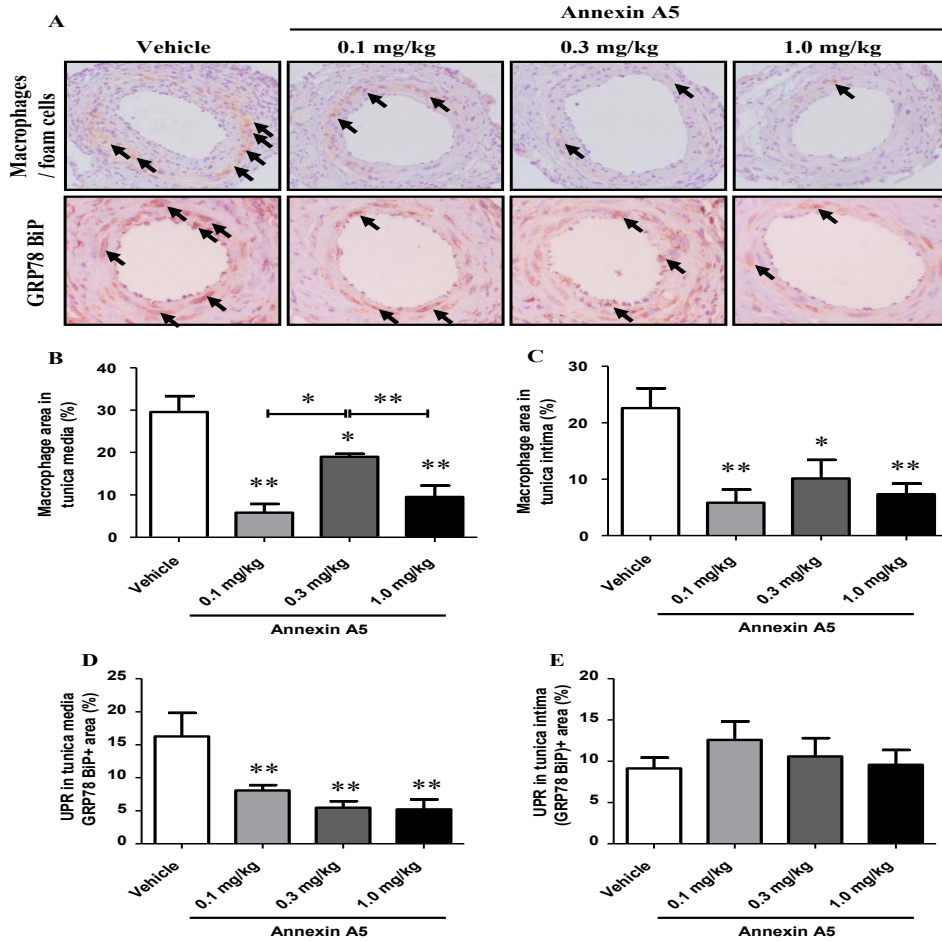


Figure 3 Annexin A5 reduces accelerated atherosclerosis development in a dose-dependent fashion. Representative cross-sections of cuffed arteries of $\text{ApoE}^{-/-}$ mice receiving vehicle or 0.1, 0.3 or 1.0 mg/kg AnxA5 (A) after 14d (HPS and Weigert's elastin staining, magnification 40x, arrows indicate internal elastic laminae). Quantification of intimal thickening (μm^2) (B), medial area (μm^2) (C), intima / media ratio (D) and luminal stenosis (%) (E). Results indicated as mean \pm SEM, n=10. * $p < 0.05$, ** $p < 0.01$.

Figure 4 next page.

Annexin A5 leads to a less-inflammatory phenotype with reduced intravascular signs of ER-stress. Representative cross-sections of cuffed arteries of $\text{ApoE}^{-/-}$ mice receiving vehicle or 0.1, 0.3 or 1.0 mg/kg AnxA5 (A) after 14d (macrophages and GRP78 BiP staining, magnification 40x, arrows indicate positive staining) and quantification of medial (B) and intimal (C) macrophage/foam cell area (%) and medial (D) and intimal (E) GRP78 BiP expression (%). Results indicated as mean \pm SEM, n=10. * $p < 0.05$, ** $p < 0.01$.

Figure 4



Discussion

This study demonstrates an important therapeutic role for AnxA5 in post-interventional intimal hyperplasia and accelerated atherosclerosis development. Association between AnxA5 SNPs and increased restenosis-risk in patients undergoing PCI was found. Systemic AnxA5 was effective in preventing intimal thickening and could dose-dependently reduce leukocyte and macrophage recruitment to injured arterial segments in ApoE^{-/-} mice in 0.3 and 0.1 mg/kg dosages. Finally, we demonstrate that sustained therapy reduces accelerated atherosclerosis with fewer infiltrated macrophages / foam cells and UPR-expressing cells in the injured arterial wall. Together, these data indicate high diagnostic and therapeutic potential for AnxA5 against post-PCI vascular remodeling.

Association between AnxA5 SNPs and restenosis development were investigated using a large study population that underwent PCI, the GENDER population. It has already been shown in this material that mutations in several genes associated with inflammation were associated to restenosis development (24). Our results demonstrate that SNPs rs4833229 and rs6830321 show significant association with increased risk for clinical restenosis (OR 1.29 and 1.35, **fig 1A**). This genetic variance in addition to plasma levels (19) would allow for

excellent stratification of patients that are most at risk for restenosis development, enabling individual tailor-made treatment strategy. Additionally, our results support the notion that genetic programming of not only pro-inflammatory mediators, but also the endogenous anti-inflammatory system exerts a significant role in post-interventional remodeling.

In this study, a perivascular cuff-mediated arterial injury model was applied, which allows for quick and reproducible lesion formation with continuous blood flow in a patent vessel segment, although the perivascular approach rather differs from clinical endovascular injury through balloon inflation and stent deployment during PCI. This perivascular approach could affect the amount of exposure of subendothelial thrombogenic material and thrombosis, which are important targets for AnxA5.

Therapeutic effects were shown to most likely result from local AnxA5 binding to activated cells in the injured vascular segment. Local AnxA5 can reduce adherence of platelets leukocytes and eventually prevent their inflammatory activation, with reduced signs of ER-stress and the UPR within these cells. We found reduced GRP78/BiP expression in the tunica media (**fig 4D**) but not in the intima (**fig 4E**). Prolonged intracellular cholesterol storage leads to increased ER stress in cells, which is more likely to occur in foam cells than in early monocyte/macrophages. In this study, such cells should predominantly be found among cells that have migrated towards the tunica media, which in turn may explain the difference between GRP78/BiP expression between the media and intima layers.

The fact that clearance of AnxA5 is much slower from the arterial wall than from plasma (30) and accumulates in the injured vascular wall after systemic injection (23), supports the hypothesis that AnxA5 could act anti-inflammatory in levels lower than originally investigated (<1.0 mg/kg). Current results confirm this, with AnxA5 already effective in reducing leukocyte (**fig 2B**) and macrophage (**fig 2C**) recruitment and intimal thickening (**fig 3B**) in dosages 3-10 times lower than previously investigated. This would favour clinical application, where undesired side-effects can be kept to a minimum.

In conclusion, this study shows that systemic AnxA5 treatment strongly influences post-interventional accelerated atherosclerosis development and can dose-dependently prevent vascular remodeling. AnxA5 has previously been successfully applied to diagnose atherosclerotic patients non-invasively (19). These results therefore may have important clinical implications. Immune-mediated interventions directed towards therapeutically controlling the leukocyte recruitment and vascular remodeling process could strongly benefit from systemic AnxA5, which could be applied in an early phase following revascularization or bypass grafting to prevent accelerated atherosclerosis development. AnxA5 SNPs could function as biomarkers in the assessment of restenosis risk in patients undergoing PCI, improving patient screening. Together, these data indicate high clinical potential for AnxA5 against post-interventional remodeling.

Disclosures

K. Pettersson is an employee of Athera Biotechnologies, Stockholm, Sweden. None of the other authors has any disclosure to report.

Reference List

1. van der Hoeven, B. L., N. M. Pires, H. M. Warda, P. V. Oemrawsingh, B. J. van Vlijmen, P. H. Quax, M. J. Schalij, E. E. van der Wall, and J. W. Jukema. 2005. Drug-eluting stents: results, promises and problems. *Int. J. Cardiol.* 99: 9-17.
2. Hansson, G. K. 2005. Inflammation, atherosclerosis, and coronary artery disease. *N. Engl. J. Med.* 352:

- 1685-1695.
3. Ross, R. 1999. Atherosclerosis--an inflammatory disease. *N. Engl. J Med.* 340: 115-126.
 4. Moore, K. J., and I. Tabas. 2011. Macrophages in the pathogenesis of atherosclerosis. *Cell* 145: 341-355.
 5. Tabas, I. 2011. Pulling down the plug on atherosclerosis: Finding the culprit in your heart. *Nat. Med.* 17: 791-793.
 6. Hotamisligil, G. S. 2010. Endoplasmic reticulum stress and atherosclerosis. *Nat. Med.* 16: 396-399.
 7. Tabas, I. 2010. The role of endoplasmic reticulum stress in the progression of atherosclerosis. *Circ. Res.* 107: 839-850.
 8. Andree, H. A., M. C. Stuart, W. T. Hermens, C. P. Reutelingsperger, H. C. Hemker, P. M. Frederik, and G. M. Willems. 1992. Clustering of lipid-bound annexin V may explain its anticoagulant effect. *J Biol Chem.* 267: 17907-17912.
 9. Thiagarajan, P., and C. R. Benedict. 1997. Inhibition of arterial thrombosis by recombinant annexin V in a rabbit carotid artery injury model. *Circulation* 96: 2339-2347.
 10. van Heerde, W. L., K. S. Sakariassen, H. C. Hemker, J. J. Sixma, C. P. Reutelingsperger, and P. G. De Groot. 1994. Annexin V inhibits the procoagulant activity of matrices of TNF-stimulated endothelium under blood flow conditions. *Arterioscler. Thromb.* 14: 824-830.
 11. Gerke, V., and S. E. Moss. 2002. Annexins: from structure to function. *Physiol Rev.* 82: 331-371.
 12. van Heerde, W. L., S. Poort, van, V, C. P. Reutelingsperger, and P. G. De Groot. 1994. Binding of recombinant annexin V to endothelial cells: effect of annexin V binding on endothelial-cell-mediated thrombin formation. *Biochem. J* 302 (Pt 1): 305-312.
 13. Ravassa, S., A. Bennaghmouch, H. Kenis, T. Lindhout, T. Hackeng, J. Narula, L. Hofstra, and C. Reutelingsperger. 2005. Annexin A5 down-regulates surface expression of tissue factor: a novel mechanism of regulating the membrane receptor repertoire. *J Biol Chem.* 280: 6028-6035.
 14. Kenis, H., L. Hofstra, and C. P. Reutelingsperger. 2007. Annexin A5: shifting from a diagnostic towards a therapeutic realm. *Cell Mol. Life Sci.* 64: 2859-2862.
 15. van Genderen, H. O., H. Kenis, L. Hofstra, J. Narula, and C. P. Reutelingsperger. 2008. Extracellular annexin A5: functions of phosphatidylserine-binding and two-dimensional crystallization. *Biochim. Biophys. Acta* 1783: 953-963.
 16. Leon, C., D. Nandan, M. Lopez, A. Moeenrezkhanlou, and N. E. Reiner. 2006. Annexin V associates with the IFN-gamma receptor and regulates IFN-gamma signaling. *J Immunol.* 176: 5934-5942.
 17. Kietselaer, B. L., C. P. Reutelingsperger, G. A. Heidendal, M. J. Daemen, W. H. Mess, L. Hofstra, and J. Narula. 2004. Noninvasive detection of plaque instability with use of radiolabeled annexin A5 in patients with carotid-artery atherosclerosis. *N. Engl. J Med.* 350: 1472-1473.
 18. Balasubramanian, K., B. Mirnikjoo, and A. J. Schroit. 2007. Regulated externalization of phosphatidylserine at the cell surface: implications for apoptosis. *J. Biol. Chem.* 282: 18357-18364.
 19. Boersma, H. H., B. L. Kietselaer, L. M. Stolk, A. Bennaghmouch, L. Hofstra, J. Narula, G. A. Heidendal, and C. P. Reutelingsperger. 2005. Past, present, and future of annexin A5: from protein discovery to clinical applications. *J Nucl. Med.* 46: 2035-2050.
 20. van Tits, L. J., W. L. van Heerde, G. M. van der Vleuten, J. de Graaf, D. E. Grobbee, L. P. van de Vijver, A. F. Stalenhoef, and H. M. Princen. 2007. Plasma annexin A5 level relates inversely to the severity of coronary stenosis. *Biochem. Biophys. Res. Commun.* 356: 674-680.
 21. Ravassa, S., A. Gonzalez, B. Lopez, J. Beaumont, R. Querejeta, M. Larman, and J. Diez. 2007. Upregulation of myocardial Annexin A5 in hypertensive heart disease: association with systolic dysfunction. *Eur. Heart J.* 28: 2785-2791.
 22. Peetz, D., G. Hafner, S. Blankenberg, A. A. Peivandi, R. Schweigert, K. Brunner, M. Dahm, H. J. Rupprecht, and M. Mockel. 2002. Annexin V does not represent a diagnostic alternative to myoglobin for early detection of myocardial infarction. *Clin. Lab* 48: 517-523.

23. Ewing, M. M., M. R. de Vries, M. Nordzell, K. Pettersson, H. C. de Boer, A. J. van Zonneveld, J. Frostegard, J. W. Jukema, and P. H. Quax. 2010. Annexin A5 Therapy Attenuates Vascular Inflammation and Remodeling and Improves Endothelial Function in Mice. *Arterioscler. Thromb. Vasc. Biol.*
24. Wever, K. E., F. A. Wagener, C. Frielink, O. C. Boerman, G. J. Scheffer, A. Allison, R. Masereeuw, and G. A. Rongen. 2011. Diannexin Protects against Renal Ischemia Reperfusion Injury and Targets Phosphatidylserines in Ischemic Tissue. *PLoS. One.* 6: e24276.
25. Cheng, E. Y., V. K. Sharma, C. Chang, R. Ding, A. C. Allison, D. B. Leeser, M. Suthanthiran, and H. Yang. 2010. Diannexin decreases inflammatory cell infiltration into the islet graft, reduces beta-cell apoptosis, and improves early graft function. *Transplantation* 90: 709-716.
26. Monraats, P. S., N. M. Pires, W. R. Agema, A. H. Zwinderman, A. Schepers, M. P. de Maat, P. A. Doevendans, R. J. de Winter, R. A. Tio, J. Waltenberger, R. R. Frants, P. H. Quax, B. J. van Vlijmen, D. E. Atsma, L. A. van der, E. E. van der Wall, and J. W. Jukema. 2005. Genetic inflammatory factors predict restenosis after percutaneous coronary interventions. *Circulation* 112: 2417-2425.
27. Sampietro, M. L., D. Pons, K. P. de, P. E. Slagboom, A. Zwinderman, and J. W. Jukema. 2009. A genome wide association analysis in the GENDER study. *Neth. Heart J.* 17: 262-264.
28. Lardenoye, J. H., D. J. Delsing, M. R. de Vries, M. M. Deckers, H. M. Princen, L. M. Havekes, V. W. van Hinsbergh, J. H. van Bockel, and P. H. Quax. 2000. Accelerated atherosclerosis by placement of a perivascular cuff and a cholesterol-rich diet in ApoE*3Leiden transgenic mice. *Circ. Res.* 87: 248-253.
29. Pires, N. M., A. Schepers, B. L. van der Hoeven, M. R. de Vries, L. S. Boesten, J. W. Jukema, and P. H. Quax. 2005. Histopathologic alterations following local delivery of dexamethasone to inhibit restenosis in murine arteries. *Cardiovasc. Res.* 68: 415-424.
30. Kemerink, G. J., X. Liu, D. Kieffer, S. Ceyskens, L. Mortelmans, A. M. Verbruggen, N. D. Steinmetz, J. L. Vanderheyden, A. M. Green, and K. Verbeke. 2003. Safety, biodistribution, and dosimetry of ^{99m}Tc-HYNIC-annexin V, a novel human recombinant annexin V for human application. *J. Nucl. Med.* 44: 94

Online supplements

Annexin A5 prevents post-interventional accelerated atherosclerosis development in a dose-dependent fashion

Materials and Methods

GENDER project

The GENetic DEterminants of Restenosis (GENDER) study was designed to investigate the association between genetic polymorphisms and clinical restenosis (1). In brief, it is a large multicenter prospective follow-up study conducted during 1999-2001 and comprised of patients treated successfully by percutaneous coronary intervention (PCI) for an acute coronary syndrome. Clinical restenosis was established during a nine-month follow-up period for death, myocardial infarction and target vessel revascularization (TVR), which occurred in 9.8% of all patients. Eight Single Nucleotide Polymorphisms (SNPs) included in the AnxA5 gene were extracted from the GENDER genome wide association study (GWAS) dataset (2) composed of 866 patients (295 cases that developed restenosis following PCI and 571 controls that did not develop restenosis after PCI). The GWAS was conducted using Illumina Human 610-Quad Beadchips (Illumina) and the Infinium II assay, following the manufacturer's instructions. After genotyping, samples and genetic markers were subjected to a stringent quality control protocol, described in detail elsewhere (2). The open source

software PLINK (3) was used to perform genetic association analysis. All p values were corrected for multiple testing. For linkage disequilibrium (LD) analyses in terms of r^2 and haplotype block delineation, we used Haploview software (4).

Mice

All experiments were approved by the Institutional Committee for Animal Welfare of the Leiden University Medical Center (LUMC). ApoE^{-/-} mice, purchased from the Jackson Laboratory (Bar Harbor) on a C57BL/6J background were used for these studies. All animals were 10-12 weeks at the start of a dietary run-in period before surgery. ApoE^{-/-} mice were fed a Western-type diet containing 0.15% cholesterol (Lantmännen Lantbruk, diet R638). The diet was given three weeks prior to surgery and was continued throughout the entire experiment. All animals received food and water ad libitum during the experiment.

Femoral artery cuff mouse model

Mice were subjected to arterial femoral arterial cuff placement to induce intimal thickening and accelerated atherosclerosis development, as described previously (5-7). In brief, animals were anesthetized before surgery with a combination of intraperitoneally (IP)-injected Midazolam (5 mg/kg, Roche), Medetomidine (0.5 mg/kg, Orion) and Fentanyl (0.05 mg/kg, Janssen). The right femoral artery was isolated and sheathed with a rigid non-constrictive polyethylene cuff (Portex, 0.40mm inner diameter, 0.80mm outer diameter and an approximate length of 2.0mm).

Animals received vehicle (0.9% sterile NaCl) or AnxA5 (Athera Biotechnologies AB) through IP injection. Three and 14 days after cuff placement, mice were anesthetized as before and euthanized. At sacrifice, blood was drawn in EDTA collection tubes (Sarstedt B.V.) and centrifuged at 6000 r.p.m. for 10 min at 4°C to obtain plasma, which was stored at -20°C. Next, the thorax was opened and mild pressure-perfusion (100mm Hg) with phosphate-buffered saline for 5 min by cardiac puncture in the left ventricle. After perfusion, the cuffed femoral artery was harvested, fixed in 3.7% formaldehyde in water (w/v) and paraffin-embedded. Serial cross-sections (5 µm thick) were made from the entire length of the artery for analysis.

Biochemical analysis

Total plasma cholesterol (Roche Diagnostics, kit 1489437) concentration was measured enzymatically before randomization at surgery.

Quantification of cuffed femoral artery lesions

Immunohistochemical (IHC) staining was performed using positive and negative tissue-specific controls as indicated by the antibody manufacturer. Samples were stained with hematoxylin-phloxine-saffron (HPS) and specific vessel wall composition was visualized for elastin (Weigert's elastin staining) and with antibodies against GRP78 BiP (1:200, Abcam, to identify cells displaying signs of UPR), CD45 for leukocytes (1:200, Pharmingen), MAC3 for monocytes/macrophages/foam cells (1:200, BD Biosciences) and anti-annexin V for injected protein accumulation (1:100, BioVision). Using image analysis software (Leica Qwin), total cross-sectional medial area was measured between the external and internal elastic laminae; total cross-sectional intimal area was measured between the endothelial cell monolayer and the internal elastic lamina, as was GRP78 BiP⁺ surface area. The luminal stenosis is expressed as the percentage of surface area (µm²) within the internal elastic lamina

(comprised of the luminal and neointimal areas) that is taken up by neointimal tissue (in μm^2). The number of leukocytes and monocytes/macrophages attached to the endothelium, within the neointimal tissue or infiltrated in the medial layer of the femoral arteries was quantified and is displayed as a percentage of the total number of present cells. All quantification in this study was performed on six equally spaced (150 μm distance) serial stained perpendicular cross-sections throughout the entire length of the vessel and was performed by blinded observers.

Statistical analysis

All data are presented as mean \pm standard error of the mean (SEM). Association between clinical outcome and individual SNPs was tested using an allelic association test. Groups were compared using a Mann-Whitney sum test for non-parametric data. Total plasma cholesterol concentrations in time were compared using a Wilcoxon matched pairs test. All statistical analyses were performed with SPSS 17.0 software for Windows or using Prism software. P-values <0.05 were regarded as statistically significant and are indicated with an asterisk (*).

1. Monraats, P. S., N. M. Pires, W. R. Agema, A. H. Zwinderman, A. Schepers, M. P. de Maat, P. A. Doevendans, R. J. de Winter, R. A. Tio, J. Waltenberger, R. R. Frants, P. H. Quax, B. J. van Vlijmen, D. E. Atsma, L. A. van der, E. E. van der Wall, and J. W. Jukema. 2005. Genetic inflammatory factors predict restenosis after percutaneous coronary interventions. *Circulation* 112: 2417-2425.
2. Sampietro, M. L., D. Pons, K. P. de, P. E. Slagboom, A. Zwinderman, and J. W. Jukema. 2009. A genome wide association analysis in the GENDER study. *Neth. Heart J.* 17: 262-264.
3. Purcell, S., B. Neale, K. Todd-Brown, L. Thomas, M. A. Ferreira, D. Bender, J. Maller, P. Sklar, P. I. de Bakker, M. J. Daly, and P. C. Sham. 2007. PLINK: a tool set for whole-genome association and population-based linkage analyses. *Am. J. Hum. Genet.* 81: 559-575
4. Barrett, J. C., B. Fry, J. Maller, and M. J. Daly. 2005. Haploview: analysis and visualization of LD and haplotype maps. *Bioinformatics.* 21: 263-265.
5. Lardenoye, J. H., D. J. Delsing, M. R. de Vries, M. M. Deckers, H. M. Princen, L. M. Havekes, V. W. van Hinsbergh, J. H. van Bockel, and P. H. Quax. 2000. Accelerated atherosclerosis by placement of a perivascular cuff and a cholesterol-rich diet in ApoE*3Leiden transgenic mice. *Circ. Res.* 87: 248-253.
6. Pires, N. M., A. Schepers, B. L. van der Hoeven, M. R. de Vries, L. S. Boesten, J. W. Jukema, and P. H. Quax. 2005. Histopathologic alterations following local delivery of dexamethasone to inhibit restenosis in murine arteries. *Cardiovasc. Res.* 68: 415-424.
7. Ewing, M. M., M. R. de Vries, M. Nordzell, K. Pettersson, H. C. de Boer, A. J. van Zonneveld, J. Frostegard, J. W. Jukema, and P. H. Quax. 2011. Annexin A5 therapy attenuates vascular inflammation and remodeling and improves endothelial function in mice. *Arterioscler. Thromb. Vasc. Biol.* 31: 95-101.

Figure I

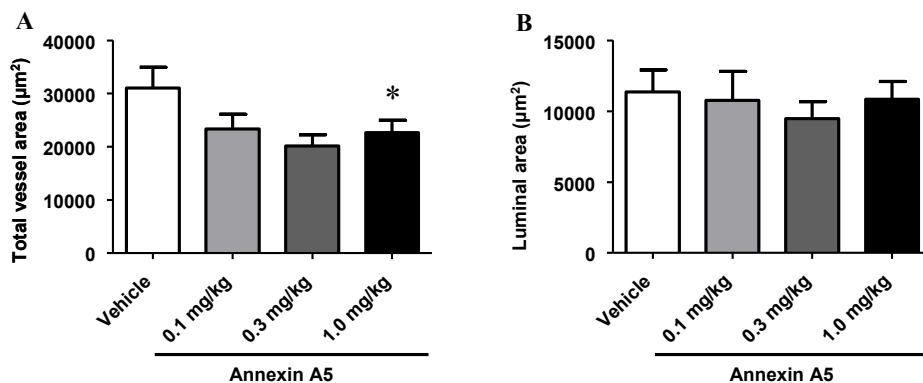


Figure I. Annexin A5 reduces accelerated atherosclerosis development in a dose-dependent fashion. Quantification of total vessel area (μm^2) (A) and luminal area (μm^2) (B) in ApoE^{-/-} mice receiving vehicle or 0.1, 0.3 or 1.0 mg/kg AnxA5 after 14d. Results indicated as mean \pm SEM, n=10. * p<0.05, ** p<0.01, n.s. not significant.

Figure II

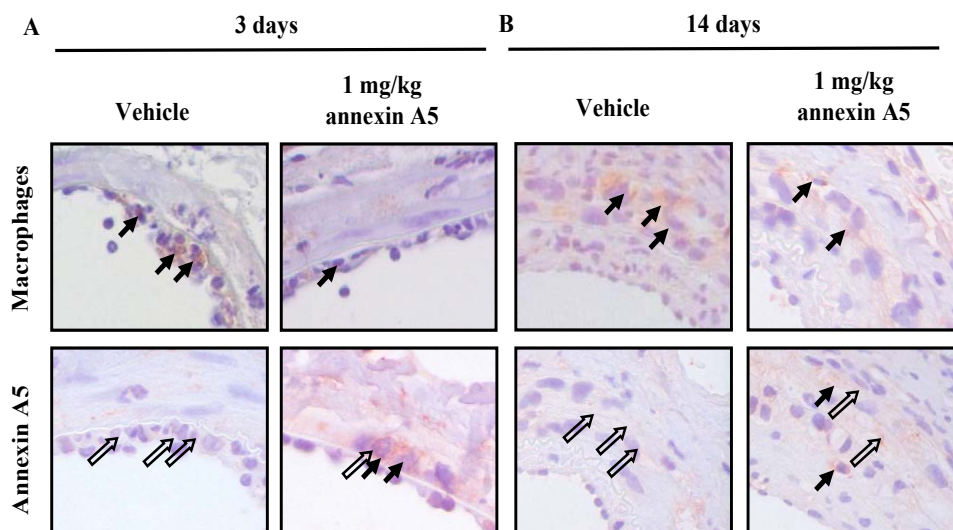


Figure II. Co-localization of injected AnxA5 at macrophage (3d) and macrophage/foam cell (14d) areas after 3d (A) and 14d (B). Representative cross-sections of cuffed arteries of ApoE^{-/-} mice receiving vehicle or 1.0 mg/kg AnxA5 (MAC3 and annexin A5 staining, magnification 80x, closed arrows indicate positive macrophage and AnxA5 staining, open arrows indicate projected macrophages in consecutive slides (5 μm distance) in annexin A5 stained femoral artery cross-sections to indicate co-localization).

Table I. Plasma cholesterol in mice undergoing annexin A5 dose-response investigations.

Group	Total plasma cholesterol (mmol/L)	
	Surgery	Sacrifice
Early time point (3d)		
Vehicle	19.5±1.3	25.0±0.8
1.0 mg/kg annexin A5	15.4±0.4	19.8±1.6
0.3 mg/kg annexin A5	16.6±0.6	20.0±1.7
0.1 mg/kg annexin A5	19.6±1.8	22.8±2.2
Late time point (14d)		
Vehicle	23.7±2.7	21.1±2.4
1.0 mg/kg annexin A5	18.0±2.7	17.1±2.7
0.3 mg/kg annexin A5	19.9±4.1	19.2±3.3
0.1 mg/kg annexin A5	19.3±1.6	19.8±1.6

Plasma total cholesterol (mmol/L) of *ApoE*^{-/-} mice receiving vehicle or annexin A5 (1.0, 0.3 or 0.1 mg/kg/d) through IP injection, measured at surgery or at sacrifice (day 3 or 14). No significant differences were observed (mean±SEM, n=10).

“It always seems impossible until it's done”

Nelson Mandela